



Sudan University of Science & Technology

College of Graduated Studies

Evaluation of Concordance of Breast Imaging Reporting and Data System with Interpretation of Digital Mammography

تقويم توافق برنامج تشخيص وبيانات تصوير الثدي مع قراءة صورة الأشعة

الرقمية للثدي

Thesis submitted to fulfillment of Academic Requirements for the
award the degree of PhD in Diagnostic Radiologic Technology

By

Mayson Ahmed Wanasi Mohammed Khair

Master of Diagnostic Radiologic Technology

Supervisor:

Co-Supervisor:

Prof. Caroline Edward AyadKhilla

Dr. Duha Abdu Mohamed Abdu

2019

بِسْمِ اللَّهِ الرَّحْمَنِ الرَّحِيمِ

قال تعالى:

اقْرَأْ بِاسْمِ رَبِّكَ الَّذِي خَلَقَ (1) خَلَقَ الْإِنْسَانَ مِنْ عَلَقٍ (2) اقْرَأْ وَرَبُّكَ

الْأَكْرَمُ (3) الَّذِي عَلَّمَ بِالْقَلَمِ (4) عَلَّمَ الْإِنْسَانَ مَا لَمْ يَعْلَمْ (5)

"صدق الله العظيم"

سورة العلق (1-5)

Abstract

Mammography is a valuable tool in the early detection of breast cancer, the American College of Radiology's (ACR) Breast Imaging Reporting and Data System (BI-RADS) provide a lexicon that give a standard way of reporting mammogram that help constant reporting and ensure better follow up of benign and suspicious findings.

The research conduct to assess the concordance of final findings of mammograms reported using BI-RADS lexicons and the final impression of radiologist those using routine interpretation of mammogram. The research was retrospective study design, and included 300 mammographic image for women aged between 15 to 90 years old, the mammograms obtained by digital mammography machine and used the basic mammographic projections (CC: Craniocaudal and MLO: Mediolateral Oblique).The data descriptively analyzed and measured the different variables in the research and determined the relationship between them, Kappa value was determined to measure the concordance. Regarding to age, the most abundant group was (46-60 years) as (40%).Regarding to **Breast composition**, the most abundant group was scattered fibroglandular breast (b) group for both routine interpretation and BIRAD.The result appeared as the concordance of the breast composition was ($k = 0.5$) that point Moderate agreement. All pathological findings were founded and the concordance among the descriptive terms measured, According to **Mass**, the presence of the mass was ($k = 0.83$) that was a Very Good agreement, the shape of the mass was ($k = 0.53$) that a Moderate agreement, the margin of the mass was ($k = 0.475$) that point Moderate agreement, the density of the mass was ($k = 0.74$) that point a good agreement, in addition the associate calcifications was ($k = 1$) that point a total agreement. According to **Calcification** the

Kappa value was for presence ($k = 0.87$) that point to Very Good agreement, the morphology of the calcifications was ($k = 0.85$) that point to Very Good agreement and distribution was ($k = 1$) that point Very Good agreement. In addition, the **Architectural distortion** was ($k = 0.85$) that point to Very Good agreement, and **A symmetry** was ($k = 1.3$) it was poor agreement. **The intramammary lymph node** was ($k = 0.65$) that point a good agreement and the overall agreement and concordance to the **Final finding** (BIRAD Categories) was ($k = 0.58$) that point to a moderate agreement. The research found a significant relationship between the different variables such as breast composition with age as (P-value = 0.000), final findings with age (P-value = 0.000), mass presence (P-value = 0.000), mass shape (P-value = 0.000), mass margin (P-value = 0.000), mass density (P-value = 0.000), mass associated calcification (P-value = 0.000), mass location (P-value = 0.000), presence of calcification (P-value = 0.000), architectural distortion (P-value = 0.001), presence of asymmetry (P-value = 0.000), presence of inflammatory lymph node (P-value = 0.000), presence of associated features (P-value = 0.000) and presence of solitary dilated duct as (P-value = 0.000).

As the conclusion to the research, there is a moderate agreement with radiologist when reporting mammogram, which mean some variation in wording of the mammography report between the radiologists. Therefore, it is very importance to the similarity wording of the mammography report to avoid any misunderstanding or confusion, and following of BIRAD lexicon leads to this goal.

ملخص البحث

يعد تصوير الثدي بالأشعة أداة قيّمة للكشف المبكر عن سرطان الثدي، ويوفر نظام بيانات وتصوير الثدييات التابع للكلية الأمريكية للأشعة معجمًا يوفر طريقة قياسية لتشخيص صور الثدي بالأشعة السينية الذي يساعد على ثبات التشخيص وضمان أفضل متابعة للنتائج الحميدة والخبيثة.

تم إجراء البحث لتقييم توافق النتائج النهائية لأشعة الثدي المشخصة باستخدام برنامج بيانات و تشخيص الثدي والانطباع النهائي لأخصائي الأشعة الذين يستخدمون التفسير الروتيني لتصوير الثدي بواسطة الأشعة الرقمية. كان تصميم البحث من نوع دراسة بأثر رجعي، وشمل 300 صورة تصويرية للنساء الذين تتراوح أعمارهم بين 15 إلى 90 سنة، والأشعة السينية التي تم الحصول عليها بواسطة جهاز تصوير الثدي بالأشعة الرقمية واستخدمت اوضاع التصوير الاشعاعية الأساسية للثدي (الوضع الرأسي الذنبي والوضع الناصفي الوحشي المائل). وتم قياس المتغيرات المختلفة في البحث وتحديد العلاقة بينهما، تم تحديد قيمة كابا لقياس التوافق.

فيما يتعلق بالعمر، كانت المجموعة الأكثر وفرة (46-60 سنة) بنسبة (40٪). فيما يتعلق بتكوين الثدي، كانت المجموعة الأكثر وفرة هي الثدي من نوع الغدد الليفية المبعثرة النوع (ب) تكوين الثدي كان (ك = 0.5) يشير إلى اتفاق متوسط. وجددت جميع النتائج المرضية وتم قياس التوافق بين المصطلحات الوصفية، طبقًا للأورام، كان وجود الورم (ك = 0.83) كان عبارة عن اتفاق جيد جدًا، وكان شكل الورم (ك = 0.53) اتفاق معتدل، كان حدود الورم (ك = 0.475) في هذه النقطة اتفاق معتدل، وكانت كثافة الورم (ك = 0.74) تشير إلى اتفاق جيد، بالإضافة إلى أن التكلسات المصاحبة للورم (ك = 1) تشير إلى اتفاق تام. وفقًا للتكلس، كانت قيمة كابا في التواجد (ك = 0.87) التي تشير إلى اتفاق جيد جدًا، كانت تكوين التكلسات (ك = 0.85) تشير إلى اتفاق جيد جدًا والتوزيع كان (ك = 1) اتفاق تام. بالإضافة إلى ذلك، كان التشويه المعماري لبنية الثدي (ك = 0.85) يشير إلى اتفاق جيد جدًا، وكان التماثل (ك = 1.3) كان اتفاقًا ضعيفًا. كانت العقدة الليمفاوية الداخلية (ك = 0.65) التي تشير إلى اتفاق جيد وكان الاتفاق الكلي والاتفاق مع النتيجة النهائية (فئات برنامج بيانات وتشخيص الثدي) (ك = 0.58) يشير إلى اتفاق معتدل.

وجد البحث علاقة مهمة بين المتغيرات المختلفة مثل تكوين الندي مع تقدم العمر بقيمة (ب = 0.000)، والنتائج النهائية مع التقدم في العمر (ب = 0.000)، والوجود الشامل (ب = 0.000)، وشكل الكتلة (ب = 0.000)، وهامش الكتلة (ب = 0.000)، وكثافة الكتلة (ب = 0.000)، وتكلس الكتلة المرتبطة (ب = 0.000)، والموقع الشامل (ب = 0.000)، ووجود التكلس (ب = 0.000)، والتشويه المعماري (ب = 0.001)، ووجود عدم تناسق (ب = 0.000)، ووجود العقدة الليمفاوية الالتهابية (ب = 0.000)، ووجود ميزات مرتبطة (ب = 0.000) ووجود توسع قناة منعزلة بقيمة (ب = 0.000).

في ختام البحث، هناك اتفاق معتدل مع أخصائي الأشعة عند تشخيص صور الأشعة للندي، مما يعني بعض الاختلاف في صياغة تقرير التصوير الإشعاعي للندي بين أخصائي الأشعة. لذلك، من الأهمية بمكان أن تشبه صياغة تقرير التصوير الشعاعي للندي لتجنب أي سوء فهم أو ارتباك، واتباع معجم تشخيص وبيانات الندي يحقق هذا الهدف.

Dedication

To my family with my great love

Acknowledgment

Firstly, I would to thanks and dreadful to Allah, to give me a pleasure and reconciliation

I would like to express my sincere gratitude to my supervisor **Dr. Caroline Edward Ayad** for the continuous support, for his patience, motivation, and immense knowledge. Her guidance helped me in all the time of research and writing of our published papers. I could not have imagined having a better supervisor and mentor for my PhD study than you, with my great love and appreciation.

I would like to express my special thanks to Co-Supervisor of the research **Dr. Duha Abdu Mohamed Abdu** to all advices, support especially in the layout of the research, comments and encouragement, but also for the hard questions which incented me to widen my research from various perspectives and get a lot of reading.

A great thanks to the radiologists help me in diagnosis of mammograms **Dr. Mona Abu Aleez, Dr. Weshah** and **Dr. Mona** as well as all radiologist not mentioned here and I take a report of them, all of you gave me the golden opportunity to do this research and Without they precious support and knowledge it would not be possible to conduct this research.

I am grateful to my friend and my researching interesting partner **Dr. Mahasin Gamalalddin Yaqob**, whom help me in Statistical analysis of my research data with all sincerity and for unfailing support and assistance.

I would to thanks my Colleagues, whom also helped me in doing a lot of Research and reading. As well as my colleagues in hospitals which the

data of the research were collected, special mention the staff of Dal El-Elag Hospital, Antalya Medical Center and Khartoum Hospital, I am really thankful to them.

I would also like to thank my parents, my little family and friends. And all my thanks to all person let my work to be possible.

Research Contents

No.	Item	Page
Chapter One: Introduction and Research Plan		
1.1	Introduction	1
1.2	Problem of the study	5
1.3	Objectives	6
1.4	Thesis Overview	7
1.5	Ethical Consideration	7
Chapter Two: Literature Review		
2.1	Anatomy of the Breast	8
2.2	Physiology of the Breast	17
2.3	Pathology of the Breast	18
2.4	Mammography	21
2.4.1	Definition	21
2.4.2	Technical Consideration	21
2.4.3	Clinical Image Evaluation Categories	22
2.4.4	Radiation Protection	24
2.5	Digital Mammography Machine	25
2.6	Technique of Mammography	34
2.7	Interpretation of Mammography image	38
2.8	BIRADS	50
2.9	Previous studies	93

Chapter Three: Methodology of the Research		
3.1 Material		134
3.1.1	Research Type	134
3.1.2	Population and Sample Size	134
3.1.3	Exclusion criteria	134
3.1.4	Study duration	134
3.1.5	Machine	134
3.1.6	Ethical consideration	135
3.2 Method		135
3.2.1	Collection of Data	136
3.2.1.1	Data collection Sheet	136
3.2.2	Statistical Analysis	139
3.2.2.1	Kappa value scale	139
Chapter Four: Results		
4	Results	141
Chapter Five: Discussion, Conclusion and Recommendations		
5.1	Discussion	177
5.2	Conclusion	201
5.3	Recommendations	205
References		206
Appendix A		
Appendix B		
Appendix C		

Table of Figures

Number of Figure	Name of Figure	Page No.
2-1	Surface Anatomy	9
2-2	Breast Sagittal section	10
2-3	Breast tissue Sagittal section	10
2-4	Breast—anterior view	11
2-5	Breast—anterior view (three tissue types)	12
2-6	The mammogram image	13
2-7	Mammography image shows Fibroglandular breast (younger or prepregnancy).	14
2-8	Mammography image shows Fibrofattybreast.	14
2-9	Mammography image shows Fatty breast	15
2-10	Breast localization—Quadrant method.	16
2-11	Breast localization—Clock system.	16
2-12	Proper positioning for the mediolateral oblique (MLO) mammography view	23
2-13	Recommendations for labeling of mammograms	24
2-14	The geometry of a mammography unit and the relative locations of the x-ray tube	26
2-15	Geometry of a mammography x-ray tube.	27
2-16	The acquisition workstation (AW).	28
2-17	The acquisition console.	28
2-18	Review Workstation (RW)	29

2-19	Cross sectional view of a computed radiography imaging plate and readout schematic.	30
2-20	Cross sectional view of a cesium iodide (CsI) with charge-coupled device (CCD) slot-scan detector.	31
2-21	Cross-sectional view of a cesium iodide (CsI) with thin film transistors (TFT) detector.	32
2-22	Cross-sectional view of an amorphous selenium with thin film transistors (TFT) detector.	33
2-23	Part position for CC projection.	35
2-24	Mammographic image of CC projection	35
2-25	Part position for MLO projection.	37
2-26	Mammographic image of MLO projection	37
2-27	Diagrammatic illustration of invasive ductal carcinoma: the larger the central tumor mass, the longer the spicules	41
2-28	Demonstrate the characteristics of atypical malignant stellate tumor	41
2-29	Right breast, MLO and CC projections. Centrally located, large (5cmdiameter) stellate tumor.	42
2-30	Enlarged view of the portion of theleft breast containing the palpable tumor. There are numerous fragmented casting type.	44
2-31	Details of the MLO project ionmicrofocus magnification.	45
2-32	Left breast, MLO projection. Two Clusters of microcalcifications.	46
2-33	Right LMO and CC projections. The de novo	47

	density associated with powdery calcifications.	
2-34	Right breast, craniocaudal (CC) projection. Extreme skin thickening over the entire breast.	47
2-35	Oval, circumscribed mass	51
2-36	Oval, circumscribed mass with two undulations	51
2-37	Round, circumscribed mass	52
2-38	Irregular, Mass with primarily obscured margin.	52
2-39	Circumscribed Mass, Oval Circumscribed mass.	53
2-40	Margin: Obscured. Oval mass	54
2-41	Margin: Microlobulated. Irregular mass with Microlobulated margin	54
2-42	Margin: Indistinct. Because it is difficult to determine the shape of mass	55
2-43	Margin: Spiculated. Irregular Spiculated mass	55
2-44	Margin: Spiculated. Irregular Spiculated mas	56
2-45	Density: High Density. Oval, high density mass	57
2-46	Density: High Density. Irregular, spiculated high density mass	57
2-47	Density: Equal Density. Oval Equal Density mass.	58
2-48	Density: Low Density. Round, Low density mass	58
2-49	Density: Fat-Containing. Irregular, Fat Containing mass.	59
2-50	Typically Benign: Skin. Tightly, grouped, lucent skin calcifications.	60

2-51	Typically Benign: Vascular. Fully developed vascular calcifications	61
2-52	Typically Benign: Corse or Popcorn like calcifications.	61
2-53	Typically Benign: Large Rod-like Calcifications	62
2-54	Typically Benign: Round. Regional round calcifications.	63
2-55	Typically Benign: Rim. Rim Calcifications	64
2-56	Typically Benign: Dystrophic. Dystrophic Calcification.	64
2-57	Typically Benign: Milk of Calcium	65
2-58	Typically Benign: Suture. Suture Calcifications.	66
2-59	Suspicious Morphology: Amorphous. Grouped Amorphous calcifications.	67
2-60	Suspicious Morphology: Coarse Heterogeneous. Grouped of Coarse Heterogeneous Calcifications.	68
2-61	Suspicious Morphology: Fine Pleomorphic. Grouped Fine Pleomorphic Calcifications.	69
2-62	Suspicious Morphology: Fine Linear or Fine Linear Branching. Regional Fine Linear Calcifications.	70
2-63	Distribution: Diffuse. Diffuse, primarily round calcifications.	71
2-64	Distribution: Regional. Regional, dystrophic Calcifications.	71
2-65	Distribution: Grouped. Grouped, fine, pleomorphic Calcifications.	72

2-66	Distribution: Linear. Linear, fine calcifications.	73
2-67	Distribution: segmental. Segmental fine linear calcifications.	73
2-68	Architectural distortion. Manifested by thin radiating lines with fatty tissue at the point of origin.	74
2-69	Asymmetry. Note the asymmetric area of dense tissue in the lateral aspect of the left breast seen only on the CC.	75
2-70	Global asymmetry. The large volume of asymmetric dense tissue occupies at least one quadrant of the right breast.	76
2-71	Focal Asymmetry. The Asymmetric dense tissue occupies less than the entire upper inner quadrant of the right breast.	77
2-72	Developing Asymmetry. The asymmetric dense tissue in the upper inner quadrant of the right breast is larger on current examination than on the previous examination.	78
2-73	Intramammary Lymph Node. Note the fatty hilum projected tangentially, at the peripheral of the oval circumscribed mass.	79
2-74	Skin Lesion. Raised skin lesion, air tapped around the skin lesion.	79
2-75	Solitary Dilated Duct.	80
2-76	Skin Retraction. Note the double skin line (indicate skin retraction).	81
2-77	Nipple Retraction. Adjacent to a spiculated high-density mass.	81
2-78	Skin Thickening. Diffuse skin thickening.	82

2-79	Axillary Adenopathy. Enlarge axillary lymph node.	83
2-80	Depth Diagram.	85
2-81	Fatty breast	87
2-82	Scattered areas of fibroglandular density	87
2-83	Heterogeneous breast	88
2-84	Dense breast	88
3-1	GE Mammographic Machine	135
4-1	Distribution of sample according to age	141
4-2	Distribution of samples according to breast composition	142
4-3	Distribution of samples according to presence of breast masses	143
4-4	Distribution of samples according to the shape of mass	144
4-5	Distribution of samples according to the margin of mass	145
4-6	Distribution of samples according to the mass density	146
4-7	Distribution of samples according to the mass associated calcification	147
4-8	Distribution of samples according to mass location	148
4-9	Distribution of samples according to calcification presence	149
4-10	Distribution of samples according to calcification morphology	150

4-11	Distribution of samples according to calcification distribution	151
4-12	Distribution of samples according to calcification location	152
4-13	Distribution of samples according to architectural distortion	153
4-14	Distribution of samples according to presence of asymmetry	154
4-15	Distribution of samples according to inflammatory lymph node	155
4-16	Distribution of samples according to associated features	156
4-17	Distribution of samples according to solitary dilated duct	157
4-18	Distribution of samples according to final findings	158

List of Tables

Number of Table	Name of Table	Page No.
2-1	Hormone Effects on the Mammary Glands	17
4-1	Distribution of sample according to age	141
4-2	Distribution of samples according to breast composition	142
4-3	Distribution of samples according to presence of breast masses	143
4-4	Distribution of samples according to the shape of mass	144
4-5	Distribution of samples according to the margin of mass	145
4-6	Distribution of samples according to the mass density	146
4-7	Distribution of samples according to the mass associated calcification	147
4-8	Distribution of samples according to mass location	148
4-9	Distribution of samples according to calcification presence	149
4-10	Distribution of samples according to calcification morphology	150
4-11	Distribution of samples according to calcification distribution	151
4-12	Distribution of samples according to calcification location	152

4-13	Distribution of samples according to architectural distortion ¹⁵⁶	153
4-14	Distribution of samples according to presence of asymmetry	154
4-15	Distribution of samples according to inflammatory lymph node	155
4-16	Distribution of samples according to associated features	156
4-17	Distribution of samples according to solitary dilated duct	157
4-18	Distribution of samples according to final findings	158
4-19	Correlation of breast composition with age	159
4-20	Correlation of final findings with age.	160
4-21	Correlation of breast composition with final findings.	161
4-22	Correlation of mass presence with final findings.	162
4-23	Correlation of mass shape with final findings.	163
4-24	Correlation of mass margin with final findings.	164
4-25	Correlation of mass density with final findings.	165
4-26	Correlation of mass associated calcification with final findings.	166
4-27	Correlation of mass location with final findings.	167
4-28	Correlation of presence of calcification with final findings.	168
4-29	Correlation of morphology with final findings.	169
4-30	Correlation of calcification distribution with final findings.	169

4-31	Correlation of calcification location with final findings.	170
4-32	Correlation of architectural distortion with final findings.	171
4-33	Correlation of presence of asymmetry with final findings.	172
4-34	Correlation of presence of inflammatory lymph node with final findings.	173
4-35	Correlation of presence of associated features with final findings.	174
4-36	Correlation of presence of solitary dilated duct with final findings.	175
4-37	Concordance of BIRAD findings with the findings in the routine interpretation (Kappa (K) value)	176

Chapter One:
Introduction

1.1 Introduction:

The American College of Radiology (ACR) came up with a standard way to describe mammogram findings and results. In this system, the results are sorted into categories numbered 0 through 6. This system is called the *Breast Imaging Reporting and Data System (BI-RADS)*. Having a standard way of reporting mammogram results lets doctors use the same words and terms, which can help ensure better follow up of suspicious findings. (Valerie, 2011)

Also the important of diagnosis and detection of any breast lesions and helps in early detection of breast cancer, give this system very important value to be used every ware. (Valerie, 2011)

In Sudan, the Breast Imaging Reporting and Data system is very new technique of reporting and there is no more radiologist working with this system, so in this study the researcher will be studied and evaluated the system and concordance of it with the traditional way of reporting.

BIRAD system have a very significant impact because the importance of diagnosis and detection of any breast lesions and helps in early detection of breast cancer (Ferreira et al. 2011).

The practice of breast imaging has transitioned through a wide variety of technologic advances from the early days of direct-exposure film mammography to xeromammography to screen-film mammography to the current era of full-field digital mammography and digital breast. Along with these technologic advances, organized screening, federal regulations based on the Mammography Quality Standards Act, and the development of the American College of Radiology Breast Imaging Reporting and Data System have helped to shape the specialty of breast imaging. (Antonio, 2012)

The standardized terminology of the BI-RADS lexicon allows quantification of the likelihood of carcinoma in an impalpable breast lesion.(Lieberman et al. 1998).

As mentioned by saeed et al, The most commonly diagnosed cancer among women in Khartoum Sudan was breast, so the accurate diagnosis of mammogram and U/S has a very important issue. In addition, The BI-RADS lexicon offers multiple area of strengths, including the standardization of common language to facilitate communication between radiologists, physicians, and patients. The system also clarifies the reporting of mammography results and offer a clinical management. (Eberl et al. 2015)

BI-RADS is an acronym for Breast Imaging-Reporting and Data System, a quality assurance tool originally designed for use with mammography. The system is a collaborative effort of many health groups but is published and trademarked by the American College of Radiology (ACR).

The system is designed to standardize reporting, and is used by medical professionals to communicate a patient's risk of developing breast cancer. The document focuses on patient reports used by medical professionals, not "lay reports" that are provided to patients.

Automatic parsers have been developed to automatically extract BI-RADS features, categories and breast composition from structured mammography reports.

While BI-RADS is a quality control system, in day-to-day usage the term "BI-RADS" refers to the mammography assessment categories. These are standardized numerical codes typically assigned by a radiologist after interpreting a mammogram. This allows for concise and unambiguous understanding of patient records between multiple doctors and medical facilities.

The assessment categories were developed for mammography and later adapted for the MRI and Ultrasound Atlases. The summary of each category, given below, is identical for all 3 modalities. (Martin ,1988)

Category 6 was added in the 4th edition of the Mammography Atlas.

BI-RADS Assessment Categories are: 0 :Inconclusive, 1: Negative, 2: Benign finding(s), 3: Probably benign, 4: Suspicious abnormality, 5: Highly suggestive of malignancy and 6: Known biopsy – proven malignancy. (Spak et al. 2017)

An incomplete (BI-RADS 0) classification warrants either an effort to ascertain prior imaging for comparison or to call the patient back for additional views and/or higher quality films. A BI-RADS classification of 4 or 5 warrants biopsy to further evaluate the offending lesion. Some experts believe that the single BI-RADS 4 classification does not adequately communicate the risk of cancer to doctors and recommend a sub classification scheme: 4A: low suspicion for malignancy, 4B: intermediate suspicion of malignancy and 4C: moderate concern, but not classic for malignancy. (D’Orsi, 2013)

Breast Composition Categories, As of the BI-RADS 5th edition

- a. The breasts are almost entirely fatty
- b. There are scattered areas of fibroglandular density
- c. The breasts are heterogeneously dense, which may obscure small masses
- d. The breasts are extremely dense, which lowers the sensitivity of mammography (D’Orsi, 2013)

As a compare to other studies, among Bent study on 2010, that was about assess the likelihood of malignancy of microcalcifications according to the BI-RADS descriptors in a digital mammography environment. They found that BI-RADS morphology and distribution descriptors can aid in assessing

the risk of malignancy of microcalcifications detected on full-field digital mammography (Bent et al, 2010). Our study take all descriptors and lexicons of BIRADS related to Normal, Benign and malignant findings to show the importance of the BIRAD system in all case using digital mammogram.

As compere with Lazarus study on 2006, that was about evaluation of interobserver variability between breast radiologists by using terminology of the fourth edition of the Breast Imaging Reporting and Data System (BI-RADS) to categorize lesions on mammograms and sonograms. They found that Interobserver agreement with the new BI-RADS terminology is good. As a match with our study in both radiologists retrospectively reviewed mammogram. Each observer described each lesion with BI-RADS terminology and assigned a final BI-RADS category. Interobserver variability was assessed with the kappa value (Lazarus et al, 2006). In our study, the mammogram double-checked and reported using different way of reporting to assess the concordance between them.

Berg et al, on 2000 mentioned that Inter- and intraobserver variability in mammographic interpretation is substantial for both feature analysis and management. Continued development of methods to improve standardization in mammographic interpretation is needed. They found previous conclusion when evaluate the use of the Breast Imaging Reporting and Data System (BI-RADS) standardized mammography lexicon among and within observers and to distinguish variability in feature analysis from variability in lesion management (Berg et al, 2000). In related to Berg study, our study use the Kappa value to measure the agreement degree.

So standardized language for physicians to describe lesions and using the same descriptors to define Benign and Malignant lesions contribute the quality of mammography diagnosis and good management.

According to Rastogi, global cancer mortality is expected to increase by 104% by 2020, but it is also estimated that one-third of all cancers are preventable and potentially curable provided that detection is made early in the course of the cancer (Rastogi, Hildesheim, and Sinha 2004). According to Kanavos, much of the disparity in cancer mortality in developing countries is due to the lack of early detection and prevention (Kanavos 2006). So that it is very important to accurate diagnosis of mammography and standardizing the reporting system using BIRAD.

1.2 Problem of the study:

In Sudan, the Breast Imaging Reporting and Data system is very new technique of reporting and there is no more radiologist working with this system. As a new topic of research, this research highlighted and demonstrate the BIRAD system and give a knowledge about it. In addition, the area of study is different from other researches, and using of digital mammography.

1.3 Objectives:

1.3.1 General Objectives:

To Concord Breast Imaging Reporting and Data System with Interpretation of Digital Mammography

1.3.2 Specific Objectives:

- To evaluate the Breast Imaging Reporting and Data System across the Khartoum.
- To correlate final diagnosis in reporting and interpretation of mammography with BI-RAD categories.

- To Concord finding description in Breast Imaging and Data System with the interpretation of Mammography.
- To assess the Breast composition value according to BI-RAD.
- To correlate the Breast composition value according to BI-RAD with routine reporting system.
- To correlate between location of the mass and the final diagnosis.
- To correlate the age of the patient with the breast composition and Malignancy.
- To correlate between the mass morphology and malignancy.
- To correlate between presence of mass, calcifications, architectural distortion, associated features and BIRAD category.
- To identify the associated features related to malignancy.
- To assess the findings and Features related to Benignancy and Malignancy.

1.4 Thesis Overview:

The Research contains:

Chapter One includes introduction and Proposal

Chapter Two includes theoretical background & Previous study

Chapter Three includes Material & Method

Chapter Four includes Result

Chapter Five includes Discussion, Conclusion and Recommendations

References

Appendix

Chapter Two:
Theoretical background
&
Previous study

2.1 Anatomy of the Breast:

Each of the mammary glands or breasts in a woman is a conic or hemispheric eminence that is located on the anterior and lateral chest walls. Breast size varies from one individual to another and often even within the same woman, depending on her age and the interplay of various hormones. These hormones are very influential in tissue development, growth, and eventually milk production in the woman. Each breast comprises 15 to 20 lobes, which are covered by adipose tissue that primarily accounts for its size and shape (Standering and others 2005).

2.1.1 Surface Anatomy:

The surface anatomy includes the nipple, a small projection that contains a collection of 15 to 20 duct openings from secretory glands within the breast tissue. The circular, darker pigmented area surrounding the nipple is termed the areola. The Montgomery glands are small oil glands whose purpose is to keep the nipple lubricated and protected, especially during nursing. The junction of the inferior part of the breast with the anterior chest wall is called the inframammary fold (IMF). The axillary tail (AT) is a band of tissue that wraps around the pectoral muscle laterally (Fig. 2-1). The width of the breast, called the mediolateral diameter, on most women is greater than the vertical measurement, from top to bottom. (Scanlon and Sanders 2018)

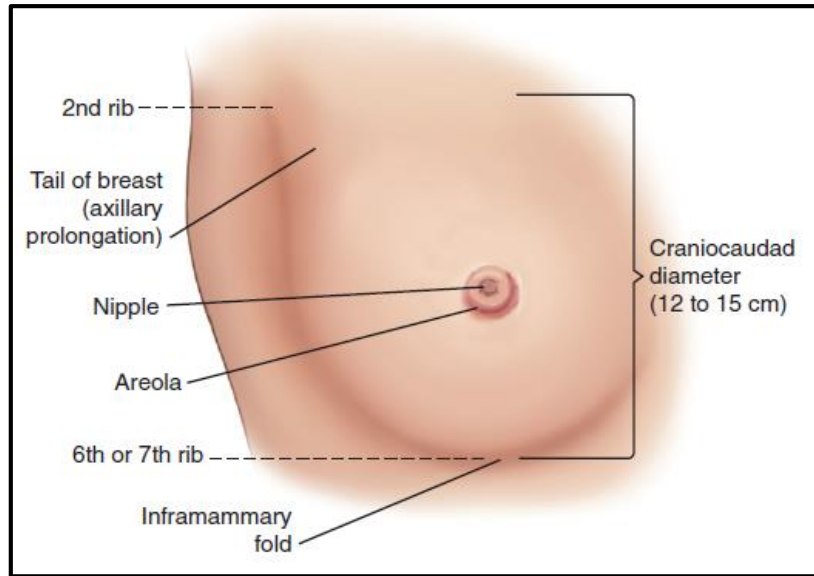


Fig. 2.1 Surface Anatomy (Standering,2017)

2.1.2 Sagittal Section Anatomy:

A sagittal section through a mature breast is illustrated in (Fig.2-2), which shows the relationship of the mammary gland to the underlying structures of the chest wall. In this illustration, the IMF is at the level of the sixth rib, but a great deal of variation can exist among individuals. The large muscle, known as the pectoralis major, is seen overlying the bony thorax. A layer of fibrous tissue encompasses the breast because of its location below the skin surface and covering the pectoralis major muscle. The area where these tissues meet superiorly to inferiorly is termed the retromammary space. This retromammary space must be demonstrated on at least one projection during the radiographic study of the mammary gland, as an indication that all breast tissue has been visualized. This task is achievable because the connections within the retromammary space are loose, and the area of the IMF is the most mobile within the normal breast. The relative position of glandular tissue versus adipose (fatty) tissue is illustrated in (Fig. 2-3). (Scanlon and Sanders 2018)

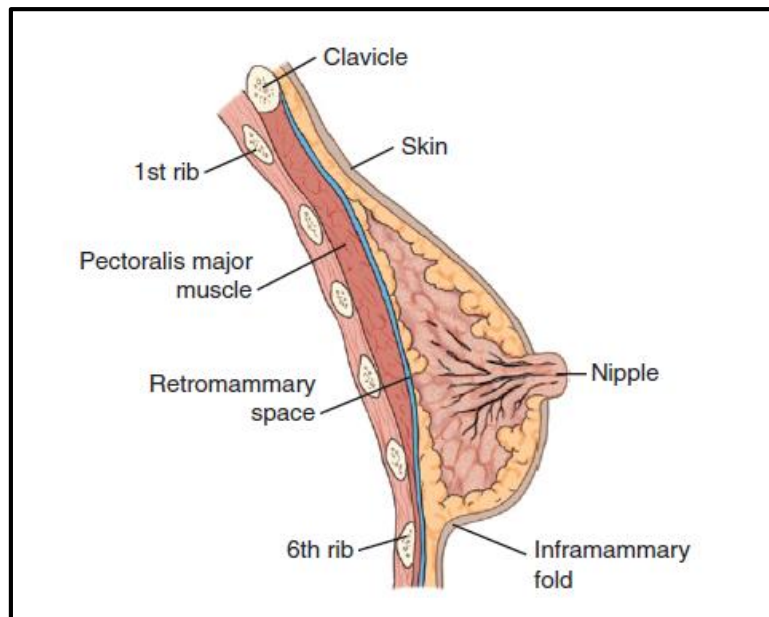


Fig. 2.2 Breast Sagittal section (Bontrager and Lampignano 2013)

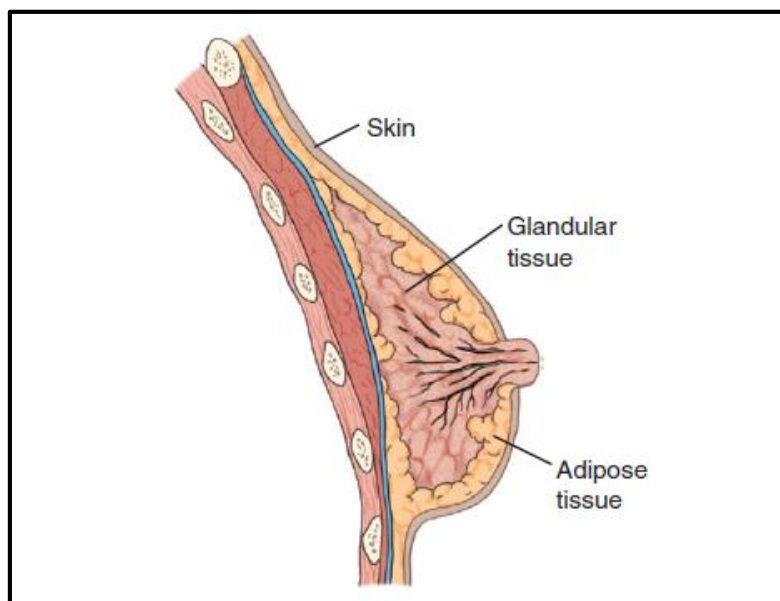


Fig. 2.3 Breast tissue Sagittal section (Bontrager and Lampignano 2013)

2.1.3 Frontal View Anatomy:

The glandular tissue of the breast is divided into 15 or 20 lobes that are arranged similarly to the spokes of a wheel surrounding the nipple (Fig. 2-4). The glandular lobes, which include several individual lobules,

are not clearly separated but are grouped in a radial arrangement, as shown on this drawing. Distally, the smallest lobules consist of clusters of rounded alveoli. On glandular stimulation, peripheral cells of the alveoli form oil globules in their interior, which, when ejected into the lumen of the alveoli, constitute milk globules. The clusters of alveoli that make up the lobules are interconnected and drain through individual ducts. Each duct enlarges into a small ampulla that serves as a reservoir for milk just before terminating in a tiny opening on the surface of the nipple. (Bontrager and Lampignano 2013)

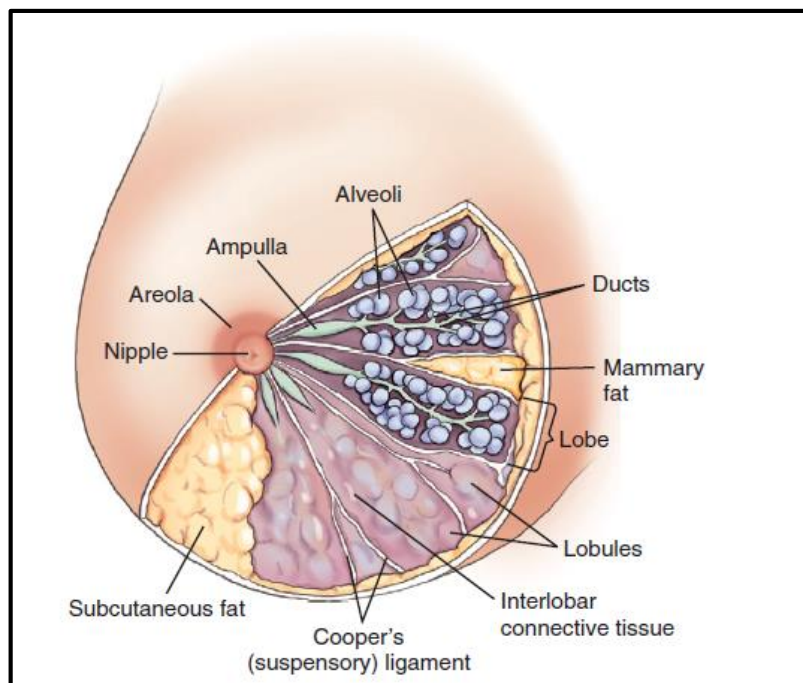


Fig. 2.4 Breast—anterior view (Bontrager and Lampignano 2013)

2.1.4 Breast Tissue Types:

A major challenge associated with imaging the breast radiographically is that the various tissues have low inherent subject contrast or breast tissue “makeup.” Breast tissue can be divided into three main types:

(1) Glandular,

(2) Fibrous or connective, and

(3) Adipose (Fig. 2-5).

Because the breast is a soft tissue structure, no high-density or air-filled tissue is present to provide contrast. The fibrous and glandular tissues are of almost heterogeneous density, which means that radiation is absorbed by these tissue types in a similar fashion. (Bontrager and Lampignano 2013)

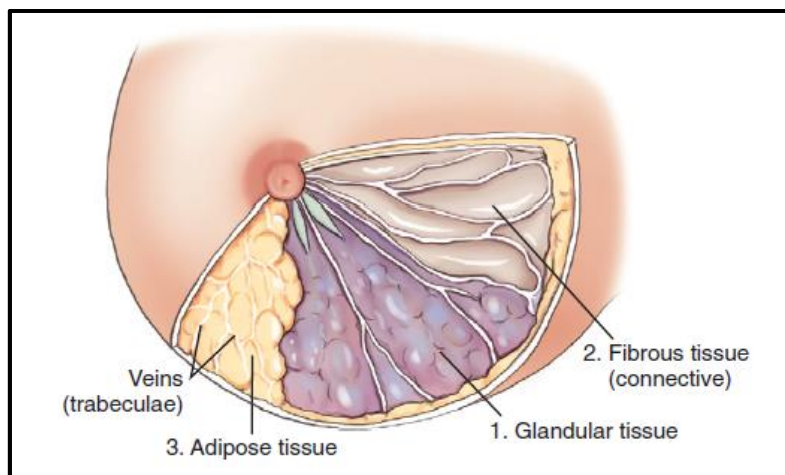


Fig. 2.5 Breast—anterior view (three tissue types)
(Frank, Long, and Smith 2013)

The major difference among breast tissues is that adipose or fatty tissue is less dense than either fibrous or glandular tissue. This difference in density between the fatty tissue and the remaining tissues accounts for the contrast differences that are apparent on the final image. (Bontrager and Lampignano 2013)

The mammogram image (Fig. 2-6) shows the differences in tissue density. These differences provide the basis for the radiographic image of the breast. The more dense glandular and fibrous or connective tissues appear as “light” structures or regions. The less dense adipose or fatty tissues appear as various shades of gray, depending on the thickness of these tissues. (Bontrager and Lampignano 2013)

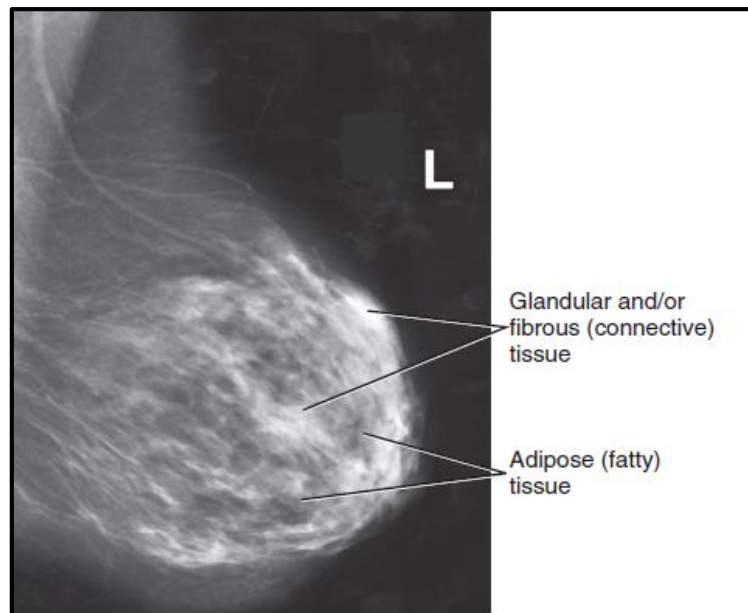


Fig. 2.6 **The mammogram image** (B. Hashimoto 2010)

2.1.5 Breast Classifications:

The relative density of the breast is affected primarily by the patient's inherent breast characteristics (genetics), hormone status, age, and number of pregnancies. (Ikeda and Miyake 2017)

Generally, breasts can be classified into three broad categories, depending on the relative amounts of fibroglandular tissue versus fatty tissue. These three categories are:

2.1.5.1 Fibroglandular Breast

The first category is the fibroglandular breast. The younger breast normally is quite dense because it contains relatively little fatty tissue. The common age group for the fibroglandular category is post puberty to about 30 years old. (Ikeda and Miyake 2017)

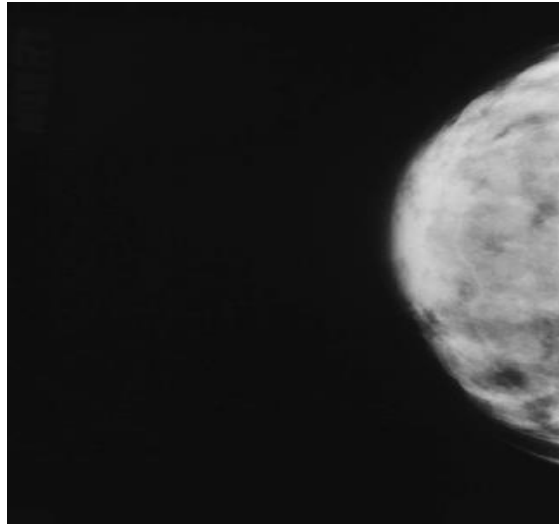


Fig. 2.7 Mammography image shows **Fibroglandular breast (younger or pre pregnancy)**. (Flowers and Holzhauser 2014)

2.1.5.2 Fibrofatty Breast

A second general category is the fibrofatty breast. As a woman ages and changes in breast tissue continue to occur, the low amount of fatty tissue gradually shifts to a more equal distribution of fat and fibroglandular tissue. In the 30-year-old to 50-year-old group, the breast is not quite as dense as in the younger group. (see Fig. 2-8). (Ikeda and Miyake 2017)



Fig. 2.8 Mammography image shows **Fibrofatty breast (30 to 50 years old, post pregnancy)**. (Bontrager and Lampignano 2013)

2.1.5.3 Fatty Breast

A third and final grouping is the fatty breast, which generally occurs after menopause, commonly in women 50 years old and older. After a woman's ability to reproduce has ended, most glandular breast tissue is converted to fatty tissue in a process called *involution*. This type of breast tissue is compressed easily, requiring less exposure (Fig. 2-9). (Flowers and Holzhauer 2014)

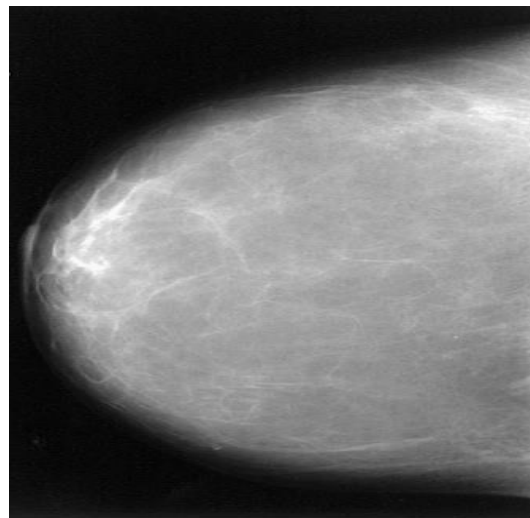


Fig. 2.9 Mammography image shows Fatty breast (Shah and Mandava 2014)

2.1.6 Methods of Localization

Two methods are commonly used to subdivide the breast into smaller areas for localization purposes.

The quadrant system and the clock system are shown in (Figs. 2-10) and (2-11). Of the two, the quadrant system is easier to use for generalized lesion localization. Four quadrants can be described by using the nipple as the center. These quadrants are the UOQ (upper outer quadrant), the UI Q (upper inner quadrant), the LOQ (lower outer quadrant), and the LIQ (lower inner quadrant). (NG et al. 2013)

The second method (Fig. 2-11), the clock system, compares the surface of the breast with the face of a clock. Although this method provides a more

accurate description of a lesion, what is described at 3 o'clock in the right breast has to be described at 9 o'clock in the left breast. (NG et al. 2013)

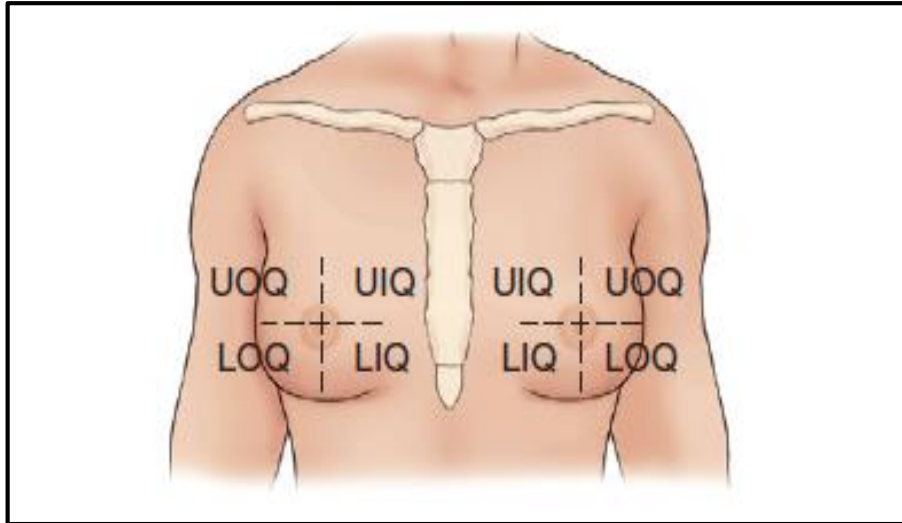


Fig. 2.10 Breast localization—Quadrant method. (Tabár and Dean 2012)

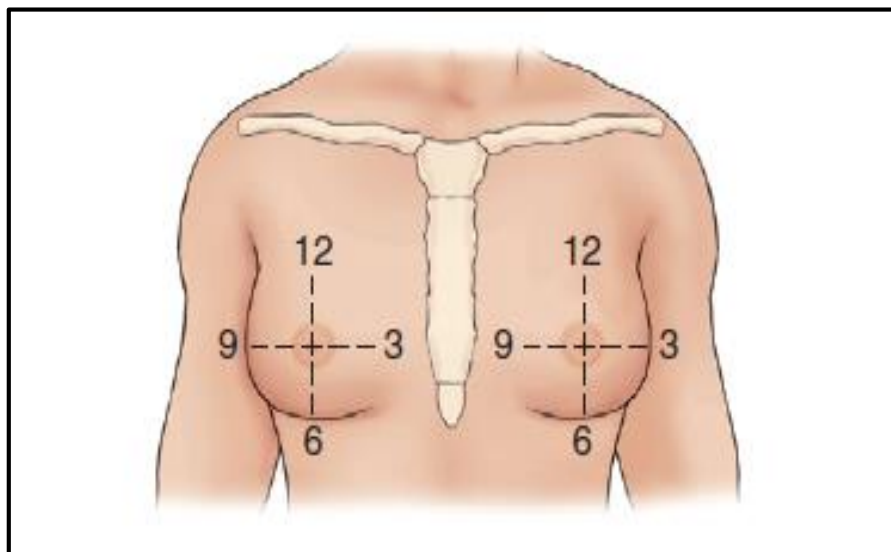


Fig. 2.11 Breast localization—Clock system. (Tabár and Dean 2012)

2.2 Physiology of Breast

The alveolar glands produce milk after pregnancy; the milk enters lactiferous ducts that converge at the nipple. The formation of milk is under hormonal control. During pregnancy, high levels of estrogen and progesterone prepare the glands for milk production. Prolactin from the anterior pituitary gland causes the actual synthesis of milk after pregnancy. The sucking of the infant on the nipple stimulates the hypothalamus to send nerve impulses to the posterior pituitary gland, which secretes oxytocin to cause the release of milk. (Scanlon and Sanders 2018)

Hormone	Secreted by	Functions
Estrogen	Ovary (follicle) Placenta	Promotes growth of duct system
Progesterone	Ovary (corpus luteum) Placenta	Promotes growth of secretory cells
Prolactin	Anterior pituitary	Promotes production of milk after birth
Oxytocin	Posterior pituitary (hypothalamus)	Promotes release of milk

Table 2-1 Hormone Effects on the Mammary Glands (Scanlon and Sanders 2018)

2.3 Pathology of the Breast:

Screening mammography is important for the early detection of pathologic changes in the breast. These changes can be either benign (noncancerous) or malignant (cancerous). The ACR Breast Imaging Reporting and Data Systems (BI-RADS) defines a breast mass as a 3D space-occupying lesion seen on at least two mammographic images. Benign masses do not invade the surrounding tissue. The most common benign or malignant pathologic findings in the breast include the following. (Scanlon and Sanders 2018)

2.3.1 Breast carcinoma (cancer)

Carcinoma of the breast is divided into two categories, noninvasive and invasive. Noninvasive carcinoma is a distinct lesion of the breast that has the potential to become invasive cancer. These lesions are restricted to the glandular lumen and do not have access to the lymphatic system or blood vessels. Noninvasive cancer also may be termed in situ. Ductal carcinoma in situ is isolated within the breast duct and has not spread to other areas of the breast. Lobular carcinoma in situ consists of abnormal cells that have been detected in one or more of the breast lobes. Noninvasive cancers (ductal carcinoma in situ and lobular carcinoma in situ) account for approximately 15% to 20% of all breast cancer diagnoses. The most common form of breast cancer is invasive or infiltrating ductal carcinoma. This type accounts for approximately 90% of all breast cancer diagnoses. Invasive cancer is believed to arise in the terminal duct lobular unit. (Dronkers 2002)

2.3.2 Benign Breast Lesions

2.3.2.1 Cysts

Cysts are fluid-filled sacs that are benign and appear as well circumscribed masses. Their density is usually that of the surrounding tissue; however,

they may appear denser. In some cases, high concentrations of calcium particles may be suspended within the cyst fluid.. (Dronkers 2002)

2.3.2.2 Fibroadenoma

Fibroadenomas are the most common benign, solid lumps or tumors composed of fibrous and glandular tissue. They are well-circumscribed lesions with clearly defined edges that may be felt during palpation. They typically have the same density as the surrounding tissue. The mass is an overgrowth of fibrous tissue of the breast lobule. (Dronkers 2002)

2.3.2.3 Fibrocystic changes

Fibrocystic changes constitute a common, benign condition that is usually bilateral and occurs in premenopausal women. It includes a variety of conditions; the most obvious are fibrosis and cystic dilation of ducts. Multiple cysts with increased fibrous tissue commonly are distributed throughout the breasts. (Dronkers 2002)

2.3.2.4 Gynecomastia

The term *gynecomastia* is derived from a Greek term meaning “woman like breasts.” In this benign condition of the male breast, a benign glandular enlargement of the breast occurs. Gynecomastia may be unilateral or bilateral but seems to be more pronounced in one breast. It typically manifests as a palpable mass near the nipple. (Dronkers 2002)

2.3.2.5 Intraductal papilloma

An intraductal papilloma is a small growth that occurs inside the duct of the breast near the nipple. Symptoms may include spontaneous, unilateral nipple discharge that may be bloody to clear in color. The mammographic appearance is typically normal. Papillomas are usually removed to exclude ductal carcinoma in situ or papillary cancer. (Dronkers 2002)

2.3.2.6 Paget’s disease of the nipple

Paget’s disease of the nipple first appears as a crusty or scaly nipple sore or as a discharge from the nipple. Slightly more than half of the patients

who have this cancer also have a lump in the breast. Paget's disease may be invasive or noninvasive. (Dronkers 2002)

2.4 Mammography

2.4.1 Definition

Mammography is the radiographic examination of the breast tissue (soft tissue radiography). To visualize normal structures and pathology within the breast, it is essential that sharpness, contrast and resolution are maximized. This optimizes, in the image, the relatively small differences in the absorption characteristics of the structures comprising the breast. (Whitley et al. 2005)

2.4.2 Technical Consideration

2.4.2.1 Patient Preparation

Before the examination begins, the technologist asks the patient to put on a gown, preferably one designed for mammography, which allows exposure of only the breast that is being examined. The patient is instructed to remove any jewelry, talcum powder, or antiperspirant that may cause artifacts on the radiographic image. Certain lotions, especially lotions with sparkles or glitter, can cause artifacts as well on the image. (Whitley et al. 2005)

2.4.2.2 Breast Positioning

In mammography, the previously mentioned tissue types, the shape and contour of the breast, and the patient's individual tolerance for the examination can pose challenges to the mammographer who is striving to produce the highest quality diagnostic images for interpretation.

The base of the breast is the portion near the chest wall, and the area near the nipple is termed the apex. In either the craniocaudal (CC) or the mediolateral (ML) projection, the base of the breast is much thicker and contains denser tissues than are found at the apex. To overcome this normal

anatomic difference found in the breast, a compression device is used in combination with a specially designed tube, so that the more intense central ray (CR) of the x-ray beam penetrates the thicker base of the breast. (Appleton and Wiele 2012).

2.4.3 Clinical Image Evaluation Categories

According to the American College of Radiology Mammography Accreditation Program (ACR MAP). The clinical image evaluation includes an assessment of these following eight categories:

(1) positioning; (2) compression; (3) exposure; (4) contrast; (5) sharpness; (6) noise; (7) artifacts; and (8) labeling. (McLelland et al. 1991)

2.4.3.1 Positioning

Breast positioning has improved dramatically over the years. This is due to a better understanding of the anatomy and mobility of the breast and improved capabilities of modern dedicated mammography equipment.

The standard screening views are the mediolateral oblique (MLO) and the craniocaudal (CC). The goal should be to image as much breast tissue as possible on these views. (Flowers and Holzhauer 2014)

2.4.3.1.1 Positioning for the Mediolateral Oblique View

The MLO is the view that provides the best opportunity to show all of the breast tissue in a single image. Because the breast lies primarily on the pectoralis muscle, a generous amount of pectoralis muscle should be included to ensure that far posterior breast tissues are shown. It is desirable for the muscle to extend inferiorly to the posterior nipple line (PNL) or below; this can be achieved in greater than 80% of women. (Whitley et al. 2005)

On the MLO, the PNL is drawn at an angle approximately perpendicular to the muscle (usually about 45 degrees), extending from the nipple to the

pectoralis muscle or to the edge of the film, whichever comes first (Whitley et al. 2005).

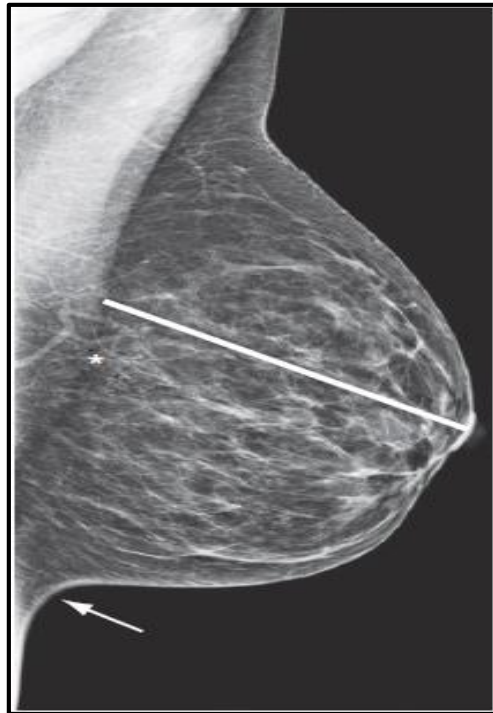


Fig. 2.12 Proper positioning for the mediolateral oblique (MLO) mammography view

2.4.3.1.2 Positioning for the Craniocaudal View

The overriding goal for positioning the CC view should be to include all of the posteromedial tissue, because this is the area of the breast most likely to be excluded in an MLO. If proper methods are used, the radiologic technologist can include all of the posteromedial fibroglandular tissue without resorting to exaggerated medial positioning of the CC (NG et al. 2013).

2.4.3.8 Labeling

Standardized methods for labeling films have been developed to ensure correct identification of facilities, patients, laterality, and view (Fig. 2-13). These labeling guidelines for mammography films can be divided into

those that are considered essential or required, highly recommended, or just recommended. Required items include identification label, view and laterality, cassette number, and initials of the radiologic technologist who performed the examination. (Tabár and Dean 2012)

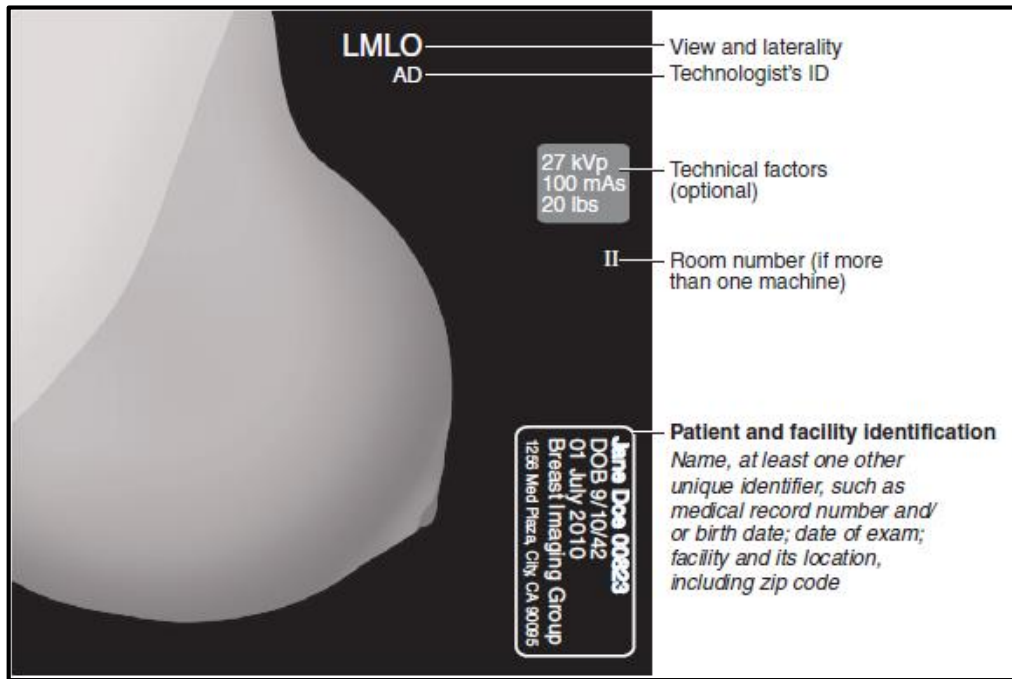


Fig: 2.13 Recommendations for labeling of mammograms

2.4.4 Radiation Protection

Absorbed doses are high in mammography due to the low kVp necessary to maximize the small differences in attenuation between tissues in the breast. A considerable proportion of the X-ray spectrum will, at the kVp used, not contribute to image formation but will increase breast dose. The breast is one of the most radio-sensitive tissues in the body.

In radiation protection as it reduces dose because exposure factors are reduced. Additionally, it maintains close object-to-film contact, thus reducing geometric unsharpness and reducing movement unsharpness. It improves contrast by reducing the production of scattered radiation, flattens out tissues resulting in a film of even density that will demonstrate

both anterior and posterior parts of the breast, and spreads out intramammary structures, allowing them to be visualized more easily. (Whitley et al. 2005)

2.5 Digital Mammography Machine

2.5.1 The Mammography Machine Units:

A mammography unit consists of an x-ray generator and control, U-arm, x-ray source assembly, collimator, compression device, breast support and grid assemblies, an image receptor— either screen-film or digital—and automatic exposure control (AEC) subsystem. A detailed diagram can be seen in Figure (3-1). (Whitman and Haygood 2012)

The U-arm can be raised or lowered via a motor drive and can be rotated clockwise and counterclockwise. The x-ray source assembly (x-ray tube, tube housing, and filters) is mounted to the top of the U-arm and covered with a shroud. The collimator is mounted directly below the source assembly and is also covered by the source assembly shroud. The compression device is built into the vertical section of the U-arm. A horizontal mounting plate for attaching the grid assemblies and magnification stand is located at the bottom. The AEC subsystem consists of an AEC sensor and associated electronics for SFM systems while for FFDM systems, the AEC system is built into the detector itself. Figure (2-14) shows the geometry of a mammography unit and the relative locations of the x-ray tube, x-ray target, the tube housing, tube port, x-ray tube filtration, collimator, compression paddle, patient breast, grid, and image receptor. (Hogg and Mercer 2015)

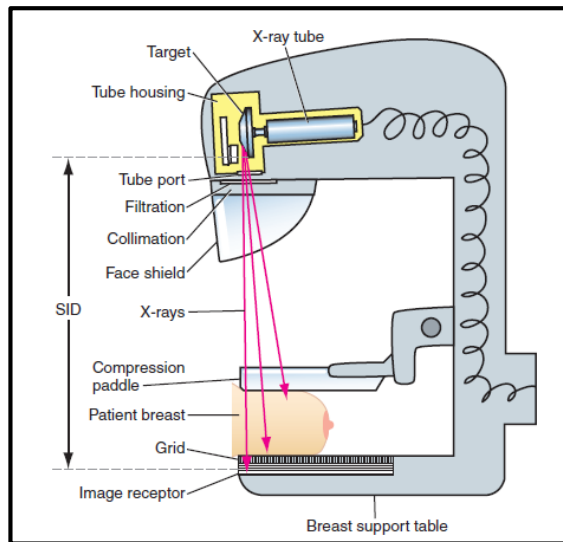


Fig: 2.14 The geometry of a mammography unit and the relative locations of the x-ray tube, x-ray target.

As illustrated in Figure (2-14), the x-ray tube focal spot or source is located directly above the chest wall edge of the image receptor. The geometry of the x-ray tube target is illustrated in Figure (2-15). A number of factors depend on the x-ray tube target angle: Heel effect (less radiation intensity on the anode side than on the cathode side along the x-ray tube axis); coverage (the cathode-anode field-of-view dimension before the radiation falls off to an unusable degree in the anode direction); and the effective or projected focal spot being smaller (in the tube axis direction) than the area of the target struck by high-speed electrons or line focus principle.

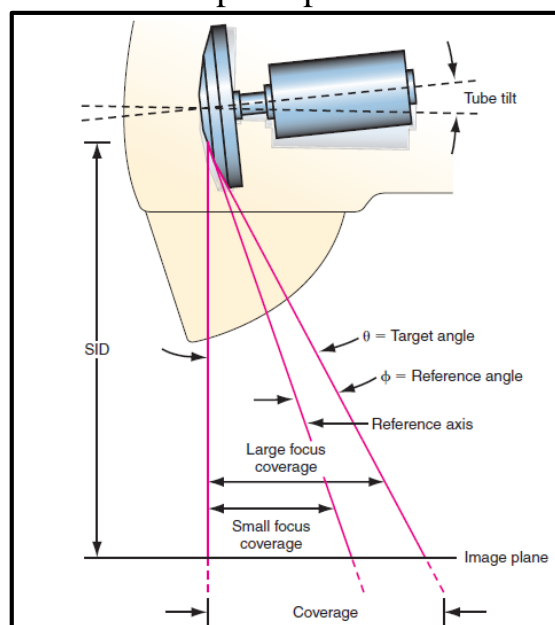


Fig: 2.15 Geometry of a mammography x-ray tube. Illustrated are the rotor and target, focal spot, target angle, reference angle and axis, source-to-image distance (SID), and coverage, or field of view (FOV). (Butler et al. 2017)

2.5.1.1 Acquisition Workstation

Digital mammography (FFDM) has an acquisition workstation (AW) which is the first place the mammography technologist will experience the difference between SFM and FFDM. The AW is where the technologist will interact with the FFDM unit to acquire and manage images (Fig. 2-16). The AW consists of a computer, computer monitor, keyboard, mouse or trackball, and software specific to the FFDM manufacturer. The technologist will use the AW to perform patient acquisitions starting with entering patient data manually or obtaining patient data from a radiology information system (RIS). Once the patient data is entered, the technologist will adjust technique parameters using the acquisition console (Fig. 2-17). The technologist can also select things such as image view, image laterality, and technologist ID. (Hogg and Mercer 2015)



Fig: 2.16 The acquisition workstation (AW) consisting of a computer, computer monitor, keyboard, mouse or trackball, and software specific to the full-field digital mammography (FFDM) manufacturer.



Fig: 2.17 The acquisition console

2.5.2.3 Review Workstation

At the end of the FFDM imaging chain the radiologist has a review workstation (RW) which usually houses a pair of high-resolution monitors where the digital mammography images are interpreted. A typical radiologist RW consists of two high-resolution 5-megapixel (MP) monitors and a single lower resolution 2-MP monitor (Fig. 3-18).

(Whitman and Haygood 2012)



Fig: 2.18

Review workstation (RW)

A typical RW consists of two high-resolution 5-megapixel (MP) monitors and a single lower resolution 2-MP monitor.

2.5.2.4 Image Receptor

2.5.2.4.1 Computed Radiography System

Computed radiography (CR) systems in digital mammography are similar to those used in conventional radiography. These detectors employ a

plastic sheet coated with a photostimulable phosphor material as the x-ray absorber. The phosphor plates are exposed to x-rays and an electronic charge is stored at the location of the absorbed x-ray. The charges are stored in “traps” and are proportional to the amount of incident x-rays. The image is read in a CR reader by a precision laser beam. During the scanning process a red laser beam discharges the traps causing stimulated emission of blue light that is collected by light guides that funnel the light into photomultiplier tubes (Fig. 2-19). The resulting signal from the photomultiplier tubes is logarithmically amplified, digitized, and processed for display (Hogg and Mercer 2015).

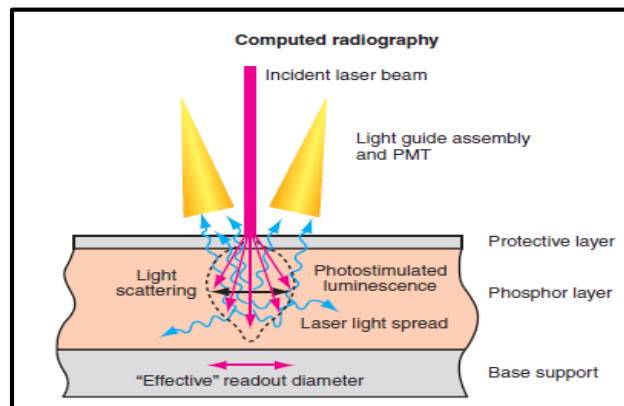


Fig: 2.19 Cross sectional view of a computed radiography imaging plate and readout schematic.

2.5.2.4.2 Digital Detectors

There are several different types of digital detectors being used in digital mammography. These include slot scanning with a scintillator and a charge-coupled device (CCD) array, a flat-panel scintillator and an amorphous silicon diode array, a flat-panel amorphous selenium array. These different detectors are described in the following section.

2.5.2.4.2.1 Slot-Scan Charge-Coupled Device System

The Slot-Scan CCD system used by Fischer Medical Imaging uses a long, narrow, rectangular detector that is approximately 1 cm × 24 cm. The detector is made from thallium activated cesium iodide (CsI) phosphor with fiber optic coupling to a CCD (Fig. 2-20).

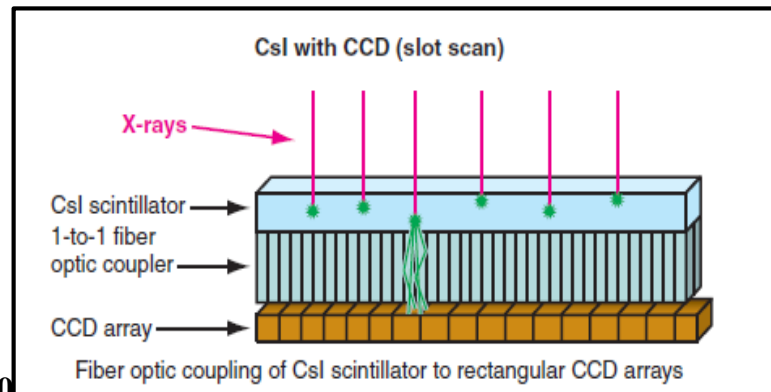


Fig: 2.20 Cross-sectional view of a cesium iodide (CsI) with charge-coupled device (CCD) slot-scan detector. X-rays pass through the CsI scintillator producing visible light.

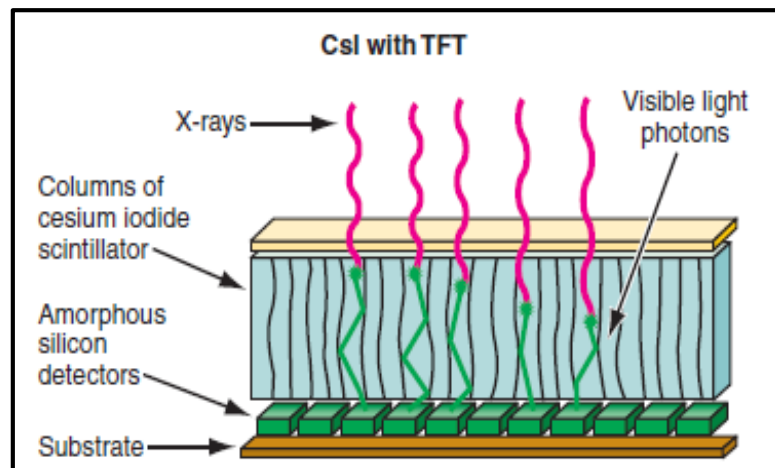


Fig: 2.21 Cross-sectional view of a cesium iodide (CsI) with thin film transistors (TFT) detector. *(Image courtesy of GE Medical Systems.)*

2.5.2.4.2.2 Flat-Panel Phosphor System

The flat-panel phosphor system uses a large area glass plate onto which a large two dimensional matrix of light sensitive diodes and thin film transistors (TFTs) have been deposited. On top of this, a layer of linear

columns of CsI crystals are deposited (Fig. 2-21). crystal. This property works to reduce lateral spread and allows the detector to be made thicker to provide high quantum efficiency.

2.5.2.4.2.3 *Selenium Flat-Panel System*

The Selenium flat-panel system is currently employed by both Hologic and Siemens Medical Systems for their FFDM systems. This detector design utilizes an x-ray absorber made of amorphous selenium (Fig. 2-22). (Butler et al. 2017)

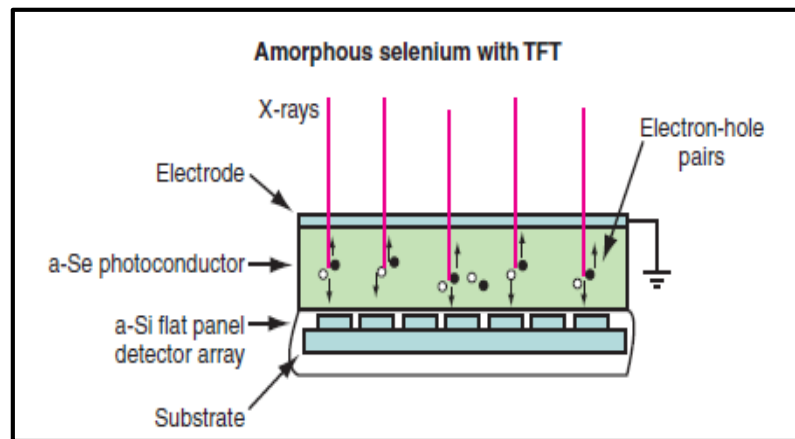


Fig: 2.22 Cross-sectional view of an amorphous selenium with thin film transistors (TFT) detector.

2.6 Technique of Mammography

2.6.1 Routine Projections

Routine projections, also sometimes referred to as departmental routines, are projections or positions that are commonly performed in most mammography departments. (Whitley et al. 2005)

2.6.1.1.1 Bilateral CC

Part Position (Fig. 2-22)

- IR height is determined by lifting the breast to achieve a 90° angle to the chest wall. The IR is at the level of the IMF at its upper limits. (The mammographer should always position from the patient's medial side to ensure that breast tissue is parallel to the IR. Positioning from the lateral aspect of the breast makes tasks more difficult.)
- The breast is pulled forward onto the IR centrally with the nipple in profile whenever possible.
- The arm on the side that is being imaged is relaxed at the side, and the shoulder is back out of the way.
- The head is turned away from the side being imaged (facing the technologist).

NOTE: The posterior nipple line (PNL) is used to evaluate the depth of breast tissue. The PNL is determined by drawing an imaginary line from the nipple to the pectoral muscle or edge of the image, whichever is the shorter distance. The PNL on CC projection (Fig. 2-23) should be within 1 cm of the PNL. (Whitley et al. 2005)

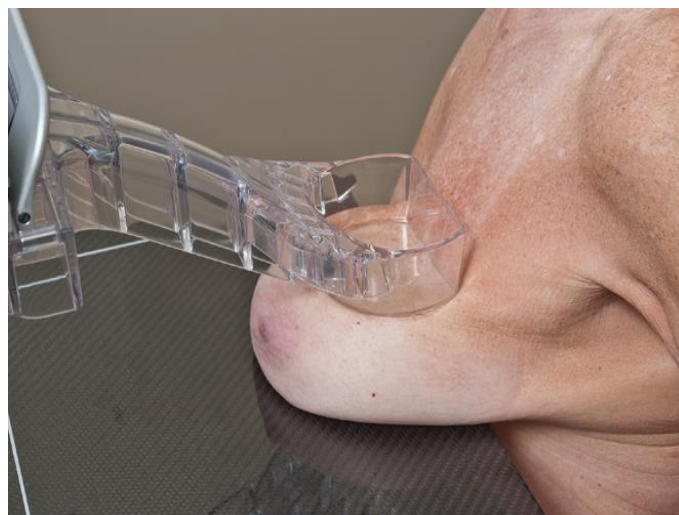


Fig: 2.23 Part position for CC projection. (Whitley et al. 2005)

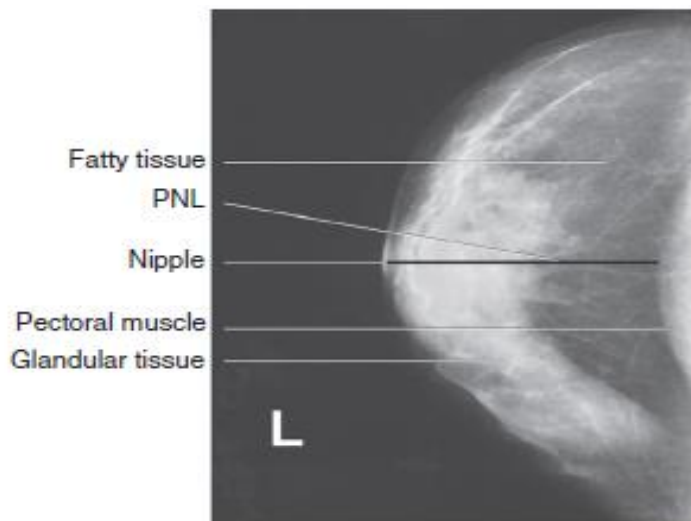


Fig: 2.24 CC projection. (Bontrager and Lampignano 2013)

2.6.1.1.2 Bilateral MLO

Part Position (Fig. 2-24)

- Tube and IR remain at right angles to each other; CR enters the breast medially, perpendicular to the patient's pectoral muscle.

Proper assessment as to the angle of the pectoral muscle on the patient's chest wall is a must if the image is going to demonstrate the maximum amount of breast tissue. This angle can be properly determined by the technologist using the extended palm along the lateral aspect of the breast and lifting it slightly away from the body and matching the angle of the palm.

- Adjust IR height so that top of IR is at the level of the axilla.
- With the patient facing the unit and feet forward exactly as in CC view, place the arm of the side being imaged forward and the hand on the bar toward the front.
- Pull breast tissue and pectoral muscle anteriorly and medially away from chest wall. Assess the angle of the pectoral muscle, and adjust the unit accordingly. Push the patient slightly toward the angled IR until the inferolateral aspect of the breast is touching the IR. The nipple should be in profile.

NOTE: To show *all* of the breast tissue on this projection with a large breast, two images may be needed, one positioned higher to get all of the axillary region and a second positioned lower to include the main part of the breast. (Fig. 2-25)



Fig: 2.25 Part position for MLO projection.
(Note x-ray tube/film unit is angled about 45°)
(Bontrager and Lampignano 2013)

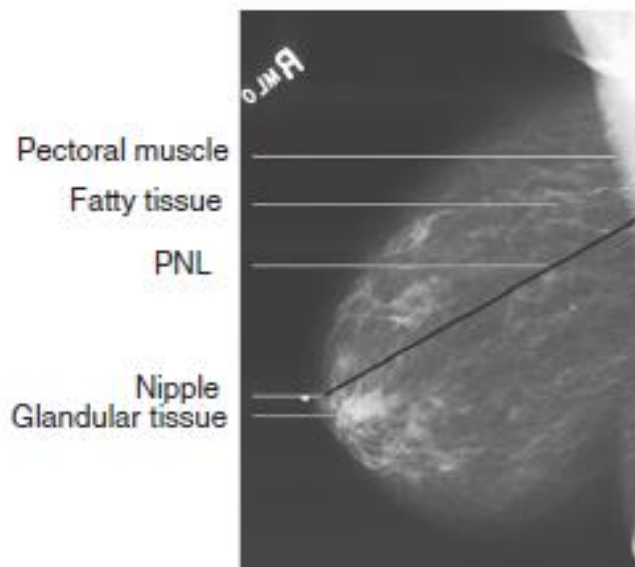


Fig: 2.26 **MLO projection.**
PNL should be within 1 cm of PNL of CC projection. (Modified from Ikeda DM: Breast imaging, St. Louis, 2005, Mosby.)

2.7 Interpretation of Mammography image

When interpreting a mammographic examination, three steps should be taken:

- Determine whether the image is of diagnostic quality in terms of positioning of the breast, image contrast, and spatial resolution. Poor-quality images or improper positioning often cause diagnostic errors.
- Perform a systematic, step-by-step survey of the mammograms to evaluate details of the breast structure while searching for a lesion.
- The systematic viewing should include side-by-side comparison of the corresponding regions of the right and left breasts.
- Carefully analyze each detected lesion. (Tabár and Dean 2012)
- First, place each lesion in to one of the five following classification groups:
 - I. Circular/oval lesions that may be solitary or multiple
 - II. Stellate/speculated lesions and architectural distortion
 - III. Calcifications that may or may not be associated with a tumor.
 - IV. Thickened skin syndrome: thickened skin in the dependent portion or most of the breast, associated with increased density and a reticular pattern on the mammogram
 - V. Any combination of two or more of the above findings.
- Second, after classification, each detected lesion should undergo detailed analysis. (Tabár and Dean 2012)

2.7.1 Circular/oval lesions

May be sharply or poorly outlined; circular, oval, or lobulated; solitary or multiple. If a circular/oval lesion is associated with calcifications, the lesion and the calcifications are analyzed separately. The two analyses are then combined. Contour and density analysis of circular/ oval lesions should rapidly lead to a benign or malignant mammographic diagnosis (Appleton and Wiele 2012).

2.7.1.1 Halo Sign or Capsule: Present or Absent

The halo sign is a narrow radiolucent ring (Mach band) or a segment of a ring around the periphery of a lesion characteristic of benign, growing circular/oval tumors. A capsule is a thin, curved, radiopaque line that is seen only when it surrounds lesions containing radiolucent material (fat as in a lipoma or fibroadenolipoma, and oil as in an oil cyst) (Conant and Brennecke 2006).

2.7.1.2 Density of the Circular/Oval Lesion

Density should be evaluated in relation to the surrounding parenchyma, or, in the case of fatty involution, to the nipple. The tumor, in comparison with the surrounding parenchyma, is either:

- Radiolucent
- Radiolucent and radiopaque combined
- Low-density radiopaque (equal to the surrounding parenchyma), or
- High-density radiopaque (greater than the surrounding parenchyma). (Tabár and Dean 2012)

2.7.2 Stellate/ Spiculated Lesions and Architectural Distortion

The majority of breast carcinomas have the mammographic appearance of a radiating structure, either a definite stellate/ spiculated lesion or architectural distortion with no central tumor mass. (Ikeda and Miyake 2017) Analysis of the central portion may show either a distinct mass or oval/circular radiolucent areas. Each is associated with its own characteristic surrounding radiating structure, resulting in one of two mammographic images that are diagnostic:

2.7.2.1 **White star:** sharp, dense, fine lines of variable length radiating in all directions from a distinct central tumor mass.(fig 2.27)

The spicules may reach the skin or muscle, causing retraction and localized skin thickening, which is often present in large or superficial invasive ductal carcinomas. (fig 2.28)

2.7.2.2 **Black star:** a radiating structure consisting of linear densities interspersed with linear radiolucencies; this picture, combined with the circular or oval radiolucent areas at the center, dominates the mammographic image black star. (fig 2.29) (Tabár and Dean 2012)

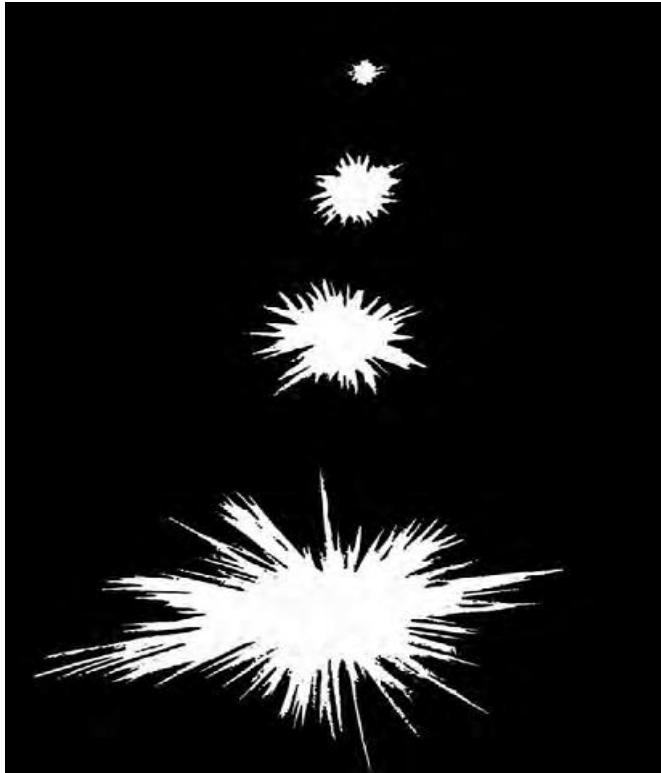


Fig (2.27) Diagrammatic illustration of invasive ductal carcinoma: the larger the central tumor mass, the longer the spicules (Salkowski 2013)

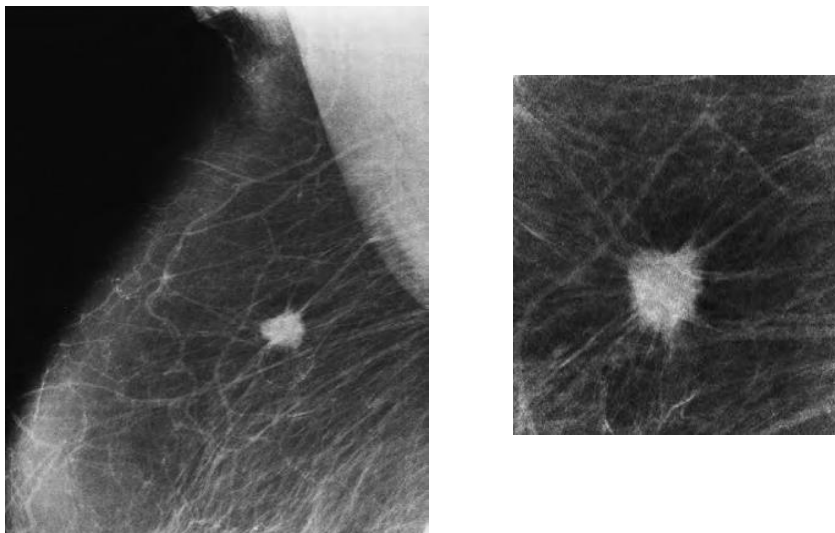


Fig. (2.28) demonstrate the characteristics of atypical malignant stellate tumor. (Tabár and Dean 2012)

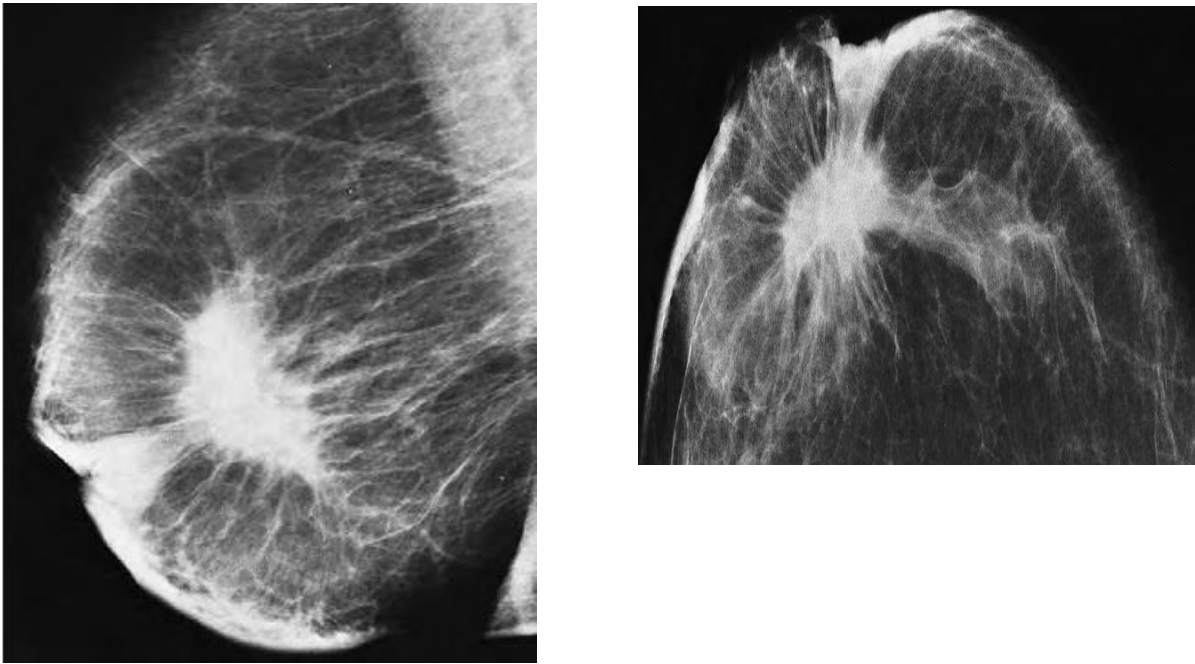


Fig. (2.29) a, b: Right breast, MLO and CC projections. Centrally located, large (5 cm diameter) stellate tumor. The nipple and areola are retracted. The skin is thickened and retracted over the lower and outer portions of the breast. (Tabár and Dean 2012)

2.7.3 Calcifications on the Mammogram

When analyzing calcifications on the mammogram, the goal is to determine the pathological process that has produced them. The analysis starts with determining the precise site of origin of the calcifications. If the calcifications arise within structures that do not contain breast epithelium (stroma, skin, blood vessels, scar tissue), then they are not malignant type, and are classified as miscellaneous-type calcifications. They are usually easily recognized, and their differential diagnosis presents few problems. Calcifications surrounding the ducts and within the arterial walls, sebaceous glands, oil cysts. The remaining calcifications are formed within the glandular tissue, that is, within anatomic cavities lined by epithelial cells (Terminal ductal lobular units/TDLUs or ducts). Analyzing the distribution of the calcifications on the mammogram will help to determine whether they are located within the TDLU(s) or within the ducts. Linear, fragmented, branching calcifications are located within dilated ducts. Individual or multiple clusters indicate that the pathological process takes place within the TDLUs.

Once the location of the calcifications has been determined, analysis of the form, size, and density of the individual calcifications will help in distinguishing benign from malignant-type calcifications through a closer understanding of the underlying processes producing them. Microfocus magnification mammography is often essential for this analysis, since it provides higher-resolution images. (Tabár and Dean 2012)

2.7.3.1 Form: Despite their wide variation in appearance, the malignant-type calcifications can be classified in to four basic forms:

2.7.3.1.1 **Casting type calcifications.** When high grade carcinoma in situ extensively fills in the ducts and their branches, the central portion of the lumen will contain necrotic cellular debris. Within this necrosis, amorphous calcifications are formed (Fig. 2.30) (Tabár and Dean 2012)

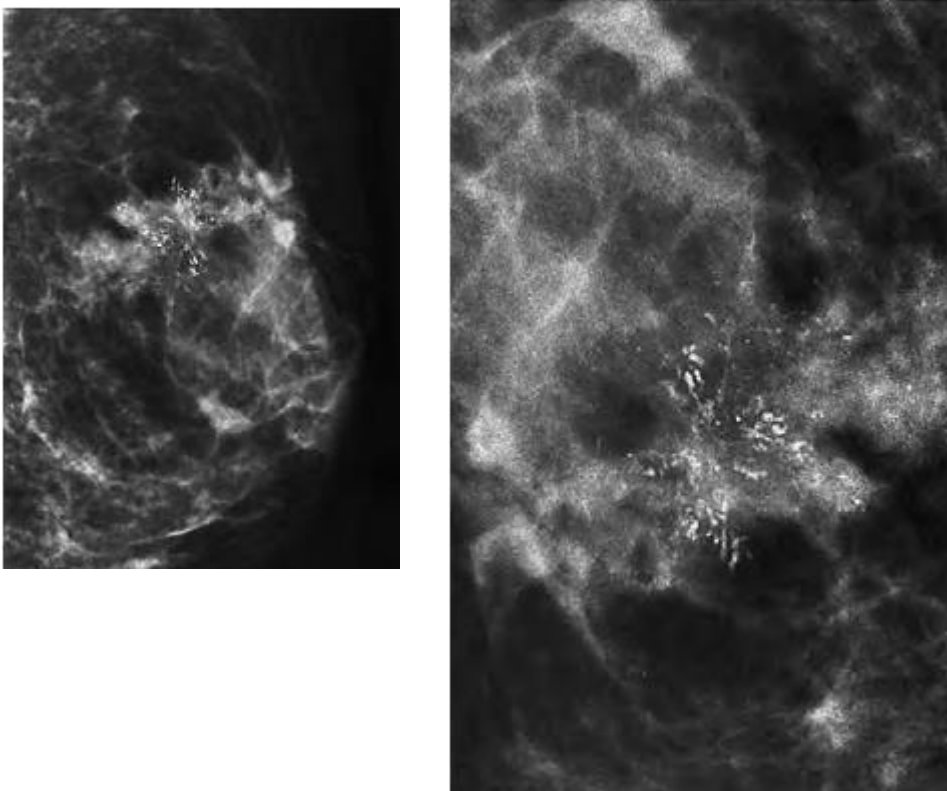


Fig. 2.30 (a): Detailed view of the MLO projection, left breast.(b): Enlarged view of the portion of the left breast containing the palpable tumor. There are numerous fragmented casting type

2.7.3.1.2 **Skipping stone-like calcifications in the ducts.** When the growth pattern of the malignant cells is micropapillary/

cribriform and the cancer cells produce proteinaceous fluid, filling the spherical, intra tumoral cavities of the cribriform cancer and distending the ducts containing the micropapillary growths, large, spheroid calcifications may be formed within the fluid. These flat, smooth contoured calcifications are reminiscent of skipping stones (fig. 2.31) (Tabár and Dean 2012)

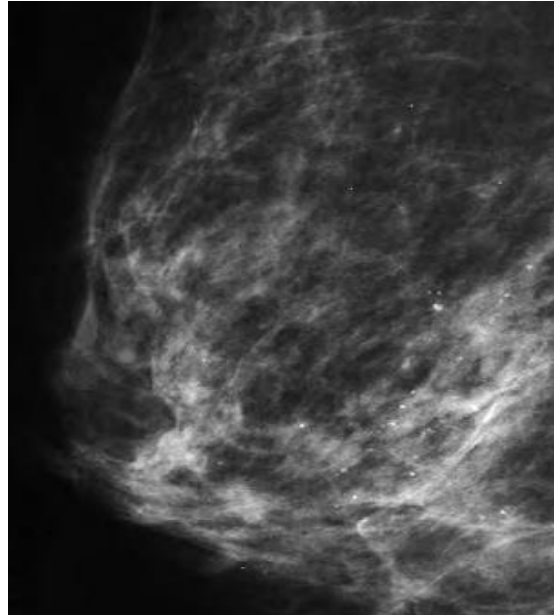


Fig. (2.31) Details of the MLO projection microfocus magnification. There are numerous dilated ducts in one lobe, containing scattered calcifications. (Tabár and Dean 2012)

2.7.3.1.3 Crushed stone-like/pleomorphic calcifications (BI-RADS: pleomorphic, heterogeneous). The individually discernible particles resemble crushed stones or Granulated sugar crystals. They are irregular in form, size, and density, and grouped very close together in single or multiple clusters. The malignant cells and the associated necrosis distend the acini within the TDLU. The amorphous calcifications are formed within this necrosis (fig. 2.32). (Tabár and Dean 2012)

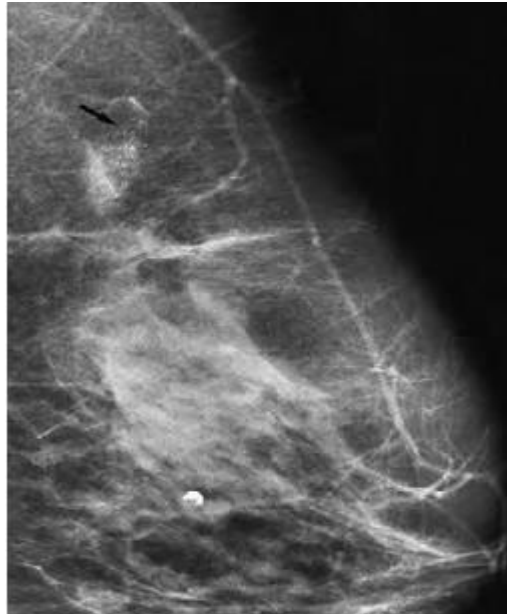


Fig. (2.32) Left breast, MLO projection. Two Clusters of microcalcifications are seen (arrow). In addition, a solitary, 4-mm eggshell-like calcification is seen in the central portion of the breast, mammographically benign. (Tabár and Dean 2012)

2.7.3.1.4 Powdery/cotton ball-like calcifications. Psammoma-body-like calcifications may be formed within the mucin secreted by grade 1 in situ carcinoma cells, which proliferate within the acini of the TDLUs. The calcium particles are far too small to be individually perceptible, but the summation of many of them can be seen on the mammogram as multiple clusters of powdery/cotton ball-like calcifications (fig. 2.33) (Tabár and Dean 2012)

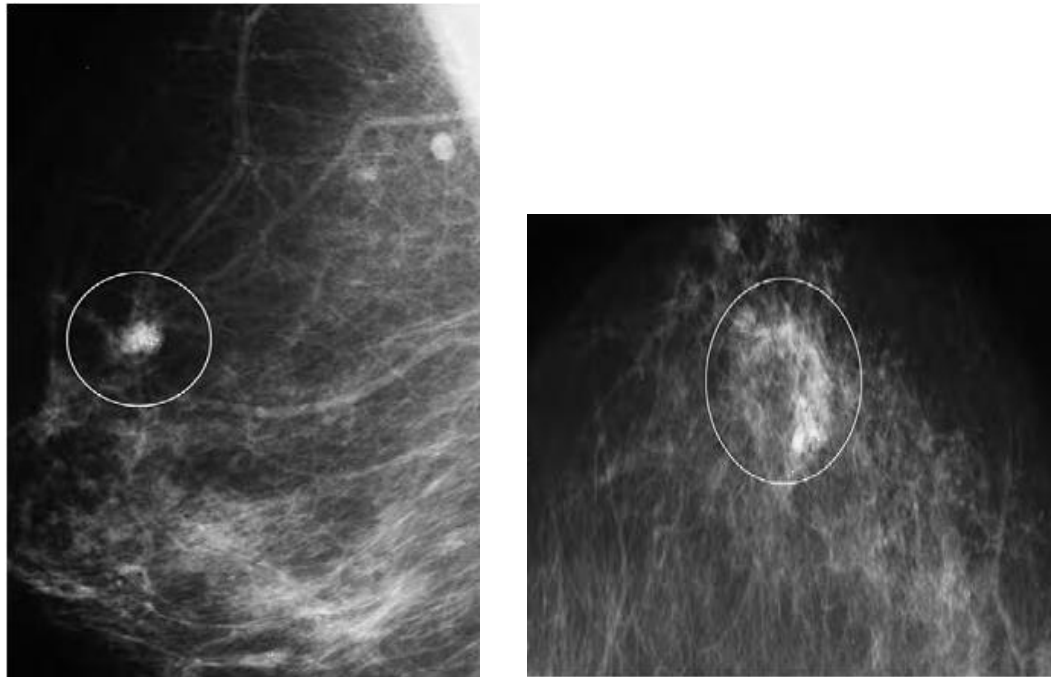


Fig. 2.33 a, b: Right LMO (a) and CC (b) projections. The de novo density associated with powdery calcifications is seen encircled.

2.7.4 Thickened Skin Syndrome of the Breast

This is a syndrome produced by lymphedema, usually secondary to obstruction of the axillary lymphatics (fig. 2.34). (B. E. Hashimoto 2010)

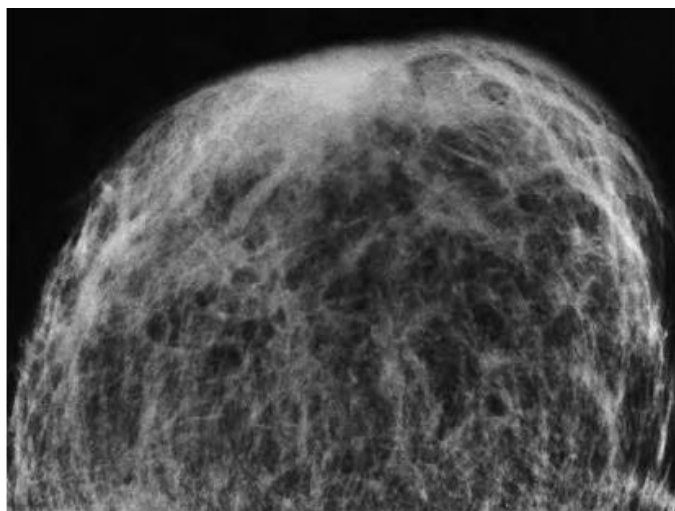


Fig. (2.34) Right breast, craniocaudal (CC) projection. Extreme skin thickening over the entire breast.

2.7.5 Overall Strategy

Perception of pathological lesions in the breast can be difficult, especially perception of stellate tumors. Superior image quality, optimal viewing conditions, and a systematic viewing technique are prerequisites for the perception of breast abnormalities. (Tabár and Dean 2012)

Analysis of the perceived lesions should be carefully performed as outlined. The strategy differs according to the type of the tumor.

- Circular/oval tumors: there is usually no perception problem. Careful analysis of the mammograms and frequent use of ancillary methods such as ultrasound and percutaneous needle biopsy can often make surgical biopsy unnecessary. The most frequent examples of this are cysts and fibroadenomas.
- Stellate lesions: the majority of breast carcinomas present as stellate tumors. Once found, 93% of stellate tumors will represent an invasive carcinoma; the remainder are radial scars, postsurgical scars or, rarely, ductal carcinoma in situ.

Radiological differential diagnosis can be highly accurate and important for directing further management. Finding these cancers at an early stage, when they are small (<10mm) may require considerable skill and experience in perception.

- Most calcifications in the breast represent benign processes. Since only 20% of consecutively biopsied clusters of calcifications represent malignant disease, detailed mammographic analysis of the calcifications and frequent use of stereotactic needle biopsy will help to avoid most unnecessary surgical biopsies.
- Thickened skin syndrome presents with a striking clinical and mammographic appearance. The underlying cause of this syndrome can be determined through a careful analysis of the clinical and mammographic findings. (Salkoweski 2013)

2.8 BI-RAD System

The ACR BI-RADS® is a quality assurance tool designed to standardize reporting, reduce confusion in breast imaging interpretations and management recommendations, and facilitate outcomes monitoring. Through a medical audit and outcomes monitoring, BI-RADS® provides important structure for collecting peer-review and quality assurance data that may improve the quality of patient care. (Sickles, CJ, and LW 2013)

2.8.1 Breast Imaging Lexicon — Mammography

The terminology used to describe mammographic findings has evolved over many years, and the diversity of this terminology may cause confusion. The descriptive terms and definitions that follow have been approved by the ACR Committee on BI-RADS®, and it is hoped that all those involved in breast imaging will adopt these terms and use them exclusively so that reports will be clear, concise, and standardized. (Sickles et al. 2013)

2.8.1.1 Masses

2.8.1.1.1 Shape

a. Oval:

An oval mass is elliptical or egg-shaped (may include two or three undulations). (Sickles et al. 2013)

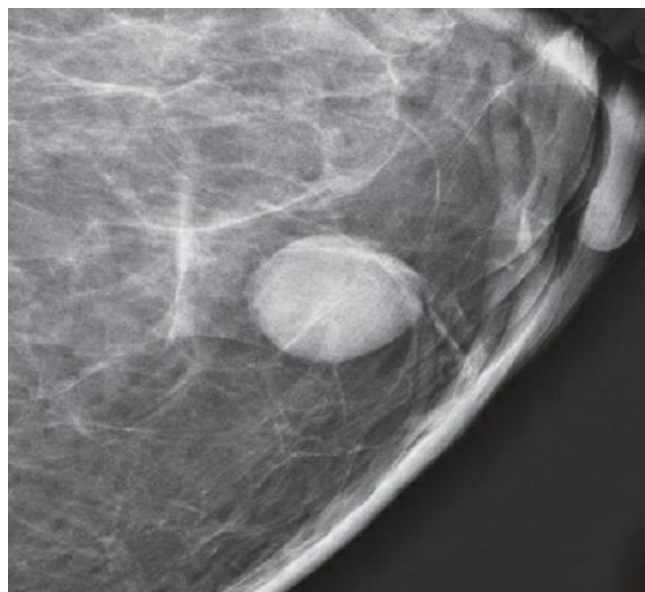


Fig 2.35 Shape: Oval, circumscribed mass (Bassett et al. 2010)

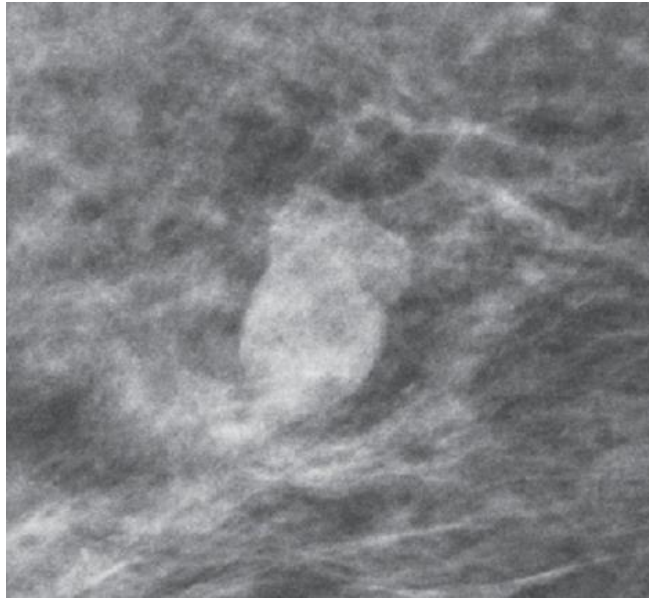


Fig 2.36 Shape: Oval, circumscribed mass with two undulations (Sickles et al. 2013)

b. Round

A round mass is spherical, ball-shaped, circular, or globular in shape.

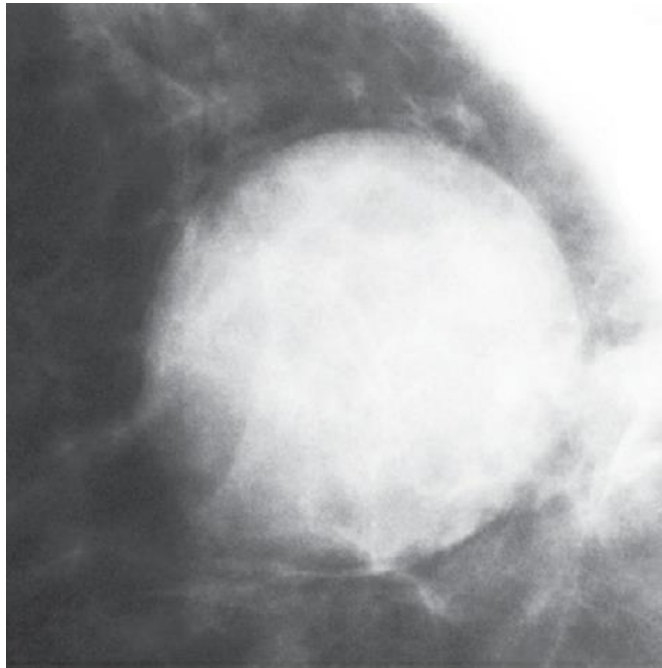


Fig 2.37 Shape: Round, circumscribed mass (Sickles et al. 2013)

c. Irregular

The shape of the mass is neither round nor oval. For mammography, use of this descriptor usually implies a suspicious finding. (Sickles et al. 2013)

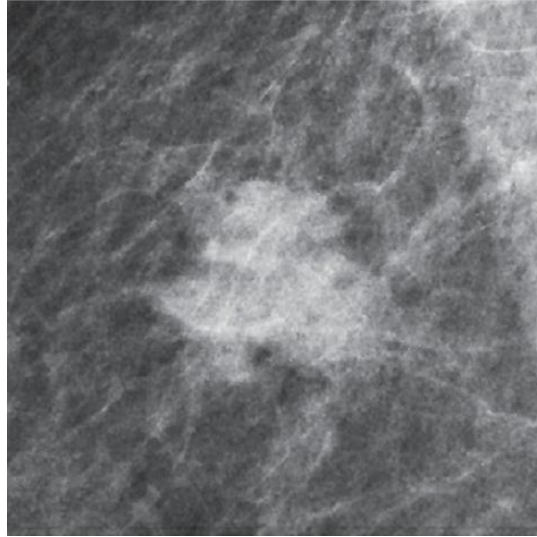


Fig 2.38 Shape: Irregular, Mass with primarily obscured margin.

2.8.1.1.2 Margin

- a. Circumscribed (historically, “well defined” or “sharply defined” The margin is sharply demarcated with an abrupt transition between the lesion and the surrounding tissue.

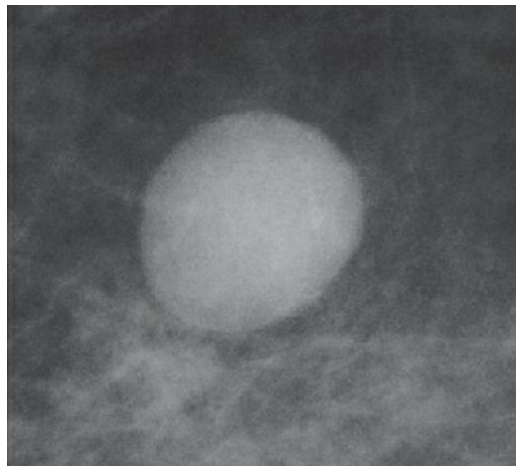


Fig. 2.39 Margin: Circumscribed Mass, Oval Circumscribed mass. (Sickles et al. 2013)

b. Obscured

An obscured margin is one that is hidden by superimposed or adjacent fibroglandular tissue. This is used primarily when some of the margin of the mass is circumscribed, but the rest (> 25%) is hidden.

(Sickles et al. 2013)

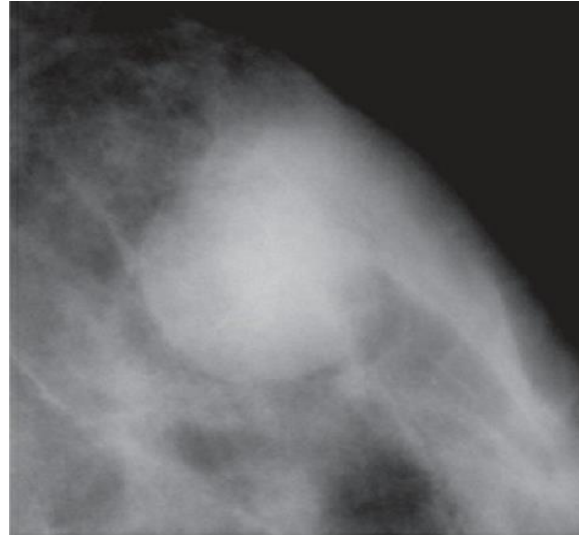


Fig. 2.40 Margin: Obscured. Oval mass (Conant and Brennecke 2006)

c. Microlobulated

The margin is characterized by short cycle undulations. For mammography, use of this descriptor usually implies a suspicious finding.

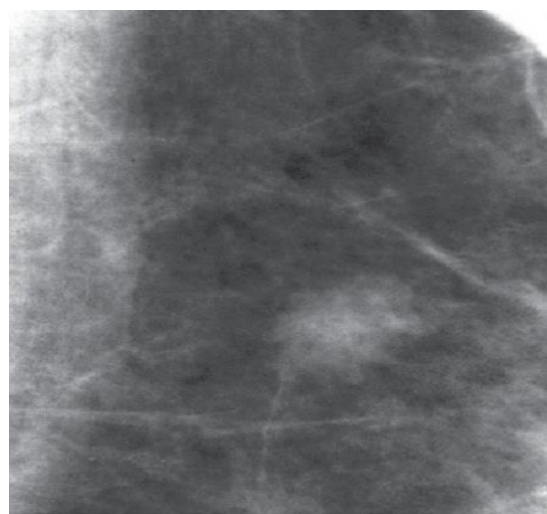


Fig. 2.41 Margin: Microlobulated. Irregular mass with Microlobulated margin.(Conant and Brennecke 2006)

d. Indistinct (historically, “ill defined”)

There is no clear demarcation of the entire margin, or of any portion of the margin, from the surrounding tissue. Use of this descriptor usually implies a suspicious finding. (Sickles et al. 2013)

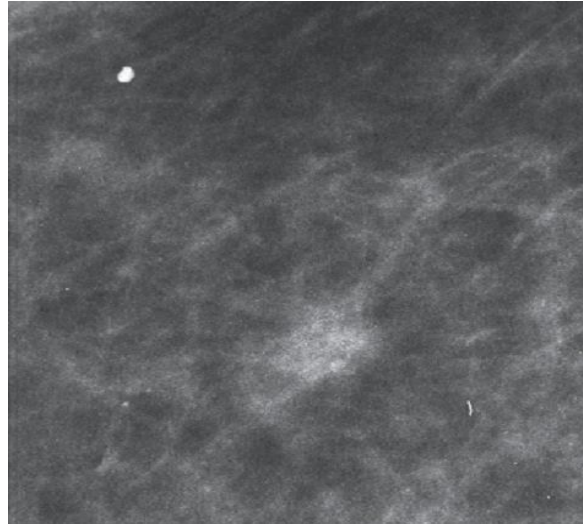


Fig. 2.42 Margin: Indistinct. Because it is difficult to determine the shape of mass. (Dronkers 2002)

e. Spiculated

The margin is characterized by lines radiating from the mass. Use of this descriptor usually implies a suspicious finding. (Sickles et al. 2013)

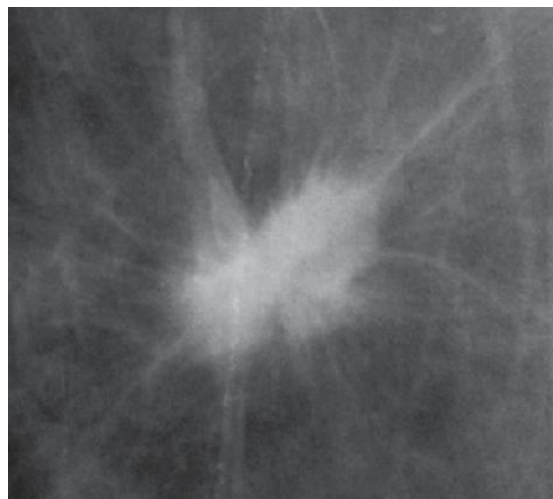


Fig. 2.43 Margin: Spiculated. Irregular Spiculated mass (Flowers and Holzhauer 2014)

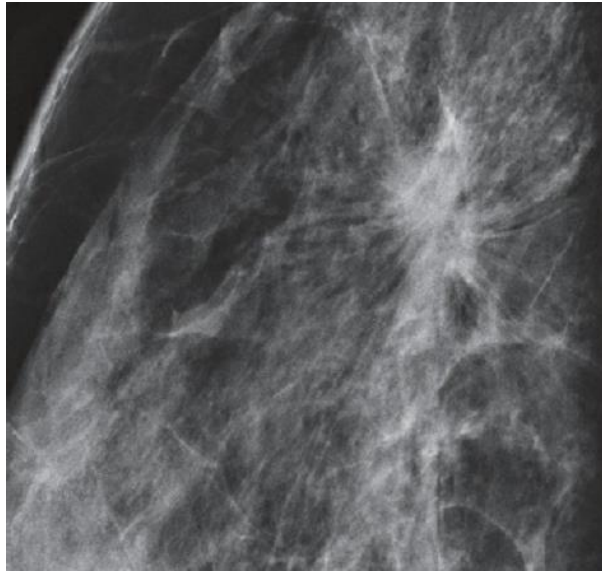


Fig. 2.44 Margin: Spiculated. Irregular Spiculated mas (B. E. Hashimoto 2010)

2.8.1.1.3 Density

This is used to define the x-ray attenuation of the mass relative to the expected attenuation of an equal volume of normal fibroglandular breast tissue.

a. High Density

X-ray attenuation of the mass is greater than the expected attenuation of an equal volume of fibroglandular breast tissue. (NG et al. 2013)

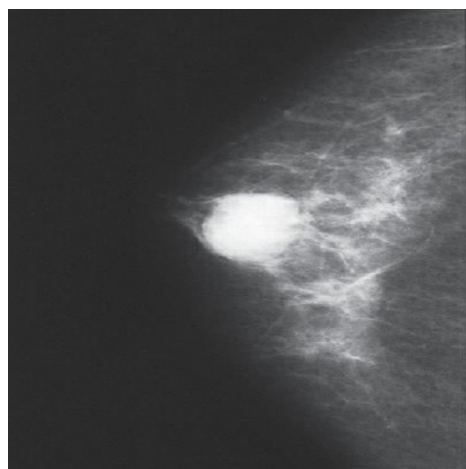


Fig. 2.45 Density: High Density. Oval, high density mass (Sickles et al. 2013)

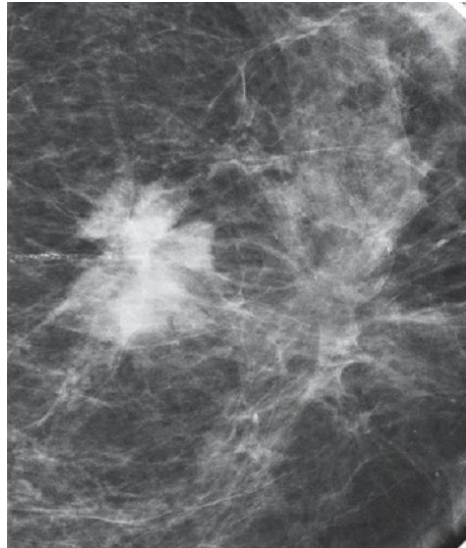


Fig. 2.46 Density: High Density. Irregular, spiculated high density mass (Sickles et al. 2013)

b. Equal Density (historically, “iso dense”)

X-ray attenuation of the mass is the same as the expected attenuation of an equal volume of fibroglandular breast tissue. (Sickles et al. 2013)

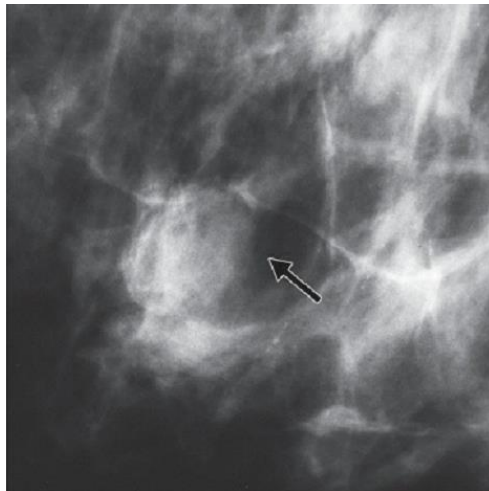


Fig. 2.47 Density: Equal Density. Oval Equal Density mass

c. Low Density

X-ray attenuation of the mass is less than the expected attenuation of an equal volume of fibroglandular breast tissue. A low-density mass may be a group of microcysts.

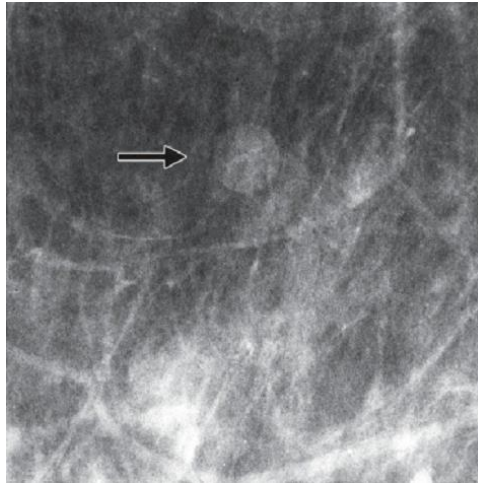


Fig. 2.48 Density: Low Density. Round, Low density mass

d. Fat-Containing

This includes all masses containing fat, such as oil cyst, lipoma, or galactocele, as well as mixed-density masses such as hamartoma. A fat-containing mass will almost always represent a benign mass.

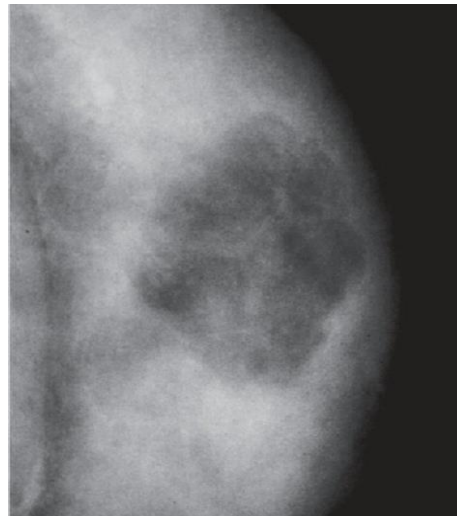


Fig. 2.49 Density: Fat-Containing. Irregular, Fat Containing mass

2.8.1.2 Calcifications

Calcifications that are assessed as benign at mammography are typically larger, coarser, round with smooth margins, and more easily seen than malignant calcifications.

Calcifications associated with malignancy (and many benign calcifications as well) are usually very small and often require the use of magnification to be seen well. When a specific, typically benign etiology cannot be assigned, a description of calcifications should include their morphology and distribution. (Sickles et al. 2013)

2.8.1.2.1 Typically Benign

a. Skin

These are usually lucent-centered and pathognomonic in their appearance. Skin calcifications are most commonly seen along the inframammary fold, parasternally, over lying the axilla, and around the areola. The individual calcific particles usually are tightly grouped, with individual groups < 5 mm in greatest dimension. (Sickles et al. 2013)



Fig. 2.50 Typically Benign: Skin. Tightly, grouped, lucent skin calcifications.

b. Vascular

These are parallel tracks, or linear tubular calcifications that are clearly associated with blood vessels. While most vascular calcification is not difficult to identify, if only a few discontinuous calcific particles are visible in a single location and if association with a tubular structure is questionable, then additional spot-compression magnification views may be needed to further characterize their nature. (Sickles et al. 2013)

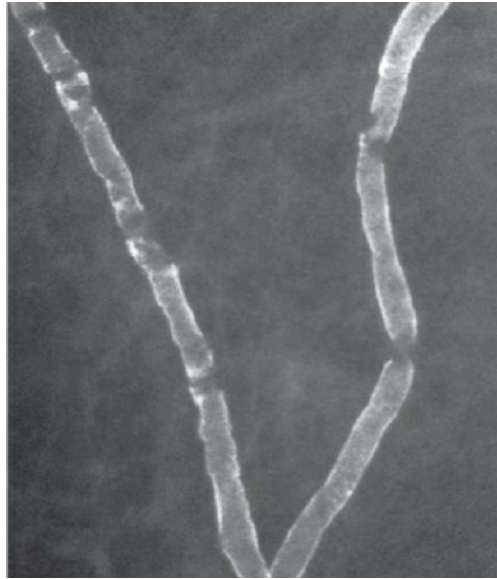


Fig. 2.51 Typically Benign: Vascular. Fully developed vascular calcifications (Appleton and Wiele 2012)

c. Coarse or “Popcorn -Like”

These calcifications are classic, large (>2–3 mm in greatest diameter), and produced by an involuting fibroadenoma.

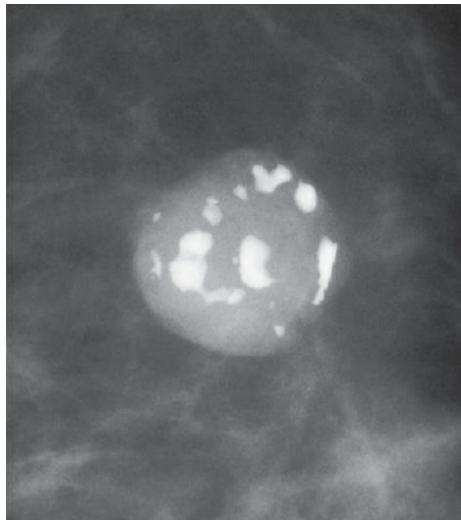


Fig. 2.52 Typically Benign: Coarse or Popcorn like calcifications (Appleton and Wiele 2012)

d. Large Rod-Like

These benign calcifications associated with ductal ectasia may form solid or discontinuous smooth linear rods, most of which are 0.5 mm or larger in diameter. A small percentage of these calcifications may have lucent centers if the calcium is in the wall of the duct (periductal), but most are

intraductal, when calcification forms with in the lumen of the duct. The calcifications usually are bilateral, although they may be seen in only one breast, especially when few calcific particles are visible. These calcifications usually are seen in women older than 60 years. (Sickles et al. 2013)

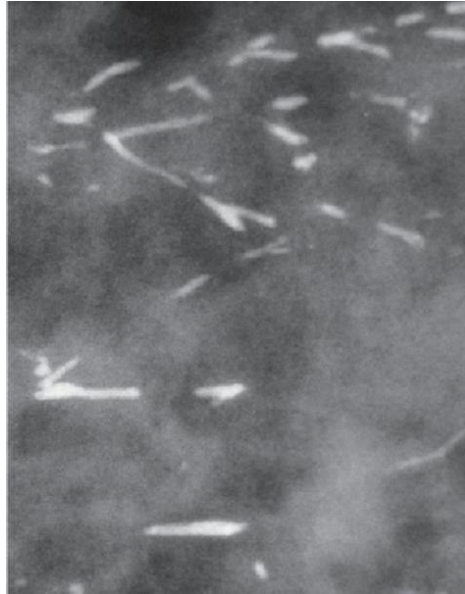


Fig. 2.53 Typically Benign: Large Rod-like Calcifications

e. Round (Punctate is a subset of Round)

When multiple, they may vary in size, and therefore in opacity. They may be considered benign when diffuse and small (< 1 mm), and are frequently formed in the acini of lobules. When smaller than 0.5 mm, the term “punctate” should be used.

An isolated group of punctate calcifications may warrant probably benign assessment and mammographic surveillance if no prior examinations are available for comparison, or image -guided biopsy if the group is new, increasing, linear, or segmental in distribution, or if adjacent to a known cancer. (Sickles et al. 2013)

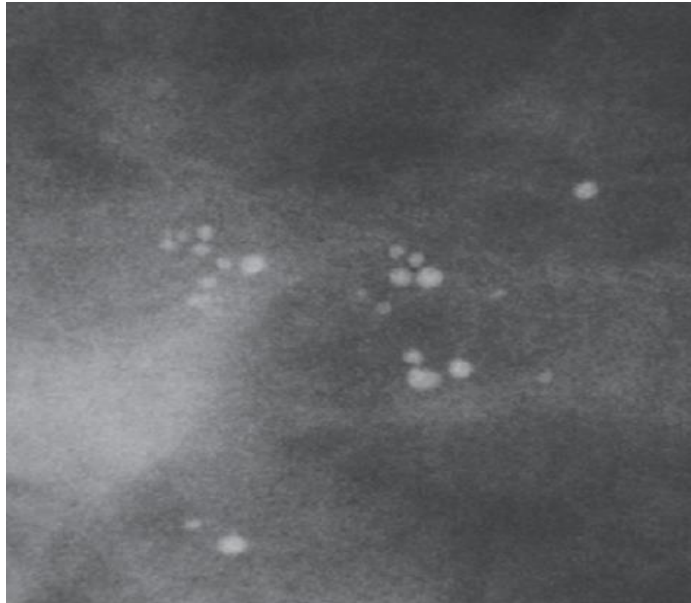


Fig. 2.54 Typically Benign: Round. Regional round calcifications (Appleton and Wiele 2012)

f. Rim (historically, “egg shell”, “lucent-centered”)

These are thin benign calcifications that appear as calcium deposited on the surface of a sphere. The calcific deposits are usually less than 1 mm in thickness when viewed on edge. Fat necrosis and calcifications in the walls of cysts are the most common rim calcifications, although more extensive (and occasionally thicker- rimmed) calcifications in the walls of oil cysts or simple cysts may be seen. (Sickles et al. 2013)

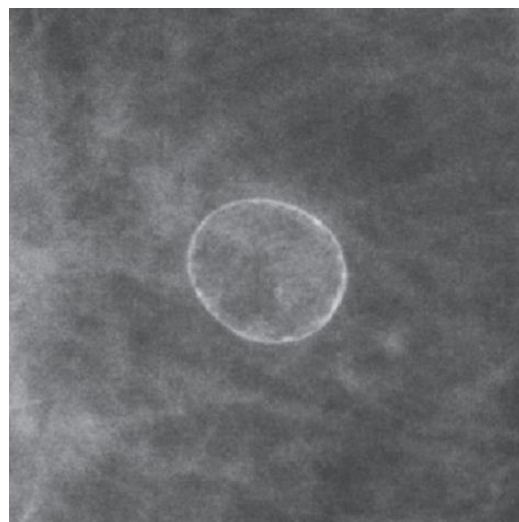


Fig. 2.55 Typically Benign: Rim. Rim Calcifications (Flowers and Holzhauser 2014)

g. Dystrophic

These typically form in the irradiated breast or in the breast following trauma or surgery. The calcifications are irregular in shape, and they are usually > 1 mm in size. They often have lucent centers. (Sickles et al. 2013)



Fig. 2.56 Typically Benign: Dystrophic. Dystrophic Calcification, at the site of previous surgical excision marked by several metallic clips. (Bassett et al. 2010)

h. Milk of Calcium

This is a manifestation of sedimented calcifications in macro- or microcysts, usually but not always grouped. On the craniocaudal image they are often less evident and appear as round, smudgy deposits, while occasionally on MLO and especially on 90° lateral (LM/ML) views, they are more clearly defined and often semilunar, crescent shaped, curvilinear (concave up), or linear, defining the dependent portion of cysts. (Sickles et al. 2013)

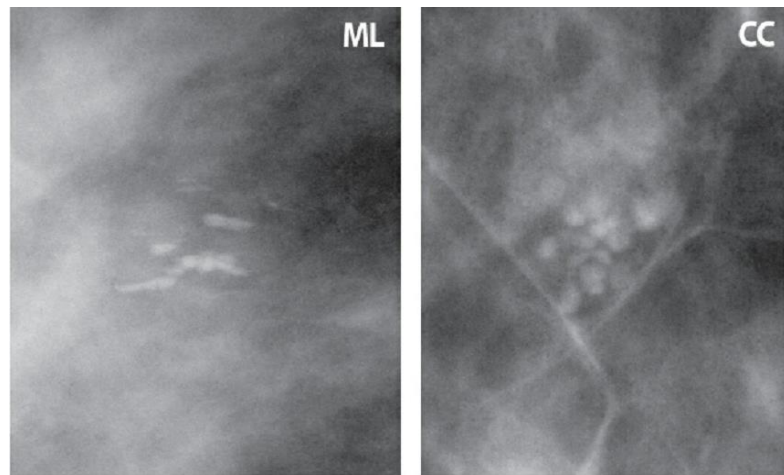


Fig. 2.57 Typically Benign: Milk of Calcium. Grouped milk of calcium the calcifications appear smudgy on CC, linear and crescent shaped on MLO. (Sickles et al. 2013)

i. Suture

These represent calcium deposited on suture material. They are typically linear or tubular in appearance and, when present, knots are frequently visible. (Sickles et al. 2013)

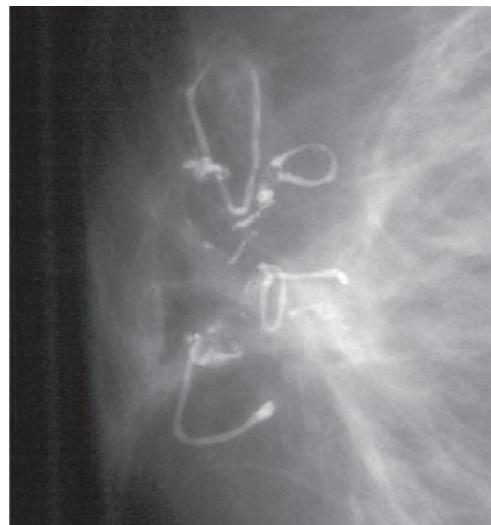


Fig. 2.58 Typically Benign: Suture. Suture Calcifications (Dronkers 2002)

2.8.1.2.2 Suspicious Morphology

Classification of breast calcifications by morphology is useful in predicting the likelihood of malignancy. There are four descriptors of calcification morphology that usually indicate sufficient suspicion of malignancy to prompt a recommendation for biopsy.

a. Amorphous (historically, “indistinct”)

These are so small and/or hazy in appearance that a more specific particle shape cannot be determined. Amorphous calcifications in a grouped, linear, or segmental distribution are suspicious and generally warrant biopsy. Bilateral, diffuse, amorphous calcifications usually may be dismissed as benign, although baseline magnification views may be helpful. The positive predictive value (PPV) of amorphous calcifications is reported to be approximately 20%.

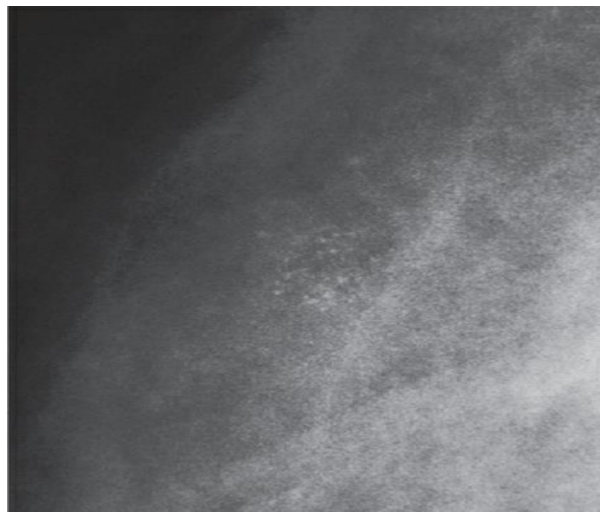


Fig. 2.59 Suspicious Morphology: Amorphous. Grouped Amorphous calcifications (Flowers and Holzhauser 2014)

b. Coarse Heterogeneous

These are irregular, conspicuous calcifications that are generally between 0.5 mm and 1 mm and tend to coalesce, but are smaller than dystrophic calcifications. They may be associated with malignancy, but more frequently are present in a fibroadenoma, or in areas of fibrosis, or trauma representing evolving dystrophic calcifications. Numerous bilateral groups of coarse heterogeneous calcifications usually may be dismissed as benign, although base line magnification views may be helpful. However, a single group of coarse heterogeneous calcifications has a positive predictive value of slightly less than 15%. (Sickles et al. 2013)

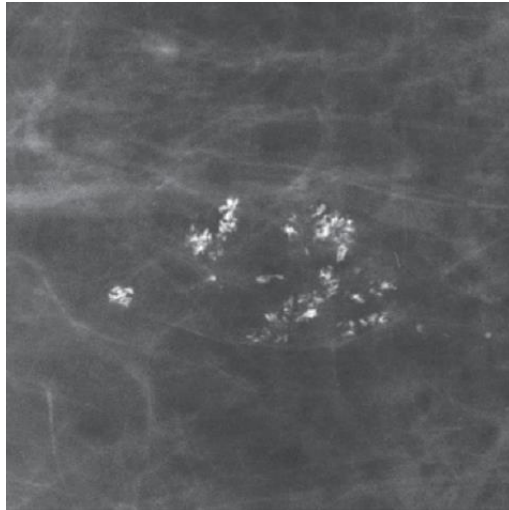


Fig. 2.60 Suspicious Morphology: Coarse Heterogeneous. Grouped of Coarse Heterogeneous Calcifications (Bassett et al. 2010)

c. Fine Pleomorphic

These calcifications are usually more conspicuous than amorphous forms and are seen to have discrete shapes. These irregular calcifications are distinguished from fine linear and fine -linear branching forms by the absence of fine- linear particles. Fine pleomorphic calcifications vary in size and shape and are usually < 0.5 mm in diameter. They have a somewhat higher PPV for malignancy (29%) than amorphous or coarse heterogeneous calcifications. (Sickles et al. 2013)

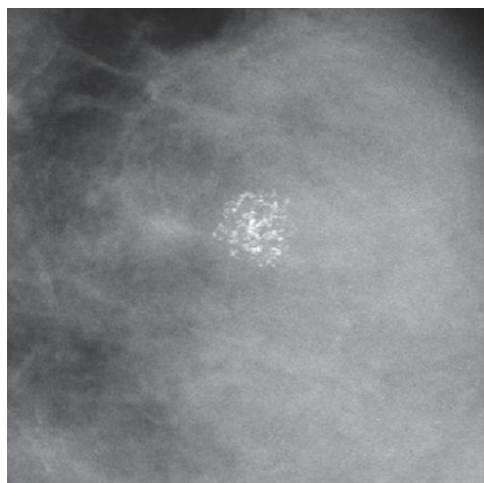


Fig. 2.61 Suspicious Morphology: Fine Pleomorphic. Grouped Fine Pleomorphic Calcifications (Flowers and Holzhauser 2014)

d. Fine Linear or Fine -Linear Branching

These are thin, linear, irregular calcifications, which may be discontinuous and which are < 0.5 mm in caliber. Occasionally, branching forms may be seen. Their appearance suggests filling of the lumen of a duct or ducts involved irregularly by breast cancer. Among the suspicious calcifications, fine linear and fine-linear branching calcifications have the highest PPV (70%). (Flowers and Holzhauser 2014)

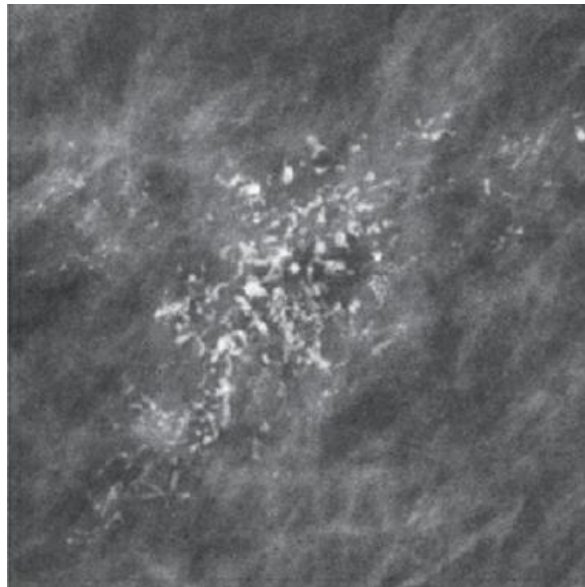


Fig. 2.62 Suspicious Morphology: Fine Linear or Fine – Linear Branching. Regional Fine Linear Calcifications. (Flowers and Holzhauser 2014)

2.8.1.2.3 Distribution

These descriptors are used to indicate the arrangement of calcifications in the breast. Multiple similar groups may be described in the report when there is more than one group of calcifications that are similar in morphology and distribution. In evaluating the likelihood of malignancy for calcifications, distribution is at least as important as morphology.

a. Diffuse (historically, “scattered”)

These are calcifications that are distributed randomly throughout the breast. Punctate and amorphous calcifications in this distribution are almost always benign, especially if they are bilateral. (Sickles et al. 2013)

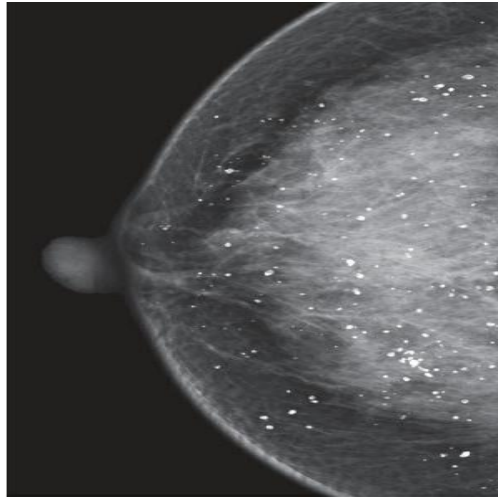


Fig. 2.63 Distribution: Diffuse. Diffuse, primarily round calcifications. (Conant and Brennecke 2006)

b. Regional

This descriptor is used for numerous calcifications that occupy a large portion of breast tissue (> 2 cm in greatest dimension). (Sickles et al. 2013)

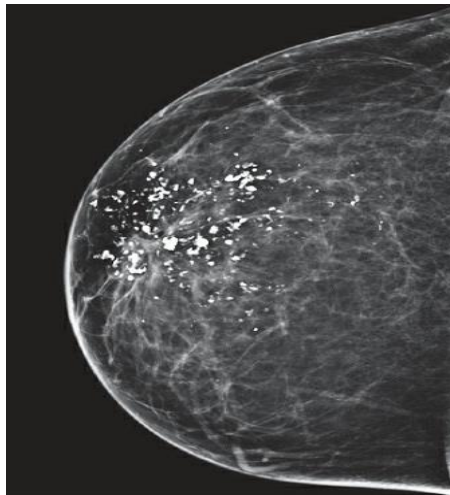


Fig. 2.64 Distribution: Regional. Regional, dystrophic Calcifications (Conant and Brennecke 2006)

c. Grouped (historically, “clustered”)

This term should be used when relatively few calcifications occupy a small portion of breast tissue. The lower limit for use of this descriptor is usually when five calcifications are grouped within 1 cm of each other or when a definable pattern is identified. (Sickles et al. 2013)

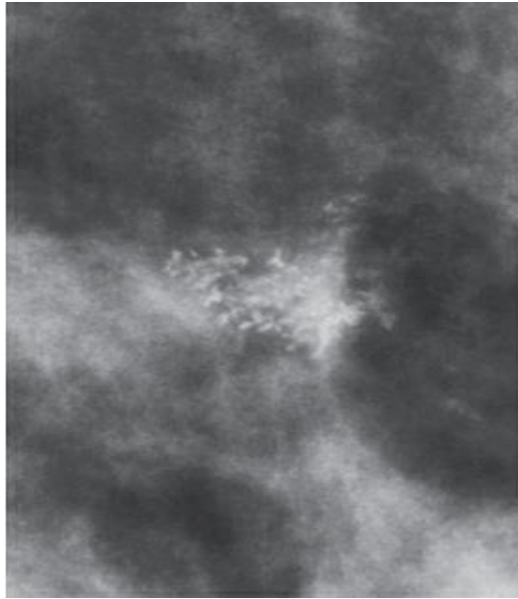


Fig. 2.65 Distribution: Grouped. Grouped, fine, pleomorphic Calcifications (D'Orsi 2013)

d. Linear

These are calcifications arrayed in a line. This distribution may elevate suspicion for malignancy, as it suggests deposits in a duct. Note that both vascular and large rodlike calcifications also are usually linear in distribution, but that these typically benign calcifications have a characteristically benign morphology.

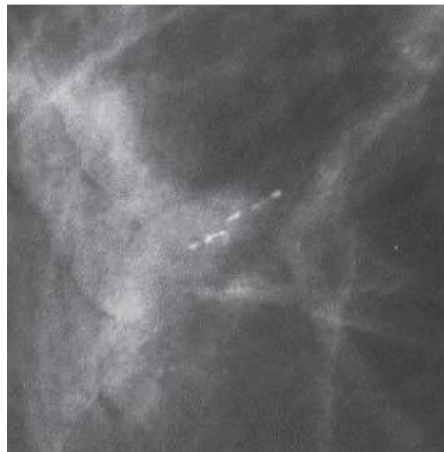


Fig. 2.66 Distribution: Linear. Linear, fine calcifications (D'Orsi 2013)

e. Segmental

Calcifications in a segmental distribution are of concern because they suggest deposits in a duct or ducts and their branches, which raises the

possibility of extensive or multifocal breast cancer in a lobe or segment of the breast. (D'Orsi 2013)



Fig. 2.67 Distribution: segmental. Segmental fine linear calcifications (D'Orsi 2013)

2.8.1.3 Architectural Distortion

The parenchyma is distorted with no definite mass visible. For mammography, this includes thin straight lines or spiculations radiating from a point, and focal retraction, distortion, or straightening at the anterior or posterior edge of the parenchyma. Architectural distortion may also be associated with asymmetry or calcifications. In the absence of appropriate history of trauma or surgery, architectural distortion is suspicious. For malignancy or radial scar, and tissue diagnosis is appropriate.

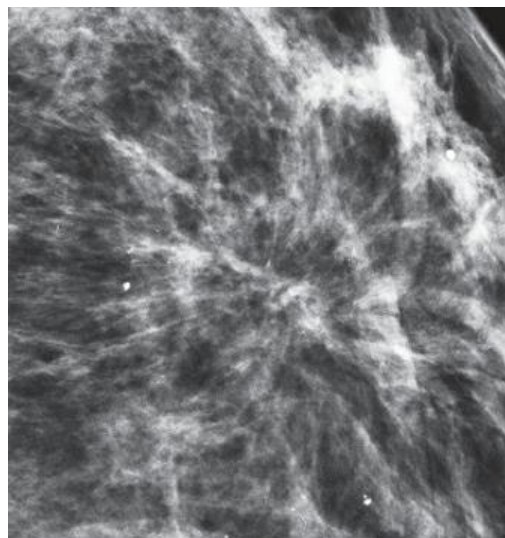


Fig. 2.68 Architectural distortion. Manifested by thin radiating lines with fatty tissue at the point of origin.

2.8.1.4 Asymmetries

The several types of asymmetry involve a spectrum of mammographic findings that represent unilateral deposits of fibroglandular tissue not conforming to the definition of a radiodense mass. The asymmetry, unlike a mass, is visible on only one mammographic projection. (D’Orsi 2013)

2.8.1.4.1 Asymmetry

This is an area of fibroglandular-density tissue that is visible on only one mammographic projection. Most such findings represent summation artifacts, a superimposition of normal breast structures, whereas those confirmed to be real lesions (by subsequent demonstration on at least one more projection) may represent one of the other types of asymmetry or a mass.

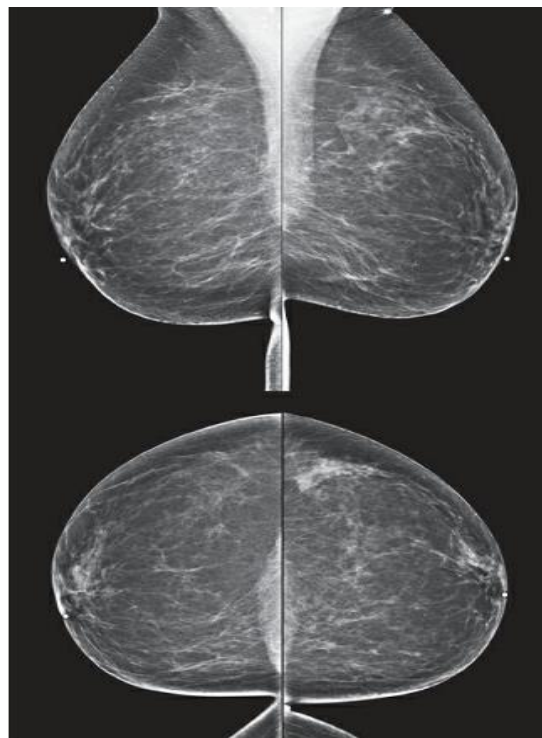


Fig. 2.69 Asymmetry. Note the asymmetric area of dense tissue in the lateral aspect of the left breast seen only on the CC. (Conant and Brennecke 2006)

2.8.1.4.2 Global Asymmetry

Global asymmetry is judged relative to the corresponding area in the contralateral breast and represents a large amount of fibroglandular-density tissue over a substantial portion of the breast (at least one quadrant). Global asymmetry usually represents a normal variant. (D'Orsi 2013)

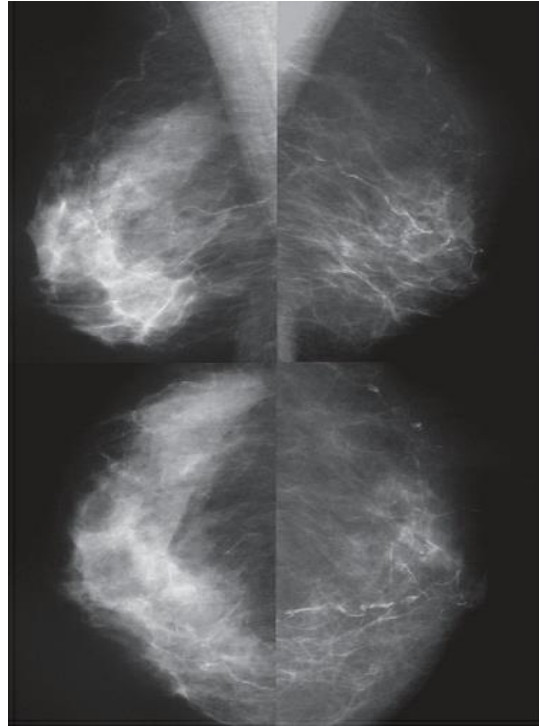


Fig. 2.70 Global asymmetry. (D'Orsi 2013)

2.8.1.4.3 Focal Asymmetry

A focal asymmetry is judged relative to the corresponding location in the contralateral breast, and represents a relatively small amount of fibroglandular-density tissue over a confined portion of the breast (less than one quadrant). (D'Orsi 2013)

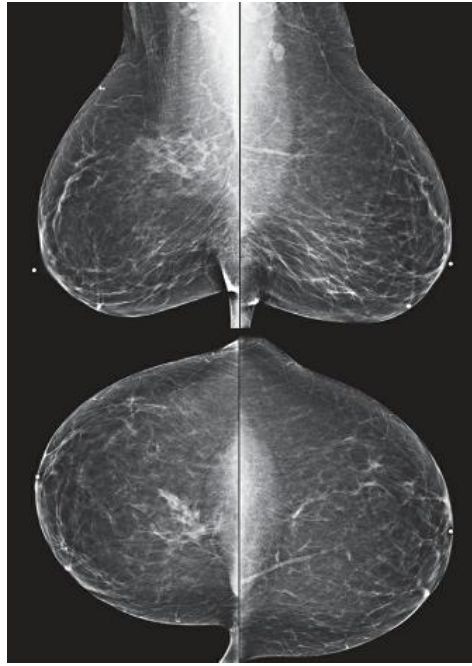


Fig. 2.71 Focal Asymmetry. The Asymmetric dense tissue occupies less than the entire upper inner quadrant of the right breast. (Conant and Brennecke 2006)

2.8.1.4.4 Developing Asymmetry

This is a focal asymmetry that is new, larger, or more conspicuous than on a previous examination. Approximately 15% of cases of developing asymmetry are found to be malignant. (D’Orsi 2013)

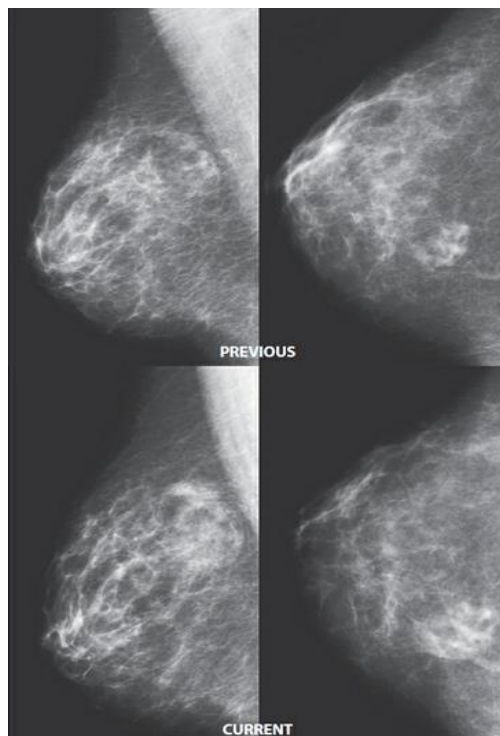


Fig. 2.72 Developing Asymmetry. The asymmetric dense tissue in the upper inner quadrant of the right breast is larger on current examination than on the previous examination. (Ikeda and Miyake 2017)

2.8.1.5 Intramammary Lymph Node

Intramammary lymph nodes are circumscribed masses that are reniform and have hilar fat. They are generally ≤ 1 cm. They may be > 1 cm and characterized as normal when fat replacement is pronounced. They frequently occur in the lateral and usually upper portions of the breast closer to the axilla, although they may occur anywhere in the breast. They often are seen adjacent to a vein, because the lymphatic drainage of the breast parallels the venous drainage. (D'Orsi 2013)

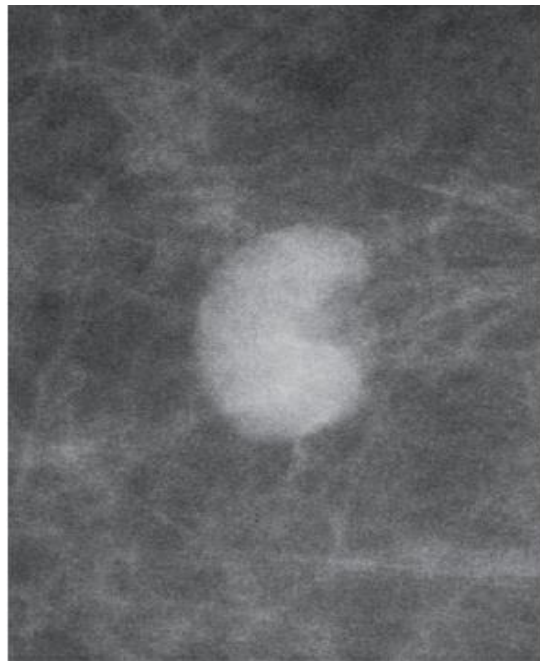


Fig. 2.73 Intramammary Lymph Node. (Ikeda and Miyake 2017)

2.8.1.6 Skin Lesion

This finding may be described in the mammography report or annotated on the mammographic image when it projects over the breast (especially on two different projections), and may be mistaken for an intramammary lesion. (D'Orsi 2013)

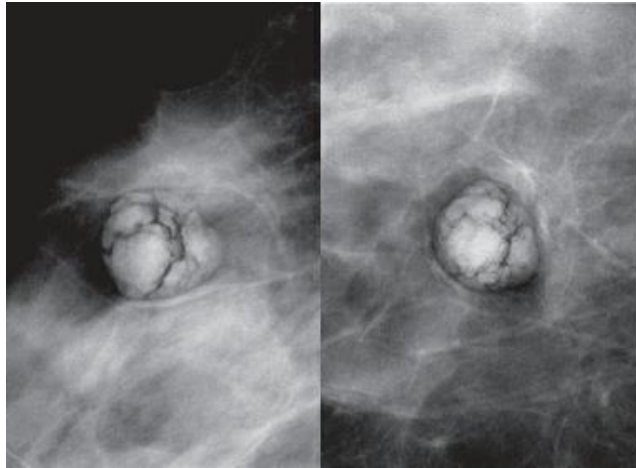


Fig. 2.74 Skin Lesion. Raised skin lesion, air trapped around the skin lesion (Conant and Brennecke 2006)

2.8.1.7 Solitary Dilated Duct

This is a unilateral tubular or branching structure that likely represents a dilated or otherwise enlarged duct. It is a rare finding. Even if unassociated with other suspicious clinical or mammographic findings, it has been reported to be associated with noncalcified DCIS. (D’Orsi 2013)

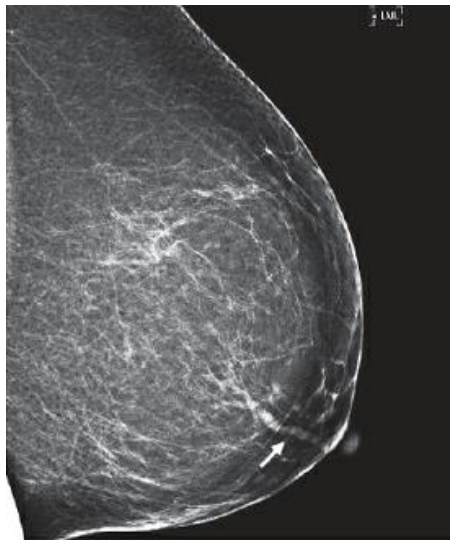


Fig. 2.75 Solitary Dilated Duct. (Dronkers 2002)

2.8.1.8 Associated Features

Used with masses, asymmetries, or calcifications or may stand alone as findings when no other abnormality is present.

2.8.1.8.1 Skin Retraction

The skin is pulled in abnormally.

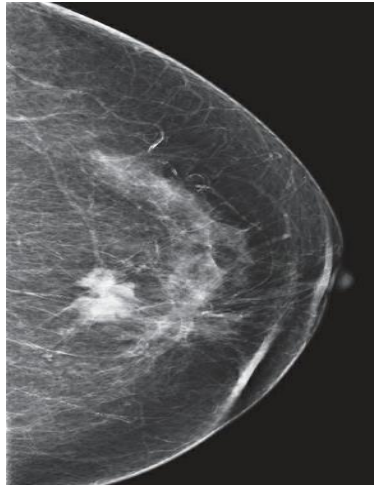


Fig. 2.76 Skin Retraction. Note the double skin line (indicate skin retraction) (D'Orsi 2013)

2.8.1.8.2 Nipple Retraction

The nipple is pulled in. This should not be confused with nipple inversion, which is often bilateral and which in the absence of any suspicious findings and when stable for a long period of time, is not a sign of malignancy. However, if nipple retraction is new, suspicion for underlying malignancy is increased. (D'Orsi 2013)

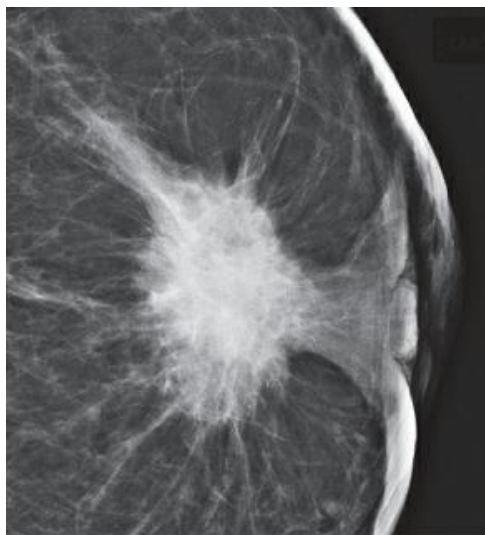


Fig. 2.77 Nipple Retraction. Adjacent to a spiculated high-density mass (Sickles et al. 2013)

2.8.1.8.3 Skin Thickening

Skin thickening may be focal or diffuse, and is defined as being greater than 2 mm in thickness. (D'Orsi 2013)

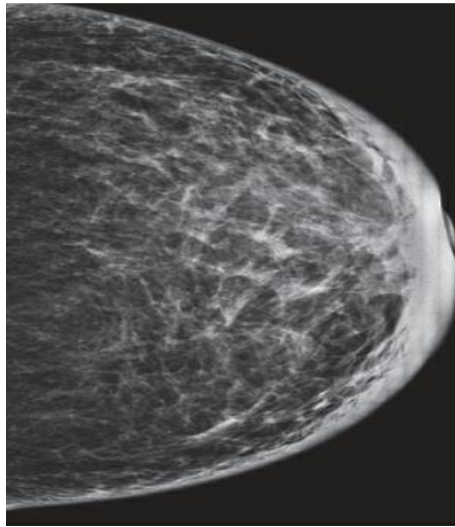


Fig. 2.78 Skin Thickening. Diffuse skin thickening. (D'Orsi 2013)

2.8.1.8.4 Trabecular Thickening

This is a thickening of the fibrous septa of the breast.

2.8.1.8.5 Axillary Adenopathy

Enlarged axillary lymph nodes may warrant comment, clinical correlation, and additional evaluation, especially if they are new or considerably larger or rounder when compared to previous examination. (D'Orsi 2013)

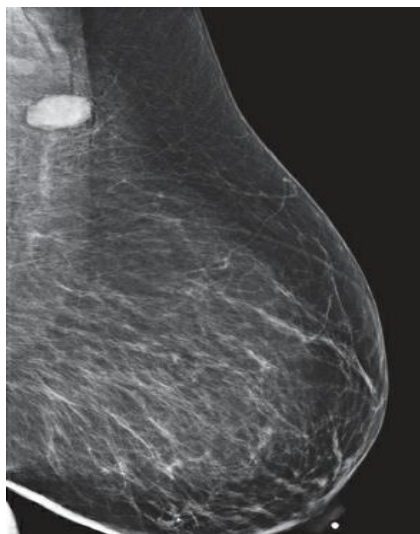


Fig. 2.79 Axillary Adenopathy. Enlarge axillary lymph node (Dronkers 2002)

2.8.1.8.6 Architectural Distortion

As an associated feature, architectural distortion may be used in conjunction with another finding to indicate that the parenchyma is distorted or retracted adjacent to the finding. (D’Orsi 2013)

2.8.1.8.7 Calcifications

As an associated feature, this may be used in conjunction with one or more other findings to describe calcifications with in or immediately adjacent to the finding(s). (D’Orsi 2013)

2.8.1.9 Location of Lesion

The location of a suspicious lesion should be described using standard clock-face clinical orientation, as extrapolated from image location. The breast is viewed as the face of a clock with the patient facing the observer. Use of both clock-face position and quadrant location is encouraged because clinicians use these location descriptors interchangeably; this also provides an internal consistency check for possible right-left confusion.

The side is given first, followed by the quadrant, clock-face location, and the depth of the lesion. Depth descriptors arbitrarily divide the breast in to anterior, middle, and posterior thirds. In addition, description of the distance of the lesion from the nipple provides a more precise indication of its depth. This may be particularly helpful in determining whether an imaging finding matches the location of a palpable mass or in directing US examination or a post imaging clinical breast examination. (Sickles et al. 2013)

The following is an example of a lesion location description:

Right, upper outer quadrant, 10:00, anterior third, 3 cm from nipple

2.8.1.9.1 Laterality

Indicate right or left breast.

2.8.1.9.2 Quadrant And Clock Face

Use upper outer quadrant, upper inner quadrant, lower outer quadrant, or lower inner quadrant. Twelve o'clock lesions may be described as upper central, 6 o'clock lesions as lower central, and lesions at 3:00 or 9:00 as either outer central or inner central depending on laterality. Central is directly behind the nipple-areolar complex on all projections. Retroareolar indicates central location in the anterior third of the breast close to the nipple. Axillary tail indicates upper outer quadrant location adjacent to the axilla but within the breast mound. The clock-face notation for a lesion in a given quadrant will depend on whether the lesion is in the right or left breast. Note that central, retroareolar, and axillary tail descriptors are used instead of quadrant descriptors and do not require indication of clock-face location. (D'Orsi 2013)

2.8.1.9.3 Depth

Indicate depth in the breast (anterior, middle, posterior third).

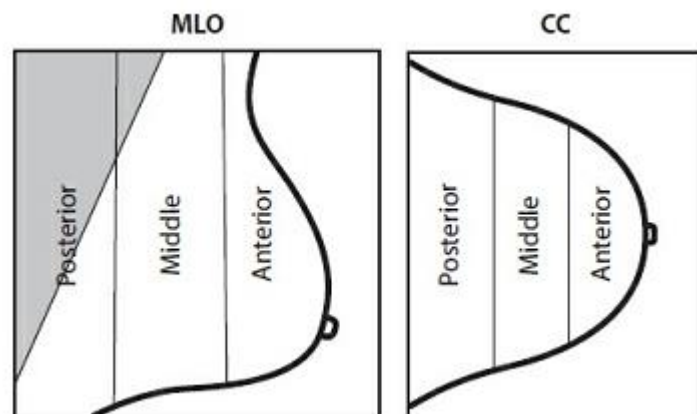


Fig. 2.80 Depth Diagram

2.8.1.9.4 Distance From The Nipple

2.8.2 Reporting System

The reporting system is designed to provide an organized approach to image interpretation and reporting.

2.8.2.1 REPORT ORGANIZATION

The reporting system should be concise and organized using the following structure.

2.8.2.1.1 Indication for Examination

Provide a brief description of the indication for examination. This may be screening for an asymptomatic woman, recall of a screening-detected finding, evaluation of a clinical finding (specify the finding and its location), or follow-up of either a probably benign lesion or cancer treated with breast conservation. If an implant is present, both standard and implant-displaced views should be performed, and this should be stated in the mammography report.

2.8.2.1.2 Succinct Description Of The Overall Breast Composition

This is an overall assessment of the volume of attenuating tissues in the breast, to help indicate the relative possibility that a lesion could be obscured by normal tissue and that the sensitivity of examination thereby may be compromised by dense breast tissue. A few coalescent areas of dense tissue may be present in breasts with as little as 10% dense tissue, whereas primarily fatty are as may be present in breasts with as much as 90% dense tissue.

The following four categories of breast composition are defined by the visually estimated content of fibroglandular-density tissue with in the breasts. The categories are listed as a, b, c, and d so as not to be confused with the numbered BIRADS® assessment categories. (D'Orsi 2013)

- a. The breasts are almost entirely fatty.

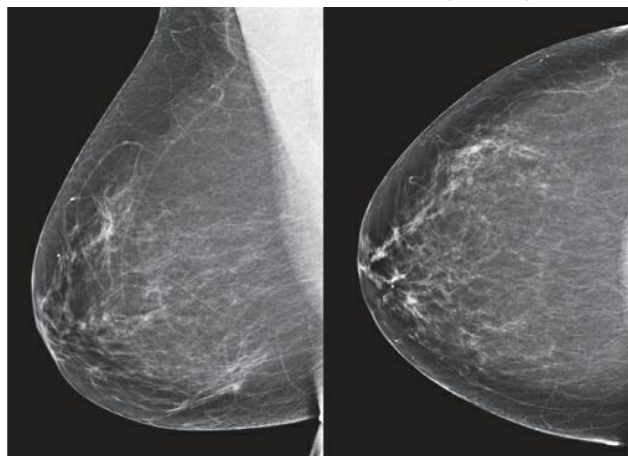


Fig. 2.81 Fatty breast (D'Orsi 2013)

- b. There are scattered areas of fibroglandular density.

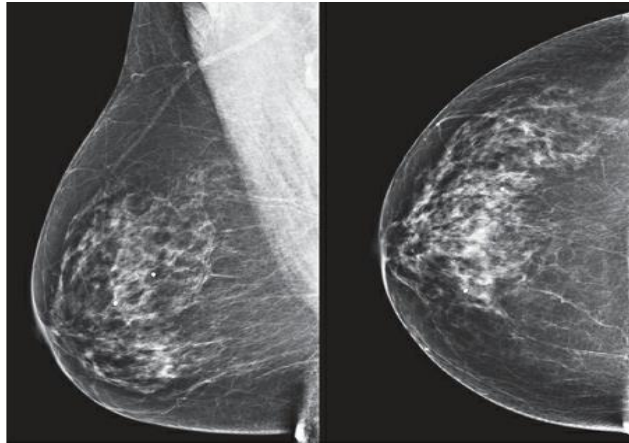


Fig. 2.82 Scattered areas of fibroglandular density (D'Orsi 2013)

c. The breasts are heterogeneously dense

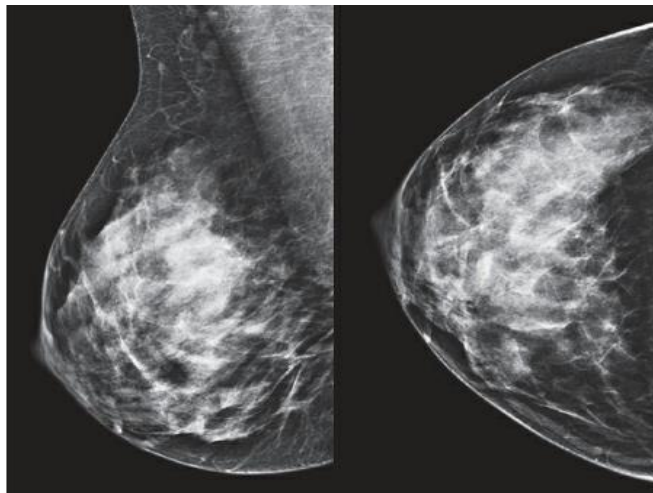


Fig. 2.83 Heterogeneous breast (D'Orsi 2013)

d. The breasts are extremely dense

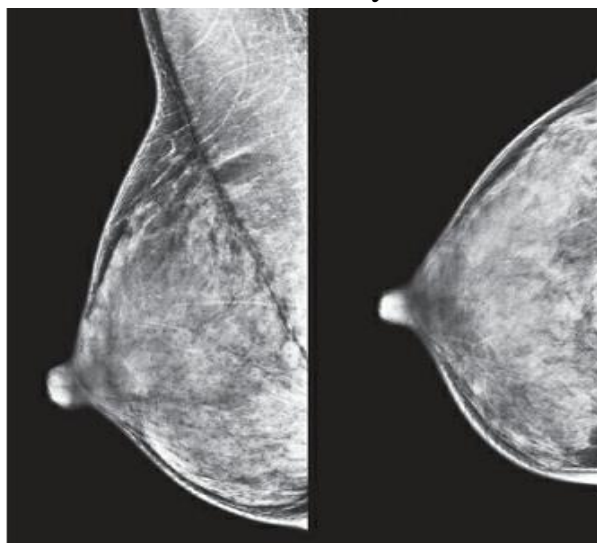


Fig. 2.84 Dense breast (D’Orsi 2013)

2.8.2.1.3 Clear Description Of Any Important Findings

The most important findings are either of concern at screening, inherently suspicious, new, or seen to be larger/more extensive when compared to previous examination.

2.8.2.1.4 Comparison to Previous Examination(S), If Deemed Appropriate By the Interpreting Physician. Comparison to previous examination may assume importance if the finding of concern requires an evaluation of change or stability. Comparison is not important when a finding has unequivocally benign features. Comparison may be irrelevant when the finding is inherently suspicious for malignancy.

2.8.2.1.5 Assessment

All final assessments (BI-RADS® categories 1, 2, 3, 4, 5, and 6) should be based on thorough evaluation of the mammographic features of concern or after determination that an examination is negative or benign.

2.8.2.1.6 Management

If a suspicious abnormality is identified, the report should indicate that a biopsy should be performed in the absence of clinical contraindication.

2.8.2.2 ASSESSMENT CATEGORIES

2.8.2.2.1 **Category 0:** Incomplete — Need Additional Imaging Evaluation and /or Prior Mammograms for Comparison For this assessment category, the text may be shortened to “Incomplete — Need Additional Imaging Evaluation” or “Incomplete — Need Prior Mammograms for Comparison”, as appropriate.

This is almost always used in a screening situation. Under certain circumstances this assessment category may be used in a diagnostic mammography report, such as when US equipment or personnel are not immediately available, or when the patient is unable or unwilling to wait for completion of a full diagnostic examination. A recommendation for additional imaging evaluation includes the use of spot-compression (with

or without magnification), special mammographic views, and US. (D’Orsi 2013)

2.8.2.2.2 **Category 1:** Negative

There is nothing to comment on. This is a normal examination. (D’Orsi 2013)

2.8.2.2.3 **Category 2:** Benign

This is a normal assessment, but here the interpreter chooses to describe a benign finding in the mammography report. Involuting calcified fibroadenomas, skin calcifications, metallic foreign bodies (such as core biopsy and surgical clips), and fat-containing lesions (such as oil cysts, lipomas, galactoceles, and mixed-density hamartomas) all have characteristically benign appearances and may be described with confidence. The interpreter may also choose to describe intramammary lymph nodes, vascular calcification, implants, or architectural distortion clearly related to prior surgery while still concluding that there is no mammographic evidence of malignancy. (D’Orsi 2013)

2.8.2.2.4 **Category 3:** Probably Benign

A finding assessed using this category should have a $\leq 2\%$ likelihood of malignancy, but greater than the essentially 0% likelihood of malignancy of a characteristically benign finding. A probably benign finding is not expected to change over the suggested period of imaging surveillance, but the interpreting physician prefers to establish stability of the finding before recommending management limited to routine mammography screening. (D’Orsi 2013)

2.8.2.2.5 **Category 4:** Suspicious

This category is reserved for findings that do not have the classic appearance of malignancy but are sufficiently suspicious to justify a recommendation for biopsy. The ceiling for category 3 assessment is a 2% likelihood of malignancy and the floor for category 5 assessment is 95%, so category 4 assessments cover the wide range of likelihood of malignancy in between. Thus, almost all recommendations for breast interventional procedures will come from assessments made using this category. By subdividing category 4 in to 4A, 4B, and 4C. (D’Orsi 2013)

2.8.2.2.6 **Category 5:** Highly Suggestive of Malignancy

These assessments carry a very high probability ($\geq 95\%$) of malignancy. This category initially was established to involve lesions for which 1-stage surgical treatment was considered with or without preliminary biopsy. (Sickles et al. 2013)

2.8.2.2.7 **Category 6:** Known Biopsy-Proven Malignancy

This category is reserved for examinations performed after biopsy proof of malignancy (imaging performed after percutaneous biopsy but prior to complete surgical excision), in which there are no mammographic abnormalities other than the known cancer that might need additional evaluation. (Sickles et al. 2013)

2.8.2.3 **WORDING THE REPORT**

The current examination should be compared to prior examination(S) when appropriate. The Indication for Examination, such as screening or diagnostic, should be stated. The report should be organized with a brief description of the Composition of the breast and any pertinent Findings, followed by the Assessment and Management Recommendations. Any verbal discussions between the interpreting physician and the referring clinician or patient should be documented in the original report or in attach to the report. (Sickles et al. 2013)

2.9 Previous Studies

Arzehgar et al (2019) have a study named Assessment and Classification of Mass Lesions Based on Expert Knowledge Using Mammographic Analysis, the research based on fact that Masses are one of the most important indicators of breast cancer in mammograms, and their classification into two groups as benign and malignant is highly necessary. Computer Aided Diagnosis (CADx) helps radiologists enhance the accuracy of their decision. Hence, the system is required to support and assess with radiologist's interaction as an expert, in this research, classification of breast masses using mammography in the two main views which include MLO and CC, is evaluated with respect to the shape, texture and asymmetry aspect. Additionally, a method was developed and proposed using the classification of breast tissue density based on the decision tree, Results show that the proposed system for entirely fat, scattered fibroglandular densities, heterogeneously dense, and extremely dense breast achieved 100, 99, 99 and 98% true malignant rate, respectively with cross-validation procedure (Arzehgar, Khalilzadeh, and Varshoei 2019).

Ahmed et al (2018), studied mass in a research named: Digital Mammography: a useful tool for differentiating benign from malignant breast masses, the study conduct to assess the efficiency of digital mammography in differentiation of benign and malignant breast masses, this validity study was conducted in radiology department, Islamabad, Pakistan from September 2016 to September 2017. 55 patients with BIRADS 0, 3, 4 and 5 on digital mammography underwent histopathological analysis. Diagnosis accuracy of digital mammography was calculated by taking histopathological analysis as gold stander. The result was mean age for disease 46.30 +8.30 years. Overall Sensitivity, Specificity, Positive Predictive Value and Negative Predictive Value for digital mammography were found to be 93.75%, 97.44%, 93.75% and 97.44%. both Sensitivity and Specificity were higher below age of 50 than for patient above 50 (Ahmed, Riaz, and Malik 2018).

Hjerkind et al (2018), their study was name: Volumetric Mammographic Density, Age-Related Decline, and Breast Cancer Risk Factors in a National Breast Cancer Screening Program. The study aimed to assess the relationship between Volumetric mammographic density (VMD) and breast cancer risk factors. The cohort consisted of 46,428

women (ages 49–71 years) who participated in Breast Screen Norway between 2007 and 2014 and had information on VMD and breast cancer risk factors. The study estimated means of percent and absolute VMD associated with age, menopausal status, body mass index (BMI), and other factors. The associations between VMD and most breast cancer risk factors were modest, although highly significant. BMI was positively associated with absolute VMD, whereas inversely associated with percent VMD. Percent VMD was inversely associated with a 5-year older age at screening in premenopausal and postmenopausal women (-0.18% vs. -0.08% for percent VMD and -0.11 cm^3 vs. -0.03 cm^3 for absolute VMD). This difference was largest among postmenopausal women with BMI $< 25 \text{ kg/m}^2$ (P for interaction with percent VMD < 0.0001), never users of postmenopausal hormone therapy (P for interaction < 0.0001), and premenopausal women with a family history of breast cancer (P for interaction with absolute VMD = 0.054). The study conclude that VMD is associated with several breast cancer risk factors, the strongest being BMI, where the direction of the association differs for percent and absolute VMD. The inverse association with age appears modified by menopausal status and other breast cancer risk factors (Hjerkind et al. 2018).

Lee et al (2018), their study named: BI-RADS 3: Current and Future Use of Probably Benign Karen. The study conduct to review the best uses and evidence for using BI-RADS 3 assessment category in mammography, breast ultrasound, and breast MRI. The result was BI-RADS 3 is not appropriate at screening mammography. After a complete diagnostic evaluation, classifying a mammographic finding as a BI-RADS 3 is highly predictive of benignity and allows for short interval follow-up rather than biopsy. While a BI-RADS 3 categorization allows for a decrease in the number of biopsies and their associated risks and costs, it should only be used to describe specific findings including a solitary group of round or punctate calcifications, a non-calcified well-circumscribed solitary mass, or a focal asymmetry without calcification or architectural distortion (Lee et al. 2018).

Mohindra et al (2018), studied lesion characterization under name: Impact of Addition of Digital Breast Tomosynthesis to Digital Mammography in Lesion Characterization in Breast Cancer Patients. The aim is to interrogate whether addition of Digital breast tomosynthesis (DBT) to digital mammography (DM) helps in better characterization of

mammographic abnormalities in breast cancer patients in general and in different breast compositions. The study was Retrospective, analytical cross-sectional study, Mammographic findings in 164 patients with 170 pathologically proven lesions were evaluated by using first DM alone and thereafter with addition of DBT to DM. The perceived utility of adjunct DBT was scored using a rating of 0–2. A score of 0 indicating that DM plus DBT was comparable to DM alone, 1 indicating that DM plus DBT was slightly better, and 2 indicating that DM plus DBT was definitely better. The result was On DM, 149 lesions were characterized mass with or without calcifications, 18 asymmetries with or without calcifications, 2 as architectural distortion, and 1 as microcalcification alone. Adjunct DBT helped in better morphological characterization of 17 lesions, with revelation of underlying masses in 16 asymmetries and one architectural distortion. Adjunct DBT was perceived to be slightly better than DM alone in 44.7% lesions, and definitely better in 22.9% lesions. Lesions showing score 1 or 2 improvement were significantly higher in heterogeneously and extremely dense breasts ($P < 0.001$), the study conclude that Adjunct DBT improves morphological characterization of lesions in patients with breast cancer. It highlights more suspicious features of lesions that indicate the presence of cancer, particularly in dense breasts (Mohindra et al. 2018).

Zeeshan et al (2018), their study named: Diagnostic Accuracy of Digital Mammography in the Detection of Breast Cancer, the study conduct to calculate the diagnostic accuracy of digital mammography in the detection of breast cancer, using histopathology as a gold standard in women aged over 30 years, who are undergoing mammography for screening and diagnostic purposes. This was a cross-sectional analytical study, conducted in the department of radiology, for a total duration of 10 months. A total of 122 patients of age above 30 years, referred for digital mammography for the evaluation of different symptoms related to breast diseases, followed by biopsy/surgery and histopathology, were included in the study. The result confirmed that digital mammography is a highly accurate tool for breast cancer detection having a sensitivity of 97%, a specificity of 64.5%, a positive predictive value of 89%, and a negative predictive value of 90.9%, with a diagnostic accuracy of 89.3% (Zeeshan et al. 2018).

Chan et al (2017), their study named: Characterization of Breast Masses in Digital Breast Tomosynthesis and Digital Mammograms: An Observer Performance Study, the study aimed to compare Breast Imaging Reporting and Data System (BI-RADS) assessment of lesions in two-view digital mammogram (DM) to two-view wide-angle digital breast tomosynthesis (DBT) without DM. two-view DBTs were acquired from 134 subjects and the corresponding DMs were collected retrospectively.

The study included 125 subjects with 61 malignant (size: 3.9–36.9 mm, median: 13.4 mm) and 81 benign lesions (size: 4.8–43.8 mm, median: 12.0 mm), and 9 normal subjects. The cases in the two modalities were read independently by six experienced. The result was Lesion conspicuity was significantly higher ($P \ll .0001$) and fewer lesion margins were considered obscured in DBT. The mean area under the receiver operating characteristic curve for the six readers increased significantly ($P = .0001$) from 0.783 (range: 0.723–0.886) for DM to 0.911 (range: 0.884–0.936) for DBT. Of the 366 ratings for malignant lesions, 343 on DBT and 278 on DM were rated as BI-RADS 4a and above. Of the 486 ratings for benign lesions, 220 on DBT and 206 on DM were rated as BI-RADS 4a and above. On average, 17.8% (65 of 366) more malignant lesions and 2.9% (14 of 486) more benign lesions would be recommended for biopsy using DBT. The inter-radiologist variability was reduced significantly (Chan et al. 2017).

Spak et al (2017), their study named: BI-RADS fifth edition: A summary of changes. The Breast Imaging Reporting and Data System (BI-RADS) is a standardized system of reporting breast pathology as seen on mammogram, ultrasound, and magnetic resonance imaging. It encourages consistency between reports and facilitates clear communication between the radiologist and other physicians by providing a lexicon of descriptors, a reporting structure that relates assessment categories to management recommendations, and a framework for data collection and auditing. This article highlights the changes made to the BI-RADS atlas 5th edition by comparison with its predecessor, provide a useful resource for a radiologist attempting to review the recent changes to the new edition, and serve as a quick reference to those who have previously become familiar with the material (Spak et al. 2017).

Durand et al (2016), their study named: Tomosynthesis-detected Architectural Distortion: Management Algorithm with Radiologic-Pathologic Correlation. Architectural distortions are often better seen and characterized at tomosynthesis. The differential diagnosis for lesions that manifest as tomosynthesis-detected architectural distortion is variable and includes benign entities such as radial scars and other benign proliferative lesions, as well as malignant invasive ductal and invasive lobular cancers. Workup should be directed toward sampling the lesion and usually involves another modality such as US or MR imaging, but in some cases

workup can include stereotactic biopsy, tomosynthesis-guided biopsy, or tomosynthesis-guided needle localization (Durand et al. 2016).

Ekpo et al (2016), their study named: Assessment of Interradiologist Agreement Regarding Mammographic Breast Density Classification Using the Fifth Edition of the BI-RADS Atlas, the study conduct to assess interradiologist agreement regarding mammographic breast density assessment performed using the rating scale out-lined in the fifth edition of the BI-RADS atlas of the American College of Radiology. Breast density assessments of 1000 cases were conducted by five radiologists from the same institution who together had recently undergone re-training in mammographic breast density classification based on the fifth edition of BI-RADS. The readers assigned breast density grades (A–D) on the basis of the BI-RADS classification scheme. Repeat assessment of 100 cases was performed by all readers 1 month after the initial assessment. A weighted kappa was used to calculate intrareader and interreader agreement. The study conclude that with regard to mammographic breast density classification, radiologists had substantial interreader agreement when a four-category scale was used and almost perfect interreader agreement when a dichotomous scale was used (Ekpo et al. 2016).

Irshad et al (2016), their study named: Effects of Changes in BI-RADS Density Assessment Guidelines (Fourth Versus Fifth Edition) on Breast Density Assessment: Intra- and Interreader Agreements and Density Distribution. The objective of the study was to determine intra- and interreader agreements for density assessment using the fifth edition of the BI-RADS guidelines and to compare with those for density assessment using the fourth edition of the BI-RADS guidelines. Five radiologists assessed breast density four times in 104 mammographic examinations: twice using the fourth edition of the BI-RADS guidelines and twice using the fifth edition. The intra- and interreader agreements for density assessment based on each guideline were determined and compared. The density distribution pattern under each of the four BI-RADS density categories using each guideline was also noted and compared. The result was the intrareader agreement for density assessment using the fifth-edition criteria was lower than that using the fourth-edition criteria ($p = 0.0179$). The overall intrareader agreement (weighted kappa) using the old criteria was 0.84 (95% CI, 0.80–0.87), and the individual intrareader agreement values in five readers ranged from 0.78 (95% CI, 0.69–0.88) to

0.92 (95% CI, 0.87–0.97). The overall intrareader agreement using the new BI-RADS criteria was 0.77 (95% CI, 0.73–0.81), and the individual intrareader agreement values in five readers ranged from 0.74 (95% CI, 0.64–0.84) to 0.99 (95% CI, 0.98–1.00). The interreader agreement values obtained using the fifth-edition criteria were also lower than those obtained using the fourth-edition criteria ($p = 0.006$). The overall interreader agreement using the old BI-RADS criteria was 0.65 (95% CI, 0.61–0.69), whereas the overall interreader agreement using the new BI-RADS criteria was 0.57 (95% CI, 0.53–0.61). Overall a higher number of dense assessments were given when the fifth-edition guidelines were used ($p < 0.0001$) (Irshad et al. 2016).

M.A. et al (2016), their study named: Architectural distortion of the breast: the best way to confront it. The study aimed to determine with which imaging method it is possible to better visualize and characterize an architectural distortion (AD) of the breast. Material and method: A retrospective study, Mammographic studies, with a diagnosis of architectural distortion (AD) in the study center between August 2015 and August 2016, were selected. Included were cases studied with at least 3 of the available PACS imaging modalities: digital mammography (2D), tomosynthesis (TS), ultrasound (US), magnetic resonance (MRI) and which were biopsied at our institution. AD cases associated with micro-calcifications and post-surgical changes were excluded. The detection rate, imaging characteristics and the histopathological concordance were evaluated. The result was in 15 months, 81 cases of AD were detected via mammography; of these, 52 met the inclusion criteria. According to the histopathology, 23 (44%) were malignant, 17 (33%) were benign and 12 (23%) were high-risk lesions (HRL). All were detected with TS and US, and classified as suspicious lesions (BI-RADS 4 or 5). In 2D mammography, 24 cases (46%) were hidden, and of these, 8 (33%) were malignant. The malignant lesions presented a dense center in 87% of the cases. The most frequent lesion on ultrasound was the hypoechogenic area (60%), in 86% of the lesions with penetrating vessels. There were 21 MRI, with mass type uptake being identified in the malignant pathologies. Conclusion: AD of the breast is best viewed in TS than in 2D mammography (M.Á. et al. 2016).

Sprague et al (2016), their study named: Variation in Mammographic Breast Density Assessments Among Radiologists in Clinical Practice: A Multicenter Observational Study, the study conduct to examine variation in breast density assessment across radiologists in clinical practice. Cross-sectional and longitudinal analyses of prospectively collected observational data. The Participants **was** Radiologists who interpreted at least 500 screening mammograms during 2011 to 2013 ($n = 83$). Data on 216 783 screening mammograms from 145 123 women aged 40 to 89 years were included. Mammographic breast density, as clinically recorded using the 4 Breast Imaging Reporting and Data System categories (heterogeneously dense and extremely dense categories were considered “dense” for analyses), and patient age, race, and body mass index (BMI). The result was overall, 36.9% of mammograms were rated as showing dense breasts. Across radiologists, this percentage ranged from 6.3% to 84.5% (median, 38.7% [interquartile range, 28.9% to 50.9%]), with multivariable adjustment for patient characteristics having little effect (interquartile range, 29.9% to 50.8%). Examination of patient subgroups revealed that variation in density assessment across radiologists was pervasive in all but the most extreme patient age and BMI combinations. Among women with consecutive mammograms interpreted by different radiologists, 17.2% (5909 of 34 271) had discordant assessments of dense versus nondense status. During 2011 to 2013 ($n = 83$). Data on 216 783 screening mammograms from 145 123 women aged 40 to 89 years were included (Sprague et al. 2016).

Youk et al (2016), their study named: Automated Volumetric Breast Density Measurements in the Era of the BI-RADS Fifth Edition: A Comparison with Visual Assessment. The purpose of this study is to evaluate automated volumetric measurements in comparison with visual assessment of mammographic breast density by use of the fifth edition of BI-RADS. A total of 1185 full-field digital mammography examinations with standard views were retrospectively analyzed. All images were visually assessed by two blinded radiologists according to breast density category in the fifth edition of the BI-RADS lexicon. Automated volumetric breast density assessment was performed using two different software programs, Quantra and Volpara. A weighted kappa value was calculated to assess the degree of agreement among the visual and volumetric assessments of the density category. The volumes of

fibroglandular tissue or total breast and the percentage breast density provided by the two software programs were compared. The result was compared with a visual assessment, the agreement of density category ranged from moderate to substantial in Quantra ($\kappa = 0.54\text{--}0.61$) and fair to moderate in Volpara ($\kappa = 0.32\text{--}0.43$). The distribution of density category was statistically significantly different among visual and volumetric measurements ($p < 0.0001$). Quantra assigned category A and B (43.5%) more frequently than did the radiologists (25.6%) or Volpara (16.0%). Volpara assigned category D (42.1%) more frequently than did the radiologists (19.5%) or Quantra (15.4%). Between the two software programs, the means of all volumetric data were statistically significantly different ($p < 0.0001$), but were well correlated ($\gamma = 0.79\text{--}0.99$; $p < 0.0001$). The study concludes that more mammographic examinations were classified as nondense breast tissue using the Quantra software and as dense breast tissue using the Volpara software, as compared with visual assessments according to the BI-RADS fifth edition (Youk et al. 2016).

Perera et al (2016), their study named: Demographic, Clinical And Mammographic Characteristics of Invasive Ductal Carcinoma of The Breast: A Sri Lankan Experience, the study aimed at describing the demographic, clinical and mammographic characteristics of histologically proven invasive ductal carcinoma (IDC) of breast in a group of Sri Lankan women. The study was carried out using a database on mammography maintained by the principal investigator. Study sample consisted of 177 subjects. The mean age of subjects was 52.2 years ($SD \pm 1.1$). Majority (63.8%) were postmenopausal women. 93% of them presented with symptomatic breast disease, and the commonest symptom was a palpable mass (90.7%). Presentation for mammography after observing symptoms showed a median delay of 28 days. BC was found mostly in involuting type of breasts. Commonest mammography characteristic was a mass (86.4%). Size of the mass was between 2 cm to 5 cm in majority (84.3%) with T stage II disease (Perera et al. 2016).

Bertrand et al (2015), their study named: Dense and Non-dense Mammographic Area and Risk of Breast Cancer by Age and Tumor Characteristics, to assess Mammographic Density Phenotypes & Breast Cancer, they examined the components of percent MD (dense area (DA) and non-dense area (NDA) with breast cancer subtypes. Methods: Data were pooled from six studies including 4095 breast cancers and 8558

controls. DA and NDA were assessed from digitized film-screen mammograms and standardized across studies. Breast cancer odds by density phenotypes and age according to histopathological characteristics and receptor status were calculated using polytomous logistic regression, the result was DA and NDA have differential associations with ER+ vs. ER- tumors that vary by age (Bertrand et al. 2015).

Ribnikar et al (2015), their study named: Breast Cancer Under Age 40: a Different Approach, Breast cancer (BC) under age 40 is a complex disease to manage due to the additionally fertility-related factors to be taken in consideration. More than 90 % of young patients with BC are symptomatic. Women <40 years are more likely to develop BC with worse clinicopathological features and more aggressive subtype. This has been frequently associated with inferior outcomes. Recently, the prognostic significance of age <40 has been shown to differ according to the BC subtype, being associated with worst recurrence-free survival (RFS) and overall survival (OS) for luminal BC. The biology of BC <40 has also been explored through analysis of large genomic data set, and specific pathways overexpressed in these tumors have been identified which can lead to the development of targeted therapy in the future. A multidisciplinary tumor board should determine the optimal locoregional and systemic management strategies for every individual patient with BC before the start of any therapy including surgery (Ribnikar et al. 2015).

Bahl et al (2015), their study named: Architectural Distortion on Mammography: Correlation With Pathologic Outcomes and Predictors of Malignancy, The objective of the study was to determine the risk of malignancy associated with architectural distortion and to evaluate the imaging and clinical features that may contribute to the prediction of malignancy in the setting of architectural distortion. The was retrospective review of architectural distortion cases from January 1, 2004, to December 31, 2013. Imaging findings and pathology outcomes were reviewed, the result of the study was Over the 10-year study period, architectural distortion that was considered to be suspicious for or highly suggestive of malignancy was present in 435 of 231,051 (0.2%) mammographic examinations. Cases were excluded if the main finding described was a mass with an associated feature of architectural distortion (n = 62) or if no pathology results were available (n = 4). Two hundred seventy-five cases of invasive adenocarcinoma or ductal carcinoma in situ (DCIS) were

identified; the positive predictive value (PPV) was therefore 74.5% (275/369). DCIS alone was identified in only 4.1% (15/369). The most common benign finding on pathology was a radial scar or complex sclerosing lesion (27/369, 7.3%). Architectural distortion was less likely to represent malignancy on screening mammography than on diagnostic mammography (67.0% vs 83.1%, respectively; $p < 0.001$). Architectural distortion without a sonographic correlate was less likely to represent malignancy than architectural distortion with a correlate (27.9% vs 82.9%, respectively; $p < 0.001$). There was no statistically significant difference in the malignancy rate between pure architectural distortion and architectural distortion with calcifications or asymmetries (73.0% vs 78.8%; $p = 0.26$). The PPV of architectural distortion for malignancy is 74.5%. Architectural distortion is less likely to represent malignancy if detected on screening mammography than on diagnostic mammography or if there is no sonographic correlate (Bahl et al. 2015).

Gard et al (2015), their study named: Misclassification of Breast Imaging Reporting and Data System (BI-RADS) Mammographic Density and Implications for Breast Density Reporting Legislation. . The aim of this study was to assess reproducibility of the four-category BI-RADS density measure and examine its relationship with a continuous measure of percent density. We enrolled 19 radiologists, experienced in breast imaging, from a single integrated health care system. Radiologists interpreted 341 screening mammograms at two points in time 6 months apart. We assessed intra- and interobserver agreement in radiologists' interpretations of BI-RADS density and explored whether agreement depended upon radiologist characteristics. The result was Intraradiologist agreement was moderate to substantial, with kappa varying across radiologists from 0.50 to 0.81 (mean = 0.69, 95% CI [0.63, 0.73]). Intraradiologist agreement was higher for radiologists with ≥ 10 years experience interpreting mammograms (difference in mean kappa = 0.10, 95% CI [0.01, 0.24]). Interradiologist agreement varied widely across radiologist pairs from slight to substantial, with kappa ranging from 0.02 to 0.72 (mean = 0.46, 95% CI [0.36, 0.55]). Of 145 examinations interpreted as “nondense” (BI-RADS density a or b) by the majority of radiologists, 82.8% were interpreted as “dense” (BI-RADS density c or d) by at least one radiologist. Of 187 examinations interpreted as “dense” by the majority of radiologists, 47.1% were interpreted as “nondense” by at

least one radiologist. While the examinations of almost half of the women in the study were interpreted clinically as having BI-RADS density c or d, only about 10% of examinations had percent density >50%. The results suggest that breast density reporting based on a single BI-RADS density interpretation may be misleading due to high interradiologist variability and a lack of correspondence between BI-RADS density and percent density (Gard et al. 2015).

DeSantis et al (2015), their study named: International Variation in Female Breast Cancer Incidence and Mortality Rates. The study conduct to examine global trends in female breast cancer rates using the most up-to-date data available. Breast cancer incidence and mortality estimates were obtained from GLOBOCAN 2012 (globocan.iarc.fr), the study analyzed trends from 1993 onward using incidence data from 39 countries from the International Agency for Research on Cancer and mortality data from 57 countries from the World Health Organization. The result was Breast cancer mortality rates are decreasing in most high-income countries, despite increasing or stable incidence rates. In contrast and of concern are the increasing incidence and mortality rates in a number of countries, particularly those undergoing rapid changes in human development. Wide variations in breast cancer rates and trends reflect differences in patterns of risk factors and access to and availability of early detection and timely treatment (DeSantis et al. 2015).

Eberl et al (2015), their study named: BI-RADS Classification for Management of Abnormal Mammograms. The study conduct to give knowlge about BIRADS caterogaries and final management, the study conclude that the Breast Imaging Reporting and Data System (BI-RADS), developed by the American College of Radiology, provides a standardized classification for mammographic studies. This system demonstrates good correlation with the likelihood of breast malignancy. The BI-RADS system can inform family physicians about key findings, identify appropriate follow-up and management and encourage the provision of educational and emotional support to patients (Eberl et al. 2015).

Ekpo et al (2015), their study named: Breast Composition: Measurement and Clinical Use Ernest, in this paper, the historical background to breast density measurement is outlined and current evidence based practice is explained. The relevance of breast density knowledge to mammographic practice and image interpretation is considered in the light of clinical

assessment and notification of mammographic breast density (MBD). Automated volumetric approaches are explained while ultrasound, digital breast tomosynthesis, molecular breast imaging, and magnetic resonance imaging are introduced as valuable adjuncts to digital mammography for imaging the dense breast. The work concludes on the important note that screened women should be notified of their breast density, and such notification should be accompanied with clear and adequate information about breast density and cancer risk, strategies associated with lower MBD, as well as best screening intervals and pathways for women with dense breasts. Adoption of these strategies may be crucial to early detection and treatment of cancer and improving survival from the disease (Ekpo et al. 2015).

Van Der Waal et al (2015), their study named: Comparing Visually Assessed BI-RADS Breast Density and Automated Volumetric Breast Density Software: A Cross-Sectional Study in a Breast Cancer Screening Setting. The objective of this study is to compare different methods for measuring breast density, both visual assessments and automated volumetric density, Digital mammographic exams (N = 992) of women participating in the Dutch breast cancer screening programme (age 50–75y) in 2013 were included. Breast density was measured in three different ways: BI-RADS density (5th edition) and with two commercially available automated software programs (Quantra and Volpara volumetric density). BI-RADS density (ordinal scale) was assessed by three radiologists. Quantra (v1.3) and Volpara (v1.5.0) provide continuous estimates. Different comparison methods were used, including Bland-Alt-man plots and correlation coefficients (e.g., intraclass correlation coefficient [ICC]). The result was Based on the BI-RADS classification, 40.8% of the women had ‘heterogeneously or extremely dense’ breasts. The median volumetric percent density was 12.1% (IQR: 9.6– 16.5) for Quantra, which was higher than the Volpara estimate (median 6.6%, IQR: 4.4– 10.9). The mean difference between Quantra and Volpara was 5.19% (95% CI: 5.04–5.34) (ICC: 0.64). There was a clear increase in volumetric percent dense volume as BI-RADS density increased. The highest accuracy for predicting the presence of BI-RADS c+d (heterogeneously or extremely dense) was observed with a cut-off value of 8.0% for Volpara and 13.8% for Quantra (Van Der Waal et al. 2015).

Berment et al (2014), their study named: Masses in mammography: What are the underlying anatomopathological lesions?, The semiological description of masses in mammography is based on the BI-RADS system provided by the American College of Radiology. The contour is the most discriminating morphological criterion between benign and malignant masses. Most circumscribed masses are benign. Nevertheless, due to specific histological characteristics, certain malignant lesions or lesions with a risk of malignancy may appear in the mammography in this falsely reassuring form. An indistinct contour in the mammography is suspicious and requires a tissue sample. The positive predictive value of malignancy varies according to the morphology of the contour (Berment et al. 2014).

Boyer and Russ (2014), their study named: Anatomical-radiological correlations: Architectural distortions. The study conduct to examine the semiologic features of the distortions and their different causes, together with their pathological anatomy correlations, the result of study was Architectural distortions consist of convergence areas and local retractions at the border of the gland. The predominant benign causes are the proliferative Aschoff body and the main malignant cause is infiltrating lobular carcinoma (Boyer and Russ 2014).

Huo et al (2014), their study named: Mammographic density—a review on the current understanding of its association with breast cancer. The study conduct to review the current literature on MD (Mammographic Density) and summarize the current evidence for its association with breast cancer. In this study Keywords “mammographic dens*”, “dense mammary tissue” or “percent dens*” were used to search the existing literature in English on PubMed and Medline. All reports were critically analyzed. The data was assigned to one of the following aspects of MD: general association with BC, its relationship with the breast hormonal milieu, the cellular basis of MD, the generic variations of MD, and its significance in the clinical setting. The result was MD adjusted for age and BMI is associated with increased risk of BC diagnosis, advanced tumour stage at diagnosis, and increased risk of both local recurrence and second primary cancers. The MD measures that predict BC risk have high heritability, and to date several genetic markers associated with BC risk have been found to also be associated with these MD risk-predictors. Change in MD could be a predictor of the extent of chemoprevention with tamoxifen (Huo et al. 2014).

Saeed et al (2014), their study named: Cancer incidence in Khartoum, Sudan: first results from the Cancer Registry, 2009–2010. this study report the first data from the National Population-based Cancer Registry (NCR) for Khartoum State for the period 2009–2010. The NCR staff used passive and active approaches to collect data on cancer diagnosed by all means in Khartoum State. Rates were age standardized to the 2010 Sudan Standard Population and 1966 and 2000 World Standard Population and expressed per 100,000 populations. During 2009–2010, 6771 new cancer cases were registered. The result was Of those, 3646 (53.8%) cases were in women and 3125 (46.2%) were in men. The most commonly diagnosed cancer among women was breast followed by leukemia, cervix, and ovary, and among men it was prostate cancer followed by leukemia, lymphoma, oral, colorectal, and liver. In children less than 15 years of age, leukemia was the most common cancer followed lymphoma, and cancer of the eye, bone, kidney, and the brain (Saeed et al. 2014).

Cupido et al (2013), their study named: Evaluation and correlation of mammographically suspicious lesions with histopathology at Addington Hospital, Durban. The research conduct to assess the PPV of SCNB (Stereotactic core-needle biopsies) in Addington Hospital, and to compare it with that of BIRADS, Mammographically detected lesions were assigned to 3 categories: benign, indeterminate and suspicious. A retrospective review of 67 SCNBs was performed for lesions falling within the suspicious category, and the PPV and rates of ductal carcinoma in situ (DCIS) were determined. The result was a PPV of 20.9%. This correlated well with international studies for BIRADS 4 and 5 lesions. DCIS accounted for 21.4% of detected malignancies (Cupido et al. 2013).

Gaur et al (2013), their study named: Architectural Distortion of the Breast. The study aimed to discuss the benign and malignant causes of architectural distortion and illustrates its various manifestations in an effort to reduce undiagnosed architectural distortion on screening mammography, the study conclude that On mammography, the architectural distortion associated with either IDC or ILC may appear as spicules radiating from a central mass. In response to local infiltration into the surrounding tissue, the architectural distortion may have a star-shaped pattern. There may be no ultrasound correlate to the architectural distortion in the absence of a palpable or mammographically apparent mass. In the presence of a correlate, ultrasound can provide guidance for biopsy. In

conclusion, architectural distortion represents the third most common imaging appearance of malignancy. Biopsy is often necessary to exclude malignancy unless it is possible to identify an obvious benign cause, such as postsurgical or postprocedural change or fat necrosis (Gaur et al. 2013).

Baum et al (2011), their study named: Use of BI-RADS 3–Probably Benign Category in the American College of Radiology Imaging Network Digital Mammographic Imaging Screening Trial, the study conducted to determine (a) how often the Breast Imaging Reporting and Data System (BI-RADS) category 3 was used in the American College of Radiology Imaging Network (ACRIN) Digital Mammographic Imaging Screening Trial (DMIST), either at the time of screening mammography or after work-up, (b) how often subjects actually returned for the recommended follow-up examination, and (c) the rate and stages of any malignancies subsequently found in subjects for whom short-term interval follow-up was recommended. The method was a total of 47 599 subjects, all of whom consented to undergo both digital and screen-film mammography, were included in this analysis. Cases referred for short-term interval follow-up based on digital, screen-film, or both imaging examinations were determined. Compliance with the recommendations and the final outcome (malignancy diagnosis at biopsy or no malignancy confirmed through follow-up) of each evaluable case were determined. The result was A total of 1114 of the 47 599 (2.34%) subjects had tumors assigned a BI-RADS 3 category and were recommended to undergo short-interval follow-up. In this study, 791 of 1114 (71%) of the subjects were compliant with the recommendation and returned for short-interval follow-up. Of the women who did not return for short-interval follow-up, 70% (226 of 323) did return for their next annual mammography. Among all subjects whose tumors were assigned a BI-RADS 3 category either at screening mammography or after additional work-up, nine of 1114 (0.81%) were found to have cancer. Of the nine biopsy-proved cancers, six were invasive cancers and three were ductal carcinoma in situ stage Tis–T1c. The invasive cancers were all less than 2 cm in size. The conclusion was In DMIST, radiologists used the BI-RADS 3 classification infrequently (2.3% of patients). Tumors assigned a BI-RADS 3 category had a low rate of malignancy. The relatively high rate of noncompliance with short-interval follow-up recommendations (323 of 1114, or 29%) supports prior recommendations that radiologists

thoroughly evaluate lesions before placing them in this category (Baum et al. 2011).

Burivong and Amornvithayacharn (2011), their study named: Accuracy of subcategories A, B, C in BI-RADS 4 lesions by combined mammography and breast ultrasound findings, the research conduct to determine the accuracy of BI-RADS 4 subcategories, mammographic and ultrasound images of 143 patients were independently and blindly reviewed by two radiologists and later compared with pathologic diagnosis. The result was Sixty-eight of 143 (47%) were classified as subcategory 4A, 54 (37%) were 4B and 21 (14%) were 4C. The positive predictive value after consensus evaluation in subcategory 4A, 4B and 4C are 4.4%, 43.3% and 52.1%, respectively. Interobserver agreement for mammographic and ultrasound descriptions varies from perfect to fair agreement. The research conclude that the malignancy rate in subcategories 4B and 4C was significantly higher than in subcategory 4A (Burivong and Amornvithayacharn 2011).

Ferreira, Pedro et al (2011), their study named: Predicting Malignancy from Mammography Findings and Surgical Biopsies, the main goal of this work is to produce machine learning models that predict the outcome of a mammography from a reduced set of annotated mammography findings. In the study we used a data set consisting of 348 consecutive breast masses that underwent image guided or surgical biopsy performed between October 2005 and December 2007 on 328 female subjects. The main conclusions are threefold: (1) automatic classification of a mammography, independent on information about mass density, can reach equal or better results than the classification performed by a physician; (2) as previous studies suggested; (3) a machine learning model can predict mass density with a quality as good as the specialist blind to biopsy, which is one of our main contributions. Our model can predict malignancy in the absence of the mass density attribute, since we can fill up this attribute using our mass density predictor.

Tzikopoulos et al (2011), their study named: A fully automated scheme for mammographic segmentation and classification based on breast density and asymmetry, This paper presents a fully automated segmentation and classification scheme for mammograms, based on breast density estimation and detection of asymmetry. First, image preprocessing and segmentation techniques are applied, including a breast boundary extraction algorithm

and an improved version of a pectoral muscle segmentation scheme. Features for breast density categorization are extracted, including a new fractal dimension- related feature, and support vector machines (SVMs) are employed for classification, achieving accuracy of up to 85.7%. Most of these properties are used to extract a new set of statistical features for each breast; the differences among these feature values from the two images of each pair of mammograms are used to detect breast asymmetry, using an one-class SVM classifier, which resulted in a success rate of 84.47%. This composite methodology has been applied to the miniMIAS database, consisting of 322 (MLO) mammograms -including 15 asymmetric pairs of images-, obtained via a (noisy) digitization procedure. The results were evaluated by expert radiologists and are very promising, showing equal or higher success rates compared to other related works, despite the fact that some of them used only selected portions of this specific mammographic database (Tzikopoulos et al. 2011).

Koch et al (2010), their study named: Quality of the interpretation of diagnostic mammographic images, the study aimed to demonstrate the knowledge of mammogram readers working in the public healthcare system in the State of Rio de Janeiro, RJ, Brazil, and to evaluate their progress in the early diagnosis of breast cancer after a training course specifically developed for medical professionals, the material and method was a group of 53 physicians with experience in mammography reports were invited. A pre-test was given to assess their initial knowledge level. Afterwards, they were trained by experts mammographers, and for final conclusion, requested to take a post-test for comparison and evaluation of gained knowledge. The Result was the course, with emphasis on theoretical classes, has not resulted in a significant improvement on the quality of mammogram reading, highlighting the persistence of errors in morphological description of fundamental lesions of the breast, in the classification of such lesions according to the BI-RADS®, besides the lack of coherence between the BI-RADS classification and follow-up recommendation as observed in both the pre- and posttest.

Antonio and Crespi (2010), their study named: Predictors of interobserver agreement in breast imaging using the Breast Imaging Reporting and Data System (BI-RADS), the study conduct to identify predictors of reliability as measured by the kappa statistic, the researcher identified studies conducted between 1993 and 2009 which reported kappa

values for interpreting mammograms using any edition of BI-RADS. Bivariate and multivariate multilevel analyses were used to examine associations between potential predictors and kappa values. The research identified ten eligible studies, which yielded 88 kappa values for the analysis. Potential predictors of kappa included: whether or not the study included negative cases, whether single-view or two-view mammograms were used, whether or not mammograms were digital vs. screen-film, whether or not the 4th edition of BI-RADS was utilized, the BI-RADS category being evaluated, whether or not readers were trained, whether or not there was an overlap in readers' professional activities, the number of cases in the study and the country in which the study was conducted. Our best multivariate model identified training, use of two-view mammograms and BI-RADS categories (masses, calcifications and final assessments) as predictors of kappa. The result was: Training, use of two-view mammograms and focusing on mass description may be useful in increasing reliability in mammogram interpretation. Calcification and final assessment descriptors are areas for potential improvement. These findings are important for implementing policies in BI-RADS use before introducing the system in different settings and improving current implementations (Antonio and Crespi 2010).

Bent (2010), their study named: The Positive Predictive Value of BI-RADS Microcalcification Descriptors and Final Assessment Categories, The purpose of this article is to retrospectively assess the likelihood of malignancy of microcalcifications according to the BI-RADS descriptors in a digital mammography environment. The study included 146 women with calcifications who underwent imaging-guided biopsy between April 2005 and July 2006. Digital mammograms procured before biopsy were analyzed independently by two breast imaging subspecialists blinded to biopsy results. Lesions described discordantly were settled by consensus. One of the radiologists provided a BI-RADS final assessment score. The result was the overall positive predictive value of biopsies was 28.8%. The individual morphologic descriptors predicted the risk of malignancy as follows: fine linear/branching, 16 (70%) of 23 cases; fine pleomorphic, 14 (28%) of 50 cases; coarse heterogeneous, two (20%) of 10 cases; amorphous, 10 (20%) of 51 cases; and typically benign, zero (0%) of 12 cases. Fisher-Freeman-Halton exact testing showed statistical significance among morphology descriptors ($p < 0.001$) and distribution descriptors (p

< 0.001). The positive predictive value for malignancy according to BI-RADS assessment categories were as follows: category 2, 0%; category 3, 0%; category 4A, 13%; category 4B, 36%; category 4C, 79%; and category 5, 100%. The conclusion was BI-RADS morphology and distribution descriptors can aid in assessing the risk of malignancy of microcalcifications detected on full-field digital mammography. The positive predictive value increased in successive BI-RADS categories (4A, 4B, and 4C), verifying that subdivision provides an improved assessment of suspicious microcalcifications in terms of likelihood of malignancy (Bent et al. 2010).

Chang et al (2010), their study named: Solitary Dilated Duct Identified at Mammography: Outcomes Analysis. The study conduct to review the clinical and pathologic outcomes for cases of solitary dilated duct identified at mammography. For all screening mammography examinations during a 22-year period and all diagnostic mammography examinations during the last 10 of these years, the radiologists recorded the principal finding of each abnormal mammographic examination during image interpretation. Only examinations with the recorded finding of solitary dilated duct were studied. The result was the finding of solitary dilated duct was recorded for nine (0.0038%) of 235,209 consecutive screenings and for 12 (0.041%) of 29,267 consecutive diagnostic mammography examinations. Five screening and five diagnostic cases were stable at follow-up (minimum interval, 2 years) and did not undergo biopsy; tumor registry linkage showed no subsequent cancer diagnosis. Biopsy was performed for four (44%) of nine screening and seven (58%) of 12 diagnostic cases. One cancer each (ductal carcinoma in situ) was identified from the screening and diagnostic populations, yielding positive predictive values of 11% (1/9) and 8% (1/12), respectively (Chang et al. 2010).

Burnside et al (2009), their study named: The ACR BI-RADS® Experience: Learning From History, the researcher in this study said that Breast Imaging Reporting and Data System® (BI-RADS®) initiative, instituted by the ACR, was begun in the late 1980s to address a lack of standardization and uniformity in mammography practice reporting. An important component of the BI-RADS initiative is the lexicon, a dictionary of descriptors of specific imaging features. The BI-RADS lexicon has always been data driven, using descriptors that previously had been shown

in the literature to be predictive of benign and malignant disease. Once established, the BI-RADS lexicon provided new opportunities for quality assurance, communication, research, and improved patient care. The history of this lexicon illustrates a series of challenges and instructive successes that provide a valuable guide for other groups that aspire to develop similar lexicons in the future (Burnside et al. 2009).

Naeem et al (2008), their study named: Pattern of Breast Cancer: Experience at Lady Reading Hospital, Peshawar, The aim of this Descriptive study was to see the various features of breast cancer in order to know the pattern of disease in the recent time. The study was conducted from Jan. 2007 to Dec. 2007 in Surgical C Unit, Postgraduate Medical Institute, Lady Reading Hospital, Peshawar, Pakistan. Study included all patients presenting to and admitted in Surgical C Unit LRH, with carcinoma of breast during the above mentioned period. Name, age, sex, other relevant data, history and examination findings and results of histopathology and other investigations were recorded. The result was Total of 46 patients was included in the study, out of which there were 46 female and 1 male patients. Most common age group was 40–49 years with 14 patients, followed by 50–59 years with 12 patients. Most common type of carcinoma was infiltrating ductal carcinoma with no specific features with 38 patients. Other types included 2 infiltrating ductal carcinomas of papillary type, 1 mucinous type and 1 medullary type; 3 invasive lobular carcinomas, and 1 mixed lobular and ductal carcinoma. The disease was left sided in 24 cases, right sided in 20 cases while it was bilateral in 2 cases. Upper outer quadrant of the breast was most commonly involved (n=26). There were 2 cases of stage I, 16 stage II, 20 stage III and 08 cases of stage IV disease. There were 2 cases of grade I, 16 grade II, and 28 cases of grade III (Naeem et al. 2008).

Balleyguier et al (2007), their study named: BIRADS classification in mammography, the study conduct to review describes the mammographic items of the BIRADS classification with its more recent developments, while detailing the advantages and limits of this classification, the result was The Breast Imaging Report and Data System (BIRADS) of the American College of Radiology (ACR) is today largely used in most of the countries where breast cancer screening is implemented. It is a tool defined to reduce variability between radiologists when creating the reports in mammography, ultrasonography or MRI. Some changes in the last version

of the BIRADS have been included to reduce the inaccuracy of some categories, especially for category 4. The BIRADS includes a lexicon and descriptive diagrams of the anomalies, recommendations for the mammographic report as well as councils and examples of mammographic cases (Balleyguier et al. 2007).

Shi et al (2007), their study named: Characterization of mammographic masses based on level set segmentation with new image features and patient information. Computer-aided diagnosis (CAD) for characterization of mammographic masses as malignant or benign has the potential to assist radiologists in reducing the biopsy rate without increasing false negatives. The purpose of this study was to develop an automated method for mammographic mass segmentation and explore new image based features in combination with patient information in order to improve the performance of mass characterization. The authors' primary data set consisted of 427 biopsy proven masses (200 malignant and 227 benign) in 909 regions of interest (ROIs) (451 malignant and 458 benign) from multiple mammographic views. Leave-one-case-out resampling was used for training and testing. The new CAD system based on the level set segmentation and the new mammographic feature space achieved a view-based Az value of 0.83 ± 0.01 . The improvement compared to the previous CAD system was statistically significant ($p=0.02$). When patient age was included in the new CAD system, view-based and case-based Az values were 0.85 ± 0.01 and 0.87 ± 0.02 , respectively. The study also demonstrated the consistency of the newly developed CAD system by evaluating the statistics of the weights of the LDA classifiers in leave-one-case-out classification. Finally, an independent test on the publicly available digital database for screening mammography with 132 benign and 197 malignant ROIs containing masses achieved a view-based Az value of 0.84 ± 0.02 (Shi et al. 2007).

Ciatto et al (2006), their study named: Reader variability in reporting breast imaging according to BI-RADS® assessment categories (the Florence experience). The inter- and intraobserver agreement (K statistic) in reporting according to BI-RADS assessment categories was tested on 12 dedicated breast radiologists, with little prior working knowledge of BI-RADS, reading a set of 50 lesions (29 malignant, 21 benign). The result was Interobserver agreement (four categories) was fair, moderate or substantial for three, six, or three radiologists, or (six categories) slight, fair

or moderate for one, six, or five radiologists. Major disagreement occurred for intermediate categories ($R_3=0.12$, $R_4=0.25$, $R_{4a}=0.08$, $R_{4b}=0.07$, $R_{4c}=0.10$). The research found insufficient intra- and interobserver consistency of breast radiologists in reporting BI-RADS assessment categories. (Ciatto et al. 2006)

Lazarus et al (2006), their study named: BI-RADS Lexicon for US and Mammography: Interobserver Variability and Positive Predictive Value. The study aimed to retrospectively evaluate interobserver variability between breast radiologists by using terminology of the fourth edition of the Breast Imaging Reporting and Data System (BI-RADS) to categorize lesions on mammograms and sonograms and to retrospectively determine the positive predictive value (PPV) of BI-RADS categories 4a, 4b, and 4c. Ninety-four consecutive lesions in 91 women who underwent image-guided biopsy comprised 59 masses, 32 calcifications, and three masses with calcification. Five radiologists retrospectively reviewed these lesions. Each observer described each lesion with BI-RADS terminology and assigned a final BI-RADS category. Inter-observer variability was assessed with the Cohen k statistic. A pathologic diagnosis was available for all 94 lesions; 30 (32%) were malignant and 64 (68%) were benign. Pathologic analysis of benign lesions was performed on tissue obtained with image-guided core-needle biopsy. In cases referred for excisional biopsy after needle biopsy because of atypia or discordance, final surgical pathologic analysis was used for correlation with imaging findings. PPV for category 4 or 5 lesions was determined for all readers combined. The result was for mammographic descriptors, moderate agreement was obtained for mass shape, mass margin, and calcification distribution ($k=0.48$, 0.48 , and 0.50 , respectively). Fair agreement was obtained for calcification description ($k=0.32$). Slight agreement was obtained for mass density ($k=0.18$). Fair agreement was obtained for final assessment category ($k=0.28$). PPVs of BI-RADS category 4 and 5 assignments were as follows: category 4a, six (6%) of 102; category 4b, 17 (15%) of 110; category 4c, 48 (53%) of 91; and category 5, 71 (91%) of 78 (Lazarus et al. 2006).

Scutt et al (2006), their study named: Breast asymmetry and predisposition to breast cancer, the study aimed to prove that breast asymmetry is related to several of the known risk factors for breast cancer, and that patients with diagnosed breast cancer have more breast volume

asymmetry, as measured from mammograms, than age-matched healthy women. The study compared the breast asymmetry of women who were free of breast disease at time of mammography, but who had subsequently developed breast cancer, with that of age-matched healthy controls who had remained disease-free to time of the present study. The study group consisted of 252 asymptomatic women who had normal mammography, but went on to develop breast cancer. The control group were 252 age-matched healthy controls whose mammograms were also normal and who remained free of cancer during the study period. Breast volume was calculated from the cranio-caudal mammograms for each group, and the relationships between asymmetry, established risk factors and the presence or absence of breast cancer were explored. The result was The group who went on to develop breast cancer had higher breast asymmetry than controls (absolute asymmetry odds ratio 1.50 per 100 ml, confidence interval (CI) 1.10, 2.04; relative asymmetry 1.09, CI 1.01, 1.18), increased incidence of family history of breast cancer, lower age at menarche, later menopause, later first pregnancies and a higher frequency of high risk breast parenchyma types (Scutt, Lancaster, and Manning 2006).

Kanavos (2006), their study named: The rising burden of cancer in the developing world, the study conduct as epidemiological study, predicted that by 2020, the number of new cases of cancer in the world will increase to more than 15 million, with deaths increasing to 12 million. Much of the burden of cancer incidence, morbidity, and mortality will occur in the developing world. This forms part of a larger epidemiological transition in which the burden of chronic, non-communicable disease—once limited to industrialized nations—is now increasing in less developed countries. In addition to the accumulating risks associated with diet, tobacco, alcohol, lack of exercise, and industrial exposures, the developing world is already burdened by cancers some of which are attributable to infectious diseases. These disparities in cancer risk combined with poor access to epidemiological data, research, treatment, and cancer control and prevention combine to result in significantly poorer survival rates in developing countries for a range of specific malignancies. This paper summarizes the recent trends in the epidemiology and survival of cancers in the developing and developed world, and explores potential causes and policy responses to the disproportionate and growing cancer burden in less developed countries. Such responses may include raising awareness as well

as education and training to foster better informed decision-making, together with improved cancer surveillance, early detection and emphasis on prevention. Improved health care financing and international initiatives and/or partnerships could also provide additional impetus in targeting resources where needed urgently (Kanavos 2006).

Ayres and Rangayvan (2005), their study named: Characterization of architectural distortion in mammograms, the study conduct to dedicated methods to detect architectural distortion in the absence of a central mass, the method was by employing the concept of phase portraits, a method to characterize architectural distortion in mammograms using texture orientation fields is presented. The results obtained show that the proposed technique can achieve good discrimination between architectural distortion and other parenchymal patterns. Such a technique would be applicable, in a CAD system, to images that have cleared the stages of detection of calcifications and masses with no positive findings (Ayres and Rangayvan 2005).

Berg et al (2004), their study named: Diagnostic Accuracy of Mammography, Clinical Examination, US, and MR Imaging in Preoperative Assessment of Breast Cancer, the study conduct to prospectively assess accuracy of mammography, clinical examination, ultrasonography (US), and magnetic resonance (MR) imaging in preoperative assessment of local extent of breast cancer. The method was results of bilateral mammography, US, and contrast-enhanced MR imaging were analyzed from 111 consecutive women with known or suspected invasive breast cancer. Results were correlated with histopathologic findings. The result was Analysis included 177 malignant foci in 121 cancerous breasts, of which 89 (50%) foci were palpable. Median size of 139 invasive foci was 18 mm (range, 2–107 mm). Mammographic sensitivity decreased from 100% in fatty breasts to 45% in extremely dense

breasts. Mammographic sensitivity was highest for invasive ductal carcinoma (IDC) in 89 of 110 (81%) cases versus 10 of 29 (34%) cases of invasive lobular carcinoma (ILC) ($P \leq .001$) and 21 of 38 (55%) cases of ductal carcinoma in situ (DCIS) ($P \leq .01$). US showed higher sensitivity than did mammography for IDC, depicting 104 of 110 (94%) cases, and for ILC, depicting 25 of 29 (86%) cases ($P \leq .01$ for each). US showed higher sensitivity for invasive cancer than DCIS (18 of 38 [47%], $P \leq .001$). MR showed higher sensitivity than did mammography for all tumor types ($P \leq .01$) and higher sensitivity than did US for DCIS ($P \leq .001$), depicting 105 of 110 (95%) cases of IDC, 28 of 29 (96%) cases of ILC, and 34 of 38 (89%) cases of DCIS. In anticipation of conservation or no surgery after mammography and clinical examination in 96 breasts, additional tumor (which altered surgical approach) was present in 30. Additional tumor was depicted in 17 of 96 (18%) breasts at US and in 29 of 96 (30%) at MR, though extent was now overestimated in 12 of 96 (12%) at US and 20 of 96 (21%) at MR imaging. After combined mammography, clinical examination, and US, MR depicted additional tumor in another 12 of 96 (12%) breasts and led to overestimation of extent in another six (6%); US showed no detection benefit after MR imaging. Bilateral cancer was present in 10 of 111 (9%) patients; contralateral tumor was depicted mammographically in six and with both US and MR in an additional three. One contralateral cancer was demonstrated only clinically. The conclusion was in nonfatty breasts, US and MR imaging were more sensitive than mammography for invasive cancer, but both MR imaging and US involved risk of overestimation of tumor extent. Combined mammography, clinical examination, and MR imaging were more sensitive than any other individual test or combination of tests (Berg et al. 2004).

Rastogi et al (2004), their study named: Opportunities for cancer epidemiology in developing countries, the study conduct to prove that, Most cancer epidemiology studies involve people living in North America and Europe, which represent only a fraction of the global population. The wide variety of dietary, lifestyle and environmental exposures, as well as the genetic variation among people in developing countries can provide valuable new information on factors that contribute to cancer or that protect against it. What are the challenges and advantages to performing large epidemiological studies in developing nations (Rastogi et al. 2004).

Carney et al (2003), their study named: Individual and combined effects of age, breast density, and hormone replacement therapy use on the accuracy of screening mammography. The study conduct to determine how breast density, age, and use of HRT individually and in combination affect the accuracy of screening mammography, the study was Prospective cohort study, 329 495 women 40 to 89 years of age who had 463 372 screening mammograms from 1996 to 1998; 2223 women received a diagnosis of breast cancer, the Measurements were done Breast density, age, HRT use, rate of breast cancer occurrence, and sensitivity and specificity of screening mammography. The result was Adjusted sensitivity ranged from 62.9% in women with extremely dense breasts to 87.0% in women with almost entirely fatty breasts; adjusted sensitivity increased with age from 68.6% in women 40 to 44 years of age to 83.3% in women 80 to 89 years of age. Adjusted specificity increased from 89.1% in women with extremely dense breasts to 96.9% in women with almost entirely fatty breasts. In women who did not use HRT, adjusted specificity increased from 91.4% in women 40 to 44 years of age to 94.4% in women 80 to 89 years of age. In women who used HRT, adjusted specificity was about 91.7% for all ages (Carney et al. 2003).

Geller et al (2002), their study named: Use of the American College of Radiology BI-RADS to Report on the Mammographic Evaluation of Women with Signs and Symptoms of Breast Disease, the study conduct to examine whether mammographic assessments and recommendations are linked as expected, based on the Breast Imaging Reporting and Data System (BI-RADS), for the evaluation of women with signs and symptoms of breast disease, the material and method of study was Eight mammography registries from the Breast Cancer Surveillance Consortium contributed mammographic data from 1996 through 1997 for women 25 years of age or older, with signs or symptoms of breast cancer. The association of assessments and recommendations and the relationship of self-reported symptoms to assessments are described, the result was A total of 51,673 diagnostic mammograms were included in the analyses and the expected management recommendation was provided 85%–90% of the time for mammograms classified as assessment categories 1, 2, 4, or 5. Category 3 (“probably benign finding”) had the most variability in associated management recommendations, with only 40% (2,998 of 7,423) of cases associated with the recommendation for short interval follow-up. Of the 1,648 category 0 mammograms (“needs additional imaging”) that did not have a final assessment, 64% were recommended for additional imaging, while another 20% of the cases were recommended for either a consultation or biopsy. The number of women who reported a lump as a symptom decreased with age but was associated with higher BI-RADS assessments (Geller et al. 2002).

Taplin et al. (2002), their study named: Concordance of Breast Imaging Reporting and Data System Assessments and Management Recommendations in Screening Mammography, the study conduct to examine how frequently Breast Imaging Reporting and Data System (BI-RADS) mammographic screening assessments were associated with expected clinical management recommendations. Materials and Methods

was Seven Breast Cancer Surveillance Consortium mammography registries recorded screening assessments and recommendations in 1997 to identify the proportion of women in each BI-RADS category. The first screening assessment for a woman without cancer or a prior mammogram within 9 months was associated with its independently recorded recommendation. The result was among 292,795 women, screening assessments included 269,022 (91.9%) with a “negative” or “benign finding,” and 267,103 (99.3%) of these women were recommended for normal interval follow-up. Among 11,861 (4.1%) women with screening assessments of “probably benign finding,” 4,782 (40.3%) were recommended for short interval follow-up as expected on the basis of the BI-RADS, but a high proportion (36.9%) were recommended for additional imaging. Among 1,625 (0.6%) women with “suspicious abnormality,” most were recommended for biopsy (48.7%) or clinical examination and/or surgical consult (9.0%), but many were recommended for additional imaging (38.7%). Among 243 (0.1%) women with screening assessments “highly suggestive of malignancy,” a majority were recommended for biopsy (73.3%) or clinical examination and/or surgical consult (18.1%) consistent with BI-RADS, but some were recommended for additional imaging (6.6%) (Taplin et al. 2002).

Sahiner et al (2001), their study named: Improvement of mammographic mass characterization using spiculation measures and morphological features. The goal of this work was to improve our characterization method by making use of morphological features. Toward this goal, they have developed a fully automated, three-stage segmentation method that includes clustering, active contour, and spiculation detection stages. The researchers have developed a fully automated, three-stage segmentation method that includes clustering, active contour, and spiculation detection stages. After segmentation, morphological features describing the shape of the mass were extracted. Texture features were also extracted from a band of pixels surrounding the mass. Stepwise feature selection and linear discriminant analysis were employed in the morphological, texture, and combined feature spaces for classifier design. The classification accuracy was evaluated using the area A_z under the receiver operating characteristic curve. A data set containing 249 films from 102 patients was used. When the leave-one-case-out method was applied to partition the data set into trainers and testers, the average test A_z for the task of classifying the mass

on a single mammographic view was 0.83 ± 0.02 , 0.84 ± 0.02 , and 0.87 ± 0.02 in the morphological, texture, and combined feature spaces, respectively. The improvement obtained by supplementing texture features with morphological features in classification was statistically significant ($p=0.04$). For classifying a mass as malignant or benign, we combined the leave-one-case-out discriminant scores from different views of a mass to obtain a summary score. In this task, the test Az value using the combined feature space was 0.91 ± 0.02 . Our results indicate that combining texture features with morphological features extracted from automatically segmented mass boundaries will be an effective approach for computer-aided characterization of mammographic masses (Sahiner et al. 2001).

Berg et al (2000), their study named: Breast Imaging Reporting and Data System: Inter- and Intraobserver Variability in Feature Analysis and Final Assessment, the study conduct to evaluate the use of the Breast Imaging Reporting and Data System (BI-RADS) standardized mammography lexicon among and within observers and to distinguish variability in feature analysis from variability in lesion management. The material and method was Five experienced mammographers, not specifically trained in BI-RADS, used the lexicon to describe and assess 103 screening mammograms, including 30 (29%) showing cancer, and a subset of 86 mammograms with diagnostic evaluation, including 23 (27%) showing cancer. A subset of 13 screening mammograms (two with malignant findings, 11 with diagnostic evaluation) were rereviewed by each observer 2 months later. Kappa statistics were calculated as measures of agreement beyond chance. After diagnostic evaluation, the interobserver kappa values for describing features were as follows: breast density, 0.43; lesion type, 0.75; mass borders, 0.40; special cases, 0.56; mass density, 0.40; mass shape, 0.28; microcalcification morphology, 0.36; and microcalcification distribution, 0.47. Lesion management was highly variable, with a kappa value for final assessment of 0.37. When we grouped assessments recommending immediate additional evaluation and biopsy (BI-RADS categories 0, 4, and 5 combined) versus follow-up (categories 1, 2, and 3 combined), five observers agreed on management for only 47 (55%) of 86 lesions. Intraobserver agreement on management (additional evaluation or biopsy versus follow-up) was seen in 47 (85%) of 55 interpretations, with a kappa value of 0.35–1.0 (mean, 0.60) for final assessment (Berg et al. 2000).

Orel et al (1999), their study named: BI-RADS Categorization as a Predictor of Malignancy. The purpose of the study to determine the positive predictive value (PPV) of the American College of Radiology Breast Imaging Reporting and Data System (BI-RADS) categories 0, 2, 3, 4, and 5 by using BI-RADS terminology and by auditing data on needle localizations. Materials and Methods: Between April 1991 and December 1996, 1,400 mammographically guided needle localizations were performed in 1,109 patients. Information entered into the mammographic database included where the initial mammography was performed (inside vs outside the institution), BI-RADS category, mammographic finding, and histopathologic findings. A recorded recommendation was available for 1,312 localizations in 1,097 patients, who composed the study population. The result was The 1,312 localizations yielded 449 (34%) cancers (139 [31%] were ductal carcinoma in situ [DCIS]; 310 [69%] were invasive cancers) and 863 (66%) benign lesions. There were 15 (1%) category 0 lesions; the PPV was 13% (two of 15 lesions). There were 50 (4%) category 2 lesions; the PPV was 0% (0 of 40 lesions). There were 141 (11%) category 3 lesions; the PPV was 2% (three of 141 lesions). The three cancers in this group were all non-comedotype DCIS. There were 936 (71%) category 4 lesions; the PPV was 30% (279 of 936 lesions). There were 170 (13%) category 5 lesions; the PPV was 97% (165 of 170 lesions), the study conclude that placing mammographic lesions into BI-RADS categories is useful for predicting the presence of malignancy. Perhaps, most important, a lesion placed into BI-RADS category 3 is highly predictive of benignity, and short-term interval follow-up as an alternative to biopsy would decrease the number of biopsies performed in benign lesions (Orel et al. 1999).

Boyd et al (1998), their study named: Mammographic Densities and Breast Cancer Risk, the conduct to review the relationship between mammographic parenchymal patterns to risk of breast cancer. The study found that Mammographic dense breast tissue is associated both with epithelial proliferation and with stromal fibrosis. The relationship between these histological features and risk of breast cancer may explained by the known actions of growth factors that are thought to play important roles in breast development and carcinogenesis. Mammographically dense tissue differs from most other breast cancer risk factors in the strength of the associated relative and attributable risks for breast cancer, and because it

can be changed by hormonal and dietary interventions. This risk factor may be most useful as a means of investigating the etiology of breast cancer and of testing hypotheses about potential preventive strategies (Boyd et al. 1998).

Lieberman et al (1998), their study named: The Breast Imaging Reporting and Data System: Positive Predictive Value of Mammographic Features and Final Assessment Categories. The purpose of the study was to assess the positive predictive value of mammographic features and final assessment categories described in the Breast Imaging Reporting and Data System (BI-RADS) for lesions on which biopsies have been performed, the study prospectively evaluated 492 impalpable mammographically detected lesions on which surgical biopsy (as opposed to percutaneous biopsy) was performed. Each lesion was classified according to BI-RADS descriptors for masses (margins and shape) and calcifications (morphology and distribution) and was categorized by the BI-RADS final assessment categories as category 3 (probably benign), category 4 (suspicious abnormality), or category 5 (highly suggestive of malignancy). Mammographic and pathologic findings were reviewed. The result was: Carcinoma was present in 225 (46%) of 492 lesions. For the 492 lesions subject to biopsy, BI-RADS final assessment categories were category 3 in eight lesions (2%), category 4 in 355 (72%), and category 5 in 129 (26%). The features with highest positive predictive value for carcinoma were spiculated margins (81%), irregular shape (73%), linear calcification morphology (81%), and segmental or linear calcification distribution (74% and 68%, respectively). Carcinoma was present in 105 (8 1%) of 129 category 5 lesions compared with 120 (34%) of 355 category 4 lesions ($p < .001$). The frequency of carcinoma was higher in category 5 than in category 4 lesions for all mammographic lesion types and all interpreting radiologists. The study conclude that the standardized terminology of the BI-RADS lexicon allows quantification of the likelihood of carcinoma in an impalpable breast lesion. The features with highest positive predictive value a spiculated margins, irregular shape, linear morphology, and segmental or linear distribution a warrant designation of a lesion as category 5 (Lieberman et al. 1998).

Baker et al. (1996), their study named: Breast Imaging Reporting and Data System Standardized Mammography Lexicon: Observer Variability in Lesion Description, this study conducted to measure Inter- and

Intraobserver variabilities of radiologists' descriptions of mammographic lesions with the BI-RADS standardized lexicon. Sixty mammographic studies with abnormal findings were independently evaluated by five radiologists. Readers described each lesion by selecting a single term from the BI-RADS lexicon for each of eight morphologic categories: calcification distribution, number, and description; mass margin, shape, and density; associated findings; and special cases. Additionally, each reader assessed the significance of each lesion on a five-point scale. One observer read each case twice. inter- and Intraobserver variabilities for each description and interpretation category of the BI-RADS lexicon were determined with Cohen's kappa statistic. Radiologists' specific use of calcification descriptors was evaluated in detail. The result was Substantial agreement was observed between readers for choosing terms to describe masses and caicifications (kappa value range, 0.50 ± 0.02 - 0.77 ± 0.03). Intraobserver agreement for these categories was similar (kappa value range, 0.57 ± 0.07 - 0.84 ± 0.09). Considerable inter- and intraobserver variabilities were noted for the "associated findings" and "special cases" categories (kappa value range, -0.02 ± 0.14 0.38 ± 0.12), a result that in part reflected the small number of cases to which these categories were assigned. Moderate interobserver variability and little intraobserver vanability in the interpretation of lesion significance were noted when an assessment classification similar to that of BI-RADS was used. Use of terms to describe calcifications did not always conform to Bi-RADS-defined levels of suspicion.

Chapter Three:
Material
&
Method of the Research

3.1 Material:

3.1.1 Research Type:

The study is Retrospective study type.

3.1.2 Population and Sample Size:

300 Mammographic Images for women aged between 15 to 90 years old

3.1.3 Exclusion criteria:

A mammogram of Women with a history of breast or ovarian cancer, or with breast implants, were excluded.

So the BIRADS Category 6 not included in this research

3.1.4 Study Duration:

From October 2015 to July 2019

3.1.5 Machine:

Different digital mammography machines in different institute.



Fig. 3-1 Example of Digital mammographic machine used.
(GE Full digital mammographic machine)

3.1.6 Ethical considerations:

The Research was approved by all relevant ethics committees. The patient and the breast care centers that the images taken from it have a right to inform if there is any suspicions to malignancy suggested by the opinion of radiologist while it's negative in the centers result.

3.2 Method:

The mammographic images reported using the BI-RAD system was collected, and re-reported by different radiologist according to traditional way of reporting, or vice versa then all the data recorded into recording data sheet according to categories should be assessed, to evaluate and assessed the BI-RAD and interpretation of mammography image, to define the degree of concordance between them.

3.2.1 Collection of Data

The researcher collected digital mammogram from different medical institutions and re-diagnosed by various radiologists. The samples were digital mammograms randomly selected for women between the ages of 15 to 90 years and the two basic projections of mammography (CC and MLO) were adopted.

The mammograms were diagnosed by radiologists using the usual interpretation of mammography and re-diagnosed again by different radiologist by adopting BIRAD system.

The data from different reports were collected using two different data collection sheets, for the two types of reporting. Each sheet includes:

patient No., age of the patient, breast composition, the mammographic finding (Mass, Calcifications, Architectural distortion, Asymmetry, Intramammary Lymph node, solitary Dilated ducts and Associated features), and the final diagnosis or BIRAD Category.

3.2.1.1 Data collection sheet:

The items of sheet determine using breast imaging lexicons of BIRAD system.

3.2.1.1.1 Age:

The ages of the patients grouped according to range of patient's age from 15 to 90.

The researcher divided the total patient's ages into five different groups with 15 years interval, the first one (15-30), the second group (31-45), the third group (46-60), the forth group (61-75) and the fifth group (76-90).

3.2.1.1.2 Breast Composition:

The breast composition determined by radiologist for each mammogram according to classification categories (fatty, scattered fibroglandular, heterogeneous fibroglandular or dense breast) for the usual interpretation.

And by letters ("a" for fatty, "b" for scattered fibroglandular, "c" for heterogeneous fibroglandular or "d" for dense breast) according to BIRADS lexicons.

3.2.1.1.3 Mass:

The term mass selected by the radiologist when found a 3D occupying space lesion and described the mass according to its shape either Oval, round or irregular.

The researcher add a fourth descriptive term found in the reports "lobulated".

In addition described the margin of the mass either Circumscribed or any related word (Well defined, Sharp), Obscured (Partially well defined), Microlobulated, Indistinct (ill defined), Speculated, or Irregular.

And also defined mass density as High, equal (Iso), low, and fat containing according to x-ray attenuation of the mass either greater than the attenuation of fibroglandular tissue of the breast, equal, or low also fat containing mass like oil cyst. And determined the associated calcification.

The location of mass was determined according to one or two of localization systems preferred to use in localization of the lesion. The selected terms sited according to reports of the mammograms. It was Retroareolar, Central, Upper inner, Upper outer, Lower inner, Lower outer, Upper anterior, Lower anterior, Upper posterior, Upper middle (upper central), Central posterior, Central anterior, Different locations (Multiple) and Axillary tail.

3.2.1.1.4 Calcification:

The presence of calcification was checked and calcified according to types either Typically benign like (Skin, Vascular, Coarse (Popcorn-like), Large rod-like, Round, Rim (egg shell), Dystrophic, Milk of calcium, Suture), or Suspicious Morphology like (Amorphous, Coarse heterogeneous, Fine Pleomorphic (fine calcification), Fine Linear branching calcifications).

And the location of calcifications also was identified as (Diffuse or scattered, Regional. Grouped, Linear, Segmental and single). And the location of the calcification determined as same as for mass.

3.2.1.1.5 Architectural Distortion:

It was identified when the parenchyma is distorted with no definite mass visible.

3.2.1.1.6 Asymmetry:

It was identified when the area of fibroglandular tissue that is visible on only one mammographic projection. Presence of asymmetry identified.

3.2.1.1.7 Intramammary Lymph node:

It was determined in each mammogram either present or absent.

3.2.1.1.8 Solitary Dilated Ducts:

It was determined in each mammogram either present or absent.

3.2.1.1.9 Associated Features:

It was determined in each mammogram according to what feature appear into the image (Skin retraction, Nipple retraction, Skin thickening, Trabecular distortion, Axillary lymph Adenopathy , Multiple small lesions, Dilated superficial vessels), if any two or more features appear together, they were determined (Nipple retraction and skin retraction, Nipple retraction and Lymph Adenopathy, Nipple retraction and Skin Thickening, Skin thickening and Lymph Adenopathy and Nipple retraction, skin thickening and Lymph Adenopathy).

3.2.1.1.10 Diagnosis and BIRADS Category:

Each mammogram diagnosed finally twice by different radiologist using routine interpretation and BIRADS system.

The diagnosis included (Normal finding, Benign, Probably Benign, Malignant, Highly malignancy) according to diagnosis write by radiologists.

The BIRADS Category included (0 incomplete, 1 Normal finding, 2 Benign, 3 probably benign, 4 Suspicious Malignancy and Highly suggestive Malignancy).

3.2.2 Statistical Analysis

The data analyzed used SPSS version 10, to maintained accurate analysis and results. The agreement evaluated using Kappa statistic. Kappa statistic is a statistical measure designed to assess agreement between two or more observations for categorical or nominal data.

3.2.2.1 Kappa scale

This technique determines the proportion of selections for which observers agree and accounts for the possibility of agreements attributable solely to chance. Perfect agreement is indicated by a kappa value of 1 .0, whereas a kappa value of 0 indicates the level of agreement expected by chance alone.

Kappa value	Strength of Agreement
< 0.20	Poor
0.21 to 0.40	Fair
0.41 to 0.60	Moderate
0.61 to 0.80	Good
0.81 to 1.00	Very Good

3.2.2.2 Kappa Equation

$$\kappa = \frac{p_o - p_e}{1 - p_e} = 1 - \frac{1 - p_o}{1 - p_e},$$

where:

P_o = the relative observed agreement among raters.

P_e = the hypothetical probability of chance agreement

Chapter Four

Results

CHAPTER FOUR

RESULTS

This chapter shows the statistical analysis results of the study in tables and descriptive figures.

Part I: distribution of patients` variable

Table (4.1): distribution of samples according to age

Age group	Frequency	Percent
15 - 30 y	18	6.0
31 - 45 y	69	23.0
46 - 60 y	120	40.0
61 - 75 y	78	26.0
75 - 90 y	15	5.0
Total	300	100.0

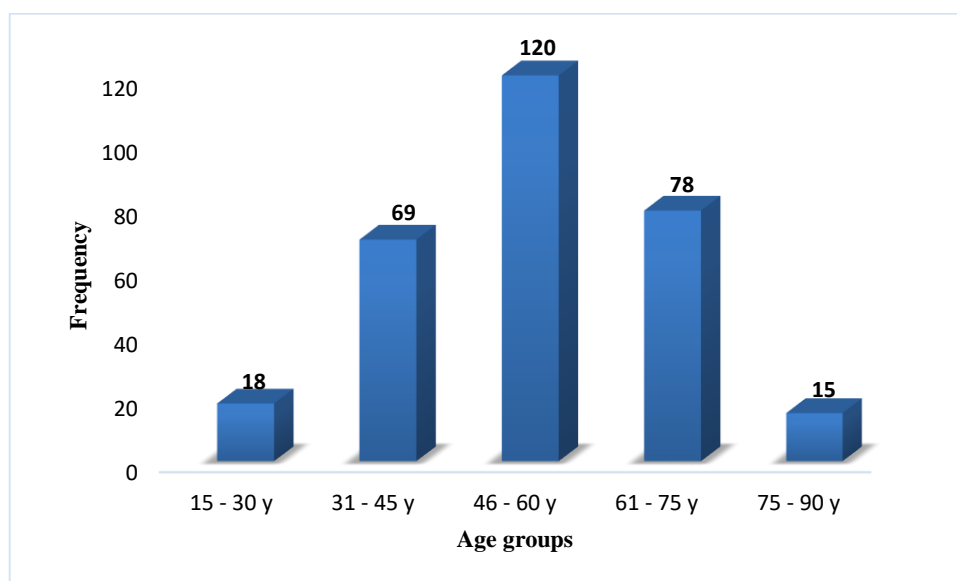


Figure (4.1): distribution of samples according to age

Part II: distribution of mammographic findings according to BIRAD system

Table (4.2): distribution of samples according to breast composition

A. In routine interpretation

Breast composition	Frequency	Percent
a	48	16.0
b	126	42.0
c	105	35.0
d	21	7.0
Total	300	100.0

B. In BIRAD interpretation

Breast composition	Frequency	Percent
a	36	12.0
b	129	43.0
c	102	34.0
d	33	11.0
Total	300	100.0

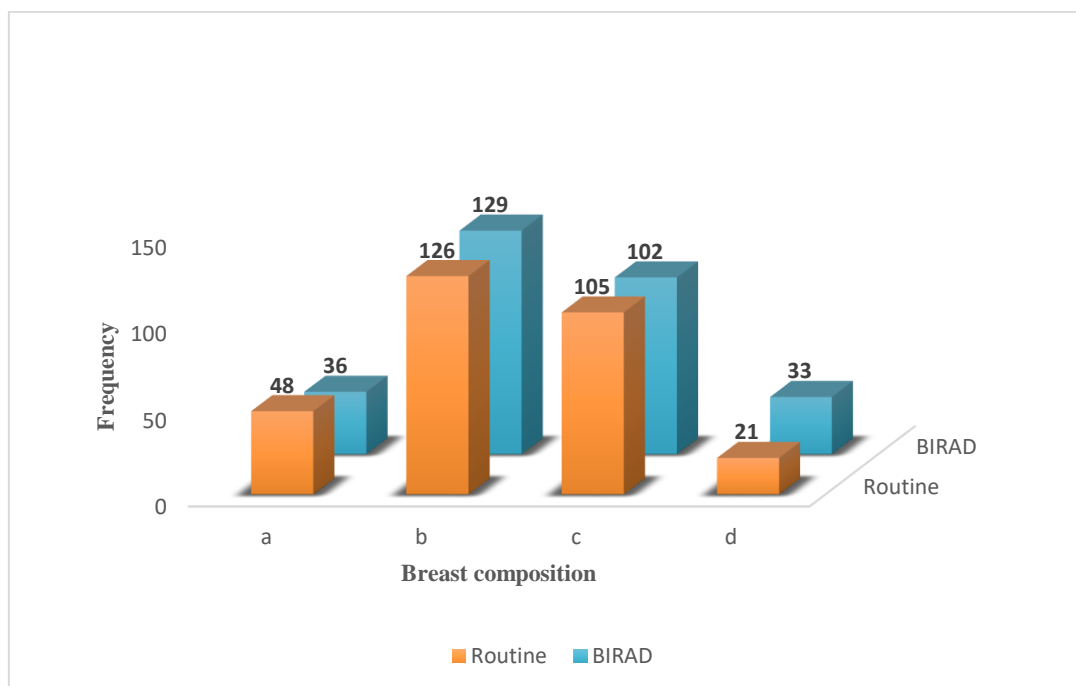


Figure (4.2): distribution of samples according to breast composition

Table (4.3): distribution of samples according to presence of breast masses

A. In routine interpretation interpretation

Breast mass	Frequency	Percent
yes	207	69.0
no	93	31.0
Total	300	100.0

B. In BIRAD

Breast mass	Frequency	Percent
Yes	186	62.0
No	102	34.0
Total	288	96.0
Undefined	12	4.0
Total	300	100.0

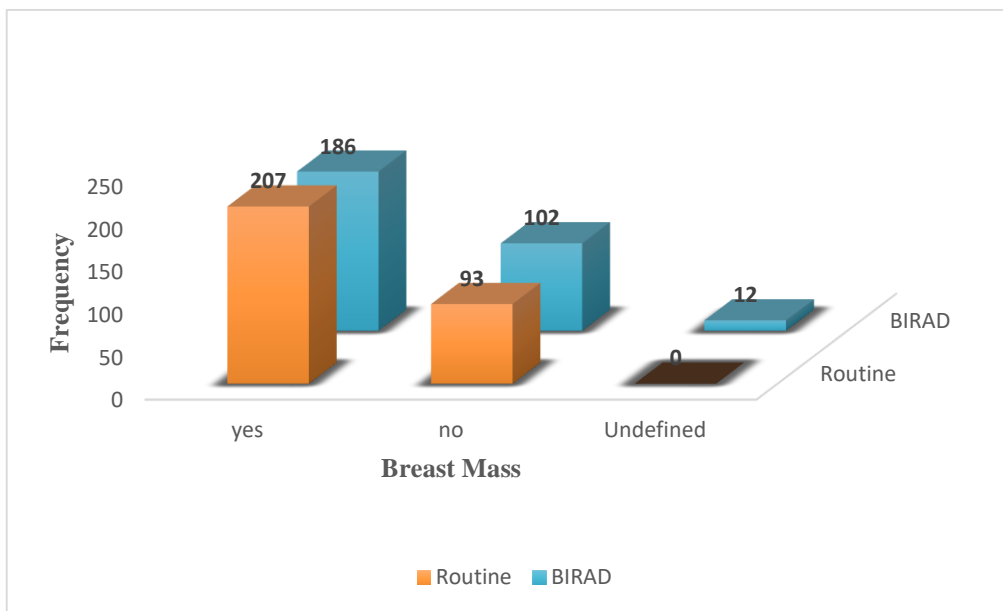


Figure (4.3): distribution of samples according to presence of breast masses

Table (4.4): distribution of samples according to the shape of mass

A. In routine interpretation

Mass shape	Frequency	Percent
Oval	51	24.6
Round	27	13.0
Irregular	126	60.9
Lobulated	3	1.5
Total	207	100

B. In BIRAD interpretation

Mass shape	Frequency	Percent
Oval	69	37.1
Round	45	24.2
Irregular	66	35.5
Lobulated	6	3.2
Total	186	100

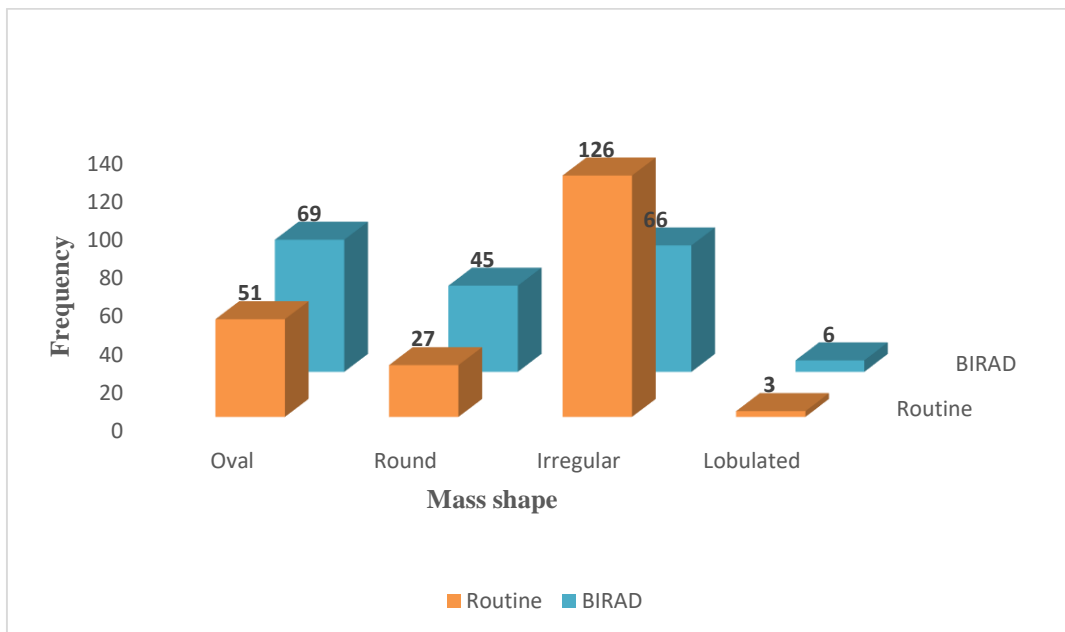


Figure (4.4): distribution of samples according to the shape of mass

Table (4.5): distribution of samples according to the margin of mass

A. In routine interpretation
interpretation

B. In BIRAD

Mass margin	Frequency	Percent
Circumscribed	45	21.7
Obscured	9	4.3
Microlobulated	3	1.4
Indistinct	66	31.9
Speculated	84	40.6
Total	207	100

Mass margin	Frequency	Percent
Circumscribed	45	24.2
Obscured	21	11.3
Microlobulated	27	14.5
Indistinct	33	17.7
Speculated	48	25.8
Irregular	12	6.5
Total	186	100

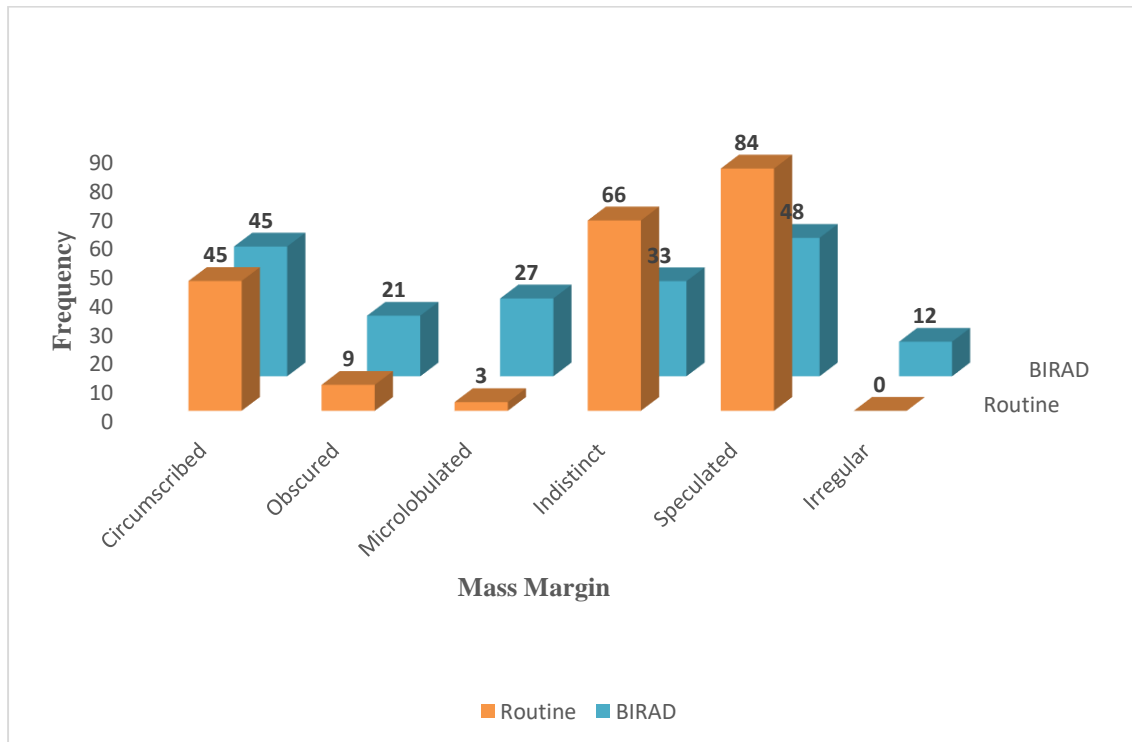


Figure (4.5): distribution of samples according to the margin of mass

Table (4.6): distribution of samples according to the mass density

A. In routine interpretation interpretation

Mass density	Frequency	Percent
High density	156	75.4
Equal density (iso)	45	21.7
Low density	6	2.9
Total	207	100

B. In BIRAD

Mass density	Frequency	Percent
High density	120	64.5
Equal density (iso)	60	32.3
Fat containing	6	3.2
Total	186	100

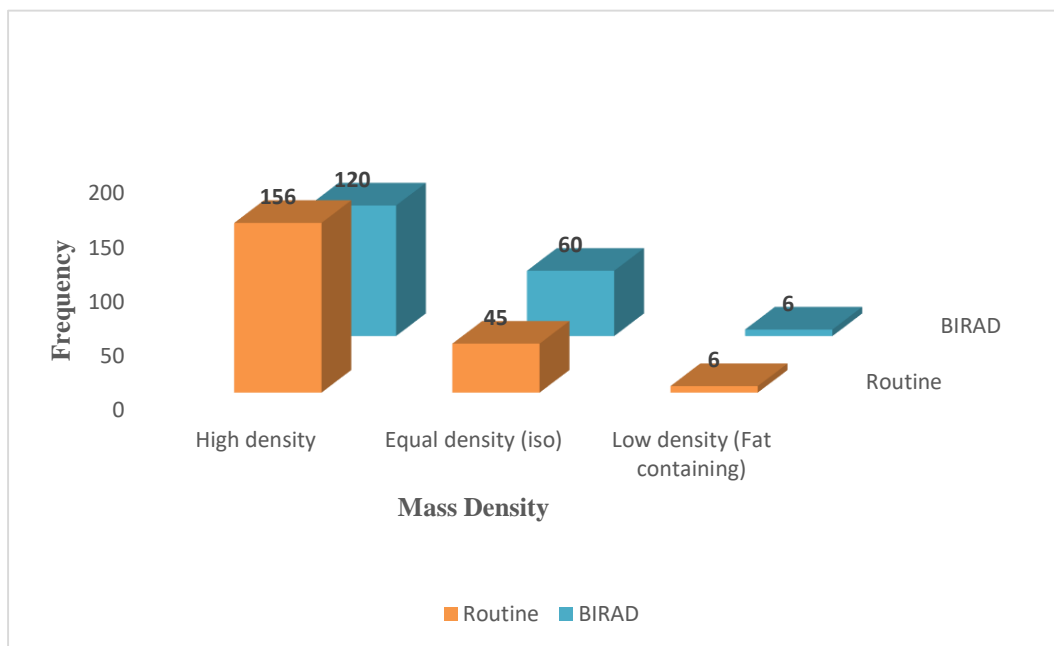


Figure (4.6): distribution of samples according to the mass density

Table (4.7): distribution of samples according to the mass associated calcification

A. In routine interpretation

Mass calcification	Frequency	Percent
Yes	6	2.9
No	201	97.1
Total	207	100

B. In BIRAD interpretation

Mass calcification	Frequency	Percent
Yes	6	3.2
No	180	96.8
Total	186	100



Figure (4.7): distribution of samples according to the mass associated calcification

Table (4.8): distribution of samples according to mass location

A. In routine interpretation

interpretation

Mass location	Frequency	Percent
Retroareolar	30	14.5
Central	3	1.4
Upper outer	57	27.5
Lower inner	6	2.9
Lower outer	12	5.8
Upper anterior	57	27.5
Lower anterior	3	1.4
Upper posterior	11	5.3
Upper middle	17	8.2
Central posterior	6	2.9
Central anterior	3	1.4
Different locations	1	.5
Axillary tail	1	.5
Total	207	100.0

B. In BIRAD

Mass location	Frequency	Percent
Retroareolar	12	6.5
Central	6	3.2
Upper inner	15	8.1
Upper outer	78	41.9
Lower inner	24	12.9
Lower outer	12	6.5
Upper middle	30	16.1
Central posterior	3	1.6
Different locations	3	1.6
Axillary tail	3	1.6
Total	186	62.0

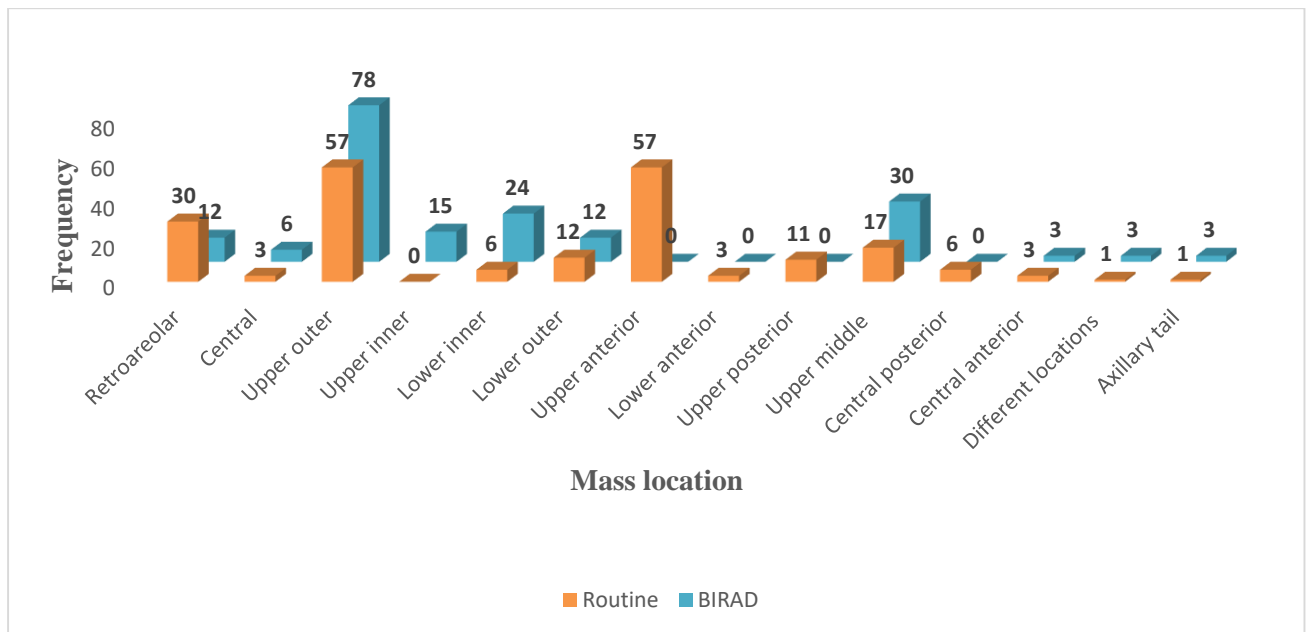


Figure (4.8): distribution of samples according to mass location

Table (4.9): distribution of samples according to calcification presence

A. In routine interpretation

Presence of calcification	Frequency	Percent
Yes	27	9.0
No	273	91.0
Total	300	100.0

B. In BIRAD interpretation

Presence of calcification	Frequency	Percent
Yes	27	9.0
No	261	87.0
Total	288	96.0
Undefined	12	4.0
Total	300	100.0

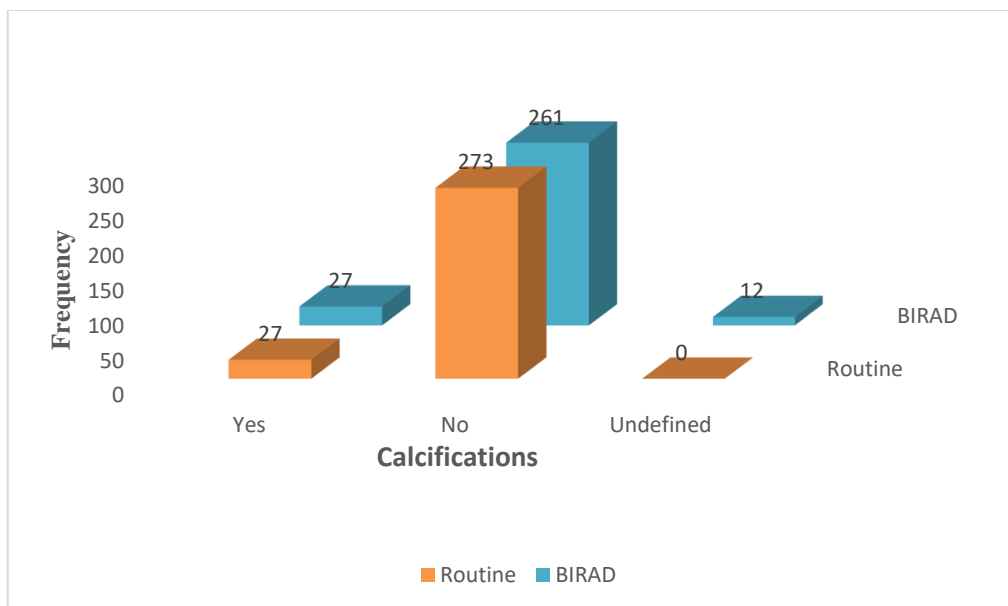


Figure (4.9): distribution of samples according to calcification presence

Table (4.10): distribution of samples according to calcification morphology

A. In routine interpretation

Calcification morphology	Frequency	Percent
Skin	3	11.1
Vascular	9	33.3
Coarse	3	11.1
Large rod-like	3	11.1
Un defined	3	11.1
Fine Pleomorphic	6	22.2
Total	27	100

B. In BIRAD interpretation

Calcification morphology	Frequency	Percent
Skin	3	11.1
Vascular	6	22.2
Coarse	6	22.2
Large rod-like	6	22.2
Fine Pleomorphic	6	22.2
Total	27	100

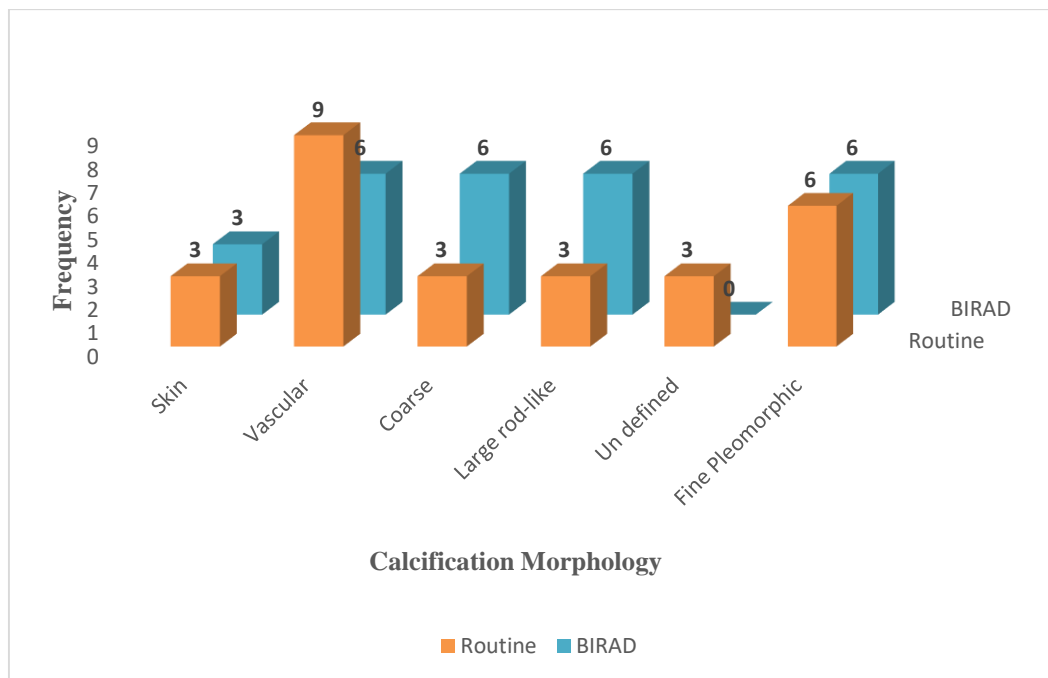


Figure (4.10): distribution of samples according to calcification morphology

Table (4.11): distribution of samples according to calcification distribution

A. In routine interpretation

Calcification distribution	Frequency	Percent
Diffuse	6	28.6
Grouped	6	28.6
Linear	6	28.6
Single	3	14.3
Total	21	100

B. In BIRAD interpretation

Calcification distribution	Frequency	Percent
Diffuse	9	50
Grouped	6	33.3
Single	3	16.7
Total	18	100

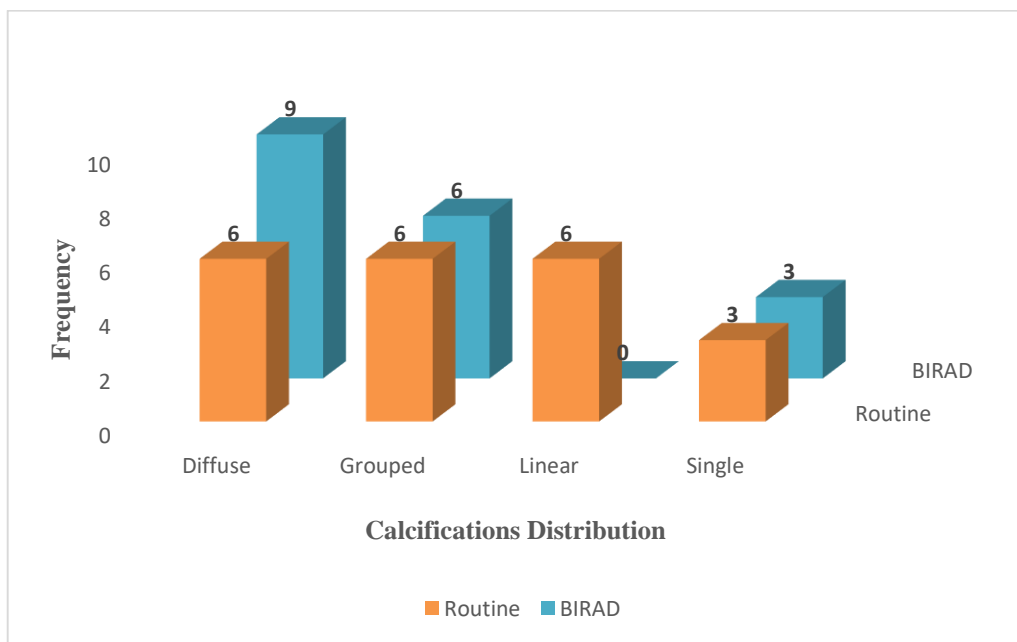


Figure (4.11): distribution of samples according to calcification distribution

Table (4.12): distribution of samples according to calcification location

A. In routine interpretation

Calcification location	Frequency	Percent
Retroareolar	3	33.3
Upper posterior	3	33.3
Upper middle	3	33.3
Total	9	100

B. In BIRAD interpretation

Calcification location	Frequency	Percent
Retroareolar	3	25
Upper outer	6	50
Lower outer	3	25
Total	12	100

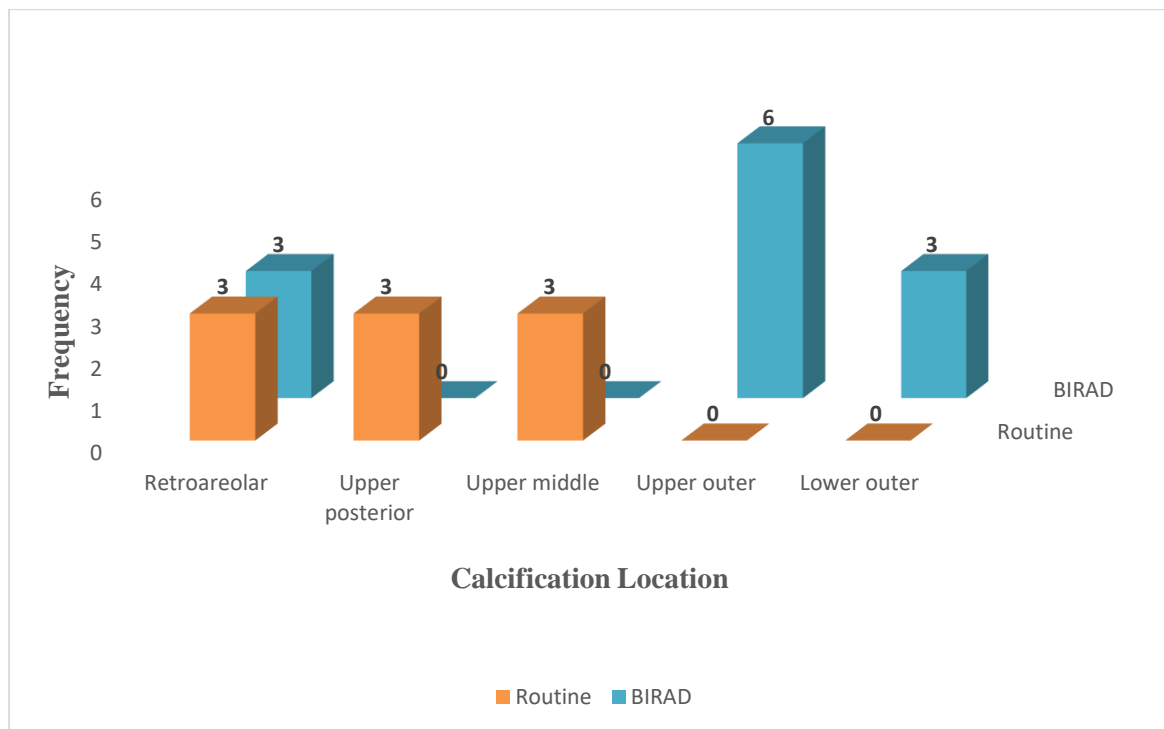


Figure (4.12): distribution of samples according to calcification location

Table (4.13): distribution of samples according to architectural distortion

B. In routine interpretation

B. In BIRAD interpretation

Architectural distortion	Frequency	Percent
Yes	138	46.0
No	162	54.0
Total	300	100.0

Architectural distortion	Frequency	Percent
Yes	117	39.0
No	171	57.0
Total	288	96.0
Undefined	12	4.0
Total	300	100.0

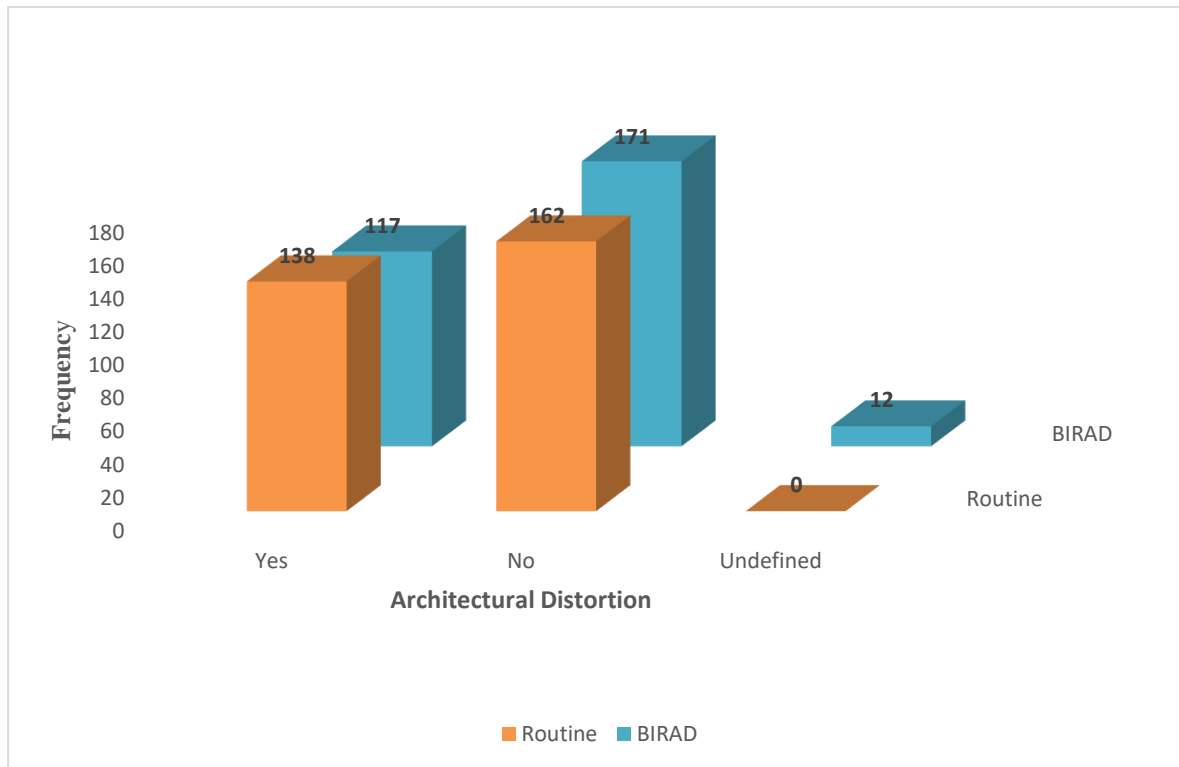


Figure (4.13): distribution of samples according to architectural distortion

Table (4.14): distribution of samples according to presence of asymmetry

A. In routine interpretation

Asymmetry	Frequency	Percent
Yes	3	1.0
No	297	99.0
Total	300	100.0

B. In BIRAD interpretation

Asymmetry	Frequency	Percent
Yes	23	7.7
No	265	88.3
Total	288	96.0
Undefined	12	4.0
Total	300	100.0

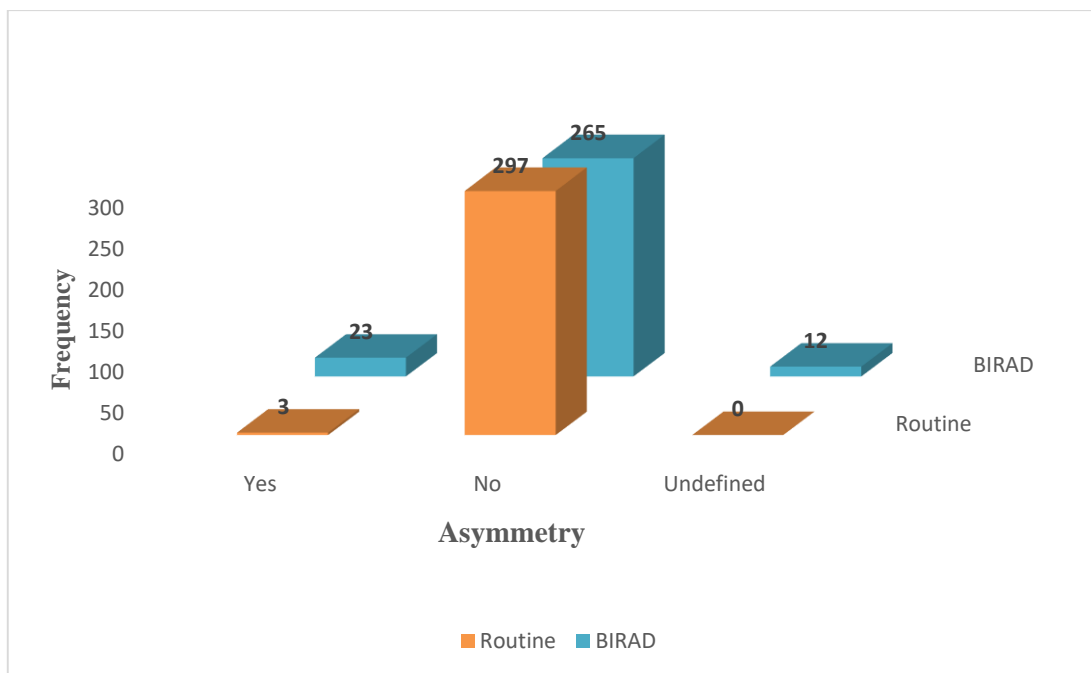


Figure (4.14): distribution of samples according to presence of asymmetry

Table (4.15): distribution of samples according to inflammatory lymph node

A. In routine interpretation

Inflammatory LN	Frequency	Percent
Yes	15	5.0
No	285	95.0
Total	300	100.0

B. In BIRAD interpretation

Inflammatory LN	Frequency	Percent
Yes	12	4.0
No	276	92.0
Total	288	96.0
Undefined	12	4.0
Total	300	100.0

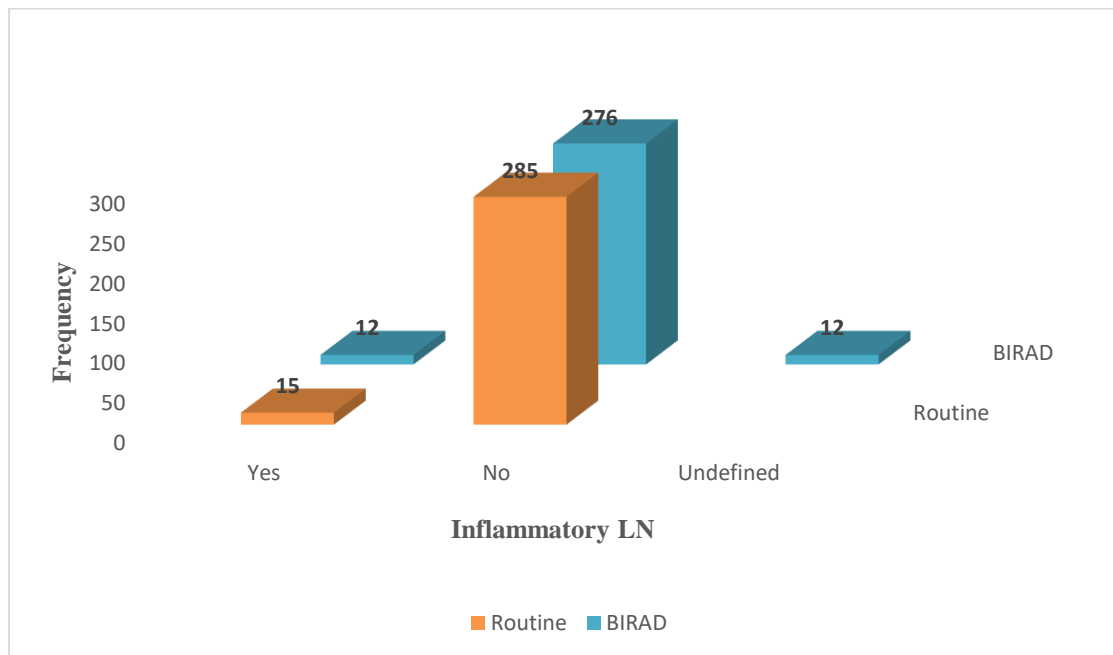


Figure (4.15): distribution of samples according to inflammatory lymph node

Table (4.16): distribution of samples according to associated features

A In routine interpretation

Associated features	Frequency	Percent
No	264	88.0
Skin thickening	15	5.0
Axillary lymph adenopathy	15	5.0
Nipple retraction and skin retraction	3	1.0
Nipple retraction and lymph adenopathy	3	1.0
Total	300	100.0

Associated features	Frequency	Percent
No	208	69.3
Skin retraction	3	1.0
Nipple retraction	6	2.0
Skin thickening	6	2.0
Axillary lymph adenopathy	43	14.3
Multiple small lesions	5	1.7
Skin thickening and lymph adenopathy	15	5.0
Nipple retraction, skin thickening and lymph adenopathy	3	1.0
Dilated superficial vessels	2	.7
Total	291	97.0
Undefined	9	3.0
Total	300	100.0

B. In BIRAD interpretation

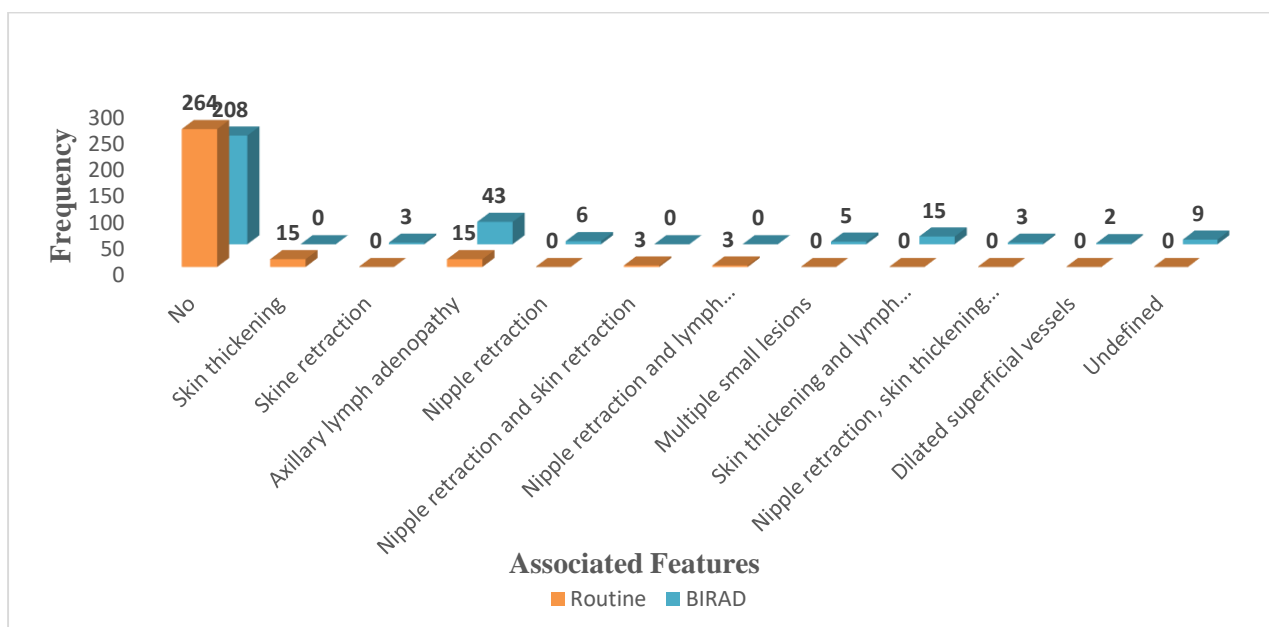


Figure (4.16): distribution of samples according to associated features

Table (4.17): distribution of samples according to solitary dilated duct

A. In routine interpretation

Dilated duct	Frequency	Percent
Yes	0	0
No	300	100.0
Total	300	100/0

B. In BIRAD interpretation

Dilated duct	Frequency	Percent
Yes	2	.7
No	286	95.3
Total	288	96.0
Undefined	12	4.0
Total	300	100.0

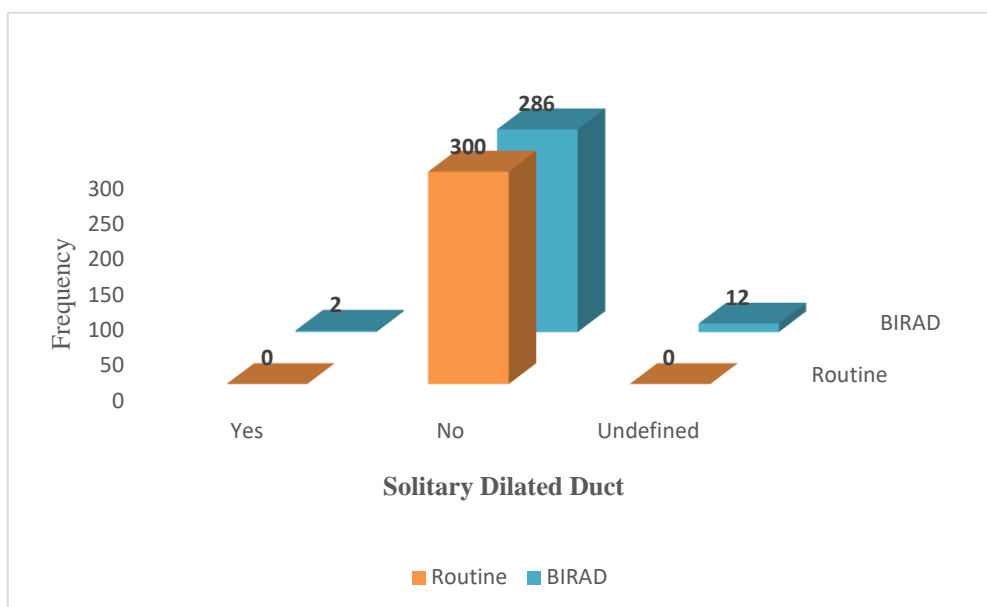


Figure (4.17): distribution of samples according to solitary dilated duct

Table (4.18): distribution of samples according to final findings

A. In routine interpretation

Final finding	Frequency	Percent
Normal finding	69	23.0
Benign	39	13.0
Probably benign	12	4.0
Malignant	165	55.0
Highly malignant	15	5.0
Total	300	100.0

B. In BIRAD interpretation

Final finding	Frequency	Percent
Incomplete	12	4.0
Negative (Normal finding)	54	18.0
Benign	33	11.0
Probably benign	36	12.0
Suspicious malignancy	132	44.0
Highly suggestive malignancy	33	11.0
Total	300	100.0

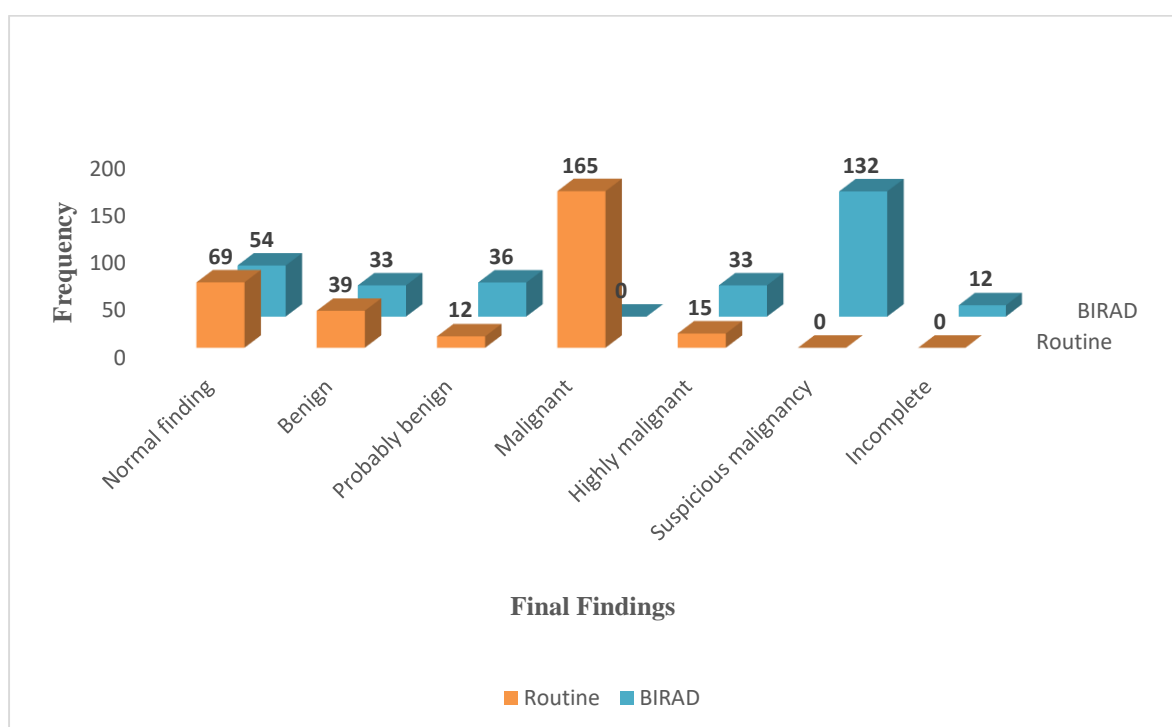


Figure (4.18): distribution of samples according to final findings

Part III: analysis of the breast composition and final findings using BIRAD system according to the age.

**Table (4.19): Correlation of breast composition with age.
(Using chi-square test, P-value = 0.000)**

Age	Distribution of breast composition				Total	
	a	b	c	d		
15 - 30 y	Count	0	0	3	15	18
	% within Distribution of age	0.0%	0.0%	16.7%	83.3%	100.0%
31 - 45 y	Count	0	15	39	15	69
	% within Distribution of age	0.0%	21.7%	56.5%	21.7%	100.0%
46 - 60 y	Count	12	69	36	3	120
	% within Distribution of age	10.0%	57.5%	30.0%	2.5%	100.0%
61 - 75 y	Count	24	36	18	0	78
	% within Distribution of age	30.8%	46.2%	23.1%	0.0%	100.0%
75 - 90 y	Count	0	9	6	0	15
	% within Distribution of age	0.0%	60.0%	40.0%	0.0%	100.0%
Total	Count	36	129	102	33	300
	% within Distribution of age	12.0%	43.0%	34.0%	11.0%	100.0%

Table (4.20): Correlation of final findings with age.
(Using chi-square test, P-value = 0.000)

Final finding		Distribution of age					Total
		15 - 30 y	31 - 45 y	46 - 60 y	61 - 75 y	75 - 90 y	
Incomplete	Count	0	6	0	6	0	12
	% within Distribution of final finding	0.0%	50.0%	0.0%	50.0%	0.0%	100.0%
Negative (Normal finding)	Count	12	9	24	9	0	54
	% within Distribution of final finding	22.2%	16.7%	44.4%	16.7%	0.0%	100.0%
Benign	Count	0	15	9	3	6	33
	% within Distribution of final finding	0.0%	45.5%	27.3%	9.1%	18.2%	100.0%
Probably benign	Count	0	12	21	0	3	36
	% within Distribution of final finding	0.0%	33.3%	58.3%	0.0%	8.3%	100.0%
Suspicious malignancy	Count	6	27	51	42	6	132
	% within Distribution of final finding	4.5%	20.5%	38.6%	31.8%	4.5%	100.0%
Highly suggestive malignancy	Count	0	0	15	18	0	33
	% within Distribution of final finding	0.0%	0.0%	45.5%	54.5%	0.0%	100.0%
Total	Count	18	69	120	78	15	300
	% within Distribution of final finding	6.0%	23.0%	40.0%	26.0%	5.0%	100.0%

Part IV: analysis of the BIRAD parameters according to the final findings.

**Table (4.21): Correlation of breast composition with final findings.
(Using chi-square test, P-value = 0.000)**

Final finding		Distribution of breast composition				Total
		a	b	c	d	
Incomplete	Count	0	6	3	3	12
	% within Distribution of final finding	0.0%	50.0%	25.0%	25.0%	100.0%
Negative (Normal finding)	Count	3	18	15	18	54
	% within Distribution of final finding	5.6%	33.3%	27.8%	33.3%	100.0%
Benign	Count	12	6	12	3	33
	% within Distribution of final finding	36.4%	18.2%	36.4%	9.1%	100.0%
Probably benign	Count	0	30	6	0	36
	% within Distribution of final finding	0.0%	83.3%	16.7%	0.0%	100.0%
Suspicious malignancy	Count	12	60	51	9	132
	% within Distribution of final finding	9.1%	45.5%	38.6%	6.8%	100.0%
Highly suggestive malignancy	Count	9	9	15	0	33
	% within Distribution of final finding	27.3%	27.3%	45.5%	0.0%	100.0%
Total	Count	36	129	102	33	300
	% within Distribution of final finding	12.0%	43.0%	34.0%	11.0%	100.0%

**Table (4.22): Correlation of mass presence with final findings.
(Using chi-square test, P-value = 0.000)**

Final finding		Distribution of presence of mass		Total
		Yes	No	
Negative (Normal finding)	Count	0	54	54
	% within Distribution of final finding	0.0%	100.0%	100.0%
Benign	Count	15	18	33
	% within Distribution of final finding	45.5%	54.5%	100.0%
Probably benign	Count	27	9	36
	% within Distribution of final finding	75.0%	25.0%	100.0%
Suspicious malignancy	Count	114	18	132
	% within Distribution of final finding	86.4%	13.6%	100.0%
Highly suggestive malignancy	Count	30	3	33
	% within Distribution of final finding	90.9%	9.1%	100.0%
Total	Count	186	102	288
	% within Distribution of final finding	64.6%	35.4%	100.0%

Table (4.23): Correlation of mass shape with final findings.
(Using chi-square test, P-value = 0.000)

Final finding		Distribution of mass shape				Total
		Oval	Round	Irregular	Lobulated	
Benign	Count	9	6	0	0	15
	% within Distribution of final finding	60.0%	40.0%	0.0%	0.0%	100.0%
Probably benign	Count	18	6	0	3	27
	% within Distribution of final finding	66.7%	22.2%	0.0%	11.1%	100.0%
Suspicious malignancy	Count	39	30	45	0	114
	% within Distribution of final finding	34.2%	26.3%	39.5%	0.0%	100.0%
Highly suggestive malignancy	Count	3	3	21	3	30
	% within Distribution of final finding	10.0%	10.0%	70.0%	10.0%	100.0%
Total	Count	69	45	66	6	186
	% within Distribution of final finding	37.1%	24.2%	35.5%	3.2%	100.0%

Table (4.24): Correlation of mass margin with final findings.
(Using chi-square test, P-value = 0.000)

Final finding	Distribution of mass margin						Total	
	Circumscribed (Well defined, Sharp)	Obscured (Partially well defined)	Microlobulated	Indistinct (Ill defined)	Speculated	Irregular		
Benign	Count	15	0	0	0	0	0	15
	% within Distribution of final finding	100.0%	0.0%	0.0%	0.0%	0.0%	0.0%	100.0%
Probably benign	Count	15	6	3	3	0	0	27
	% within Distribution of final finding	55.6%	22.2%	11.1%	11.1%	0.0%	0.0%	100.0%
Suspicious malignancy	Count	15	15	24	27	21	12	114
	% within Distribution of final finding	13.2%	13.2%	21.1%	23.7%	18.4%	10.5%	100.0%
Highly suggestive malignancy	Count	0	0	0	3	27	0	30
	% within Distribution of final finding	0.0%	0.0%	0.0%	10.0%	90.0%	0.0%	100.0%
Total	Count	45	21	27	33	48	12	186
	% within Distribution of final finding	24.2%	11.3%	14.5%	17.7%	25.8%	6.5%	100.0%

Table (4.25): Correlation of mass density with final findings.
(Using chi-square test, P-value = 0.000)

Final finding		Distribution of mass density			Total
		High density	Equal density (iso)	Fat containing	
Benign	Count	3	6	6	15
	% within Distribution of final finding	20.0%	40.0%	40.0%	100.0%
Probably benign	Count	9	18	0	27
	% within Distribution of final finding	33.3%	66.7%	0.0%	100.0%
Suspicious malignancy	Count	81	33	0	114
	% within Distribution of final finding	71.1%	28.9%	0.0%	100.0%
Highly suggestive malignancy	Count	27	3	0	30
	% within Distribution of final finding	90.0%	10.0%	0.0%	100.0%
Total	Count	120	60	6	186
	% within Distribution of final finding	64.5%	32.3%	3.2%	100.0%

Table (4.26): Correlation of mass associated calcification with final findings.
(Using chi-square test, P-value = 0.000)

Fnal finding		Distribution of mass associated calcification		Total
		Yes	No	
Benign	Count	0	15	15
	% within Distribution of final finding	0.0%	100.0%	100.0%
Probably benign	Count	0	27	27
	% within Distribution of final finding	0.0%	100.0%	100.0%
Suspicious malignancy	Count	3	111	114
	% within Distribution of final finding	2.6%	97.4%	100.0%
Highly suggestive malignancy	Count	3	27	30
	% within Distribution of final finding	10.0%	90.0%	100.0%
Total	Count	6	180	186
	% within Distribution of final finding	3.2%	96.8%	100.0%

**Table (4.27): Correlation of mass location with final findings.
(Using chi-square test, P-value = 0.000)**

Final finding	Distribution of mass location											
	Retroar eolar	Central	Upper inner	Upper outer	Lower inner	Lower outer	Upper middle (upper central)	Central posterior	Different locations (Multiple)	Axillary tail	Total	
Benign	Count	0	0	0	6	0	0	6	0	0	3	15
	% within Distribution of final finding	0.0%	0.0%	0.0%	40.0%	0.0%	0.0%	40.0%	0.0%	0.0%	20.0%	100.0 %
Probably benign	Count	3	0	9	9	0	0	3	0	3	0	27
	% within Distribution of final finding	11.1%	0.0%	33.3%	33.3%	0.0%	0.0%	11.1%	0.0%	11.1%	0.0%	100.0 %
Suspicious malignancy	Count	9	6	6	45	18	12	18	0	0	0	114
	% within Distribution of final finding	7.9%	5.3%	5.3%	39.5%	15.8%	10.5%	15.8%	0.0%	0.0%	0.0%	100.0 %
Highly suggestive malignancy	Count	0	0	0	18	6	0	3	3	0	0	30
	% within Distribution of final finding	0.0%	0.0%	0.0%	60.0%	20.0%	0.0%	10.0%	10.0%	0.0%	0.0%	100.0 %
Total	Count	12	6	15	78	24	12	30	3	3	3	186
	% within Distribution of final finding	6.5%	3.2%	8.1%	41.9%	12.9%	6.5%	16.1%	1.6%	1.6%	1.6%	100.0 %

Table (4.28): Correlation of presence of calcification with final findings.

(Using chi-square test, P-value = 0.000)

Final finding		Distribution of presence of calcifications		Total
		Yes	No	
Negative (Normal finding)	Count	0	54	54
	% within Distribution of final finding	0.0%	100.0%	100.0%
Benign	Count	15	18	33
	% within Distribution of final finding	45.5%	54.5%	100.0%
Probably benign	Count	0	36	36
	% within Distribution of final finding	0.0%	100.0%	100.0%
Suspicious malignancy	Count	9	123	132
	% within Distribution of final finding	6.8%	93.2%	100.0%
Highly suggestive malignancy	Count	3	30	33
	% within Distribution of final finding	9.1%	90.9%	100.0%
Total	Count	27	261	288
	% within Distribution of final finding	9.4%	90.6%	100.0%

Table (4.29): Correlation of morphology with final findings.
 (Using chi-square test, P-value = 0.856)

Final finding	Distribution of morphology					Total
	Skin	Vascular	Coarse (Popcorn-like)	Large rod-like	Fine Pleomorphic (fine calcification)	
Benign	3	0	6	6	0	15
Count	3	0	6	6	0	15
% within Distribution of final finding	20.0%	0.0%	40.0%	40.0%	0.0%	100.0%
Suspicious malignancy	0	3	0	0	6	9
Count	0	3	0	0	6	9
% within Distribution of final finding	0.0%	33.3%	0.0%	0.0%	66.7%	100.0%
Highly suggestive malignancy	0	3	0	0	0	3
Count	0	3	0	0	0	3
% within Distribution of final finding	0.0%	100.0%	0.0%	0.0%	0.0%	100.0%
Total	3	6	6	6	6	27
Count	3	6	6	6	6	27
% within Distribution of final finding	11.1%	22.2%	22.2%	22.2%	22.2%	100.0%

Table (4.30): Correlation of calcification distribution with final findings.
(Using chi-square test, P-value = 0.223)

Final finding		Distribution of calcifications distribution			Total
		Diffuse (scattered)	Grouped	Single	
Benign	Count	9	0	3	12
	% within Distribution of final finding	75.0%	0.0%	25.0%	100.0%
Suspicious malignancy	Count	0	6	0	6
	% within Distribution of final finding	0.0%	100.0%	0.0%	100.0%
Total	Count	9	6	3	18
	% within Distribution of final finding	50.0%	33.3%	16.7%	100.0%

Table (4.31): Correlation of calcification location with final findings.
(Using chi-square test, P-value = 0.472)

Final finding		Distribution of calcifications location			Total
		Retroareolar	Upper outer	Lower outer	
Benign	Count	3	0	3	6
	% within Distribution of final finding	50.0%	0.0%	50.0%	100.0%
Suspicious malignancy	Count	0	6	0	6
	% within Distribution of final finding	0.0%	100.0%	0.0%	100.0%
Total	Count	3	6	3	12
	% within Distribution of final finding	25.0%	50.0%	25.0%	100.0%

Table (4.32): Correlation of architectural distortion with final findings.
(Using chi-square test, P-value = 0.001)

Final finding		Distribution of architectural distortion		Total
		Yes	No	
Negative (Normal finding)	Count	0	54	54
	% within Distribution of final finding	0.0%	100.0%	100.0%
Benign	Count	0	33	33
	% within Distribution of final finding	0.0%	100.0%	100.0%
Probably benign	Count	3	33	36
	% within Distribution of final finding	8.3%	91.7%	100.0%
Suspicious malignancy	Count	84	48	132
	% within Distribution of final finding	63.6%	36.4%	100.0%
Highly suggestive malignancy	Count	30	3	33
	% within Distribution of final finding	90.9%	9.1%	100.0%
Total	Count	117	171	288
	% within Distribution of final finding	40.6%	59.4%	100.0%

Table (4.33): Correlation of presence of asymmetry with final findings.

(Using chi-square test, P-value = 0.000)

Final finding	Distribution of presence of asymmetry		Total
	Yes	No	
Negative (Normal finding)	Count	0	54
	% within Distribution of final finding	0.0%	100.0%
Benign	Count	3	33
	% within Distribution of final finding	9.1%	90.9%
Probably benign	Count	6	36
	% within Distribution of final finding	16.7%	83.3%
Suspicious malignancy	Count	12	132
	% within Distribution of final finding	9.1%	90.9%
Highly suggestive malignancy	Count	2	33
	% within Distribution of final finding	6.1%	93.9%
Total	Count	23	288
	% within Distribution of final finding	8.0%	92.0%

Table (4.34): Correlation of presence of inflammatory lymph node with final findings.
(Using chi-square test, P-value = 0.000)

Final finding		Distribution of presence of intramammary lymph node		Total
		Yes	No	
Negative (Normal finding)	Count	0	54	54
	% within Distribution of final finding	0.0%	100.0%	100.0%
Benign	Count	0	33	33
	% within Distribution of final finding	0.0%	100.0%	100.0%
Probably benign	Count	3	33	36
	% within Distribution of final finding	8.3%	91.7%	100.0%
Suspicious malignancy	Count	3	129	132
	% within Distribution of final finding	2.3%	97.7%	100.0%
Highly suggestive malignancy	Count	6	27	33
	% within Distribution of final finding	18.2%	81.8%	100.0%
Total	Count	12	276	288
	% within Distribution of final finding	4.2%	95.8%	100.0%

Table (4.35): Correlation of presence of associated features with final findings.
(Using chi-square test, P-value = 0.000)

Final finding	Distribution of presence of associated features										
	No	Skin retraction	Nipple retraction	Skin thickening	Axillary lymph adenopathy	Multiple small lesions	Skin thickening and lymph adenopathy	Nipple retraction, skin thickening and lymph adenopathy	Dilated superficial vessels	Total	
Incomplete	Count % within Distribution of final finding	0 0.0%	0 0.0%	0 0.0%	0 0.0%	3 100.0%	0 0.0%	0 0.0%	0 0.0%	0 0.0%	3 100.0%
Negative (Normal finding)	Count % within Distribution of final finding	54 100.0%	0 0.0%	0 0.0%	0 0.0%	0 0.0%	0 0.0%	0 0.0%	0 0.0%	0 0.0%	54 100.0%
Benign	Count % within Distribution of final finding	31 93.9%	0 0.0%	0 0.0%	0 0.0%	0 0.0%	0 0.0%	0 0.0%	0 0.0%	2 6.1%	33 100.0%
Probably benign	Count % within Distribution of final finding	33 91.7%	0 0.0%	0 0.0%	3 8.3%	0 0.0%	0 0.0%	0 0.0%	0 0.0%	0 0.0%	36 100.0%
Suspicious malignancy	Count % within Distribution of final finding	87 65.9%	3 2.3%	3 2.3%	3 2.3%	24 18.2%	3 2.3%	6 4.5%	3 2.3%	0 0.0%	132 100.0%
Highly suggestive malignancy	Count % within Distribution of final finding	3 9.1%	0 0.0%	3 9.1%	0 0.0%	16 48.5%	2 6.1%	9 27.3%	0 0.0%	0 0.0%	33 100.0%
Total	Count % within Distribution of final finding	208 71.5%	3 1.0%	6 2.1%	6 2.1%	43 14.8%	5 1.7%	15 5.2%	3 1.0%	2 0.7%	291 100.0%

Table (4.36): Correlation of presence of solitary dilated duct with final findings.
(Using chi-square test, P-value = 0.000)

Final finding		Distribution of presence of solitary dilated duct		Total
		Yes	No	
Negative (Normal finding)	Count	0	54	54
	% within Distribution of final finding	0.0%	100.0%	100.0%
Benign	Count	0	33	33
	% within Distribution of final finding	0.0%	100.0%	100.0%
Probably benign	Count	2	34	36
	% within Distribution of final finding	5.6%	94.4%	100.0%
Suspicious malignancy	Count	0	132	132
	% within Distribution of final finding	0.0%	100.0%	100.0%
Highly suggestive malignancy	Count	0	33	33
	% within Distribution of final finding	0.0%	100.0%	100.0%
Total	Count	2	286	288
	% within Distribution of final finding	0.7%	99.3%	100.0%

Part V: analysis of the concordance of findings

Table (4.37): concordance of BIRAD findings with the findings in the routine interpretation (Kappa (K) value)

Parameter		K- value
Breast Composition		0.465
Mass	presence	0.835
	Shape	0.529
	Margin	0.475
	Density	0.742
	Associated calcification	1.000
	Location	0.222
Calcification	Presence	0.877
	Morphology	0.846
	Distribution	1.000
	Location	0.250
Architectural Distortion		0.852
A Symmetry		0.138
Inflammatory lymph node		0.650
Solitary dilated duct		0.000
Associated Features		0.360
Final findings		0.581

Chapter Five:

Discussion, Conclusion

&

Recommendations

5.1 Discussion

Table (4.1) showed **distribution of samples according to age**, first group of the patient (15-30 years) was 18 of 300 represent (6%). Among the older group of the patient (76-90 years) was 15 of 300 represent (5%). The second group of the patients (31-45 years) was 69 of 300 represent (23%), and third group (46-60 years) was 120 of 300 as (40%), the third group of the patients (61-75 years) was 78 of 300 as (26%). the most abundant group was (46-60 years) as (40%). The result goes with previous studies, which mention Fifty-four percent of the women in their study were younger than 50 years old (Geller et al. 2002). Also Arzehger et al mentioned that in there study, both Sensitivity and Specificity were higher below age of 50 than for patient above 50 (Ahmed et al. 2018). In addition, Berg et al mention that the mean age was 48.7 years; median age was 48 years (age range, 26–81 years) (Berg et al. 2004).

According to the distribution of mammographic findings among BIRAD system.

Table (4.2) showed **distribution of samples according to breast composition**, as a classification of breast composition according to routine interpretation the first group is fatty breast that represent 48 of all population (16%), on the other hand the same group that sampled by letter (a) represent 36 of all mammogram re-reported using BIRAD system as (12%). The second group is a scattered fibroglandular that represent 126 (42%) for routine interpretation. On other hand, in BIRAD a (b) group represent 129 (43%). The third group is a heterogeneous fibroglandular represent 105 (35%), for BIRAD system the same category called (c) that represent 102 (34%). The last group describe the breast composition is a dense breast that represent 21 (7%), in BIRAD the same group represent 33 as (11%). The most abundant group was scattered fibroglandular breast

in routine interpretation and (b) group for BIRAD. All previous studies pointed to importance of the inclusion of a statement describing the general breast tissue type in the mammography report. The inclusion of 4 categories describing breast density (ranging from the almost entirely fatty breast to the extremely dense breast) in the standard mammography report is designed to improve the communication of predicted mammographic performance and breast cancer risk (Burnside et al. 2009),(Bertrand et al. 2015),(Ribnikar et al. 2015).

According to the distribution of pathological mammographic findings, the first pathological findings found in this study is **Mass**.

Table (4.3) showed **distribution of samples according to presence of breast masses**, the presence of Mass over all samples was 207 (69%) according to routine interpretation, and 93 of all cases not present a mass (31%). Among to BIRAD the mass present in 186 (62%), and absent in 102 (34%), and 12 (4%) of subject undefined because was classified as category (1), which needed more investigations.

Table (4.4) showed **distribution of samples according to the shape of mass**. According to the shape of mass, oval, round, irregular and lobulated are the descriptor terms used by the radiologist in both way of reporting. The oval shape was found in 51 (24.6%) of 207 that reported as mass in routine interpretation, in compere to finding by BIRAD the oval shape found in 69 (37%) of 186 that reported as mass. The round shape found in 27 (13%) as routine interpretation and 45 (24%) in BIRAD. Irregular shape found in 126 (61%) in routine interpretation and 66 (35.5%) in BIRAD. The lobulated shape found in 3 (1.5%) for routine interpretation and 6 (3%) for BIRAD.

The most descriptor used to describe the mass shape in routine interpretation was irregular as 61% of all cases reported by presence of mass. Moreover, most descriptor used in BIRAD was oval as 37% off all

cases 186, because the lexicon of BIRADS recommend describing the shape regardless the margin that described separately. That showed in increasing of descriptor of irregular margin in the BIRAD in the next paragraph.

Table (4.5) showed **distribution of samples according to the margin of mass**. Regarding to mass margin, the descriptor words as the following: circumscribed, obscured, Microlobulated, indistinct and speculated for routine interpretation as same as BIRAD but increased by irregular margin for BIRAD as additional word in its lexicon. The first descriptor circumscribed found as 45 (22%) for routine interpretation and 45 as (24%) for BIRAD. The second one obscured found in 9 (4%) for routine interpretation, and 21 (11%) for BIRAD. The third one is Microlobulated that found as 3 (1.5%) for routine interpretation and 27 (14.5%) for BIRAD. The fourth one is indistinct that found in 66 (32%) for routine interpretation, and in 33 (18%) for BIRAD. The speculated margin found in 84 (41%) for routine interpretation, and 48 (26%) for BIRAD. The last descriptor is Irregular margin that found only in BIRAD as 12 (7%). The most common descriptor for the mass margin was speculated margin for both routine interpretation and BIRAD.

Table (4.6) showed **distribution of samples according to the mass density**, the result was the mass with the High density found in 156 (75%) for routine interpretation and 120 (65%) for BIRAD. The equal density (iso dense) was found as 45 (22%) for routine interpretation and 60 (32%) for BIRAD. The last descriptor was low density for routine interpretation and found in 6 (3%), respective less BIRADS the word used to describe the same category is Fat containing, which found in 6 (3%). The most common descriptor for mass density was High density for both routine interpretation and BIRAD.

Table (4.7) showed **distribution of samples according to the mass associated calcification**, the result was according to presence of the calcification or not. For routine interpretation 6 masses showed associated calcification and 201 was not, for BIRAD 6 also showed associated calcification and 180 was not. As the same percentage (97%).

Table (4.8) showed **distribution of samples according to mass location**, the description show a big different in a method of location, some radiologist adopt a clock method and others a quarter method with or without pointing of the mass depth as anterior, central and posterior. A common location found in routine interpretation was Upper outer as 57 (27%) and Upper anterior 57 (27%). For BIRAD, the most common location was Upper outer 78 (42%).

Considering BIRAD system provides a standardized classification for mammographic studies (Eberl et al. 2015), so descriptive terms offered by the system helps the radiologist to describe the lesion very well. Related to the research findings for Mass, the shape and margin is the most discriminating morphological criterion between benign and malignant masses. Most circumscribed masses are benign. Nevertheless, due to specific histological characteristics, certain malignant lesions or lesions with a risk of malignancy may appear in the mammography in this falsely reassuring form (Berment et al. 2014). So the results of the research geos with those periviously search about Mass. Irregular shapes, with spicules growing margn into the surrounding tissue, which are more likely to be malignant (Ciecholewski 2017), as the most common findings of mass (irregular shape and speculated margin). In addition, the mass density is a good indicator to tumor benigncy or malignancy, mass density seems to be a good indicator of malignancy (Ferreira et al. 2011) in case of high density mass as founded in the result. Focusing on mass description may be useful

in increasing reliability in mammogram interpretation (Antonio and Crespi 2010).

The second pathological findings found in this study is **Calcification**.

Table (4.9) showed **distribution of samples according to calcification presence**, the calcification found in 27 (9%) and 273 (91%) not showed a calcification according to routine interpretation. 27 (9%) reported with presence of calcification, 261 (87%) not showed a calcification, remaining case reported as Undefined 12 (4%) in BIRAD. Table (4.9)

Table (4.10) showed **distribution of samples according to calcification morphology**. There are a many types of calcifications according to morphology, the study show distribution of samples according to calcification morphology as the following: according to routine interpretation, skin calcification as 3 (11%), vascular 9 (33%), Coarse 3 (11%), Large rod-like 3 (11%) and Fine Pleomorphic 6 (22%). In BIRAD skin as 3 (11%), %, vascular 6 (22%), Coarse 6 (66%), Large rod-like 6 (22%) and Fine Pleomorphic 6 (22%). The most descriptor of calcifications morphology was vascular 9 (33%) and Fine Pleomorphic 6 (22%). Table (4.10)

Table (4.11) showed **distribution of samples according to calcification distribution**. The descriptor for routine interpretation as: Diffuse, Grouped, Linear and single are founded as 6 (28%), 6 (28%), 6 (28%) and 3 (14%) respectively. On the other hand, for BIRAD founded as Diffuse 9 (50%), Grouped 6 (33%) and Single 3 (17%). The most descriptor used to identify to calcification distribution is grouped style.

Table (4.12) show the **distribution of samples according to calcification location**, the result was as the following: Retroareolar 3 (33%), Upper posterior 3 (33%), Upper middle 3 (33%), for routine interpretation. Whereas BIRAD results were Retroareolar 3 (25%), Upper outer 6 (50%), lower outer 3 (25%). The most common location was Upper outer in

BIRAD and equally distributed in routine interpretation between different locations.

Morphology and distribution descriptors can aid in assessing the risk of malignancy of microcalcifications (Bent et al. 2010), according to this study the most descriptive of calcification was fine linear/branching, 16 (70%) of 23 cases and fine pleomorphic, 14 (28%) of 50 cases, that goes with our study result that Fine Pleomorphic was 6 (22%). Other study mention the classifications of calcification according to risk of malignancy as following: typically benign: skin calcifications, milky calcifications. Intermediate: amorphous calcifications. Higher probability of malignant calcifications: linear, branching calcifications for morphology (Balleyguier et al. 2007).

The third pathological findings found in this study is **Architectural Distortion**.

Table (4.13) show **distribution of samples according to architectural distortion**. The result was as the following: the presence of architectural distortion as 138 (46%) and absent in 162 (54%) for routine interpretation. Whereas the presence of architectural distortion as 117 (39%) and absent in 171 (57%) for BIRAD and 12 (4%) of cases undefined because it diagnosed as category 0.

Architectural distortion is the third most common mammographic appearance of non- palpable breast cancer, representing nearly 6% of abnormalities detected on screening mammography (Gaur et al. 2013). Architectural distortion is the most difficult mammographic image to detect (Balleyguier et al. 2007). Improvement in the detection of architectural distortion may be expected to result in better prognosis for patients with early stages of breast cancer (Ayres and Rangayvan 2005). Architectural distortions are due to defective connective tissue harmony

and include convergence areas and local retractions (Boyer and Russ 2014).

The fourth pathological findings found in this study is **asymmetry**.

Table (4.14) show **distribution of samples according to presence of asymmetry**, the result was as the following: the presence of asymmetry as 3 (1%) and absent in 297 (99%) for routine interpretation. Whereas the presence of asymmetry as 23 (7%) and absent in 265 (88%) for BIRAD and 12 (4%) of cases undefined because it diagnosed as category 0.

Asymmetry between the left and the right breast in a pair of mammograms, it can provide clues about the presence of early signs of tumors such as parenchymal distortion. As mentioned by (Tzikopoulos et al. 2011) use the difference in density between two breast to determine Asymmetry of the breast. Also Asymmetry, in some cases related to pathological findings, as mentioned by (Chang et al. 2010), which said that DCIS may appear as a noncalcified focal asymmetry or solitary dilated duct.

The fifth pathological findings found in this study is **inflammatory lymph node**.

Table (4.15) show **distribution of samples according to inflammatory lymph node**, the result was as the following: the presence of inflammatory lymph node as 15 (5%) and absent in 285 (95%) for routine interpretation. Whereas the presence of inflammatory lymph node as 12 (4%) and absent in 276 (92%) for BIRAD and 12 (4%) of cases undefined because it diagnosed as category 0.

The most cases of inflammatory lymph node found in the research needed more evaluation to insure the original, is it benign or malignant and it need other imaging modality like Ultrasound to more evaluation or previous mammographic image to evaluate it. So classified as category 0, that is mean need more image to give a specific diagnosis.

The sixth pathological findings found in this study is **associated features**. Table (4.16) show **distribution of samples according to associated features**. The result was as the following: the associated features presented into 12 (22%) of all cases as: Skin thickening 15 (5%), Axillary lymph Adenopathy 15 (5%), Nipple retraction and Skin retraction 3 (1%), Nipple retraction and lymph Adenopathy 3 (1%) and absent in 264 (88%) for routine interpretation. Regarding to BIRAD, the associated features presented into 83 (28%) of all cases as, Skin retraction 3 (1%), Nipple retraction 6 (2%), Axillary lymph Adenopathy 43 (14%), Multiple small lesions 5 (2%). Skin thickening and lymph Adenopathy 15 (5%), Nipple retraction, Skin thickening and lymph Adenopathy 3 (1%), Dilated superficial vessels 2 (1 %), and 9 (3%) of cases undefined because it diagnosed as category 0. The most common associated features were skin thickening and Axillary Lymph Adenopathy (5%) for routine interpretation whereas Axillary Lymph Adenopathy (14%) for BIRADS.

The result match the previous studies that found that axillary lymph Adenopathy and skin lesion are a common associated feature in mammography. (Zeeshan et al. 2018) mention that, Skin features, such as skin thickening and nipple retraction, were present in 22 (18%) and 10 (8.2%) patients, respectively. Axillary lymph nodes were present in 106 patients (86.9%) in their study. Also (Perera et al. 2016) mention invasion of the IDC leads to skin thickening, nipple retraction.

The seventh pathological findings found in this study is **solitary dilated duct**.

Table (4.17) show **distribution of samples according to solitary dilated duct**. The result was as the following: the presence of solitary dilated duct was 0 (0%) and absent in 300 (100%) for routine interpretation. Whereas the presence of solitary dilated duct was 2 (1%) and absent in 286 (95%)

for BIRAD, and 12 (4%) of cases undefined because it diagnosed as category 0.

The mammographic finding of solitary dilated duct is rare, as found in the result that also mentioned by (Chang et al. 2010) as the isolated finding of a solitary dilated duct identified at mammography is rare. They found only 21 (0.0079%) solitary dilated duct cases in 264,476 consecutive mammography examinations. Also (Scutt et al. 2006) mentioned the group who went on to develop breast cancer had higher breast asymmetry than controls. Some of cases in the result need additional imaging to accurate diagnosis so it diagnose as category 0.

The conclusion of the pathological findings is the **final finding**.

Table (4.18) show **distribution of samples according to final findings**, which found in this study as the following: regarding to routine interpretation Normal finding as 69 (23%), Benign 39 (13%), Probably Benign 12 (4%), Malignant 165 (55%) and Highly Malignant 15 (5%). Regarding to BIRAD, incomplete (**Category 0**) was 12 (4%), Negative or Normal finding (**Category 1**) was 54 (18%), Benign (**Category 2**) 33 (11%), Probably Benign (**Category 3**) 36 (12%), Suspicious Malignant (**Category 4**) 132 (44%), Highly suggestive Malignancy (**Category 5**) 33 (11 %). The most common final findings was Malignant 165 (55%) regarding to routine interpretation also Suspicious Malignant (**Category 4**) 132 (44%) Regarding to BIRAD.

The result reflect the importance of all category in diagnosis of mammography with increasing in Suspicious Malignant and Highly suggestive Malignancy as normal result. Firstly **Category 0**, need more investigation as mentioned in previous study, as (Geller et al. 2002) mention that Category 0 appears to be used inconsistently. Some radiologists use category 0 even when imaging is complete and they are recommending biopsy. In the current study, 20% of the category 0

mammograms were associated with a recommendation for either a clinical consultation or additional imaging. The normal findings **Category 1** reflect there is no pathological findings. The result of Taplin et al, reflect exactly our result, where as in their study found that Among 292,795 women, screening assessments included 269,022 (91.9%) with a “negative” or “benign finding,”. and 11,861 (4.1%) women with screening assessments of “probably benign finding,”. Also 1,625 (0.6%) women with “suspicious abnormality,” most were recommended for biopsy (48.7%) or clinical examination and/or surgical consult (9.0. Among 243 (0.1%) women with screening assessments “highly suggestive of malignancy,” a majority were recommended for biopsy (73.3%) or clinical examination and/or surgical consult (18.1%) consistent with BI-RADS (Taplin et al. 2002). Whereas (Taplin et al. 2002) found that the most common category founded in their study was Category 4.

The correlation between variables of research considered in the BIRAD findings only.

Table (4.19) showed **Correlation of breast composition with age**. Using chi-square test, the achieved P-value was (0.000) that reflect a statistical significant relationship between increasing in age and breast composition. Where 15 (83%) of the first age group (15-30y) was reported as d (dense breast) this consider the high frequency in compere to other groups. Whereas 69 (58%) of age group (61-75y) was reported as b (scattered fibroglandular breast), 24 (31%) of age group (61-75y) was reported as a (fatty breast).

There is a high relationship between age and breast composition, when women increasing in age fibroglandular tissue decreased and replacing by fatty tissue. Berg et al reported that the frequency of dense breasts decreases with increasing age, with 62% of women in their 30s having more than 50% breast density compared with 27% of women in their 60s

(Berg et al. 2004). Several studies have shown decreased mammographic sensitivity in younger women because increasing of breast density (Carney et al. 2003). As Hjerkind et al the Percent Volumetric Mammographic Density (VMD) was inversely associated with a 5-year older age at screening in premenopausal and postmenopausal women (Hjerkind et al. 2018).

Table (4.20) showed **Correlation of final findings with age**, it was statistically significant at P-value of (0.000). The distribution of age groups among the incomplete (**Category 0**) were 6 (50%) in age group 31-45 years, whereas 6 (50%) in age group 61-75 years. Among Negative or Normal finding (**Category 1**) the result was 12 (22%) for the age group of 15-30, and 9 (17%) for age group 31-45, 24 (44%) for age group 46-60, 9 (17%) for age group 61-75 and 0 for age group 75-90. Among Benign (**Category 2**) the result was 0 for the age group of 15-30, 15 (45.5%) for age group 31-45, 9 (27%) for age group 46-60, 3 (9%) for age group 61-75 and 6 (18%) for age group 75-90. Among Probably Benign (**Category 3**) the result was 0 for age group of 15-30, 12 (33%) for age group 31-45, 21 (58%) for age group 46-60 y, 0 for age group of 61-75 y and 3 (9%) for age group of 75-90 y. Among Suspicious Malignant (**Category 4**) the result was 6 (4.5%) for age group 15-30 y, 27 (20%) for age group 31-45y, 51 (39%) for age group 46-60 y, 42 (32%) for age group 61-75 y, 6 (4.5%) for age group 75-90 y. Among Highly suggestive Malignancy (**Category 5**) the result was 0 for both age groups 15-30 and 31- 45y, 15 (45.5%) for age group 46-60 y, 18 (54.5%) for age group 61-75 y, also 0 for age group of 76-90 y.

The possibility of the malignancy increased by the age, so there is a high relation between suspicious of malignancy and increasing in age groups. The most common age group related to pathological findings (benign and malignant) was 46-60 years as 120 (40%), that is close to the study of

Ahmed et al which mention that the both benign and malignant masses were most common in 41-50 age group (Ahmed et al. 2018). (Geller et al. 2002) reported that Fifty-four percent of the women in their study were younger than 50 years old. The percentage of women with mammograms assigned assessment categories 4 and 5 increased with age. After age 40, the use of category 0 decreased with each decade of age, and a decrease in the use of category 3 was noted at age 50. (Bahl et al. 2015) mention that There was a correlation of age with malignancy: The mean age of patients diagnosed with malignancy was 59 years (SD, 12 years) ($p = 0.01$).

Table (4.21) showed **Correlation of breast composition with final findings**, it was statistically significant at P-value of (0.000). The Distribution of breast composition over the final BIRAD Categories were as the following: Among Incomplete (**Category 0**) the result was 0 for a, 6 (50%) for b and 3 (25%) for both c, d. Among Normal finding (**Category 1**) the result was 3 (6%) for a, 18 (33%) for b, 15 (28%) for c and 18 (33%) for d. Among Benign (**Category 2**) the result was 12 (36%) for a, 6 (18%) for b, 12 (36%) for c and 3 (9%) for d. Among Probably Benign (**Category 3**) the result was 0 for both a and d, 30 (83%) for b and 6 (17 %) for c. Among Suspicious Malignant (**Category 4**) the result was 12 (9%) for a, 60 (45.5%) for b, 51 (39%) for c and 9 (7%) for d. Among Highly suggestive Malignancy (**Category 5**) the result was 9 (27%) for both a and b, 15 (46%) for c and 0 for d.

The most common breast composition related with the final finding was b (scattered fibroglandular breast) as 129 (43%). There is a significant relationship as the benign findings increasing in d type and malignancy increasing in a, b types of the breast. According to (Bertrand et al. 2015) Mammographic density (MD) is a strong breast cancer risk factor. They previously reported associations of percent MD with larger and node-positive tumors across all ages.

Table (4.22) showed **Correlation of mass presence with final findings**. It was statistically significant at P-value of (0.000). Among Normal finding (**Category 1**) the result was 0 for presence of mass and 54 (100%) for absence of mass. Among Benign (**Category 2**) the result was 15 (45.5%) for presence of mass and 18 (54.5%) for absence of mass. Among Probably Benign (**Category 3**) the result was 27 (75%) for presence of mass and 9 (25%) for absence of mass. Among Suspicious Malignant (**Category 4**) the result was 114 (86%) for presence of mass and 18 (14%) for absence of mass. Among Highly suggestive Malignancy (**Category 5**) the result was 30 (91%) for presence of mass and 3 (9%) for absence of mass.

The presence of the mass give a great chance to find a suspicious findings or malignant tumor.

Table (4.23) showed **Correlation of mass shape with final findings**. It was statistically significant at P-value of (0.000). Among Benign (**Category 2**) the result was 9 (60%), 6 (40%), 0 and 0 for Oval, Round, Irregular and Lobulated respectively. Among Probably Benign (**Category 3**) the result was 18 (67%), 6 (22%), 0 and 3 (11%) for Oval, Round, Irregular and Lobulated respectively. Among Suspicious Malignant (**Category 4**) the result was 39 (34%), 30 (26%), 45 (40%) and 0 for Oval, Round, Irregular and Lobulated respectively. Among Highly suggestive Malignancy (**Category 5**) the result was 3 (10%), 3(10%), 21 (70%) and 3 (10%) for Oval, Round, Irregular and Lobulated respectively. The mass shape associated with the malignancy findings is an irregular shape.

In recent years, many researchers have investigated the use of computer-extracted image features for classification of breast masses as malignant or benign (Sahiner et al. 2001), that reflect the importance of mass morphology in classification of the mass as benign or malignant. The mass can classified as benign or malignant using morphological characteristics of the mass, as above result the Oval shape of the mass

related to (**Category 2**) that is mean benign, on other hand the irregular shape increased as Suspicious Malignant (**Category 4**) and Highly suggestive Malignancy (**Category 5**). That goes with the study reported that, the mammographic features with highest positive predictive value can be understood in terms of their pathologic correlates. Irregular shape and Spiculated margins indicate that a lesion is invading surrounding tissue or inciting adjacent desmoplastic reaction, suggestive of a malignant process (Lieberman et al. 1998).

Table (4.24) showed **Correlation of mass margin with final findings**. It was statistically significant at P-value of (0.000). Among Benign (**Category 2**) the result was 15 (100%) for Circumscribed (Well defined, Sharp). Among Probably Benign (**Category 3**) the result was 15 (56%), 6 (22%), 3 (11%) and 3 (11%) for Circumscribed (Well defined, Sharp), Obscured (Partially well defined), Microlobulated and Indistinct (Ill defined) respectively. Among Suspicious Malignant (**Category 4**) the result was 15 (13%), 15 (13%), 24 (21%), 27 (24%), 21 (18%) and 12 (10%) for Circumscribed (Well defined, Sharp), Obscured (Partially well defined), Microlobulated and Indistinct (Ill defined), Speculated and Irregular respectively. Among Highly suggestive Malignancy (**Category 5**) the result was 3 (10%) and 27 (90%) for Indistinct (Ill defined) and Speculated. The mass margin associated with the malignancy findings is Speculated margin as 48 (26%).

The mass can classified as benign or malignant using morphological characteristics of the mass as reported by different studies (Sahiner et al. 2001). The morphological features included Mass Margin. Circumscribed masses first indicate benign lesions. In mammography, circumscribed masses of typically benign appearance, placed in category 2 of the BI-RADS system (Berment et al. 2014). Conversely the lesion with irregular margin highly suspected to be malignant. Berment et al reported that the

existence of a non-circumscribed contour, whether microloubrate, masked or indistinct, justifies a biopsy for histological examination (Berment et al. 2014). As above result the circumscribed margin increased with benign findings (**Category 2**), and decreased as malignant result (**Category 4,5**). and irregular margin absent in benign findings (**Category 2**) and increased as Suspicious Malignant (**Category 4**) and Highly suggestive Malignancy (**Category 5**).

Table (4.25) showed **Correlation of mass density with final findings**. It was statistically significant at P-value of (0.000). Among Benign (**Category 2**) the result was 3 (20%), 6 (40%) and 6 (40%) for High density, Iso density and Fat containing respectively. Among Probably Benign (**Category 3**) the result was 9 (33%) and 18 (67%) for High density and Iso density respectively. Among Suspicious Malignant (**Category 4**) the result was 81 (71%) and 33(29%) for High density and Iso density respectively. Among Highly suggestive Malignancy (**Category 5**) the result was 27 (90%) and 10 (3%) for High density and Iso density respectively. The mass density associated with the malignancy findings is High density as 120 (65%).

The mass density is other factor to classify of mass as benign and malignant. As increasing of mass density the malignancy is increased and vice versa. spiculated (or stellar) masses correspond to opacities formed by a dense center from which arise multiple linear radial prolongations called spicules (Berment et al. 2014), that is mean the dense mass associated with speculating margin and malignant tumor. Most of the malignant tumors corresponding to a high-grade proliferation with a high mitotic index (strong cellularity) which justify increasing in density of them, whoever the benign tumor always contain fat or fluids. The result show that Iso density and Fat containing corresponding to (**Category 2**), and High density corresponding to (**Category 4, 5**). Also (M.Á. et al. 2016) mention

the “typical” mammographic feature described for invasive carcinoma is a dense homogeneous central mass with an ill-defined spiculated margin.

Table (4.26) showed **Correlation of mass associated calcification with final findings**. It was statistically significant at P-value of (0.000). The presence of associated classification related to malignancy findings (**Category 4 and Category 5**). Associated calcification related to malignancy. According to (Berment et al. 2014), In mammography, the classic appearance of Tubular carcinoma is that of a small spiculated mass, in 50% of the cases associated with microcalcifications. So the calcification is highly associated with malignancy.

Table (4.27) showed **Correlation of mass location with final findings**. It was statistically significant at P-value of (0.000). Among Benign findings (**Category 2**) the common location associated with it was Upper outer 6 (40%), Upper middle (Upper central) was 6 (40%) and Axillary as 3 (20%). Among Probably Benign (**Category 3**) the common location associated with it was Upper inner and upper outer as 9 (33%), Retroareolar, Upper middle (Upper central) and Different locations (Multiple) as 3 (11%). Among Suspicious Malignant (**Category 4**) the common location associated with it was Upper outer 45 (40%), Lower inner and Upper middle (Upper central) 18 (19%), Lower outer 12 (10%) and Central and Upper inner 6 (5%). Among Highly suggestive Malignancy (**Category 5**) the common location associated with it was Upper outer 18 (60%), Lower inner 6 (20%) and Upper middle (Upper central), Central posterior as 3 (10%). The most common location associated with different pathological findings is Upper outer 78 (42%). The relationship supported by previous studies. the research reflect high relationship between the pathological findings and mass location. (Perera et al. 2016) mention that the right upper outer quadrant (RUOQ) had 43.8% (n=49), left upper outer quadrant (LUOQ), left upper inner quadrant (LUIQ), and right upper inner quadrant

(RUIQ) had 23.2%, 9.8% and 8.0% respectively. Also which found by (Zeeshan et al. 2018) highest number of lesions was located in the right upper outer quadrant (40 cases; 32.8%) with the second-most common location being the left upper-outer quadrant (34 cases; 27.9%). In addition, (Naeem et al. 2008) found that the common location is Upper outer quadrant with 26 cases (56.5%).

Table (4.28) showed **Correlation of presence of calcification with final findings**. It was statistically significant at P-value of (0.000). The result was 15 (46%) of the presence of calcification associated with Benign findings and 12 (17%) associated with Malignant findings of total number of 27.

Presence of calcification is usually associated with malignancy, but when related to mass. In this case, calcifications not associated to mass, that is why it is not related to malignancy. The most calcification founded was vascular, that is classified as benign calcification.

Table (4.29) showed **Correlation of morphology of calcification with final findings**. It was no significant relationship at P-value of (0.856). It was statistically significant at P-value of (0.001).skin calcification 3 (20%), Coarse (Popcorn-like) and Large rod-like 6 (40%). Among Suspicious Malignant (**Category 4**), the result was 3 (33%) Vascular, 6 (67%) Fine Pleomorphic (fine calcification). Among Highly suggestive Malignancy (**Category 5**), the result was 3 (100%) Vascular calcification.

Orel et al reported that Lesions that proved to be malignant was associated with calcifications (Orel et al. 1999). That is match the result, where Pleomorphic (fine calcification) related to Malignant findings. The morphology and distribution of the calcifications indicated to malignancy or not, which appear in the result and match with reporting of the previous studies. Liberman et al reported that irregular calcifications with linear or branching morphology suggest filling of the lumen of a duct involved

irregularly by breast cancer (Lieberman et al. 1998). Bent et al reported that morphology descriptors progressively stratified the risk of malignancy as follows: amorphous, coarse heterogeneous, fine pleomorphic, and fine linear/branching (Bent et al. 2010).

Table (4.30) showed that **Correlation of calcification distribution with final findings**. It was no significant relationship at P-value of (0.223). Among Benign findings (**Category 2**), the result was 9 (75%) Diffuse (scattered), 3 (25%) Single. Among Suspicious Malignant (**Category 4**), the result was total 6 (100%) Grouped calcifications.

Segmental distribution raises the possibility of breast cancer involving a lobe or segment of the breast. Previous studies support the high positive predictive value of these features (Lieberman et al. 1998)

Table (4.31) showed **Correlation of calcification location with final findings**. It was no significant relationship at P-value of (0.472). Among Benign findings (**Category 2**), the result was 3 (50%) Retroareolar and 3 (50%) Lower outer. Among Suspicious Malignant (**Category 4**), the result was 6 (100%) Upper outer. The result consider not significant and that related to original of the mass, some locations related to benign calcification and another related to malignancy as classified in BIRAD atlas.

Table (4.32) showed **Correlation of architectural distortion with final findings**. It was statistically significant at P-value of (0.001). The presence of architectural distortion associate with **Category 3, Category 4** and **Category 5** that is means it related to malignant findings and some of probably benign findings.

The presence of architectural distortion associated with malignancy. According to previous studies that agree with this result. (Bahl et al. 2015) mention that, the 369 patients with architectural distortion, 197 (53.4%) presented for screening mammography and 172 (46.6%) for diagnostic

mammography. Architectural distortion detected on screening and Diagnostic mammography represented malignancy in 68.0%. the cases classified as **Category 3** may be related to benign types but need more follow up, that recommended in BIRAD system, the benign causes of architectural distortion as mentioned by Durand et al are radial scars and other benign proliferative lesions (Durand et al. 2016). Another study support the result, (Gaur et al. 2013) mention that, the two most common types of invasive breast cancers that can produce architectural distortion on mammography are invasive ductal carcinoma (IDC) and invasive lobular carcinoma (ILC), which represent about 70–90% and 5–10% of invasive breast malignancies.

Table (4.33) showed **Correlation of presence of asymmetry with final findings**. It was statistically significant at P-value of (0.000). Among Normal findings (**Category 1**), the result was there is no Asymmetry. Among Benign findings (**Category 2**), the result was 3 (9%) of total 33 with Asymmetry. Among Probably Benign (**Category 3**), the result was 6 (17%) of 36 with Asymmetry. Among Suspicious Malignant (**Category 4**), the result was 12 (9%) of 120 with Asymmetry. Among Highly suggestive Malignancy (**Category 5**), the result was 2 (6%) of 33 with Asymmetry. The most common findings associated with Asymmetry was Suspicious Malignant (**Category 4**).

The presence of asymmetry consider associated to malignancy according to findings that goes with previous studies. (Scutt et al. 2006) mentioned breast asymmetry is related to several of the known risk factors for breast cancer, and that patients with diagnosed breast cancer have more breast volume asymmetry, as measured from mammograms, than age-matched healthy women.

Table (4.34) showed **Correlation of presence of inflammatory lymph node with final findings**. It was statistically significant at P-value of

(0.000). The presence of Inflammatory lymph node associate with **Category 3, Category 4** and **Category 5**. It was related to malignant findings and some of probably benign findings.

There is an association between inflammatory lymph node and malignancy. (Walsh et al. 1997) mention that the most common axillary abnormality revealed on mammography was abnormal lymph nodes. Homogeneously dense (nonfatty) axillary lymph nodes were strongly associated with malignancy. And may be due to a benign reason so can classified as **Category 3**.

Table (4.35) showed **Correlation of presence of associated features with final findings**. It was statistically significant at P-value of (0.000). Among Incomplete (**Category 0**), the result was presence of Axillary lymph Adenopathy in 3 (100%). Among Normal findings (**Category 1**), the result was there is no associated features. Among Benign findings (**Category 2**), the result was presence of Dilated superficial vessels (2%). Among Probably Benign (**Category 3**), the result was presence of Skin thickening (8%). Among Suspicious Malignant (**Category 4**), the result was presence of Skin retraction, Nipple retraction, Skin thickening, Multiple small lesions and Nipple retraction, skin thickening and lymph Adenopathy in (2%) for each one, Axillary lymph Adenopathy (18%) and Skin thickening and lymph Adenopathy (4.5%). Among Highly suggestive Malignancy (**Category 5**), the result was presence of Multiple small lesions (6%), Nipple retraction (9%), Skin thickening and lymph Adenopathy (27%) and Axillary lymph Adenopathy (48.5%).

The most common associated feature was Axillary lymph Adenopathy at (15%). Several studies have suggested that the likelihood of cancer in an impalpable breast lesion can be predicted by careful analysis of its mammographic features and associated features. (Walsh et al. 1997) mention Most (79%) of the axillary abnormalities seen in their study were

abnormal-appearing lymph nodes. Malignant causes (55%) for our cases of abnormal lymph nodes were only slightly more common than benign causes (45%). Also for (Zeeshan et al. 2018) the associated features appear as skin thickening, and nipple retraction; these were present in 22 (18%), and 10 (8.2%) of patients, respectively.

Table (4.36) showed **Correlation of presence of solitary dilated duct with final findings**. It was statistically significant at P-value of (0.000). It was just associated with Probably Benign (**Category 3**) at (6%). The lesion meet the descriptors in the BI-RADS classification. That is mean need short-interval follow-up, usually at 6 months. (Eberl et al. 2015) mention that lack of a recent prior comparison mammogram, and the current lesion was felt to be of low suspicion that is a reason for classification of the pathological findings as (**Category 3**). Also (Chang et al. 2010) mention that Solitary dilated duct is a rare mammographic finding, this series being the largest reported to date. Although few cases are studied, solitary dilated duct appears to have a greater than 2% likelihood of malignancy.

Table (4.37) showed **Concordance of BIRAD findings with the findings in the routine interpretation** using Kappa (K) value. as regard to breast density, the degree of agreement was a Moderate agreement ($k=0.46$) that reflect the difference in visual assessment of radiologist. Determine the ratio between the breast tissue and fatty tissue, which implies the breast density; can be different between one to another. The overall weighted kappa value for breast composition achieved by Ekpo and Ujong was 0.83 (Ekpo et al. 2016).

As regard to Mass, a Very Good agreement was achieved for the presence of mass ($k=0.83$), and for the mass shape the agreement was moderate ($k=0.529$), that reflect the difference in word used to describe mass shape between BIRAD system and routine interpretation. As compere to the result achieved by (Lazarus et al. 2006). Which their study about evaluation

of interobserver variability between breast radiologists by using terminology of the fourth edition of the Breast Imaging Reporting and Data System (BI-RADS), and result was ($k=0.48$) for mass shape. In addition, among the margin of the mass ($k=0.475$) that reflect a Moderate agreement. As regard to Mass density the kappa value was ($k=0.742$) as a good agreement. Determine the mass density as hyper, iso and low may different a little bit visually, but not always an area of disagreement, As compare to the overall kappa value of 0.40 that found for mass density by (Berg et al. 2000). As regard to Associated calcification the Kappa value was ($k=1$) that was a very good agreement. Regarding to Location of the mass, the agreement was ($k=0.222$) that mean a fair agreement, which related to different types of location systems were adopted by radiologist, and not related to actual disagreement.

For Calcifications, as regard to presence of calcifications the K-value of ($k=0.877$) that was a very good agreement. Related to Morphology of Calcifications the K-value of ($k=0.846$) that was a very good agreement, also Distribution of Calcifications the k-value was ($k=1$) that consider as very good agreement. Regarding to Location of calcifications the k-value was ($k=0.250$) that reflect a fair agreement, for the same reason as mass the disagreement related to different types of location systems that adopted by radiologist.

As regard to Architectural Distortion, the k-value was (0.852), which consider a very good agreement. As a regard to The A Symmetry as a finding for both breast mammogram, the k-value= (0.138) that was a poor agreement, which a result for not using of ultrasound as aiding tools for diagnosis and other alternative projections during re-reporting.

Regarding to Inflammatory lymph node, show a Good agreement as ($k=0.650$). As regard to Associated Features, the k-value was (0.360) that reflect a Fair agreement, due to difference in description of the features.

The overall diagnostic and pathological Final findings reflect a Moderate agreement with k-value of (0.581), which a result to the radiologists may have misunderstood some time to the definition of the terms designed by BIRAD system perhaps the description. That match the result found by (Baker, Kornguth, and Floyd Jr 1996). In addition, the level of mammography training of the radiologist in this study affect the misconcordance somehow. Some of the BI-RADS terms included in the “typically benign” category 2 and need more image category 0 may not always represent by the other radiologist adapted the routine interpretation as benign findings. Possibility that, a limited number of descriptive choices by BIRADS for radiologists may not always match the choice of other group of radiologists that freely find a term that they believe adequately describes a lesion. Put this difference not affect diagnostic assessment that may not agree with the BI-RADS assessment of the term selected.

Taken broadly, the study consistent with other studies that reflect the importance of standardization of lexicon that descript the pathological findings in mammography (Bent et al. 2010), (Balleyguier et al. 2007), (Orel et al. 1999). The result of study reflect how far the importance of the controlling and standardization of the wording using in diagnosis of Mammogram. In addition the a Moderate agreement achieved by the study is acceptable for the purpose of study and reflect the normal inter observer variability, consist with others studies like (Antonio and Crespi 2010), (Burivong and Amornvithayacharn 2011) and (Ciatto et al. 2006).

5.2 Conclusion

The research conduct to assess the concordance of findings of mammograms reported using BI-RADS lexicons and the impression and findings of radiologist those using routine interpretation of mammogram. The research was retrospective study design, the data descriptively analyzed and Kappa value was determined to measure the concordance. Regarding to **age**, the most abundant group was (46-60 years) as (40%). Regarding to **Breast composition**, the most abundant group was scattered fibroglandular breast (b) group for both routine interpretation and BIRAD. However the degree of agreement was a Moderate agreement as ($k=0.46$). Regarding to pathological findings, the first pathological findings found in this study was **Mass**. The degree of concordance among the descriptive terms use to describe and define the mass as the following: regarding to the shape of the mass, the most descriptor used to describe the mass shape in routine interpretation was irregular as (61%) of all cases reported by presence of mass. Moreover, most descriptor used in BIRAD was oval as (37%), the agreement was moderate as ($k= 0.529$). Regarding to mass margin, the most common descriptor for the mass margin was speculated margin for both routine interpretation and BIRAD, the agreement was moderate as ($k=0.475$). Regarding to mass density, the most common descriptor for mass density was High density for both routine interpretation and BIRAD, the agreement was good agreement as ($k=0.742$). Regarding to mass associated calcification, 6 cases were present an associated calcifications in both routine interpretation and BIRAD, the agreement was very good agreement as ($k=1$). Regarding to mass location, the most common descriptor for the mass location were Upper outer and Upper anterior as 57 (27%) in routine interpretation. However the most common

location was Upper outer 78 (42%) in BIRAD, the agreement was fair agreement as ($k=0.222$).

The second pathological findings found in this study was **Calcification**. Regarding to presence of calcification, the calcification present in 27 (9%) cases for both routine interpretation and BIRAD, the agreement was very good agreement as ($k=0.877$). Regarding to calcification morphology, the most descriptor of calcifications morphology was vascular 9 (33%) in routine interpretation and Fine Pleomorphic 6 (22%) in BIRAD, the agreement was very good agreement as ($k=0.846$). Regarding to calcification distribution, the most descriptor used to identify to calcification distribution is grouped style, the agreement was very good agreement as ($k=1$). Regarding to calcification location, the most common location was Upper outer in BIRAD and equally distributed in routine interpretation between different locations, the agreement was that fair agreement as ($k=0.250$).

The third pathological findings found in this study was **Architectural Distortion**. Regarding to presence of Architectural Distortion, the architectural distortion present in 138 for routine interpretation. Whereas 117 for BIRAD, the agreement was very good agreement as ($k=0.852$).

The fourth pathological findings found in this study was **asymmetry**. Regarding to presence of asymmetry, the presence of asymmetry as 3 (1%) for routine interpretation. Whereas 23 (7%) for BIRAD, the agreement was a poor agreement as ($k=0.138$).

The fifth pathological findings found in this study is **inflammatory lymph node**. Regarding to presence of inflammatory lymph node, the presence of inflammatory lymph node as 15 (5%) for routine interpretation. Whereas 12 (4%) for BIRAD, the agreement was a Good agreement as ($k=0.650$).

The sixth pathological findings found in this study is **associated features**. The most common associated features were skin thickening and Axillary

Lymph Adenopathy (5%) for routine interpretation whereas Axillary Lymph Adenopathy (14%) for BIRADS, the agreement was a Fair agreement as ($k=0.360$).

The seventh pathological findings found in this study is **solitary dilated duct**. Regarding to presence of solitary dilated duct, the presence of solitary dilated duct was 0 (0%) for routine interpretation. Whereas 2 (1%) for BIRAD, there was no agreement.

Regarding to **Final Findings**, The most common final findings was Malignant 165 (55%) regarding to routine interpretation also Suspicious Malignant (**Category 4**) 132 (44%) Regarding to BIRAD, the agreement was Moderate agreement with k-value of (0.581).

The research found a significant relationship between the different variables such as breast composition with age, final findings with age, mass presence with final findings, mass shape with final findings, mass margin with final findings, mass density with final findings, mass associated calcification with final findings, mass location with final findings, presence of calcification with final findings, architectural distortion with final findings, presence of asymmetry with final findings, presence of inflammatory lymph node with final findings, presence of associated features with final findings and presence of solitary dilated duct with final findings.

Mammography is a valuable tool in the early detection of breast cancer, but radiologists can present considerably different interpretations and recommendations for follow-up. Efforts to reduce variability in interpretations may help to increase the efficacy of mammography using BI-RADS.

The great limitation of the study is that the number of readers was relatively small. Also, the generalizability of the results was limited because readers were in different level of skills, qualifications and practice and were

working in the different clinical setting. As a recommendation to reduce limitations Additional investigation with larger populations and more readers is necessary to further assessment with taken the level of experience of radiologist in consider. Finally, the implementation of the BIRAD in all mammography facilities will support the completion of quality improvement activities and clinical research in addition to diagnosis benefits. Moreover, decrease the inconsistencies in mammography reports.

5.3 Recommendation

1. Using the computed aid diagnostic program to help in accurate diagnosis of mammograms.
2. More training to the radiologist about BIRAD system.
3. The good quality control program must tightly control the technical aspect of the mammography.
4. Statement of mammography quality standards related to international standards and focused to problems meets the mammography units in Sudan.
5. Good training to the mammography technologist and radiologist because the whole procedure of imaging and interpretation depending on them.
6. Following the Special designed Mammography Accreditation program improve the quality of mammography services.
7. More researches to measure the efficiency and accuracy of using BIRAD final category in comparative to histopathology findings in Sudan.

References

- Ahmed, Aliya, Ramish Riaz, and Ghazala Malik. 2018. "Digital Mammography: A Useful Tool for Differentiating Benign from Malignant Breast Masses." *Rawal Medical Journal* 43(4):743–46.
- Antonio, Anna Liza M. and Catherine M. Crespi. 2010. "Predictors of Interobserver Agreement in Breast Imaging Using the Breast Imaging Reporting and Data System." *Breast Cancer Research and Treatment* 120(3):539–46.
- Appleton, Catherine M. and Kimberly N. Wiele. 2012. *BREAST IMAGING CASES Cases in Radiology*. Oxford.
- Arzehgar, Afrooz, Mohammad M. Khalilzadeh, and Fatemeh Varshoei. 2019. "Assessment and Classification of Mass Lesions Based on Expert Knowledge Using Mammographic Analysis." *Current Medical Imaging Reviews* 15(2):199–208.
- Ayres, Fabio J. and R. M. Rangayvan. 2005. "Characterization of Architectural Distortion in Mammograms." *IEEE Engineering in Medicine and Biology Magazine* 24(1):59–67.
- Bahl, Manisha, Jay A. Baker, Emily N. Kinsey, and Sujata V. Ghate. 2015. "Architectural Distortion on Mammography: Correlation with Pathologic Outcomes and Predictors of Malignancy." *American Journal of Roentgenology* 205(6):1339–45.
- Baker, Jay A., Phyllis J. Kornguth, and C. E. Floyd Jr. 1996. "Breast Imaging Reporting and Data System Standardized Mammography Lexicon: Observer Variability in Lesion Description." *AJR. American Journal of Roentgenology* 166(4):773–78.
- Balleyguier, Corinne, Salma Ayadi, Kim Van Nguyen, Daniel Vanel, Clarisse Dromain, and Robert Sigal. 2007. "BIRADS™ Classification in Mammography." *European Journal of Radiology* 61(2):192–94.
- Bassett, Lawrence W., Mary C. Mahoney, Sophia Apple, and Carl D'Orsi. 2010. *Breast Imaging Expert Radiology Series E-Book: Expert Radiology Series*. Elsevier Health Sciences.
- Baum, Janet K., Lucy G. Hanna, Mary C. Mahoney, Emily F. Conant,

- Lawrence W. Bassett, and Etta D. Pisano. 2011. "Use of BI-RADS 3 – Probably Benign Category in the American College of Radiology Imaging Network Digital Mammographic Imaging Screening Trial 1 Methods : Results :” *Radiology* 260(1):61–67.
- Bent, Chris K., Lawrence W. Bassett, Carl J. D’Orsi, and James W. Sayre. 2010. "The Positive Predictive Value of BI-RADS Microcalcification Descriptors and Final Assessment Categories.” *American Journal of Roentgenology* 194(5):1378–83.
- Berg, Wendie A., Cristina Campassi, Patricia Langenberg, and Mary J. Sexton. 2000. "Breast Imaging Reporting and Data System: Inter-and Intraobserver Variability in Feature Analysis and Final Assessment.” *American Journal of Roentgenology* 174(6):1769–77.
- Berg, Wendie A., Lorena Gutierrez, Moriel S. NessAiver, W. Bradford Carter, Mythreyi Bhargavan, Rebecca S. Lewis, and Olga B. Ioffe. 2004. "Diagnostic Accuracy of Mammography, Clinical Examination, US, and MR Imaging in Preoperative Assessment of Breast Cancer.” *Radiology* 233(3):830–49.
- Berment, H., V. Becette, M. Mohallem, F. Ferreira, and P. Chérel. 2014. "Masses in Mammography: What Are the Underlying Anatomopathological Lesions?” *Diagnostic and Interventional Imaging* 95(2):124–33.
- Bertrand, Kimberly A., Christopher G. Scott, Rulla M. Tamimi, Matthew R. Jensen, V. Shane Pankratz, Aaron D. Norman, Daniel W. Visscher, Fergus J. Couch, John Shepherd, Yunn Yi Chen, Bo Fan, Fang Fang Wu, Lin Ma, Andrew H. Beck, Steven R. Cummings, Karla Kerlikowske, and Celine M. Vachon. 2015. "Dense and Nondense Mammographic Area and Risk of Breast Cancer by Age and Tumor Characteristics.” *Cancer Epidemiology Biomarkers and Prevention* 24(5):798–809.
- Bontrager, Kenneth L. and John Lampignano. 2013. *Textbook of Radiographic Positioning and Related Anatomy*. eighth edi. Elsevier Health Sciences.
- Boyd, Norman F., Gina A. Lockwood, Jeff W. Byng, David L. Tritchler, and Martin J. Yaffe. 1998. "Mammographic Densities and Breast Cancer Risk.” *Cancer Epidemiology and Prevention Biomarkers* 7(12):1133–44.
- Boyer, B. and E. Russ. 2014. "Anatomical-Radiological Correlations: Architectural Distortions.” *Diagnostic and Interventional Imaging*

95(2):134–40.

- Burivong, WANAPORN and Ornsiri Amornvithayacharn. 2011. “Accuracy of Subcategories A, B, C in BI-RADS 4 Lesions. by Combined Mammography and Breast Ultrasound Findings.” *Journal of Medicine and Medical Sciences* 2(3):728–33.
- Burnside, Elizabeth S., Edward A. Sickles, Lawrence W. Bassett, Daniel L. Rubin, Carol H. Lee, Debra M. Ikeda, Ellen B. Mendelson, Pamela A. Wilcox, Priscilla F. Butler, and Carl J. D’Orsi. 2009. “The ACR BI-RADS® experience: Learning from History.” *Journal of the American College of Radiology* 6(12):851–60.
- Butler, Priscilla, Pamela Platt, Kathleen Lorig, Eric Berns, and others. 2017. “Mammography Accreditation and the New ACR Digital Mammography QC Manual.”
- Carney, Patricia A., Mark Dignan, Gary Cutter, Rachel Ballard-Barbash, Diana L. Miglioretti, Bonnie C. Yankaskas, Karla Kerlikowske, Robert Rosenberg, Carolyn M. Rutter, Berta M. Geller, Linn A. Abraham, and Steven H. Taplin. 2003. “Individual and Combined Effects of Age, Breast Density, and Hormone Replacement Therapy Use on the Accuracy of Screening Mammography.” *Annals of Internal Medicine* 138(3):168–75.
- Chan, Heang-Ping, Mark A. Helvie, Lubomir Hadjiiski, Deborah O. Jeffries, Katherine A. Klein, Colleen H. Neal, Mitra Noroozian, Chintana Paramagul, and Marilyn A. Roubidoux. 2017. “Characterization of Breast Masses in Digital Breast Tomosynthesis and Digital Mammograms: An Observer Performance Study.” *Academic Radiology* 24(11):1372–79.
- Chang, C. Belinda, Natalya M. Lvoff, Jessica W. Leung, R. James Brenner, Bonnie N. Joe, Hilda H. Tso, and Edward A. Sickles. 2010. “Solitary Dilated Duct Identified at Mammography: Outcomes Analysis.” *American Journal of Roentgenology* 194(2):378–82.
- Ciatto, S., N. Houssami, A. Apruzzese, E. Bassetti, B. Brancato, F. Carozzi, S. Catarzi, M. P. Lamberini, G. Marcelli, R. Pellizzoni, and others. 2006. “Reader Variability in Reporting Breast Imaging According to BI-RADS® assessment Categories (the Florence Experience).” *The Breast* 15(1):44–51.
- Ciecholewski, Marcin. 2017. “Malignant and Benign Mass Segmentation in Mammograms Using Active Contour Methods.” *Symmetry* 9(11).

- Conant, Emily F. and Cecilia Brennecke. 2006. *BREAST IMAGING: CASE REVIEW*. MOSBY ELSEVIER.
- Cupido, B. D., F. Vawda, A. Sabri, and C. T. Sikwila. 2013. "Evaluation and Correlation of Mammographically Suspicious Lesions with Histopathology at Addington Hospital, Durban." *South African Medical Journal* 103(4):251–54.
- D’Orsi, Carl J. 2013. *ACR BI-RADS Atlas: Breast Imaging Reporting and Data System*. American College of Radiology.
- DeSantis, Carol E., Freddie Bray, Jacques Ferlay, Joannie Lortet-Tieulent, Benjamin O. Anderson, and Ahmedin Jemal. 2015. "International Variation in Female Breast Cancer Incidence and Mortality Rates." *Cancer Epidemiology Biomarkers and Prevention* 24(10):1495–1506.
- Dronkers, Daniel J. 2002. *The Practice of Mammography: Pathology, Technique, Interpretation, Adjunct Modalities*. Thieme Medical Publishers.
- Durand, Melissa A., Steven Wang, Regina J. Hooley, Madhavi Raghu, and Liane E. Philpotts. 2016. "Tomosynthesis-Detected Architectural Distortion: Management Algorithm with Radiologic-Pathologic Correlation." *Radiographics* 36(2):311–21.
- Eberl, Margaret M., Chester H. Fox, Stephen B. Edge, Cathleen a Carter, and Martin C. Mahoney. 2015. "BI-RADS Classification for Management of Abnormal Mammograms." *Journal of the American Board of Family Medicine : JABFM* 19(2):161–64.
- Ekpo, E. U., P. Hogg, R. Highnam, and M. F. McEntee. 2015. "Breast Composition: Measurement and Clinical Use." *Radiography* 21(4).
- Ekpo, Ernest U., Ujong Peter Ujong, Claudia Mello-Thoms, and Mark F. McEntee. 2016. "Assessment of Interradiologist Agreement Regarding Mammographic Breast Density Classification Using the Fifth Edition of the BI-RADS Atlas." *American Journal of Roentgenology* 206(5):1119–23.
- Ferreira, Pedro, Nuno A. Fonseca, Inês Dutra, Ryan Woods, and Elizabeth Burnside. 2011. "Predicting Malignancy from Mammography Findings and Surgical Biopsies." Pp. 339–44 in *Bioinformatics and Biomedicine (BIBM), 2011 IEEE International Conference on*.
- Flowers, Chris I. and Markus K. Holzhauser. 2014. *BREAST IMAGING*.

McGraw-Hill Education.

Frank, Eugene D., Bruce W. Long, and Barbara J. Smith. 2013. *Merrill's Atlas of Radiographic Positioning and Procedures*. Vol. 3. Elsevier Health Sciences.

Gard, Charlotte C., Erin J. Aiello Bowles, Diana L. Miglioretti, Stephen H. Taplin, and Carolyn M. Rutter. 2015. "Misclassification of Breast Imaging Reporting and Data System (BI-RADS) Mammographic Density and Implications for Breast Density Reporting Legislation." *Breast Journal* 21(5).

Gaur, Shantanu, Vandana Dialani, Priscilla J. Slanetz, and Ronald L. Eisenberg. 2013. "Architectural Distortion of the Breast." *American Journal of Roentgenology* 201(5):662–70.

Geller, Berta M., William E. Barlow, Rachel Ballard-Barbash, Virginia L. Ernster, Bonnie C. Yankaskas, Edward A. Sickles, Patricia A. Carney, Mark B. Dignan, Robert D. Rosenberg, Nicole Urban, and others. 2002. "Use of the American College of Radiology BI-RADS to Report on the Mammographic Evaluation of Women with Signs and Symptoms of Breast Disease." *Radiology* 222(2):536–42.

Hashimoto, Beverly. 2010. *Multimodality Breast Imaging: A Correlative Atlas*. Thieme New York.

Hashimoto, Beverly E. 2010. *Multimodality Breast Imaging*. Second edi. Thieme New York.

Hjerkind, Kirsti Vik, Merete Ellingjord-Dale, Anna L. V Johansson, Hildegunn Siv Aase, Solveig Roth Hoff, Solveig Hofvind, Siri Fagerheim, Isabel dos-Santos-Silva, and Giske Ursin. 2018. "Volumetric Mammographic Density, Age-Related Decline, and Breast Cancer Risk Factors in a National Breast Cancer Screening Program." *Cancer Epidemiology and Prevention Biomarkers* 27(9):1065–74.

Hogg, Peter and Claire Mercer. 2015. *Digital Mammography A Holistic Approach*. Springer.

Huo, C. W., G. L. Chew, K. L. Britt, W. V. Ingman, M. A. Henderson, J. L. Hopper, and E. W. Thompson. 2014. "Mammographic Density - A Review on the Current Understanding of Its Association with Breast Cancer." *Breast Cancer Research and Treatment*.

Ikeda, Debra M. and Kanae Kawai Miyake. 2017. *THE REQUISITES BREAST IMAGING*. Third edit. Elsevier.

- Irshad, Abid, Rebecca Leddy, Susan Ackerman, Abbie Cluver, Dag Pavic, Ahad Abid, and Madelene C. Lewis. 2016. "Effects of Changes in BI-RADS Density Assessment Guidelines (Fourth versus Fifth Edition) on Breast Density Assessment: Intra-and Interreader Agreements and Density Distribution." *American Journal of Roentgenology* 207(6).
- Kanavos, P. 2006. "The Rising Burden of Cancer in the Developing World." *Annals of Oncology* 17(SUPPL. 8):15–23.
- Lazarus, Elizabeth, Martha B. Mainiero, Barbara Schepps, Susan L. Koelliker, and Linda S. Livingston. 2006. "BI-RADS Lexicon for US and Mammography: Interobserver Variability and Positive Predictive Value." *Radiology* 239(2):385–91.
- Lee, Karen A., Nishi Talati, Rebecca Oudsema, Sharon Steinberger, and Laurie R. Margolies. 2018. "BI-RADS 3 : Current and Future Use of Probably Benign." *Current Radiology Reports*.
- Liberman, L., A. F. Abramson, F. B. Squires, J. R. Glassman, and E. A. at al Morris. 1998. "The Breast Imaging Reporting and Data System : Positive Predictive Value of Mammographic Features and Final Assessment Categories." *AJR* 73(July):35–40.
- M.Á., Pinochet Tejos, Altamirano Salazar A.V., Horvath Polos E., Uchida Silva M., Silva Fuente-Alba C., and Darrás Ismael C. 2016. "Distorsion of Breast Architecture: The Best Way to Confront It." *Revista Chilena de Radiologia* 22(4):158–63.
- Martin, John E. 1988. *Atlas of Mammography: Histologic and Mammographic Correlations*. Williams & Wilkins Baltimore, MD.
- McLelland, Robert, R. E. Hendrick, Mane D. Zininger, and Pamela A. Wilcox. 1991. "The American College of Radiology Mammography Accreditation Program." *AJR. American Journal of Roentgenology* 157(3):473–79.
- Mohindra, Namita, Zafar Neyaz, Vinita Agrawal, Gaurav Agarwal, and Prabhakar Mishra. 2018. "Impact of Addition of Digital Breast Tomosynthesis to Digital Mammography in Lesion Characterization in Breast Cancer Patients." *International Journal of Applied and Basic Medical Research* 8(1):33.
- Naeem, Muhammad, Nadim Khan, Zahid Aman, Amir Nasir, Ambreen Samad, and Abbas Khattak. 2008. "Pattern of Breast Cancer: Experience at Lady Reading Hospital, Peshawar." *Journal of Ayub*

Medical College, Abbottabad : JAMC 20(4):22–25.

- NG, E. Y. K., U. Rajendra Acharya, R. M. Rangayvan, and Jasjit S. Suri. 2013. *Multimodality Breast Imaging Diagnosis and Treatment*. First edit. Washington USA: SPIE.
- Orel, Susan G., Nicole Kay, Carol Reynolds, and Daniel C. Sullivan. 1999. “BI-RADS Categorization As a Predictor of Malignancy.” *Radiology* 211(3):845–50.
- Perera, D. C., G. B. Hettiarachchi, N. V. I. Ratnatunga, P. V. R. Kumarasiri, and P. B. Hewavithana. 2016. “Demographic, Clinical and Mammographic Characteristics of Invasive Ductal Carcinoma of the Breast; A Sri Lankan Experience.” *Sri Lanka Journal of Radiology* 2(2):1.
- Rastogi, Tanuja, Allan Hildesheim, and Rashmi Sinha. 2004. “Opportunities for Cancer Epidemiology in Developing Countries.” *Nature Reviews Cancer* 4(11):909.
- Ribnikar, D., J. M. Ribeiro, D. Pinto, B. Sousa, A. C. Pinto, E. Gomes, E. C. Moser, M. J. Cardoso, and F. Cardoso. 2015. “Breast Cancer Under Age 40: A Different Approach.” *Current Treatment Options in Oncology* 16(4).
- Saeed, Intisar E., Hsin Yi Weng, Kamal H. Mohamed, and Sulma I. Mohammed. 2014. “Cancer Incidence in Khartoum, Sudan: First Results from the Cancer Registry, 2009-2010.” *Cancer Medicine* 3(4):1075–84.
- Sahiner, B., H. P. Chan, N. Petrick, M. A. Helvie, and L. M. Hadjiiski. 2001. “Improvement of Mammographic Mass Characterization Using Spiculation Measures and Morphological Features.” *Medical Physics* 28(7):1455–65.
- Salkoweski, Lonie. 2013. *RadCases Breast Imaging*. Thieme.
- Scanlon, Valerie C. and Tina Sanders. 2018. *Essentials of Anatomy and Physiology*. fifth edit. FA Davis.
- Scutt, Diane, Gillian A. Lancaster, and John T. Manning. 2006. “Breast Asymmetry and Predisposition to Breast Cancer.” *Breast Cancer Research* 8(2):1–7.
- Shah, Biren A. and Sabala R. Mandava. 2014. *Breast Imaging : A Core Review*. first edit. LIPPINCOTT WILLIAMS & WILKINS, a WOLTERS KLUWER health.

- Shi, Jiazheng, Berkman Sahiner, Heang-Ping Chan, Jun Ge, Lubomir Hadjiiski, Mark A. Helvie, Alexis Nees, Yi-Ta Wu, Jun Wei, Chuan Zhou, Yiheng Zhang, and Jing Cui. 2007. "Characterization of Mammographic Masses Based on Level Set Segmentation with New Image Features and Patient Information." *Medical Physics* 35(1):280–90.
- Sickles, EA, D’Orsi CJ, and Bassett LW. 2013. *ACR BI-RADS® Atlas, Breast Imaging Reporting and Data System*.
- Spak, D. A., J. S. Plaxco, L. Santiago, M. J. Dryden, and B. E. Dogan. 2017. "BI-RADS® fifth Edition: A Summary of Changes." *Diagnostic and Interventional Imaging* 98(3):179–90.
- Sprague, Brian L., Emily F. Conant, Tracy Onega, Michael P. Garcia, Elisabeth F. Beaber, Sally D. Herschorn, Constance D. Lehman, Anna N. A. Tosteson, Ronilda Lacson, Mitchell D. Schnall, Despina Kontos, Jennifer S. Haas, Donald L. Weaver, and William E. Barlow. 2016. "Variation in Mammographic Breast Density Assessments among Radiologists in Clinical Practice: A Multicenter Observational Study." *Annals of Internal Medicine* 165(7).
- Standerling, Susan and others. 2005. *Gray’s Anatomy. The Anatomical Basis of Clinical Practice*. London: Elsevier Churchill Livingstone.
- Tabár, László and Peter B. Dean. 2012. *Teaching Atlas of Mammography*. 4 th. New York: Thieme New York.
- Taplin, Stephen H., Karla Kerlikowske, Stephen H. Taplin, Laura E. Ichikawa, Karla Kerlikowske, Virginia L. Ernster, Robert D. Rosenberg, Bonnie C. Yankaskas, Patricia A. Carney, Berta M. Geller, Nicole Urban, Mark B. Dignan, William E. Barlow, Rachel Ballard-barbash, and Edward A. Sickles. 2002. "Concordance of BI-RADS Assessments and Management Recommendations in Screening Mammography Concordance of Breast Imaging Reporting and Data System Assessments and Management." (November 2015).
- Tzikopoulos, Stylianos D., Michael E. Mavroforakis, Harris V. Georgiou, Nikos Dimitropoulos, and Sergios Theodoridis. 2011. "A Fully Automated Scheme for Mammographic Segmentation and Classification Based on Breast Density and Asymmetry." *Computer Methods and Programs in Biomedicine* 102(1):47–63.
- Van Der Waal, Daniëlle, Gerard J. Den Heeten, Ruud M. Pijnappel, Klaas H. Schuur, Johanna M. H. Timmers, André L. M. Verbeek, and Mireille J. M. Broeders. 2015. "Comparing Visually Assessed BI-

RADS Breast Density and Automated Volumetric Breast Density Software: A Cross-Sectional Study in a Breast Cancer Screening Setting.” *PLoS ONE* 10(9).

Walsh, Ruth, Phyllis J. Kornguth, Rex Bentley, and David M. DeLong. 1997. “Axillary Lymph Nodes : Mammographic, Pathologic and Clinical Correlation.” *American Journal of Roentgenology* (January):33–38.

Whitley, A. Stewart, Gail Jefferson, Charles Sloane, and Graham Hoadley. 2005. *Clark’s Positioning in Radiography*. 12 th edit. crc Press.

Whitman, Gary J. and Tamara Milner Haygood. 2012. *Digital Mammography: A Practical Approach*. Cambridge University Press.

Youk, Ji Hyun, Hye Mi Gweon, Eun Ju Son, and Jeong Ah Kim. 2016. “Automated Volumetric Breast Density Measurements in the Era of the BI-RADS Fifth Edition: A Comparison with Visual Assessment.” *American Journal of Roentgenology* 206(5).

Zeeshan, Muhammad, Basit Salam, Qazi Saad B. Khalid, Shahbaz Alam, and Raza Sayani. 2018. “Diagnostic Accuracy of Digital Mammography in the Detection of Breast Cancer.” *Cureus* 10(4).

Appendix

A- Data Sheet

B- Published papers

C- Selected Mammographic Images

A- Data Sheet

Sudan University of Science & Technology

College of Graduated Studies

Concordance of Breast Imaging Reporting and Data System with Interpretation of Digital Mammography

Data Collection Sheet

1. Age groups:

1. 15-30
2. 31-45
3. 46-60
4. 61-75
5. 76-90

2. Breast Composition:

1. a
2. b
3. c
4. d

Mammographic Findings according to BIRAD System

1. Mass
2. Calcification
3. Architectural Distortion
4. A Symmetry
5. Intramammary lymph node
6. Skin Lesion
7. Solitary dilated duct
8. Associated Features

Mass:

1. Yes
2. No

Shape:

1. Oval
2. Round
3. Irregular
4. Lobulated

Margin:

1. Circumscribed (Well defined, Sharp)
2. Obscured (Partially well defined)
3. Microlobulated
4. Indistinct (Ill defined)
5. Speculated
6. Irregular

Density:

1. High density
2. Equal density (iso)
3. Low density
4. Fat-Containing

Associated calcification:

1. Yes
2. No

Location:

1. Retroareolar
2. Central
3. Upper inner
4. Upper outer
5. Lower inner
6. Lower outer
7. Upper anterior
8. Lower anterior
9. Upper posterior
10. Upper middle (upper central)
11. Central posterior
12. Central anterior
13. Different locations (Multiple)
14. Axillary tail

Calcification:

1. Yes
2. No

Typically benign:

1. Skin
2. Vascular
3. Coarse (Popcorn-like)
4. Large rod-like
5. Round
6. Rim (egg shell)
7. Dystrophic
8. Milk of calcium
9. Suture
10. Un defined

Suspicious Morphology:

11. Amorphous
12. Coarse heterogeneous
13. Fine Pleomorphic (fine calcification)
14. Fine linear (Fine linear branching)

Distribution:

1. Diffuse (scattered)
2. Regional
3. Grouped
4. Linear
5. Segmental
6. Single

Location:

1. Retroareolar
2. Central
3. Upper inner
4. Upper outer
5. Lower inner
6. Lower outer
7. Upper posterior
8. Upper middle
9. Different locations (Multiple)
10. Axillary tail

Architectural Distortion:

1. Yes
2. No

Asymmetry:

1. Asymmetry
2. Global Asymmetry
3. Focal Asymmetry
4. Developmental Asymmetry
5. No

Intramammary lymph node

1. Yes
2. No

Associated Features:

1. No
2. Skin retraction
3. Nipple retraction
4. Skin thickening
5. Trabecular distortion
6. Axillary lymph Adenopathy
7. Multiple small lesions
8. Nipple retraction and skin retraction
9. Nipple retraction and Lymph Adenopathy
10. Nipple retraction and Skin Thickening
11. Skin thickening and Lymph Adenopathy
12. Nipple retraction, skin thickening and Lymph Adenopathy
13. Dilated superficial vessels

Solitary dilated duct:

1. Yes
2. No

Final Finding:

Final Diagnosis	1 Normal finding		2 benign	3 probably benign	4 malignant	5 highly malignant
BIRADS Category	0 incomplete	1 negative Normal Finding	2 Benign	3 probably benign	4 suspicious malignancy	5 highly suggestive malignancy

B- Published papers

Concordance of Breast Imaging Reporting and Data System with Routine Interpretation of Digital Mammography

Mayson A. Wanasi¹, Caroline Edward Ayad¹, Duha Abdu Mohamed Abdu¹, Mahasin Gamalalddin Yaqob.²

¹Collage of Medical Radiological Science, Sudan University for science and technology, Khartoum, Sudan

²Princess Nora Bint Abdul Rahman University, Riyadh, KSA

Abstract

The American College of Radiology's (ACR) Breast Imaging Reporting and Data System (BI-RADS) provide a lexicon that give a standard way of reporting mammogram that help ensure better follow up of suspicious findings. The study conduct to assess the concordance of final findings of mammograms reported using BI-RADS lexicons and the final impression of radiologist those using routine interpretation of mammogram. The data descriptively analyzed and Kappa value was determined to measure the concordance. The result appeared as the concordance of the breast composition was ($k = 0.5$) that point Moderate agreement. According to mass, the presence of the mass was ($k = 0.83$) that was a Very Good agreement, the shape of the mass was ($k = 0.53$) that a Moderate agreement, the margin of the mass was ($k = 0.475$) that point Moderate agreement, the density of the mass was ($k = 0.74$) that point a good agreement, in addition the associate calcifications was ($k = 1$) that point a total agreement. According to calcification the Kappa value was for presence ($k = 0.87$) that point to Very Good agreement, the morphology of the calcifications was ($k = 0.85$) that point to Very Good agreement and distribution was ($k = 1$) that point Very Good agreement. In addition, the architectural distortion was ($k = 0.85$) that point to Very Good agreement, and A symmetry was ($k = 1.3$) it was poor agreement. The intramammary lymph node was ($k = 0.65$) that point a good agreement and the overall agreement and concordance to the final finding was ($k = 0.58$) that point to a moderate agreement. As the conclusion to the study, there is a wide variation in wording of the mammography report between the radiologists. Therefore, it is very importance to the similarity wording of the mammography report to avoid any misunderstanding or confusion, and following of BIRAD lexicon leads to this goal.

Keywords: BIRADS, Mammography, Breast imaging

1. Introduction

BIRAD system have a very significant impact because the importance of diagnosis and detection of any breast lesions and helps in early detection of breast cancer (Ferreira et al. 2011). The American College of Radiology designed the Breast Imaging Reporting and Data System (BI-RADS), which includes six assessment categories numbered 0–5 with associated management recommendations (Taplin et al. 2002). And also category 6 for proven malignancy ((Balleyguier et al. 2007). Since developed the BIRAD system terms used in reporting have been developed to describe breast composition, lesion morphology, final impression, and recommendations (Berg et al. 2004). Because the wide variability of the mammography practice and difference in description of the lesions between radiologist comes the importance of the BIRAD system (Lazarus et al. 2006), that provide a complete system to standardization Both lesion description and management recommendations (Burnside et al. 2009). The standardized terminology of the BI-RADS lexicon allows quantification of the likelihood of carcinoma in an impalpable breast lesion. (Liberman, L., Abramson, A.F., Squires, F.B.,

Glassman, J.R., Morris 1998). The BI-RADS lexicon offers multiple area of strengths, including the standardization of common language to facilitate communication between radiologists, physicians, and patients. The system also clarifies the reporting of mammography results and offer a clinical management. (Eberl et al. 2015)

2. Method

The subject of the study were 300 mammograms taken by different digital mammography machines. The study conduct between 2015 and 2018 to evaluate, assess the BI-RAD and interpretation of mammography image, and define the degree of concordance between them.

The mammographic images reported using the BI-RAD system was collected, and re-reported by different radiologist according to traditional way of reporting, or vice versa then, all the data recorded into recording data sheet according to categories should be assessed. The study exclude a mammogram of Women with a history of breast or ovarian cancer, or with breast implants. So the BIRADS Category 6 not included in this study.

2.1 Collection of Data

The researcher collected digital mammogram from different medical institutions and re-diagnosed by various radiologists. The subjects were digital mammograms randomly selected for women between the ages of 15 to 90 years and the two basic projections of mammography (CC and MLO) were adopted. The mammograms diagnosed by radiologists using the usual interpretation of mammography and re-diagnosed again by different radiologist by adopting BIRAD system. The data from different reports collected using two different data collection sheets, for the two types of reporting. Each sheet includes: patient No., age of the patient, breast composition, the mammographic finding (Mass, Calcifications, Architectural distortion, Asymmetry, Intramammary Lymph node, solitary Dilated ducts and Associated features), and the final diagnosis or BIRAD Category.

2.2 Data collection sheet:

The items of sheet determine using breast imaging lexicons of BIRAD system.

2.2.1 Age:

The ages of the patients grouped according to range of patient's age from 15 to 90. The researcher divided the total patient's ages into five different groups with 15 years interval, the first one (15-30), the second group (31-45), the third group (46-60), the forth group (61-75) and the fifth group (76-90).

2.2.2 Breast Composition:

The breast composition determined by radiologist for each mammogram according to classification categories (fatty, scattered fibroglandular, heterogeneous fibroglandular or dense breast) for the usual interpretation. And by letters ("a" for fatty, "b" for scattered fibroglandular, "c" for heterogeneous fibroglandular or "d" for dense breast) according to BIRADS lexicons.

2.2.3 Mass:

The term mass selected by the radiologist when found a 3D occupying space lesion and described the mass according to its shape either Oval, round or irregular. The researcher add a fourth descriptive term found in the reports "lobulated". In addition described the margin of the mass either Circumscribed or any related word (Well defined, Sharp), Obscured (Partially well defined), Microlobulated, Indistinct (ill defined), Speculated, or Irregular. And also defined mass density as High, equal (Iso), low, and fat containing according to x-ray attenuation of the mass either greater than the attenuation of fibroglandular tissue of the breast, equal, or low also fat containing mass like oil cyst. And determined the associated calcification. The location of mass was determined according to one or two of localization systems preferred to use in localization of the lesion. The selected terms sited according to reports of the mammograms. It was Retroareolar, Central, Upper inner, Upper outer, Lower inner,

Lower outer, Upper anterior, Lower anterior, Upper posterior, Upper middle (upper central), Central posterior, Central anterior, Different locations (Multiple) and Axillary tail.

2.2.4 Calcification:

The presence of calcification was checked and calcified according to types either Typically benign like (Skin, Vascular, Coarse (Popcorn-like), Large rod-like, Round, Rim (egg shell), Dystrophic, Milk of calcium, Suture), or Suspicious Morphology like (Amorphous, Coarse heterogeneous, Fine Pleomorphic (fine calcification), Fine Linear branching calcifications). In addition, the location of calcifications was identified as (Diffuse or scattered, Regional. Grouped, Linear, Segmental and single). Moreover, the location of the calcification determined as same as for mass.

2.2.5 Architectural Distortion:

It was identified when the parenchyma is distorted with no definite mass visible.

2.2.6 Asymmetry:

It was identified when the area of fibroglandular tissue that is visible on only one mammographic projection. Presence of asymmetry identified.

2.2.7 Intramammary Lymph node:

It was determined in each mammogram either present or absent.

2.2.8 Solitary Dilated Ducts:

It was determined in each mammogram either present or absent.

2.2.9 Associated Features:

It was determined in each mammogram according to what feature appear into the image (Skin retraction, Nipple retraction, Skin thickening, Trabecular distortion, Axillary lymph Adenopathy , Multiple small lesions, Dilated superficial vessels), if any two or more features appear together, they were determined (Nipple retraction and skin retraction, Nipple retraction and Lymph Adenopathy, Nipple retraction and Skin Thickening, Skin thickening and Lymph Adenopathy and Nipple retraction, skin thickening and Lymph Adenopathy).

2.2.10 Diagnosis and BIRADS Category:

Each mammogram diagnosed finally twice by different radiologist using routine interpretation and BIRADS system. The diagnosis included (Normal finding, Benign, Probably Benign, Malignant, Highly malignancy) according to diagnosis write by radiologists. The BIRADS Category included (0 incomplete, 1 Normal finding, 2 Benign, 3 probably benign, 4 Suspicious Malignancy and Highly suggestive Malignancy).

2.3 Statistical Analysis

The data analyzed used SPSS version 10, to maintained accurate analysis and results. Then the Kappa value was determined for each findings.

3. Result

The data was collected, reported, and analyzed to found the agreement between BIRAD and Interpretation of the mammography. The study determine the K-value and found the agreement between the different opinions. The first parameter was breast composition the K-value was 0.4 that was Moderate agreement. In overall description of mass (presence, shape, margin, density, associated calcifications and location), the agreement was good as K-value of 0.72. Regarding to calcification mean of the K-value was 0.7 that reflect a good agreement. The Architectural Distortion was 0.85 K-value, the conceder a very good agreement. In addition, the K-value of 0.13 among A Symmetry, that consider a Poor agreement. In Inflammatory lymph node the K-value was 0.65, that a Good agreement. Associated Features was 0.36, which consider a Fair agreement. Finally, the final finding was 0.58 in K-value scale, which consider a Moderate agreement. Table (1).

Parameter		K- value
Breast Composition		0.465
Mass	presence	0.835
	Shape	0.529
	Margin	0.475
	Density	0.742
	Associated calcification	1.000
	Location	0.222
Calcification	Presence	0.877
	Morphology	0.846
	Distribution	1.000
	Location	0.250
Architectural Distortion		0.852
A Symmetry		0.138
Inflammatory lymph node		0.650
Solitary dilated duct		0.000
Associated Features		0.360
Final findings		0.581

Table 1: show the K-value of different findings and final diagnosis of mammography

4. Discussion

This study conduct to found the concordance of mammography reporting using two reporting system, BIRAD and routine interpretation of the digital mammography, as regard to breast density, the degree of agreement was a Moderate agreement ($k=0.46$) that reflect the difference in visual assessment of radiologist. Determine the ratio between the breast tissue and fatty tissue, which implies the breast density; can be different between one to another. The overall weighted kappa value for breast composition achieved by Ekpo and Ujong was 0.83 (Ekpo et al. 2016).

As regard to Mass, a Very Good agreement was achieved for the presence of mass ($k=0.83$), and for the mass shape the agreement was moderate ($k= 0.529$), that reflect the difference in word used to describe mass shape between BIRAD system and routine interpretation. As compare to the result achieved by (Lazarus et al. 2006). Which their study about evaluation of interobserver variability between breast radiologists by using terminology of the fourth edition of the Breast Imaging Reporting and Data

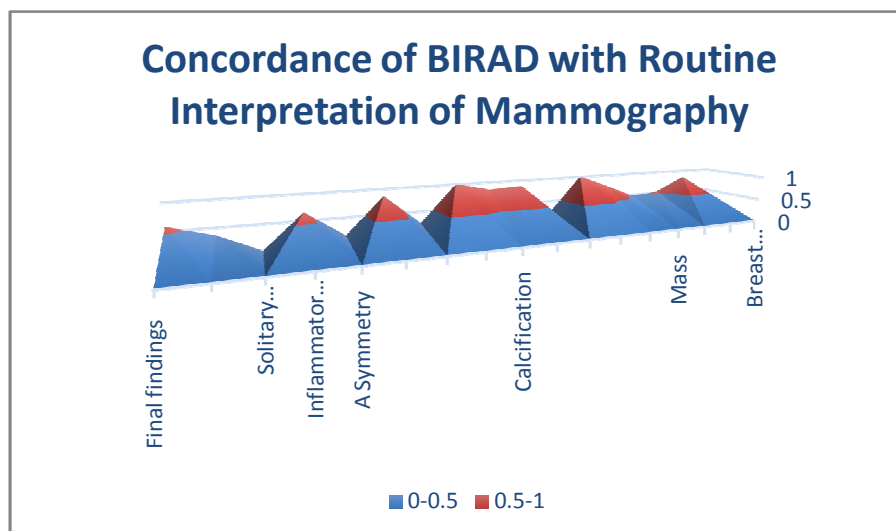
System (BI-RADS), and result was ($k=0.48$) for mass shape. In addition, among the margin of the mass ($k=0.475$) that reflect a Moderate agreement. As regard to Mass density the kappa value was ($k=0.742$) as a good agreement. Determine the mass density as hyper, iso and low may different a little bit visually, but not always an area of disagreement, As compare to the overall kappa value of 0.40 that found for mass density by (Berg et al. 2000). As regard to Associated calcification the Kappa value was ($k=1$) that was a very good agreement. Regarding to Location of the mass, the agreement was ($k=0.222$) that mean a fair agreement, which related to different types of location systems were adopted by radiologist, and not related to actual disagreement.

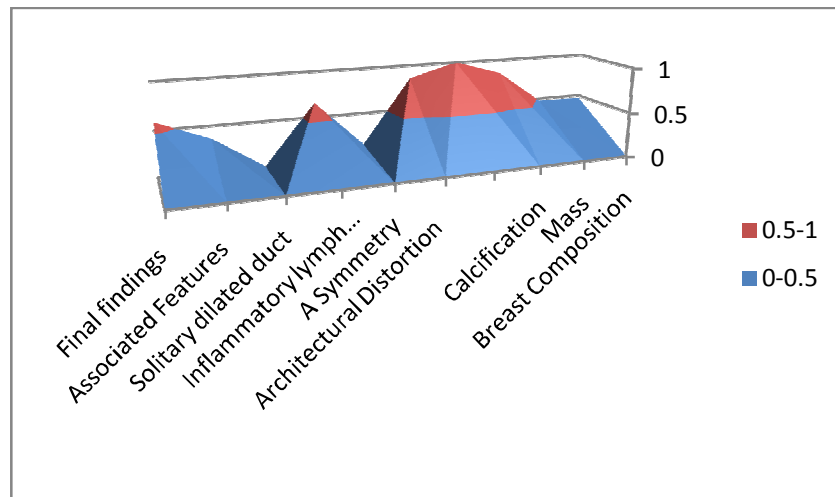
For Calcifications, as regard to presence of calcifications the K-value of ($k=0.877$) that was a very good agreement. Related to Morphology of Calcifications the K-value of ($k=0.846$) that was a very good agreement, also Distribution of Calcifications the k-value was ($k=1$) that consider as very good agreement. Regarding to Location of calcifications the k-value was ($k=0.250$) that reflect a fair agreement, for the same reason as mass the disagreement related to different types of location systems that adopted by radiologist.

As regard to Architectural Distortion, the k-value was 0.852, which consider a very good agreement. As a regard to The A Symmetry as a finding for both breast mammogram, the k-value= 0.138 that was a poor agreement, which a result for not using of ultrasound as aiding tools for diagnosis and other alternative projections during re-reporting.

Regarding to Inflammatory lymph node, show a Good agreement as ($k=0.650$). As regard to Associated Features, the k-value was 0.360 that reflect a Fair agreement, due to difference in description of the features.

The overall diagnostic and pathological Final findings reflect a Moderate agreement with k-value of (0.581), that result to the radiologists may have misunderstood some time to the definition of the terms designed by BIRAD system perhaps the description. That match the result found by (Baker, Kornguth, and Floyd Jr 1996). In addition, the level of mammography training of the radiologist in this study affect the misconcordance somehow. Some of the BI-RADS terms included in the “typically benign” category 2 and need more image category 0 may not always represent by the other radiologist adapted the routine interpretation as benign findings. Possibility that, a limited number of descriptive choices by BIRADS for radiologists may not always match the choice of other group of radiologists that freely find a term that they believe adequately describes a lesion. Put this difference not affect diagnostic assessment that may not agree with the BI-RADS assessment of the term selected.





Figure(1): show the degree of agreement according to Kappa value between routine interpretation and BIRADS



Figure (2): CC view of right breast of 62 patient show that a benign type of calcifications (Vascular Calcification)

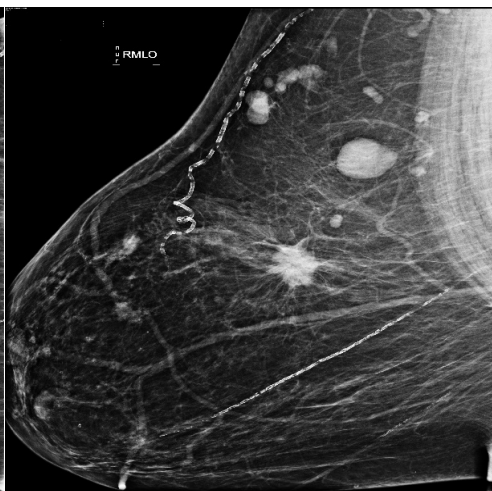


Figure (3): MLO view of right breast of 62 patient (same patient) show that a benign type of calcifications (Vascular Calcification)

Conclusion

Taken broadly, our study consistent with other studies that reflect the importance of standardization of lexicon that describe the pathological findings in mammography (Bent et al. 2010), (Balleyguier et al. 2007), (Orel et al. 1999). The result of study reflect how far the importance of the controlling and standardization of the wording using in diagnosis of Mammogram. In addition the a Moderate agreement achieved by the study is acceptable for the purpose of study and reflect the normal inter observer variability, consist with others studies like (Antonio and Crespi 2010), (Burivong and Amornvithayacharn 2011) and (Ciatto et al. 2006).

The great limitation of the study is that the number of readers was relatively small. Also, the generalizability of the results was limited because readers were in different level of skills, qualifications and practice and were working in the different clinical setting. As a recommendation Additional investigation with larger populations and more readers is necessary to further assessment with taken the level of experience of radiologist in consider. Finally, the implementation of the BIRAD in all mammography facilities will support the completion of quality improvement activities and clinical research in addition to diagnosis benefits. Moreover, decrease the inconsistencies in mammography reports.

Acknowledgments

I would like to thank all people help me to completion my work.

References

- Antonio, Anna Liza M. and Catherine M. Crespi. 2010. "Predictors of Interobserver Agreement in Breast Imaging Using the Breast Imaging Reporting and Data System." *Breast Cancer Research and Treatment* 120(3):539–46.
- Baker, Jay A., Phyllis J. Kornguth, and C. E. Floyd Jr. 1996. "Breast Imaging Reporting and Data System Standardized Mammography Lexicon: Observer Variability in Lesion Description." *AJR. American Journal of Roentgenology* 166(4):773–78.
- Balleyguier, Corinne et al. 2007. "BIRADS™ Classification in Mammography." *European Journal of Radiology* 61(2):192–94.
- Bent, Chris K., Lawrence W. Bassett, Carl J. D'Orsi, and James W. Sayre. 2010. "The Positive Predictive Value of BI-RADS Microcalcification Descriptors and Final Assessment Categories." *American Journal of Roentgenology* 194(5):1378–83.
- Berg, Wendie A. et al. 2004. "Diagnostic Accuracy of Mammography, Clinical Examination, US, and MR Imaging in Preoperative Assessment of Breast Cancer." *Radiology* 233(3):830–49.
- Berg, Wendie A., Cristina Campassi, Patricia Langenberg, and Mary J. Sexton. 2000. "Breast Imaging Reporting and Data System: Inter-and Intraobserver Variability in Feature Analysis and Final Assessment." *American Journal of Roentgenology* 174(6):1769–77.
- Burivong, WANAPORN and Ornsiri Amornvithayacharn. 2011. "Accuracy of Subcategories A, B, C in BI-RADS 4 Lesions. by Combined Mammography and Breast Ultrasound Findings." *Journal of Medicine and Medical Sciences* 2(3):728–33.
- Burnside, Elizabeth S. et al. 2009. "The ACR BI-RADS® experience: Learning from History." *Journal of the American College of Radiology* 6(12):851–60.
- Ciatto, S. et al. 2006. "Reader Variability in Reporting Breast Imaging According to BI-RADS® assessment Categories (the Florence Experience)." *The Breast* 15(1):44–51.
- Eberl, Margaret M., Chester H. Fox, Stephen B. Edge, Cathleen a Carter, and Martin C. Mahoney. 2015. "BI-RADS Classification for Management of Abnormal Mammograms." *Journal of the American Board of Family Medicine : JABFM* 19(2):161–64.
- Ekpo, Ernest U., Ujong Peter Ujong, Claudia Mello-Thoms, and Mark F. McEntee. 2016. "Assessment of Interradiologist Agreement Regarding Mammographic Breast Density Classification Using the Fifth Edition of the BI-RADS Atlas." *American Journal of Roentgenology* 206(5):1119–23.
- Ferreira, Pedro, Nuno A. Fonseca, Inês Dutra, Ryan Woods, and Elizabeth Burnside. 2011. "Predicting Malignancy from Mammography Findings and Surgical Biopsies." Pp. 339–44 in *Bioinformatics and Biomedicine (BIBM), 2011 IEEE International Conference on*.
- Lazarus, Elizabeth, Martha B. Mainiero, Barbara Schepps, Susan L. Koelliker, and Linda S. Livingston. 2006. "BI-RADS Lexicon for US and Mammography: Interobserver Variability and Positive Predictive Value." *Radiology* 239(2):385–91.
- Liberman, L., Abramson, A.F., Squires, F.B., Glassman, J.R., Morris, E. A. at al. 1998. "The Breast Imaging Reporting and Data System: Positive Predictive Value of Mammographic Features and Final Assessment Categories." *AJR* 73(July):35–40.
- Orel, Susan G., Nicole Kay, Carol Reynolds, and Daniel C. Sullivan. 1999. "BI-RADS Categorization As a Predictor of Malignancy." *Radiology* 211(3):845–50.
- Taplin, Stephen H. et al. 2002. "Concordance of BI-RADS Assessments and Management Recommendations in Screening Mammography Concordance of Breast Imaging Reporting and Data System Assessments and Management." (November 2015).

Evaluation of Breast Architecture and Mass Morphology in Digital Mammography using BIRADS

Mayson .M. Wansi¹, Caroline Edward Ayad¹
Doha Abdo Mohammed Abdo¹

¹(College Of Medical Radiological Science/ Sudan University of Science and Technology Khartoum –Sudan)
Corresponding Author: Mayson .M. Wansi

Abstract: Breast architectural distortion is an abnormal arrangement of tissue strands and happened linearly as an indicator of breast cancer and conceivably it has a benign cause also. This prospective analytic cross section study was to evaluate and correlate between breast architecture and mass morphology using Breast Imaging Reporting and Data System (BI-RADS). The study was conducted during the period from 2015 to 2018. 300 mammograms of ladies aged between 15 and 90 were evaluated. The research results showed that the architectural distortion was present in 117 of 300 (39%), and absence in 171 of 300 (57%). The architectural distortion and mass shape was correlated significantly at P-value = (0.000), the presence of architectural distortion was associated with irregular mass, whereas the absence of architectural distortion was associated with oval shape masses. The architectural distortion was associated significantly with speculated mass margin at P-value of (0.000) was found in 48 /102 cases. The relation between the architectural distortion and pathological outcomes using BIRADS was also been evaluated: 84/117 cases of distorted architecture were of BIRAD 4 (suspicious malignancy) and 54 of the cases were of BIRAD 1 with no presence of architectural distortion. Finally the study showed that there is association between architectural distortion and the features of mass morphology as well as the masses which were suspicious or highly suggestive to be malignant

Keywords: BIRAD, Distortion, Breast, Malignant masses

Date of Submission: 05-01-2019

Date of acceptance: 21-01-2019

I. Introduction

The breast parenchymal pattern consists of thin, curvilinear lines that directed toward the nipple. This radiating pattern is broken only by blood vessels. (Sickles, EA, D'Orsi CJ, Bassett LW, 2013). Architectural distortion is defined as linear alterations of breast parenchyma pulled into a central focus, without a definite visible mass, resulting in radiating spiculations or thin lines pointing toward the center, like a star. (Ikeda and Miyake, 2016) Also defined as appearance in which the normal architecture of the breast is altered by an invisible mass. (M.Á. *et al.*, 2016). The Architectural distortion can be due to malignant lesions, such as invasive cancer or ductal carcinoma in situ (DCIS), or to benign lesions, such as a radial scar or complex sclerosing lesion. (Bahl *et al.*, 2015) AD is the third mammographic manifestation of non-palpable breast cancer and is the most commonly undiagnosed anomaly in mammography, being the cause of false negatives. (Durand *et al.*, 2016) The Architectural distortion representing nearly 6% of abnormalities detected on screening mammography. (Gaur *et al.*, 2013) The suspicion of malignancy in an AD increases if it is associated with a mass. (M.Á. *et al.*, 2016). Architectural distortions appear as speculation, retraction, and distortion. Although most architectural distortions must be considered to represent cancer. (Ichikawa *et al.*, 2004)

The contour of the mass is the most discriminating morphological feature between benign and malignant. (Berment *et al.*, 2014) Characterization of lesion margin is also very important, as spiculated margins are highly suggestive of malignancy. (Mohindra *et al.*, 2018). The most significant features indicating whether the tumor is malignant or benign are its shape and the nature of its margins. (Ciecholewski, 2017) Architectural Distortion is a classical presenting appearance for infiltrating lobular carcinoma as 16% to 20%, and intra-ductal carcinoma represented 17%. (Boyer and Russ, 2014) Researchers used different methods to detect architectural distortion due to the relation between it and cancer. (Anand and Rathana, 2013), (Baeg and Kehtarnavaz, 2002). The current study aimed to evaluate the breast architecture and mass morphology in Digital Mammography using BIRADS as well to determine the risk of malignancy or suspicious lesions associated with architectural distortion and to evaluate the imaging features that may contribute to the prediction of malignancy in the setting of architectural distortion. The information from this study can be used to counsel patients and inform clinicians about expected pathologic outcomes.

II. Materials and Methods

The study was prospective cross section study for 300 mammograms of women aged between 15 and 90 years old; all mammograms were reviewed by more than 2 radiologists and reported using BIRADS Lexicons. Two basic projections of mammography (Crano- Caudal(CC) and Mediolateral(MLO) were adopted.

The purpose of the study was to evaluate breast architectural distortion and to determine the relationship between it and mass morphology, so that the data collected according to presence of the mass and architectural distortion as the following:

Criteria for Characterizing the Mass:

The term mass selected by the radiologist when found a 3D occupying space lesion and described the mass morphology (Shape, Margin) according to its shape either Oval, round or irregular. The researcher added a fourth descriptive term found in the reports as "lobulated". Moreover, the margin of the mass was described Circumscribed or (Well defined, Sharp), Obscured (Partially well defined), Microlobulated, Indistinct (ill defined), Speculated, or Irregular.

Architectural Distortion:

It identified when the parenchyma is distorted with or with no definite mass visible. Each mammogram had finally different BIRADS category. As (0 incomplete, 1 Normal finding, 2 Benign, 3 probably benign, 4 Suspicious Malignancy and Highly suggestive Malignancy). Statistical analyses were performed using statistics program (SPSS version 10) to maintained accurate analysis and results. Statistical significance was determined with the chi-square test for category variables. The researcher found the correlation between the Mass morphology, Architectural distortion and final findings.

III. Results

Table 1: Distribution of samples according to architectural distortion

Architectural distortion	Frequency	Percent
Distorted	117	39
Normal architecture	171	57
undefined	12	4
Total	300	100

Table 2: Distribution of samples according to presence of breast mass

Breast Mass	Frequency	Percent
Present	186	62.0
Absent	102	34.0
Undefined	12	4.0
Total	300	100.0

Table 3: Correlation of architectural distortion with mass shape

	Distribution of mass shape				Total
	Oval	Round	Irregular	Lobulated	
Yes	21	18	60	3	102
No	48	27	6	3	84
Total	69	45	66	6	186

(Using chi-square test, P-value = 0.000)

Table 4: Correlation of architectural distortion with mass margin

Architectural distortion	Distribution of mass margin						Total
	Circumscribed (Well defined, Sharp)	Obscured (Partially well defined)	Micro-lobulated	Indistinct (Ill defined)	Speculated	Irregular	
Yes	0	15	9	21	48	9	102
No	45	6	18	12	0	3	84
Total	45	21	27	33	48	12	186

Using chi-square test, P-value = 0.000

(Table 5) Correlation of architectural distortion with pathological outcomes.

Pathological Outcomes	Count	Distribution of architectural distortion		Total
		Yes	No	
Negative (Normal finding)		0	54	54
	% within Distribution of pathological outcomes	0.0%	100.0%	100.0%

Benign	Count	0	33	33
BIRAD 2	% within Distribution of pathological outcomes	0.0%	100.0%	100.0%
Probably benign BIRAD3	Count	3	33	36
	% within Distribution of pathological outcomes	8.3%	91.7%	100.0%
Suspicious malignancy	Count	84	48	132
BIRAD 4	% within Distribution of pathological outcomes	63.6%	36.4%	100.0%
Highly suggestive malignancy	Count	30	3	33
BIRAD 5	% within Distribution of pathological outcomes	90.9%	9.1%	100.0%
Total	Count	117	171	288
	% within Distribution of pathological outcomes	40.6%	59.4%	100.0%

(Using chi-square test, P-value = 0.001)

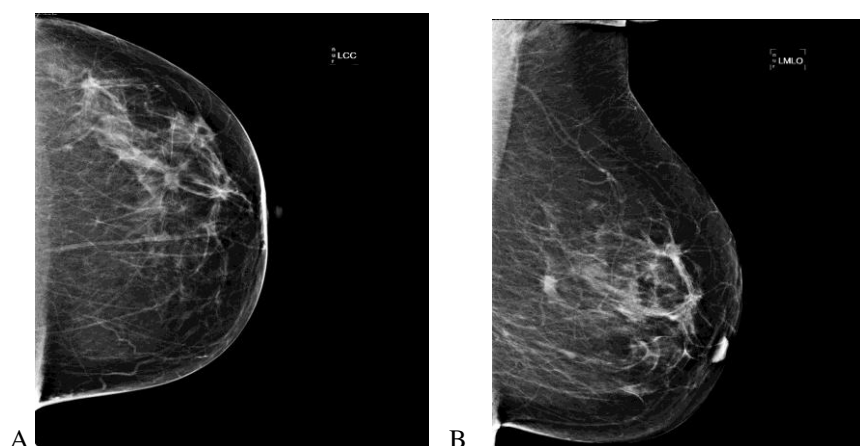


Figure 1: Cranio Caudal (CC) view of the left breast, show that multiple masses with architectural distortion associated with mass. B- Mediolateral (MLO) view of the left breast for the same patient, show that presence of architectural distortion.

IV. Discussion

The research showed that the architectural distortion was present in 117 of 300 (39%), and absent in 171 of 300 (57%) and also the breast masses were found in 186 cases and distorted with absence of masses in 102 (34%) cases as shown in tables (1 and 2) that means that the distortion happened in most of the cases that detected to be affected with mass. This was consistent with one of the most valuable published studies which informed that the architectural distortion is defined by the Breast Imaging Reporting and Data System (BIRADS) system as an appearance in which “the normal architecture of the breast is distorted with no definite mass visible. (Shantanu Gaur et al 2013) The distortion happened because of the spiculations radiating from a point and focal retraction or distortion at the edge of the parenchyma. Our study showed that architectural distortion also be an associated findings with benign causes of architectural distortion.

Table 3 showed the correlation of architectural distortion with mass shape and presented as, the oval shape was 21 of 102 associated with presence of architectural distortion, whereas the irregular shape was 60 of 102 associated with presence of architectural distortion.

Table 4 showed the correlation between architectural distortion and mass margin. The higher numbers of cases associated with architectural distortion were those of speculated mass margin 48 of 102.

The correlation was done in the cases affected with mass and determined whether architectural distortion presented or not. Therefore, the total cases taken were 186 mammograms

When characterizing the mass as Circumscribed: it was considered to be well defined, sharply demarcated with an abrupt transition between the lesion and the surrounding tissue. In some cases where part of the margin is obscured, it was defined for as circumscribed. A mass for which any portion of the margin is indistinct, microlobulated, or speculated was classified on the basis to be of suspicious component. This was clearly found in table(4) where 15 cases were obscured and partially well defined with the presence of distorted background. Micro-lobulated was found in both cases with and without distorted architecture. The margin is characterized by short cycle undulations. References have mentioned this criterion in mammography, and used this descriptor when implies a suspicious findings (Car. J.2012). The Indistinct (“ill defined”) description was applied when there is no clear demarcation of the entire margin, or of any portion of the margin, from the surrounding tissue. This was recommended to be used to implies a suspicious finding.(Carl J.2012) This was found in 21, and 12 cases with and without architecture distortion respectively. The margin was characterized by lines radiating from the mass in the speculated character. 48 cases were described as speculated margin which was associated with distortion, this descriptor implies the suspicious finding also the masses with irregular margins as mentioned by(Carl. J.2012)

The correlation of architectural distortion with mass shape was : the oval shape was 21 of 102, 18 for round shape and 3 for lobulated shape associated with presence of architectural distortion, whereas the irregular shapes were 60 of 102 associated with presence of architectural distortion , that consider statistically significant at P-value = (0.000). The result proved that the architectural distortion goes with the irregular shape more than round or oval shapes .This was consistent with what was mentioned with (Shantanu Gaur et al 2013) who stated that although an irregular mass or calcification is the most common mammographic appearance of invasive cancer, architectural distortion is generally considered the third most frequent and sometimes the only presenting finding. And a speculated mass or architectural distortion was the most common radiographic findings.

In addition our study showed that, the correlation between architectural distortion and mass margin found that the higher number of cases associated significantly at P-value = (0.000) with architectural distortion were those of speculated margin 48 of 102. The result goes with the nature of architectural distortion as linear alterations in the breast parenchyma, so that speculation margin lead to linear or appear as linear deformity, according to nature of the tumor, that almost malignant as mentioned by (Shi *et al.*, 2007).

Table(5) showed the correlation between the architectural distortion and pathological outcomes using BIRADS it presented that 84 of 117 were BIRAD 4 (suspicious malignancy)and were associated with presence of architectural distortion, and 54 of the cases were BIRAD 1 with no presence of architectural distortion it was correlated significantly at P-value = (0.001).That goes with previous studies (Bahl, M. *et al.*.2015) that showed that 75% of all mammography cases represent breast malignancy associated with architectural distortion. Moreover (M.Á., P. T. *et al.* .2016) in their study, have mentioned that 44.23% of the architectural distortion were corresponded to cancers.

V. Conclusion

The study showed that both malignant and nonmalignant pathologic masses were associated with architectural distortion. The probably benign masses BIRAD3 , the suspicious malignancy BIRAD 4 and the highly suggestive malignancy BIRAD 5 were all can be presented with distorted back ground architecture. Many limitations facing the researcher in the current study; is that the dependency upon the architectural distortion alone may be one of the highest levels of inter-observer variability among mammographic findings as mentioned by previous researchers (Baker JA et al 1996, Onega T et al 2013, Onega T et al 2012) and should be accompanied with other additional imaging methods beside the mammography. In Some cases there are difficulties in diagnosing the speculated masses because their characters appeared as architectural distortion .The study recommended to apply additional imaging method and have mentioned that the the evaluation of the breast considering the architectural distortion alone is not quit enough and less likely to represent malignancy on mammography if there is no other imaging method to be correlated with the mammographic findings. This information can be used to counsel patients about expected pathologic outcomes

Acknowledgements

We sincerely thank the participants without whom the study would not have been feasible. The Sudan University of Science and Technology, College of Medical Radiological Science and Radiology Department- in which the study was obtained, are thankfully acknowledged.

References

- [1]. Anand, S. and Rathana, R. A. V (2013) 'Architectural Distortion Detection in Mammogram using Contourlet Transform and Texture Features', *International Journal of Computer Applications*, 74(5), pp. 12–19.
- [2]. Baeg, S. and Kehtarnavaz, N. (2002) 'Classification of breast mass abnormalities using denseness and architectural distortion', *ELCVIA Electronic Letters on Computer Vision and Image Analysis*, 1(1), pp. 1–20.
- [3]. Bahl, M. *et al.* (2015) 'Architectural Distortion on Mammography: Correlation with Pathologic Outcomes and Predictors of Malignancy', *American Journal of Roentgenology*, 205(6), pp. 1339–1345. doi: 10.2214/AJR.15.14628.
- [4]. Berment, H. *et al.* (2014) 'Masses in mammography: What are the underlying anatomopathological lesions?', *Diagnostic and Interventional Imaging*. Elsevier Masson SAS, 95(2), pp. 124–133. doi: 10.1016/j.diii.2013.12.010.
- [5]. Boyer, B. and Russ, E. (2014) 'Anatomical-radiological correlations: Architectural distortions', *Diagnostic and Interventional Imaging*. Elsevier Masson SAS, 95(2), pp. 134–140. doi: 10.1016/j.diii.2014.01.003.
- [6]. Ciecholewski, M. (2017) 'Malignant and benign mass segmentation in mammograms using active contour methods', *Symmetry*, 9(11). doi: 10.3390/sym9110277.
- [7]. Durand, M. A. *et al.* (2016) 'Tomosynthesis-detected architectural distortion: management algorithm with radiologic-pathologic correlation', *Radiographics*. Radiological Society of North America, 36(2), pp. 311–321.
- [8]. Gaur, S. *et al.* (2013) 'Architectural distortion of the breast', *American Journal of Roentgenology*, 201(5), pp. 662–670. doi: 10.2214/AJR.12.10153.
- [9]. Ichikawa, T. *et al.* (2004) 'Automated detection method for architectural distortion areas on mammograms based on morphological processing and surface analysis', 5370, p. 920. doi: 10.1117/12.535116.
- [10]. Ikeda, D. and Miyake, K. K. (2016) *Breast Imaging: The Requisites E-Book*. Elsevier Health Sciences.

- [11]. Miguel Ángel Pinochet T, Aleen Vanessa Altamirano S, Eleonora Horvath P, Marcela Uchida S, Claudio Silva F-A, Carla Darrás I. (2016) 'Distorsion of breast architecture: The best way to confront it', *Revista Chilena de Radiología*, 22(4), pp. 158–163. doi: 10.1016/j.rchira.2016.11.007.
- [12]. Mohindra, N. *et al.* (2018) 'Impact of addition of digital breast tomosynthesis to digital mammography in lesion characterization in breast cancer patients', *International Journal of Applied and Basic Medical Research*. Wolters Kluwer--Medknow Publications, 8(1), p. 33.
- [13]. Shi, J. *et al.* (2007) 'Characterization of mammographic masses based on level set segmentation with new image features and patient information', *Medical Physics*, 35(1), pp. 280–290. doi: 10.1118/1.2820630.
- [14]. Sickles, EA, D'Orsi CJ, Bassett LW, *et al.* (2002) *ACR BI-RADS® Atlas, Breast Imaging Reporting and Data System*.
- [15]. Shantanu Gaur, Vandana Dialani, Priscilla J. Slanetz, Ronald L. Eisenberg, (2013) Architectural Distortion of the Breast *AJR*; 201:W662–W670
- [16]. Carl J. D'Orsi, Edward A. Sickles, Ellen B. Mendelson, Elizabeth A. Morris, 2013 *ACR BI-RADS Atlas Breast Imaging Reporting and Data System*
- [17]. Baker JA, Kornguth PJ, Floyd CE Jr. Breast Imaging Reporting and Data System standardized mammography lexicon: observer variability in lesion description. *AJR* 1996; 166:773–778
- [18]. Onega T, Anderson ML, Miglioretti DL, *et al.* Establishing a gold standard for test sets: variation
- [19]. in interpretive agreement of expert mammographers. *Acad Radiol* 2013; 20:731–739
- [20]. Onega T, Smith M, Miglioretti DL, *et al.* Radiologist agreement for mammographic recall by case difficulty and finding type. *J Am Coll Radiol* 2012; 9:788–794

Mayson .M. Wansi, "Evaluation of Breast Architecture and Mass Morphology in Digital Mammography using BIRADS." *IOSR Journal of Dental and Medical Sciences (IOSR-JDMS)*, vol. 18, no. 1, 2019, pp 75-79.

C- Selected Mammographic Images

Image (1):

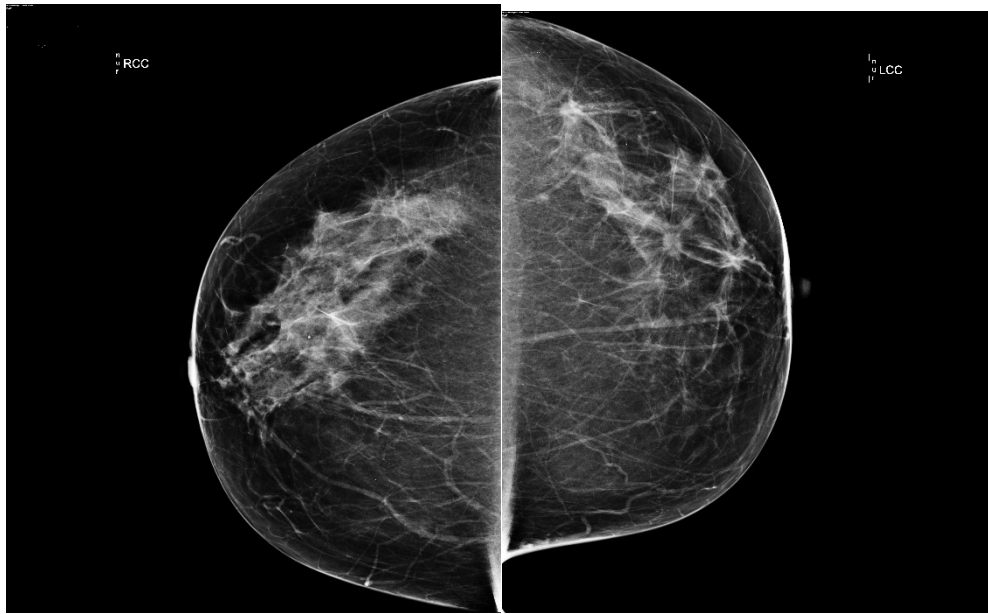


(a)

(b)

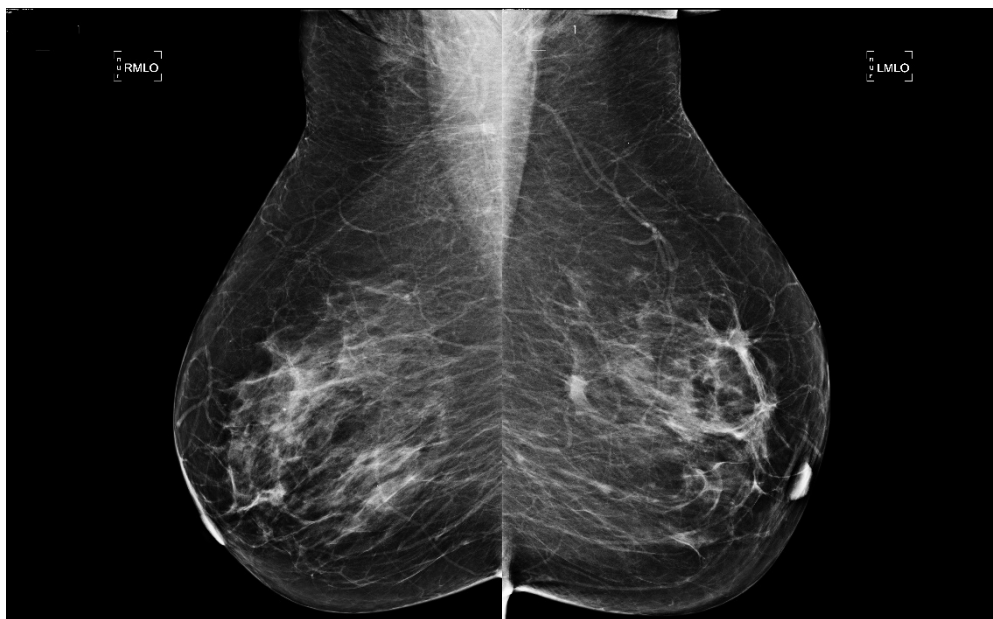
a, CC and b, MLO for left breast of the patient aged 70 years, show high density lobulated shape mass with speculated margin, the location of the mass is left upper outer quadrant (central mass). The breast composition assigned as fatty breast (a). There is associated feature as multiple axillary tail and left axillary lymph Adenopathy. Final diagnosis is highly suggestive malignancy (BITAD 5).

Image (2):



(a)

(b)

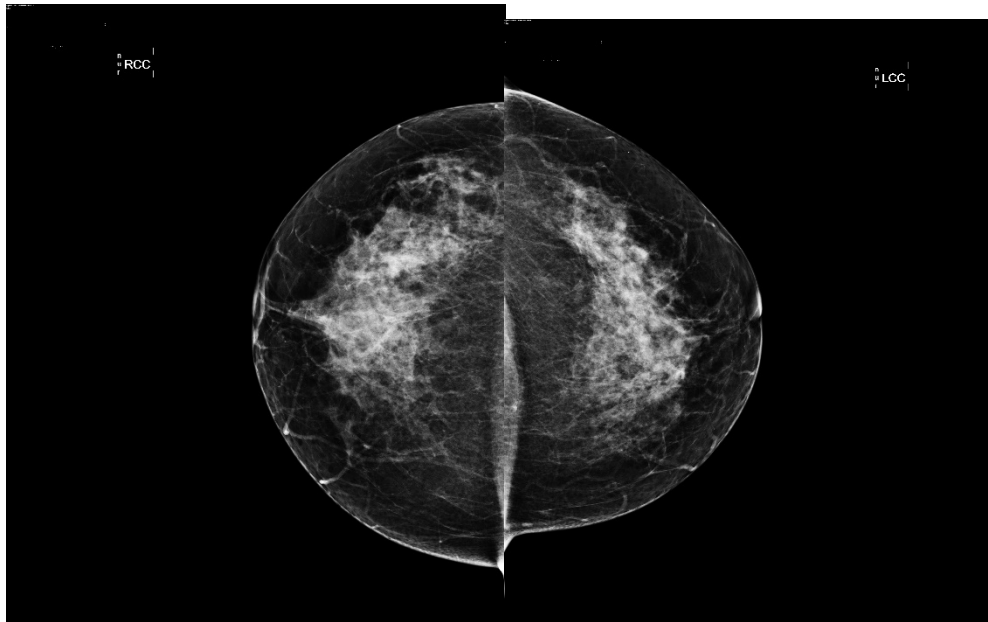


(c)

(d)

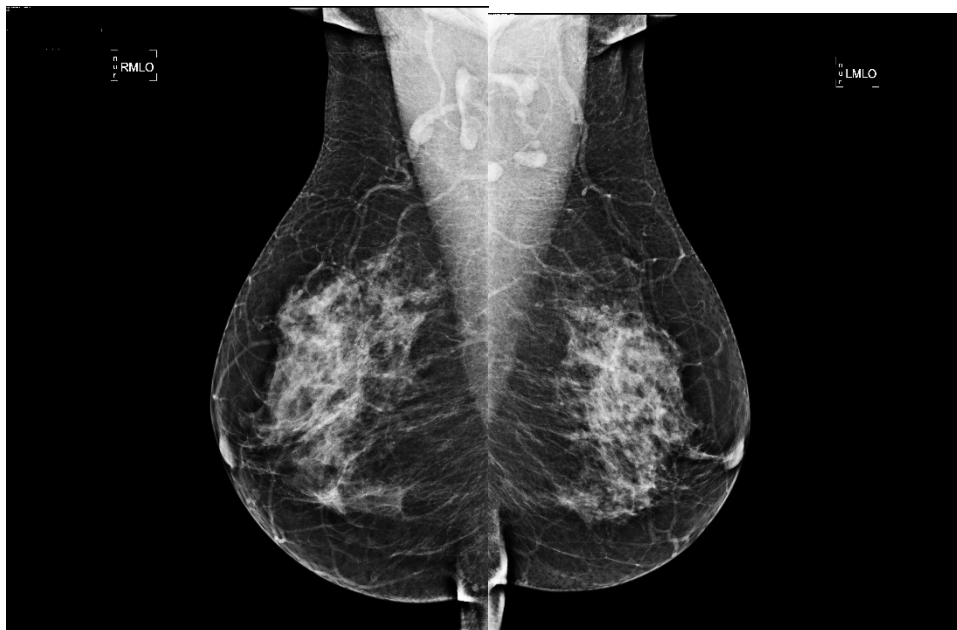
a, CC. c, MLO mammographic image of Right Breast. b, CC. d, MLO mammographic image of Left Breast. For 60 years old patient, show in left breast mass with irregular shape; ill define margin; and high density at left upper outer quadrant. The breast composition assigned as scattered fibroglandular breast (b). With Architectural Distortion. Final diagnosis is suspicious malignancy (BITAD 4).

Image (3):



(a)

(b)

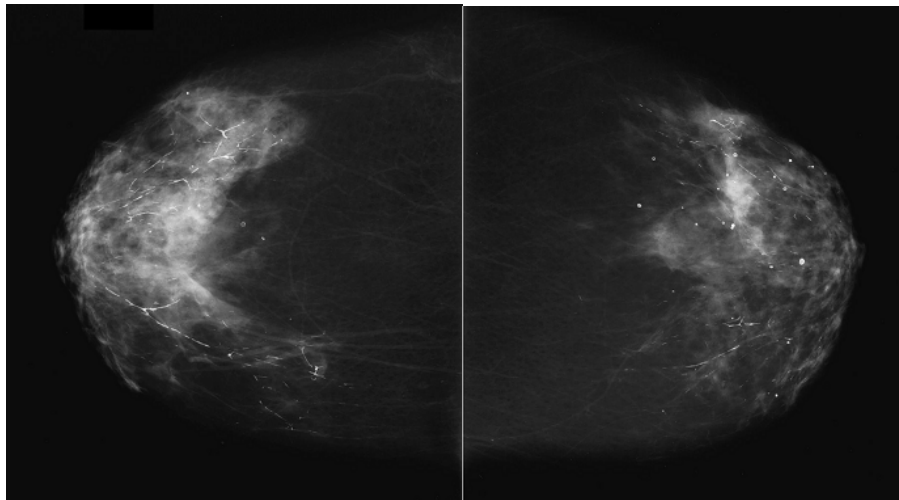


(c)

(d)

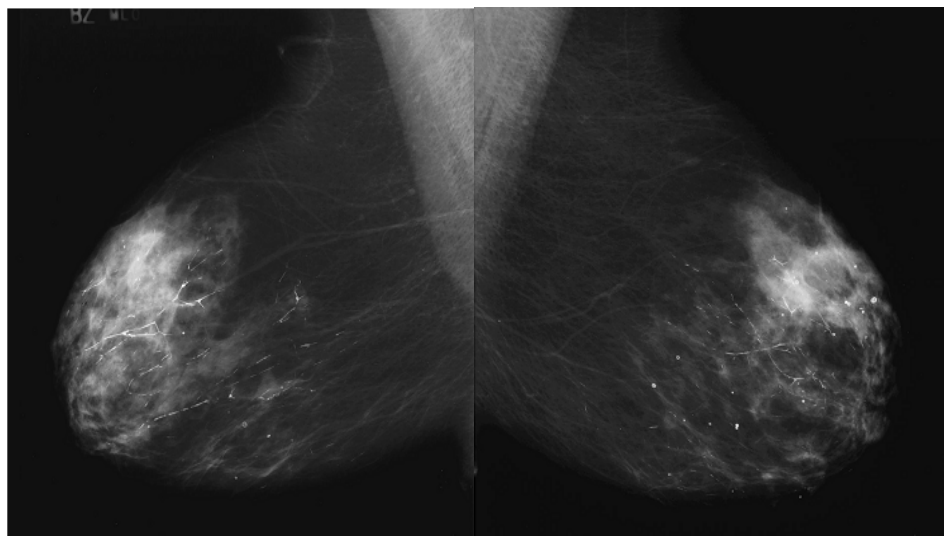
a, CC. c, MLO mammographic image of Right Breast. b, CC. d, MLO mammographic image of Left Breast. For 53 years old patient, show in left breast mass with irregular shape; speculated margin; and iso density at left lower outer quadrant. The breast composition assigned as heterogeneous fibroglandular breast (c). With Architectural Distortion. Final diagnosis is suspicious malignancy (BITAD 4).

Image (4):



(a)

(b)



(c)

(d)

a, CC. c, MLO mammographic image of Right Breast. b, CC. d, MLO mammographic image of Left Breast. For 45 years old patient, show in both breasts scatter small calcifications with vascular calcifications. The

breast composition assigned as scattered fibroglandular breast (b). Final diagnosis is benign finding (BITAD 2).